

DEVELOPMENT OF NEW METHODS TO SYNTHESIZE HETEROCYCLIC COMPOUNDS

By

Md Shafaat Al Mehedi

A DISSERTATION

Submitted to
Michigan State University
in partial fulfillment of the requirements
for the degree of

Chemistry-Doctor of Philosophy

2021

ABSTRACT

DEVELOPMENT OF NEW METHODS TO SYNTHESIZE HETEROCYCLIC COMPOUNDS

By

Md Shafaat Al Mehedi

This dissertation is focused on the development of new methods to synthesize imidazoline scaffolds. The work discusses three new procedures developed in the Tepe lab to synthesize *trans*-oxazoline, *trans*-imidazoline, and 2,3-disubstituted quinoline scaffolds. In addition, a new guanidine base mediated diastereoselective aziridine synthesis is described in this work. These new synthetic methodologies provide access to compounds that were not easily accessible using previously described methods. Paths to oxazolines and imidazolines via modified Corey-Chaykovsky sulfur ylide chemistry are presented. Here, the sulfonium salts were treated with stable precursors of acyl imines and 1,3-diaza-1,3-butadiene intermediates, respectively, for the oxazoline and imidazoline syntheses. A modified Skraup-type reaction was employed to synthesize 2,3-disubstituted quinoline scaffolds where epoxides were treated with aromatic anilines under mild conditions in the presence of a Lewis acid.

This dissertation is dedicated to my father, Md Fazlul Hoque, whose dream was to see his son be a doctorate. This is for you, Abbu (Dad).

ACKNOWLEDGEMENTS

I could not complete my graduate life without the research and mental support provided by some people in every step of this journey. I am not a person who can express emotional thoughts properly in writing, but I will try my best to write here.

First, I like to thank my supervisor Prof. Jetze J. Tepe, for his continuous support in my graduate life. I still can remember the day of my first-year committee meeting, where I was too nervous and could not do well and was very upset about it. But after the meeting, You talked to me for an hour, and you said you saw a sharp improvement in me. Those lines inspired me a lot, and I have tried my best to make it right. The more I know you in the last few years, the more I feel how caring a supervisor you are, and I want to be like you in the future.

Next, I want to thank Prof. James E. Jackson, for helping me in my Ph.D. career. I can not remember how many times I emailed you for various reasons, and sometimes I bothered you repeatedly, and you still took that calmly. Thank you for being considerate about it.

I also like to thank Prof. Melanie M. Cooper for showing me how to teach an undergraduate organic chemistry course. I am blessed that I got the opportunity to be a TA in your organic chemistry course, and this will help me in my future career in academia.

I also like to thank Prof. Robert E. Maleczka and Prof. John W. Frost for enlightening conversations and guiding me in my Ph.D. life.

I cannot thank you enough for my awesome labmates Katarina, Grace, Taylor, Sophia, Allison, Dare, Charles, Konika, Kyra, Daniel, and Evan, as well as my past labmates Evert, Corey, Shuang, and Travis.

A special thanks to Katarina for making my Ph.D. career much more comfortable. You took care of a lot of lab works and reduced my load significantly. Thank you, Grace, for your time and a lot of discussion about research and a lot of other things. I will miss those conversations for sure. Shuang, in the first year of my Ph.D., you are the person I talked to most about every failure of my reactions and how I am struggling with my work. Thank you for listening and helping me at the worst time of my Ph.D. career.

I also especially like to thanks Corey, whom I believe was my second guide in the lab after Prof. Tepe. It will be hard for me to say in some words how you helped me at the beginning of my Ph.D. I just want to say thank you and again thank you.

Dr. Tony, thank you for your help in the mass spectrometry, and Dr. Holmes, thank you for your help in the NMR. I learned a lot about these valuable instruments from you two and how to solve different chemical problems by using these instruments.

I also like to thank my friends and colleagues to whom I am grateful here at MSU: Soham, Ankush, Dan, Debarshi, Pepe, Zhilin, Ali, and many others. A special thanks to Soham for your selfless help in many steps inside and outside of work.

In the end, I like to thank my mom, Shamsun Nahar, and my dad, Md Fazlul Hoque. Every day, I miss them more than anything else in the world. I also like to thank my mother-in-law Rowshon Ara, my father-in-law Safayet Ullah Patwary, who passed away in 2019. I miss you, Baba.

Finally, I don't want to say thank you to my wife, Sajia Afrin. Those are just words, which will never show how grateful I am for you being in my life. Your hardship, your tolerance, your sacrifice, I cannot just say thank you for all of that. You are the love of my life, and I want to spend the rest of my life with you..... Because who is going to tolerate me, except you?

TABLE OF CONTENTS

LIST OF TABLES.....	viii
LIST OF FIGURES.....	ix
LIST OF SCHEMES.....	xiv
KEY TO ABBREVIATIONS.....	xix
Chapter 1: Recent advances in the synthesis of imidazolines.....	1
1.1 Introduction.....	1
1.2 Classification of imidazolines.....	2
1.3 Classification of imidazoline synthesis methods.....	3
1.4 Synthesis of imidazolines.....	4
1.4.1 Method A: Synthesis of imidazolines from 1,2-diamines.....	4
1.4.2 Method B: Synthesis of imidazolines from isocyanides.....	20
1.4.3 Method C: Synthesis of imidazolines from amidines.....	43
1.5 Conclusion.....	54
REFERENCES.....	55
Chapter 2: Synthesis of diastereoselective 2,3-disubstituted aziridine in the presence of a guanidine base.....	61
2.1 Introduction.....	61
2.2 Results and discussion.....	62
2.3 Conclusion.....	64
2.4 Experimental sections.....	64
APPENDIX.....	76
REFERENCES.....	98
Chapter 3: Synthesis of oxazolines via reaction of acyl imines with sulfur ylides.....	101
3.1 Introduction.....	101
3.2 Results and discussion.....	102
3.3 Conclusion.....	116
3.4 Experimental sections.....	116
APPENDIX.....	150
REFERENCES.....	201
Chapter 4: Synthesis of imidazolines via reaction of 1,3-diaza-1,3-butadiene with sulfur ylides.....	204
4.1 Introduction.....	204
4.2 Results and discussion.....	204
4.3 Conclusion.....	209
4.4 Experimental sections.....	209
APPENDIX.....	218
REFERENCES.....	231

Chapter 5: Synthesis of 2,3-disubstituted quinolines via reaction of anilines with epoxides in the presence of Lewis acids.....	233
5.1 Introduction.....	233
5.2 Results and discussion.....	234
5.3 Mechanistic experiments.....	244
5.4 Conclusion.....	249
5.5 Experimental sections.....	249
APPENDIX.....	264
REFERENCES.....	285
Chapter 6: Conclusion and future works.....	288

LIST OF TABLES

Table 2.1. Synthesis of aziridines.....	63
Table 3.1. Optimization of oxazoline synthesis with different leaving groups in compound X	103
Table 3.2. Lewis acid optimization.....	106
Table 3.3. Solvent screening for the synthesis of oxazoline 3a from compound 5a	107
Table 3.4. Scope of oxazoline synthesis with different sulfonium salts (2).....	108
Table 3.5. Stevens rearrangement of sulfur ylides.....	109
Table 3.6. Optimization of oxazoline synthesis with tetrahydrothiophene containing sulfonium Salt (7c).....	110
Table 3.7. Scope of oxazoline synthesis with different sulfonium salts (7)	111
Table 3.8. Regioselective formation of oxazolines.....	113
Table 3.9. Scope of oxazoline synthesis with different substitutions in the R ¹ , R ² , and R ³ positions.....	114
Table 4.1. Optimization of the amidine synthesis.....	205
Table 4.2. Optimization of new sulfur ylide reaction.....	206
Table 4.3. Optimization of imidazoline synthesis with TBD base.....	207
Table 5.1. Optimization of quinoline synthesis with different acids/bases	235
Table 5.2. Optimization of quinoline synthesis (acid).....	236
Table 5.3. Optimization of quinoline synthesis (solvent and temperature)	238

LIST OF FIGURES

Figure 1.1. Structures of imidazolines containing biologically active natural and synthetic molecules.....	1
Figure 1.2. Classification of imidazolines.....	2
Figure 1.3. Classification of imidazoline synthesis methods.....	3
Figure 2.1. Guanidine bases.....	61
Figure 2.2. ^1H and ^{13}C NMR Spectra of Compound 2.1.....	77
Figure 2.3. ^1H and ^{13}C NMR Spectra of Compound 2.2.....	78
Figure 2.4. ^1H and ^{13}C NMR Spectra of Compound 2.3.....	79
Figure 2.5. ^1H and ^{13}C NMR Spectra of Compound 2.4.....	80
Figure 2.6. ^1H and ^{13}C NMR Spectra of Compound 2.5.....	81
Figure 2.7. ^1H and ^{13}C NMR Spectra of Compound 2.6.....	82
Figure 2.8. ^1H and ^{13}C NMR Spectra of Compound 2.7a.....	83
Figure 2.9. ^1H and ^{13}C NMR Spectra of Compound 2.7.....	84
Figure 2.10. ^1H and ^{13}C NMR Spectra of Compound 2.8a.....	85
Figure 2.11. ^1H and ^{13}C NMR Spectra of Compound 2.8.....	86
Figure 2.12. ^1H and ^{13}C NMR Spectra of Compound 2.9.....	87
Figure 2.13. ^1H and ^{13}C NMR Spectra of Compound 2.10.....	88
Figure 2.14. ^1H and ^{13}C NMR Spectra of Compound A1 (trans).....	89
Figure 2.15. ^1H and ^{13}C NMR Spectra of Compound A1 (cis).....	90
Figure 2.16. ^1H and ^{13}C NMR Spectra of Compound A2 (mixture).....	91
Figure 2.17. ^1H and ^{13}C NMR Spectra of Compound A3 (trans).....	92
Figure 2.18. ^1H and ^{13}C NMR Spectra of Compound A3 (cis).....	93

Figure 2.19. ^1H and ^{13}C NMR Spectra of Compound A4.....	94
Figure 2.20. ^1H and ^{13}C NMR Spectra of Compound A5.....	95
Figure 2.21. ^1H and ^{13}C NMR Spectra of Compound A6.....	96
Figure 2.22. ^1H and ^{13}C NMR Spectra of Compound A7.....	97
Figure 3.1. ^1H and ^{13}C NMR Spectra of Compound 1.....	151
Figure 3.2. ^1H and ^{13}C NMR Spectra of Compound 2a.....	152
Figure 3.3. ^1H and ^{13}C NMR Spectra of Compound 2b.....	153
Figure 3.4. ^1H and ^{13}C NMR Spectra of Compound 2c.....	154
Figure 3.5. ^1H and ^{13}C NMR Spectra of Compound 2d.....	155
Figure 3.6. ^1H and ^{13}C NMR Spectra of Compound 2e.....	156
Figure 3.7. ^1H and ^{13}C NMR Spectra of Compound 2f.....	157
Figure 3.8. ^1H and ^{13}C NMR Spectra of Compound 2g.....	158
Figure 3.9. ^1H and ^{13}C NMR Spectra of Compound 2h.....	159
Figure 3.10. ^1H and ^{13}C NMR Spectra of Compound 3a.....	160
Figure 3.11. ^1H and ^{13}C NMR Spectra of Compound 3b.....	161
Figure 3.12. ^1H and ^{13}C NMR Spectra of Compound 3c.....	162
Figure 3.13. ^1H and ^{13}C NMR Spectra of Compound 3d.....	163
Figure 3.14. ^1H and ^{13}C NMR Spectra of Compound 3e.....	164
Figure 3.15. ^1H and ^{13}C NMR Spectra of Compound 3f.....	165
Figure 3.16. ^1H and ^{13}C NMR Spectra of Compound 3g.....	166
Figure 3.17. ^1H and ^{13}C NMR Spectra of Compound 3h.....	167
Figure 3.18. ^1H and ^{13}C NMR Spectra of Compound 3i.....	168
Figure 3.19. ^1H and ^{13}C NMR Spectra of Compound 3j.....	169

Figure 3.20. ^1H and ^{13}C NMR Spectra of Compound 3k.....	170
Figure 3.21. ^1H and ^{13}C NMR Spectra of Compound 3l.....	171
Figure 3.22. ^1H and ^{13}C NMR Spectra of Compound 3m.....	172
Figure 3.23. ^1H and ^{13}C NMR Spectra of Compound 3n.....	173
Figure 3.24. ^1H and ^{13}C NMR Spectra of Compound 3o.....	174
Figure 3.25. ^1H and ^{13}C NMR Spectra of Compound 3p.....	175
Figure 3.26. ^1H and ^{13}C NMR Spectra of Compound 3q.....	176
Figure 3.27. ^1H and ^{13}C NMR Spectra of Compound 3r.....	177
Figure 3.28. ^1H and ^{13}C NMR Spectra of Compound 3s.....	178
Figure 3.29. ^1H and ^{13}C NMR Spectra of Compound 3t.....	179
Figure 3.30. ^1H and ^{13}C NMR Spectra of Compound 3u.....	180
Figure 3.31. ^1H and ^{13}C NMR Spectra of Compound 3v.....	181
Figure 3.32. ^1H and ^{13}C NMR Spectra of Compound 3w.....	182
Figure 3.33. ^1H and ^{13}C NMR Spectra of Compound 4.....	183
Figure 3.34. ^1H and ^{13}C NMR Spectra of Compound 5a.....	184
Figure 3.35. ^1H and ^{13}C NMR Spectra of Compound 5b.....	185
Figure 3.36. ^1H and ^{13}C NMR Spectra of Compound 5c.....	186
Figure 3.37. ^1H and ^{13}C NMR Spectra of Compound 5d.....	187
Figure 3.38. ^1H and ^{13}C NMR Spectra of Compound 5e.....	188
Figure 3.39. ^1H and ^{13}C NMR Spectra of Compound 5f.....	189
Figure 3.40. ^1H and ^{13}C NMR Spectra of Compound 5g.....	190
Figure 3.41. ^1H and ^{13}C NMR Spectra of Compound 5h.....	191
Figure 3.42. ^1H and ^{13}C NMR Spectra of Compound 6a.....	192

Figure 3.43. ^1H and ^{13}C NMR Spectra of Compound 6b.....	193
Figure 3.44. ^1H and ^{13}C NMR Spectra of Compound 6c.....	194
Figure 3.45. ^1H and ^{13}C NMR Spectra of Compound 7a.....	195
Figure 3.46. ^1H and ^{13}C NMR Spectra of Compound 7b.....	196
Figure 3.47. ^1H and ^{13}C NMR Spectra of Compound 7c.....	197
Figure 3.48. ^1H and ^{13}C NMR Spectra of Compound 7d.....	198
Figure 3.49. ^1H and ^{13}C NMR Spectra of Compound 7h.....	199
Figure 3.50. ^1H and ^{13}C NMR Spectra of Compound 7i.....	200
Figure 4.1. ^1H and ^{13}C NMR Spectra of Compound 4.1a.....	219
Figure 4.2. ^1H and ^{13}C NMR Spectra of Compound 4.1b.....	220
Figure 4.3. ^1H and ^{13}C NMR Spectra of Compound 4.1c.....	221
Figure 4.4. ^1H and ^{13}C NMR Spectra of Compound 4.1d.....	222
Figure 4.5. ^1H and ^{13}C NMR Spectra of Compound 4.1e.....	223
Figure 4.6. ^1H and ^{13}C NMR Spectra of Compound 4.1f.....	224
Figure 4.7. ^1H and ^{13}C NMR Spectra of Compound 4.2a.....	225
Figure 4.8. ^1H and ^{13}C NMR Spectra of Compound 4.2b.....	226
Figure 4.9. ^1H and ^{13}C NMR Spectra of Compound 4.2c.....	227
Figure 4.10. ^1H and ^{13}C NMR Spectra of Compound 4.3a.....	228
Figure 4.11. ^1H and ^{13}C NMR Spectra of Compound 4.3b.....	229
Figure 4.12. ^1H and ^{13}C NMR Spectra of Compound 4.4.....	230
Figure 5.1. Crude mass spectrum five minutes into the reaction.....	245
Figure 5.2. Crude mass spectrum fifteen minutes into the reaction.....	246
Figure 5.3. Crude mass spectrum thirty minutes into the reaction.....	247

Figure 5.4. ^{13}C Spectrum: Reaction of styrene oxide with $\text{Sc}(\text{OTf})_3$ at 1 hour.....	248
Figure 5.5. ^{13}C NMR of phenylacetaldehyde.....	248
Figure 5.6. ^1H and ^{13}C NMR Spectra of Compound Q1.....	265
Figure 5.7. ^1H and ^{13}C NMR Spectra of Compound Q2.....	266
Figure 5.8. ^1H and ^{13}C NMR Spectra of Compound Q3.....	267
Figure 5.9. ^1H and ^{13}C NMR Spectra of Compound Q4.....	268
Figure 5.10. ^1H and ^{13}C NMR Spectra of Compound Q5.....	269
Figure 5.11. ^1H and ^{13}C NMR Spectra of Compound Q6.....	270
Figure 5.12. ^1H and ^{13}C NMR Spectra of Compound Q7.....	271
Figure 5.13. ^1H and ^{13}C NMR Spectra of Compound Q8.....	272
Figure 5.14. ^1H and ^{13}C NMR Spectra of Compound Q9.....	273
Figure 5.15. ^1H and ^{13}C NMR Spectra of Compound Q10.....	274
Figure 5.16. ^1H and ^{13}C NMR Spectra of Compound Q11.....	275
Figure 5.17. ^1H and ^{13}C NMR Spectra of Compound Q12.....	276
Figure 5.18. ^1H and ^{13}C NMR Spectra of Compound Q13.....	277
Figure 5.19. ^1H and ^{13}C NMR Spectra of Compound Q14.....	278
Figure 5.20. ^1H and ^{13}C NMR Spectra of Compound Q15.....	279
Figure 5.21. ^1H and ^{13}C NMR Spectra of Compound Q16.....	280
Figure 5.22. ^1H and ^{13}C NMR Spectra of Compound Q17.....	281
Figure 5.23. ^1H and ^{13}C NMR Spectra of Compound Q18.....	282
Figure 5.24. ^1H and ^{13}C NMR Spectra of Compound Q19.....	283
Figure 5.25. ^1H and ^{13}C NMR Spectra of Compound Q20.....	284

LIST OF SCHEMES

Scheme 1.1. The first synthesis of imidazoline.....	4
Scheme 1.2. Cellulose sulfuric acid mediated synthesis of imidazolines from diamines	4
Scheme 1.3. Synthesis of ferrocenyl imidazolines from diamines.....	5
Scheme 1.4. SiO ₂ supported tungstosilicic acid mediated synthesis of 2-imidazolines and bis-imidazolines.....	5
Scheme 1.5. Synthesis of imidazolines from fluorinated alkenes and diamines	6
Scheme 1.6. Proposed mechanism of the reaction shown in Scheme 1.5.....	7
Scheme 1.7. Synthesis of imidazolines from imidoyl chlorides and diamines	8
Scheme 1.8. Cupric indole-3-acetate mediated synthesis of imidazolines.....	8
Scheme 1.9. Proposed mechanism of the reaction shown in Scheme 1.8.....	9
Scheme 1.10. Pyridinium p-toluenesulfonate mediated synthesis of imidazolines.....	9
Scheme 1.11. Proposed mechanism of the reaction shown in Scheme 10.....	10
Scheme 1.12. Synthesis of 2-amino imidazolines.....	10
Scheme 1.13. Peroxide mediated synthesis of imidazolines.....	11
Scheme 1.14. Proposed mechanism of the reaction shown in Scheme 1.13.....	12
Scheme 1.15. Intramolecular cyclization of imidoyl chlorides to imidazolines.....	12
Scheme 1.16. Formation of imidoyl chloride 56	13
Scheme 1.17. Potassium ferricyanide mediated synthesis of imidazolines.....	13
Scheme 1.18. Trimethylsilyl polyphosphate mediated synthesis of imidazolines.....	14
Scheme 1.19. Boric acid mediated synthesis of imidazoline in kilogram scale.....	14
Scheme 1.20. Palladium-catalyzed synthesis of imidazolines.....	15
Scheme 1.21. Synthesis of chiral pybim ligand.....	15

Scheme 1.22. Mechanism of the catalytic cycle of 2-aryl-2-imidazoline (70) synthesis.....	16
Scheme 1.23. Ruthenium complex mediated synthesis of imidazolines.....	17
Scheme 1.24. Mechanism of ruthenium (II) catalyzed 2-imidazoline synthesis.....	17
Scheme 1.25. Zn-modified magnetic Si-sphere H ₂ SO ₄ mediated synthesis of imidazolines.....	18
Scheme 1.26. Synthesis of 1- <i>tert</i> -butyl-2-imidazoline.....	18
Scheme 1.27. Peroxide mediated synthesis of imidazolines.....	19
Scheme 1.28. Sulfur-mediated synthesis of phosphoryl-substituted imidazolines	19
Scheme 1.29. Mechanism of phosphoryl-substituted imidazolines synthesis.....	20
Scheme 1.30. Cinchona alkaloid-derived organocatalytic reaction to synthesize imidazolines.....	21
Scheme 1.31. Proposed mechanism of the reaction shown in Scheme 1.30.....	21
Scheme 1.32. Organocatalytic diastereoselective and enantioselective Mannich-type reaction to synthesize imidazolines.....	22
Scheme 1.33. Proposed mechanism of the reaction shown in Scheme 1.32	22
Scheme 1.34. Cinchona derived precatalyst mediated fully β -substituted imidazolines synthesis.	23
Scheme 1.35. Linked oxazole-imidazoline synthesis from bifunctional α -imino ester.....	24
Scheme 1.36. NMR studies reaction of Scheme 1.35.....	25
Scheme 1.37. Synthesis of quaternary carbon center <i>syn</i> -selective imidazolines.....	26
Scheme 1.38. Mechanism of <i>syn</i> -imidazoline synthesis.....	27
Scheme 1.39. Superbase proazaphosphatane mediated imidazoline synthesis.....	28
Scheme 1.40. Mechanism of water and PAP mediated imidazoline synthesis.....	28
Scheme 1.41. Synthesis of sulfamate-fused 2-imidazolines.....	29
Scheme 1.42. Synthesis of imidazolines from β -sulfinylamino isocyanides.....	30
Scheme 1.43. Ugi–Staudinger–aza-Wittig-sequence mediated synthesis of 2-(acetamide-2-yl)-imidazolines.....	31

Scheme 1.44. Silver-catalyzed multicomponent reaction to synthesize (2-imidazolin-4-yl) phosphonates.....	31
Scheme 1.45. Cu(I)-mediated enantioselective 2-imidazolines.....	32
Scheme 1.46. Cinchona alkaloid thiourea mediated synthesis of spirooxindole imidazolines.....	33
Scheme 1.47. Transition-state model of the Scheme 1.46 cyclization step.....	33
Scheme 1.48. Cinchona alkaloid-based amide catalyst mediated synthesis of vicinal tetra-substituted 2-imidazolines.....	34
Scheme 1.49. Proposed mechanism of the reaction shown in Scheme 1.48.....	35
Scheme 1.50. Cinchona-derived amide catalyst and Ag(I) salt mediated synthesis of vicinal tetra-substituted 2-imidazolines.....	36
Scheme 1.51. Diastereoselective synthesis of imidazolines.....	36
Scheme 1.52. Proposed mechanism of [3 + 2]- cycloaddition reaction of Scheme 1.51.....	37
Scheme 1.53. Cu-catalyzed synthesis of imidazolines.....	38
Scheme 1.54. CuI-catalyzed cascade cyclization to synthesize 1,1'-biimidazole.....	38
Scheme 1.55. Proposed mechanism of the reaction shown in Scheme 1.53 and 1.54.....	39
Scheme 1.56. Ag-catalyzed [3+2]- cycloaddition reaction to synthesize imidazolines.....	39
Scheme 1.57. Ag-mediated [3+1+1] annulation reaction to synthesize imidazolines.....	40
Scheme 1.58. Mechanism of the silver-promoted [3+1+1] annulation.....	41
Scheme 1.59. Cinchona-derived bifunctional squaramide catalyst mediated imidazoline synthesis	41
Scheme 1.60. Ag ₂ O & phosphine-based catalyst mediated enantioselective imidazoline synthesis	42
Scheme 1.61. Proposed mechanism of the reaction shown in scheme 1.60.....	43
Scheme 1.62. Synthesis of imidazolines from amidines and sulfonium salts.....	43
Scheme 1.63. The mechanism for the synthesis of imidazolinium salts (225).....	44
Scheme 1.64. Cu(I)-catalyzed aerobic reaction to synthesize bi- and tri-cyclic imidazolines.....	45

Scheme 1.65. Proposed mechanism of the [3+2]- annulation reaction of amidine.....	45
Scheme 1.66. Cu-catalyzed synthesis of imidazolines from <i>N</i> -alkenylamidines.....	46
Scheme 1.67. Proposed mechanism of the reaction shown in Scheme 1.66	47
Scheme 1.68. Cu-mediated 2-imidazoline synthesis.....	47
Scheme 1.69. Proposed mechanism of the reaction shown in Scheme 1.68.....	48
Scheme 1.70. Buckminsterfullerene fused imidazolines synthesis from amidines.....	49
Scheme 1.71. Mechanism of the synthesis of [60]fullerene-fused imidazolines.....	49
Scheme 1.72. CuI-catalyzed redox neutral C-H amination of the amidoximes to synthesize 2-imidazolines.....	50
Scheme 1.73. Hypervalent Iodine-mediated diastereoselective imidazolines synthesis.....	51
Scheme 1.74. Proposed mechanism of the reaction shown in Scheme 1.73.....	51
Scheme 1.75. Hypervalent Iodine-mediated 4-fluoroalkyl-2-imidazolines synthesis.....	52
Scheme 1.76. Pd-catalyzed cyclization of <i>N</i> -acetoxy-amidine to synthesize imidazolines.....	52
Scheme 1.77. Synthesis of 2-imidazoline from the reaction of sulfonium salt and 1,3-diaza-1,3-butadiene.....	53
Scheme 1.78. Pd-catalyzed synthesis of imidazolines.....	53
Scheme 2.1. Synthesis of aziridines.....	62
Scheme 3.1. Synthesis of oxazolines via expansion of modified Corey-Chaykovsky-type reaction and Heine Reaction.....	101
Scheme 3.2. Proposed ring-opening mechanism of aziridine to oxazoline providing two regioisomers.....	112
Scheme 3.3. Proposed mechanism of the reaction.....	115
Scheme 4.1. Synthesis of imidazoline.....	204
Scheme 4.2. Synthesis of <i>N</i> -benzylidene- <i>N'</i> -(4-methoxyphenyl)benzimidamide.....	206
Scheme 4.3. Synthesis of imidazoline 4.3a under the optimized condition.....	209
Scheme 5.1. Synthesis of quinolines from epoxides and aromatic amines.....	234

Scheme 5.2. Substrate scope of the reaction.....	242
Scheme 5.3. Proposed mechanism of the reaction.....	243

KEY TO ABBREVIATIONS

Å	Angstrom
Ac	Acetyl
AEEA	<i>N</i> -(2-aminoethyl)ethanolamine
Aq	Aqueous
Boc	<i>tert</i> -Butyloxycarbonyl-
Bn	Benzyl-
Bz	Benzoyl-
°C	Celsius
CAN	Ceric ammonium nitrate
Cbz	Carboxybenzyl-
CNS	Central Nervous System
Cu ^(II) -(IAA) ₂	Cupric indole-3-acetate
Cy	Cyclohexyl-
DABCO	1,4-Diazabicyclo[2.2.2]-octane
DBU	1,8-Diazabicyclo(5.4.0)undec-7-ene
DCE	Dichloroethane
DCM	Dichloromethane
DIPEA	<i>N,N</i> -Diisopropylethylamine
DMAP	Dimethylaminopyridine
DMF	Dimethylformamide
DMSO	Dimethyl sulfoxide
dppf	1,1'-Bis(diphenylphosphino) ferrocene
dppp	1,3-Bis(diphenylphosphino) propane
EDG	Electron donating group
Equiv	Equivalent
EtOAc	Ethyl acetate
EWG	Electron withdrawing group
h	Hours
H ₂ O ₂	Hydrogen peroxide
HMDS	Hexamethyldisilazane
HPMo	Tungstophosphoric acid
HPW	Phosphomolybdic acid
HSiW	Tungstosilicic acid
Hv	Light
LED	Light-emitting diode
Me	Methyl-
mp	Melting point
MTBD	7-Methyl-1,5,7-triazabicyclo(4.4.0)dec-5-ene
NBS	<i>N</i> -Bromosuccinimide
NCS	<i>N</i> -Chlorosuccinimide
NIS	<i>N</i> -Iodosuccinimide
OTf	Trifluoromethanesulfonate

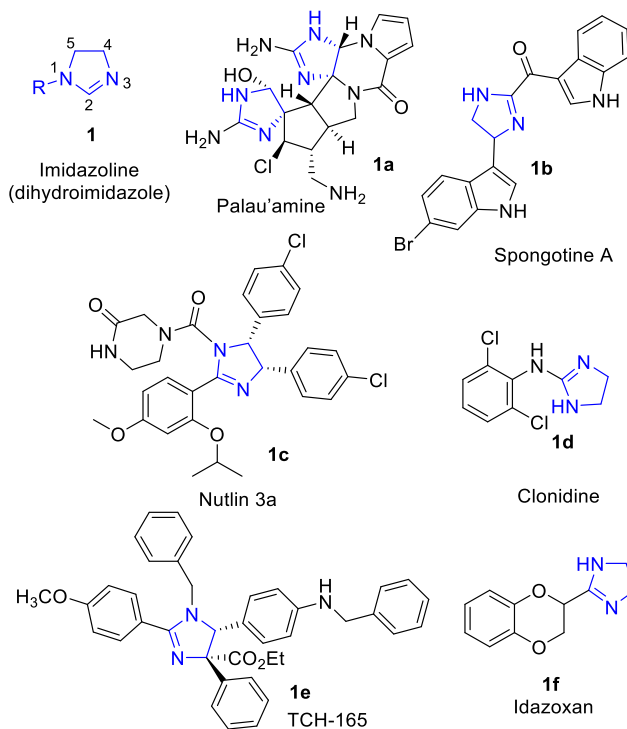
<i>p</i> -TSA	<i>p</i> -Toluenesulfonic acid
PCl ₅	Phosphorous pentachloride
Ph	Phenyl
PPSE	Trimethylsilyl polyphosphate
PPTS	Pyridinium <i>p</i> -toluenesulfonate
rt	Room temperature
SARS-CoV-2	Severe acute respiratory syndrome coronavirus 2
TBAB	Tetrabutylammonium bromide
TBAOH	<i>tetra-n</i> -Butylammonium hydroxide
TBD	1,5,7-Triazabicyclo(4.4.0)dec-5-ene
TEA	Triethylamine
TfOH	Triflic acid
TFA	Trifluoroacetic acid
TEMPO	(2,2,6,6-Tetramethylpiperidin-1-yl)oxyl
THF	Tetrahydrofuran
TMG	1,1,3,3-Tetramethylguanidine
TMS	Trimethylsilyl-
TMSOTf	trimethylsilyl trifluoromethanesulfonate
TosMIC	<i>p</i> -Toluenesulfonylmethyl isocyanide
TS	Transition state
Ts	Tosyl-

Chapter 1: Recent advances in the synthesis of imidazolines

1.1 Introduction

Imidazolines (**1**) are non-aromatic five-membered heterocyclic compounds containing two nitrogen atoms in the core part of the molecule.¹ They are an important class of molecules that can be found in various biologically active natural² (**1a,1b**) and synthetic³ (**1c-1f**) products (**Figure 1**). The discovery of the imidazoline binding site (IBS) in 1984,⁴ increased the interest in the imidazoline synthesis significantly. Moreover, different substituted imidazolines have demonstrated potential therapeutic value for the treatment of various diseases such as hyperglycemia,⁵ cancer,⁶ parasitic diseases,⁷ fungal diseases,⁸ hypertension,⁹ as well as potentially for the treatment of Alzheimer's¹⁰ and Parkinson's¹¹ disease. Furthermore, imidazolines have been used as different synthetic intermediates,¹² transition metal ligands,¹³ and as chiral catalysts.¹⁴

Figure 1.1. Structures of imidazolines containing biologically active natural and synthetic molecules

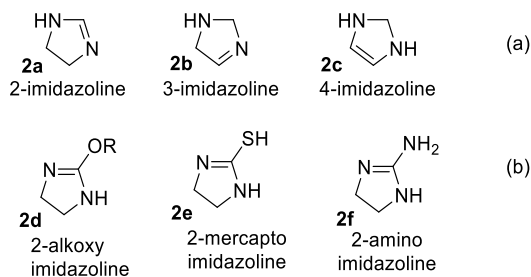


Due to the simplicity of the insertion of chirality around the imidazoline ring, the use of imidazoline compounds as chiral auxiliaries¹⁵ in enantioselective reactions has been increased significantly in the last few years. Many common reactions, including Friedel-Crafts reactions,¹⁶ Suzuki-Miyaura coupling reactions,¹⁷ Mannich-type reactions,¹⁸ Mizoroki-Heck reactions,¹⁹ Henry reactions,²⁰ Michael reactions,²¹ and Diels-Alder reactions²² have utilized imidazoline catalysts to obtain high enantioselectivities. Liu and Du published an excellent review of the imidazoline synthesis methods in 2009,²³ which is cited in 104 publications until now. After that, several efficient methods have been developed for the preparation of substituted imidazolines. This chapter discusses recent advancements in the synthesis of imidazolines, reported in the scientific literature after the imidazoline synthesis review published by Liu and Du in 2009.

1.2 Classification of imidazolines

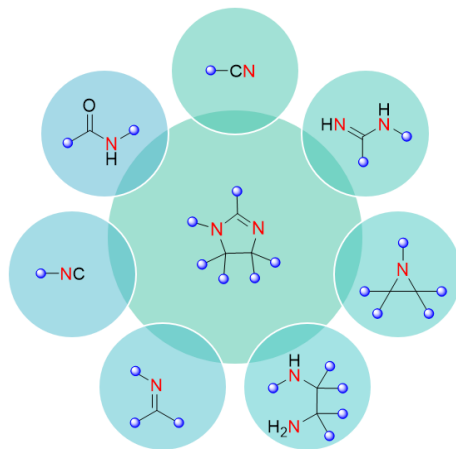
Based on the position of the double bond, imidazolines are classified as a 2-imidazoline (**2a**), 3-imidazoline (**2b**), and 4-imidazoline (**2c**) (**Figure 1.2a**).²⁴ Among them, 2-imidazolines are the most common moieties in various sectors of biology and chemistry. Different heteroatoms are incorporated as substituents in the 2-imidazolines to form subclasses of imidazolines, including 2-alkoxy imidazoline (**2d**), 2-mercapto imidazoline (**2e**), and the 2-amino imidazoline (**2f**) (**Figure 1.2b**).

Figure 1.2. Classification of imidazolines



1.3 Classification of imidazoline synthesis methods

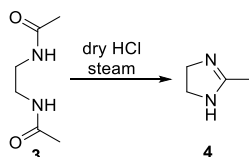
Figure 1.3. Classification of imidazoline synthesis methods



The first synthesis of 2-methyl-imidazoline (lysidine) was performed in 1988 by the German chemist A.W. Hofmann. He synthesized imidazoline (**4**) by heating *N,N'*-diacetyleneethylenediamine (**3**) in the presence of dry hydrogen chloride (HCl) (**Scheme 1**).²⁵ Since then, many synthetic methods have been developed to synthesize imidazoline compounds by using various starting materials. The most common method uses different electrophiles (aldehyde, carboxylic acid, nitrile, etc.) with ethylenediamine as a starting material. Other pathways utilizing aziridine, amidine, isocyanide, imine, or amide to obtain imidazoline moieties have been reported in recent literature. Many of those reactions implicated transition metals such as nickel (Ni), copper (Cu), palladium (Pd), tungsten (W), rhodium (Rh), silver (Ag), titanium (Ti) as catalysts. Based on the starting materials used, the methods were categorized into several groups (Method A to Method H) (**Figure 1.3**). Method A contains the methods that utilized ethylenediamine as the starting material. Method B to G comprises the synthesis of imidazolines based on the starting material; isocyanide (B), amidine (C), imine (D), aziridine (E), cyanide (F), and amide (G). Method H discusses the reports that do not fit into one of the categories mentioned above. Here, this chapter

discusses the recent advancement in imidazoline synthesis by using ethylenediamine (Method A), isocyanide (Method B), and amidine (Method C), based on the scientific literature report from 2009 until 2020.

Scheme 1.1. The first synthesis of imidazoline

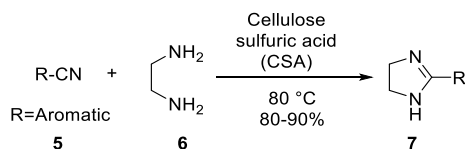


1.4 Synthesis of imidazolines

1.4.1 Method A: Synthesis of imidazolines from 1,2-diamines

Due to the relative ease of incorporating chirality, the synthesis of imidazolines from 1,2-diamines has been one of the most common methods. In 2009, Shaabani *et al.* advanced this method by reacting aromatic nitriles (**5**) and ethylenediamine (**6**) in the presence of a biopolymer-based cellulose sulfuric acid catalyst.²⁶ The imidazolines (**7**) were reported in good to excellent yields. These reactions were utilized as a green method by performing under a solvent-free condition at 80 °C with different substitutions on the aromatic nitriles (five examples) (**Scheme 1.2**).

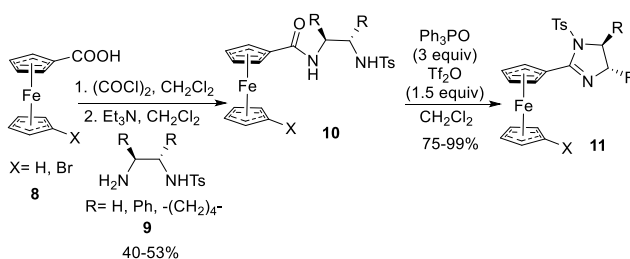
Scheme 1.2. Cellulose sulfuric acid mediated synthesis of imidazolines from diamines



In the same year, Wang and co-workers reported the synthesis of ferrocenyl imidazolines (**11**) from ferrocenyl carboxylic acids (**8**) and diamines (**9**) in good to excellent yields (**Scheme**

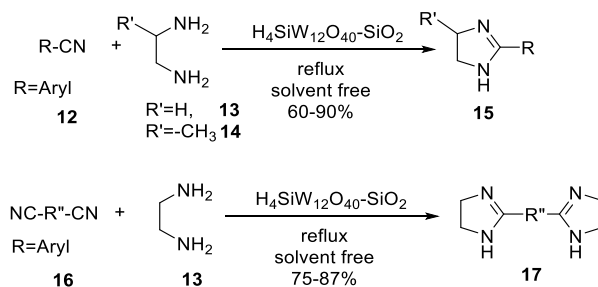
1.3).²⁷ These ferrocenyl imidazolines had been employed as ligands in the transition metal-mediated catalytic processes.²⁸ At first, the ferrocene containing carboxylic acids (**8**) and the diamines (**9**) formed intermediate amides (**10**). In the next step, the imidazolines were generated by the cyclodehydration reaction of the intermediates **10**. This step was performed in the presence of triphenylphosphine oxide and trifluoromethanesulfonic anhydride.

Scheme 1.3. Synthesis of ferrocenyl imidazolines from diamines



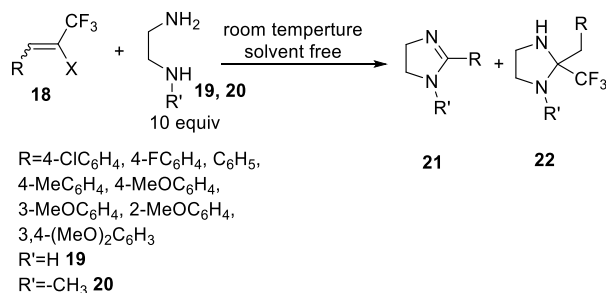
In 2010, Nasr-Esfahani *et al.* synthesized 2-imidazolines (**15**) by the reaction of 1,2-diaminoethane (**13**) or 1,2-diaminopropane (**14**) with aromatic nitriles (**12**) in the presence of SiO₂ supported tungstosilicic acid (H₄SiW₁₂O₄₀-SiO₂) (**Scheme 1.4**).²⁹ These reactions generated the imidazolines in good to excellent yields (60-90%). Moreover, the reaction of dinitriles (**16**) with 1,2-diamine (**13**), the bis-imidazolines (**17**) were also isolated in 75-87% yields. The tungsten catalyst was recovered and reused, which provided a great advantage to this method.

Scheme 1.4. SiO₂ supported tungstosilicic acid mediated synthesis of 2-imidazolines and bis-imidazolines



The same year, Nenajdenko and co-workers reported an unanticipated synthesis of imidazoline compounds from β -halogeno- β -polyfluoromethylstyrenes (**18**) with substituted and substituted ethylenediamine (**19**) (**Scheme 1.5**).³⁰ A simple reaction condition was used under solvent-free conditions at room temperature, and the reactions formed a mixture of imidazolines (**21**) and fluorinated imidazolidines (**22**), with a total isolated yield ranging from 65 to 96%. A variety of substituted aromatic groups (C₆H₅, 2-MeOC₆H₄, 3-MeOC₆H₄, 4-ClC₆H₄, 4-MeC₆H₄, 4-MeOC₆H₄, 4-FC₆H₄, 3,4-(MeO)₂C₆H₃) and halogens (X= F, Cl, Br) have been investigated. However, when *p*-MeOPh and 3,4-(MeO)₂Ph substituted substrates were used, only imidazolines product were isolated. Moreover, treatment of *N*-substituted ethylenediamine (**20**) with different vinylic halides (**18**) also solely formed imidazolines.

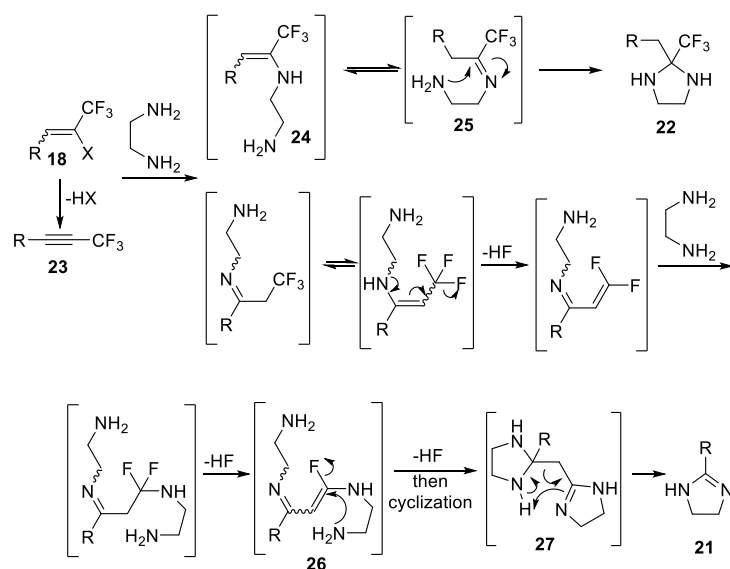
Scheme 1.5. Synthesis of imidazolines from fluorinated alkenes and diamines



Based on the proposed mechanism (**Scheme 1.6**), the reaction is initiated in two pathways. One is the dehalogenation of **18** to form acetylene (**23**), and the other one is an addition of ethane-1,2-diamine to the double bond. Depending on the conditions and reagents, ethane-1,2-diamine can attack both α - or β - position of styrene. Nucleophilic substitution at the β -position of styrene forms enamine (**24**), and then tautomerize into the intermediate imine (**25**). Finally, cyclization of **25** formed the imidazolidine **22**. However, a more complex mechanism is observed when the ethylenediamine attacks the α -position of acetylene, or styrene. This pathway advances by

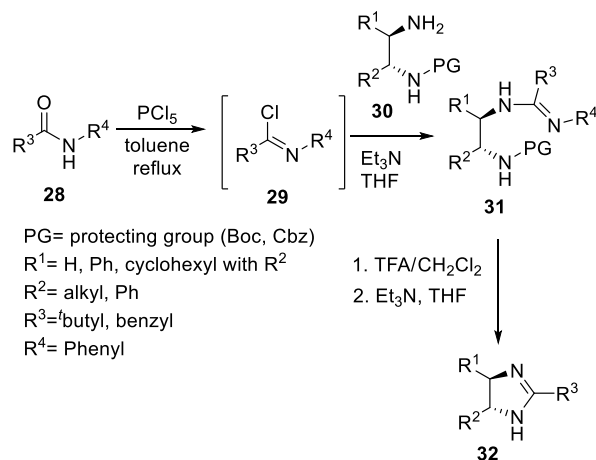
eliminating hydrogen fluoride and then adding a second ethylenediamine to generate the intermediate **26**. Next, the removal of additional hydrogen fluoride, followed by cyclization, leads to the intermediate **27**. Finally, the imidazoline **21** was formed by the C-C bond cleavage of the intermediate **27**.

Scheme 1.6. Proposed mechanism of the reaction shown in Scheme 1.5



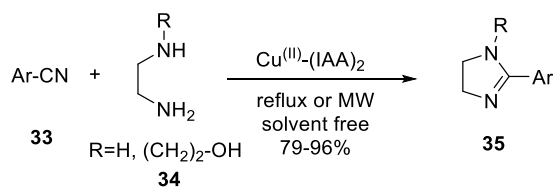
Later in 2010, Zhu and Lu reported a new method to synthesize chiral imidazolines from carboxy amides (**28**) and 1,2-diamines (**30**) (**Scheme 1.7**).³¹ The reaction commenced by the formation of *in situ* imidoyl chloride (**29**) from carboxy amide in the presence of phosphorous pentachloride (PCl₅). This intermediate **29** then reacts with diamine **30** to form the intermediate amidine (**31**). Removal of the protecting group from the intermediate **31** set the crucial stage of cyclization to generate the imidazoline (**32**). Cbz and Boc protecting groups were used in this reaction, and the imidazolines were obtained in good yields (70-88%).

Scheme 1.7. Synthesis of imidazolines from imidoyl chlorides and diamines



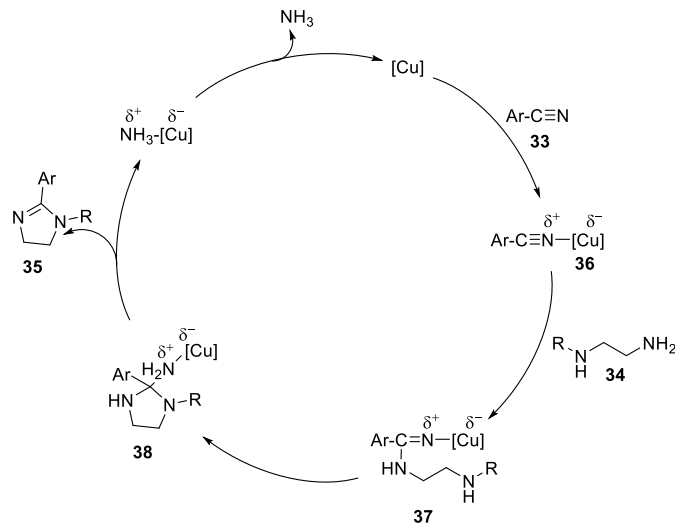
In 2011, Zhang and co-workers reported another synthesis of 2-imidazolines from the reaction of aromatic nitriles (**33**) with ethylenediamine (**34**) (**Scheme 1.8**).³² This catalytic approach was aided by reusable cupric indole-3-acetate ($\text{Cu(II)}-(\text{IAA})_2$) under a solvent-free condition. Under the same reaction conditions, *N*-(2-aminoethyl)ethanolamine (AEEA) was used with **33** to synthesize *N*-hydroxyethyl derivatives of imidazoline. The author only reported electron-withdrawing aromatic nitriles to synthesized imidazolines in good to excellent yields (79-96%).

Scheme 1.8. Cupric indole-3-acetate mediated synthesis of imidazolines



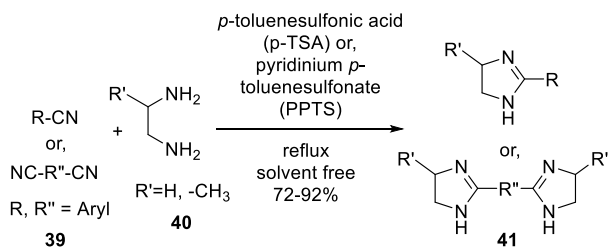
The mechanism of the reaction is illustrated in **Scheme 1.9**. At first, the cupric indole-3-acetate activates the nitrile group of **33** to generate the nitrogen cation (**36**). Then, the nucleophilic attack of **34** provides the intermediate amidine (**37**), followed by the generation of imidazolidine (**38**). Lastly, the imidazoline or *N*-substituted imidazoline (**35**) is generated by liberating NH_3 , and the copper catalyst is reused for the next cycle.

Scheme 1.9. Proposed mechanism of the reaction shown in Scheme 1.8



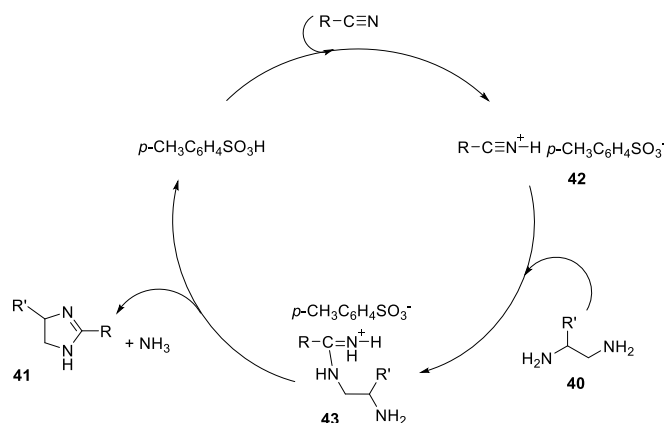
Nasr-Esfahani *et al.* demonstrated another imidazoline synthesis method, by using nitriles or dinitriles (**39**) with ethylenediamine or 1,2-diaminopropane (**40**) in the presence of pyridinium *p*-toluenesulfonate (PPTS) or, *p*-toluenesulfonic acid (*p*-TSA) (**Scheme 1.10**).³³ The reaction proceeds with a good to an excellent yield of both mono- & bis-imidazolines (**41**) (72-92%). When ethylenediamine was treated with dinitriles for a short period of time (50-60 min), the mono-imidazolines were obtained in 90-92% yields. On the contrary, longer reaction times (Above 100 min) generated the bis-imidazolines in 85-87% yields. Of all the Brønsted acids screened in the reaction, *p*-TSA performed better in terms of yield of imidazolines and reaction time.

Scheme 1.10. Pyridinium *p*-toluenesulfonate mediated synthesis of imidazolines



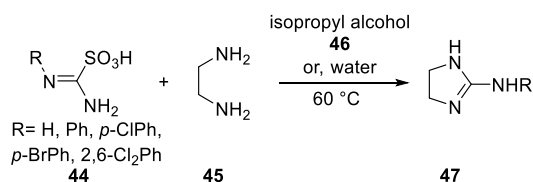
In their mechanism (**Scheme 1.11**), they showed that the nitrile is first activated by the Brønsted acid to form the intermediate **42**. Then the diamine (**40**) attacks **42** to generate the intermediate **43**. Finally, cyclization of **43** gives the product **41** and release ammonia (NH₃) and the catalyst for the next catalytic cycle.

Scheme 1.11. Proposed mechanism of the reaction shown in Scheme 10



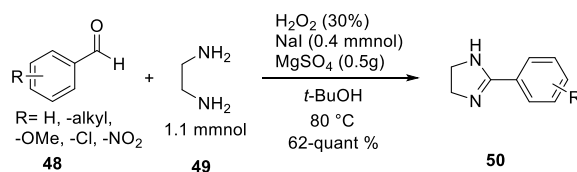
Mohanazadeh and co-workers reported the synthesis of 2-amino-imidazolines (**47**) from a reaction between sulfonic acid-containing amidine (**44**) and ethylenediamine (**45**) under mild reaction conditions (**Scheme 1.12**).³⁴ The reaction used water or, isopropyl alcohol (**46**) as reaction medium, where isopropyl alcohol affords better yields (80-93%) of **47** (yields in water 54-77%). The author only reported halogen-substituted (*p*-ClPh, *p*-BrPh, 2,6-Cl₂Ph) aromatic moieties in the acid derivatives (**44**) to synthesize imidazolines (**47**).

Scheme 1.12. Synthesis of 2-amino imidazolines



Bai and co-workers demonstrated an efficient and straightforward synthesis of 2-imidazolines (**50**) from aldehydes (**48**) with ethylenediamine (**49**), in the presence of a convenient and simple oxidant hydrogen peroxide (H_2O_2) and sodium iodide (NaI) catalyst (**Scheme 1.13**).³⁵ When the reaction carried out with H_2O_2 alone, the product formation was not observed. Incorporation of a second oxidant CAN also did not offer any product. Primarily, with 0.4 mmol of NaI, 33% product was isolated. Screening of different drying agents (anhydrous sodium sulfate (Na_2SO_4), anhydrous magnesium sulfate (MgSO_4), and 4Å molecular sieves) showed that with 0.5 gm of MgSO_4 , the yield improved to 94%. Under these optimized reaction conditions, a series of substituted aromatic aldehydes (*p*-MeOPh, -alkyl, *o,m,p*-ClPh, *o,m,p*-NO₂Ph, 2,4-Cl₂Ph) were screened with **49**, and the imidazolines (**50**) were isolated in 62% and up to quantitative yields. There were no substantial electronic effects observed, although a steric effect appeared to be critical in the reaction, as showed with the 2-NO₂PhCHO provided 62% product, compared to the 3-NO₂PhCHO, and 4-NO₂PhCHO gave 74%, and 97% of the product **50**, respectively.

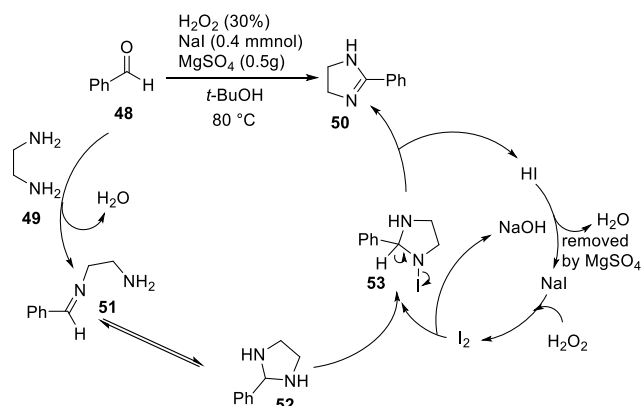
Scheme 1.13. Peroxide mediated synthesis of imidazolines



Based on the mechanistic experimental data, a mechanism was reported in the literature (**Scheme 1.14**). Initially, the Schiff base intermediate **51** is generated from the corresponding **49** and aldehyde (**48**). After that, intermediate imidazolidine **52** is formed via cyclization of **51**. Then **52** reacts with the *in situ* formed iodine (I_2), generated from the oxidation of NaI by hydrogen peroxide to form the (Iodo)-imidazolidine (**53**). Finally, the elimination of HI from **53** forms the desired imidazoline (**50**). NaOH generated from the reaction between peroxide and NaI,

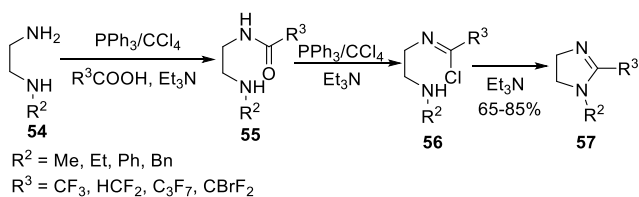
neutralizes the hydrogen iodide to regenerate the NaI catalyst. Finally, the H₂O produced from this reaction step is removed by dry MgSO₄.

Scheme 1.14. Proposed mechanism of the reaction shown in Scheme 1.13



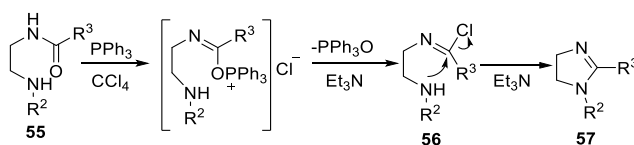
In 2012, a one-pot synthesis of 2-imidazolines (**57**) was reported by Jiang *et al.* from the condensation of a fluorinated carboxylic acid with *N*-substituted ethylenediamines (**54**) in the presence of CCl₄ and PPh₃ (**Scheme 1.15**).³⁶ The fluorinated amide (**55**) formed in the initial step, transformed to the intermediate imidoyl chloride (**56**) in the presence of TEA and PPh₃/CCl₄. In the last stage, the intramolecular imidoyl chloride **56** is cyclized to the desired 2-imidazoline (**57**). A number of halogenated carboxylic acids were investigated, including F₂BrCCOOH, F₇C₃COOH, F₃CCOOH, F₂CHCCOOH, and the imidazolines were isolated in good to excellent yields (65-85%).

Scheme 1.15. Intramolecular cyclization of imidoyl chlorides to imidazolines



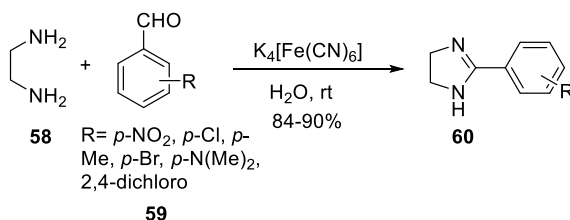
The most critical step of this reaction is the formation of imidoyl chloride (**56**) where the electron-withdrawing effect of the halogenated alkyl group (R^3) in the intermediate amide (**55**) facilitates the conversion of the amide tautomer imino alcohol to **56** (**Scheme 1.16**).

Scheme 1.16. Formation of imidoyl chloride **56**



Shaikh *et al.* reported a monosubstituted imidazoline synthesis was from the aromatic aldehyde (**59**) and ethylenediamine (**58**) in the presence of potassium ferricyanide ($K_4[Fe(CN)_6]$) in the water at room temperature (**Scheme 1.17**).³⁷ A few substituted aromatic aldehydes (4- NO_2 Ph, 4-MePh, 4-ClPh, 4-BrPh, 2,4- Cl_2 Ph, 4-(NMe_2)Ph,) were examined, and the products (**60**) were isolated in good to excellent yields (84-90%).

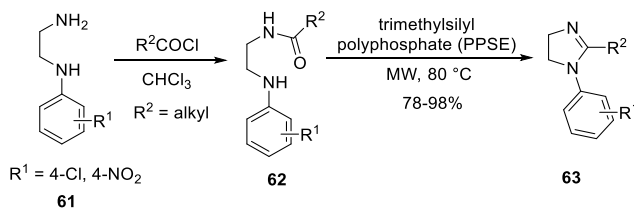
Scheme 1.17. Potassium ferricyanide mediated synthesis of imidazolines



A mild dehydrating agent, Trimethylsilyl polyphosphate (PPSE) mediated *N*-substituted 2-imidazoline (**63**) synthesis, was reported by Reverdito *et al.* (**Scheme 1.18**).³⁸ Initially, the aliphatic acyl chloride and *N*-monosubstituted ethylenediamine (**61**) reacted to form the intermediate amide (**62**). Then, the desired imidazoline was generated by cyclocondensation of **62**. The reaction was performed under both microwave irradiation (MW) and conventional heating, where the microwave irradiation produced **63** in high to excellent yields (78-98%) with short reaction times (22-29 min), whereas the conventional heating provided moderate yields (35-50%)

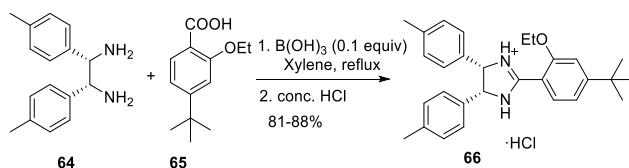
with longer reaction times (10-12 h). In this report, the author only reported 4-ClPh and 4-NO₂Ph groups as *N*-substitution in the ethylenediamine (**61**).

Scheme 1.18. Trimethylsilyl polyphosphate mediated synthesis of imidazolines



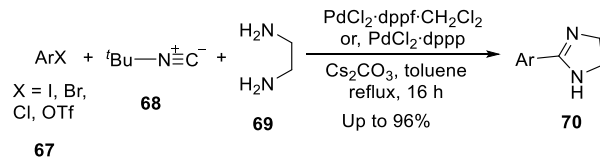
Shu *et al.* reported a direct condensation of *meso*-bis(4-chlorophenyl)ethane-1,2-diamine (**64**) with benzoic acid (**65**) in the presence of boric acid to synthesize *cis*-4,5-bis(4-chlorophenyl)imidazoline (**66**) (**Scheme 1.19**).³⁹ The synthesis of chemotherapeutic Nutlin analogs⁴⁰ has a key step that has imidazolines **66** as an intermediate, and this new process provided a simple way to generate those critical agents. The reaction was performed in both milligram (88% yield) and kilogram scale (15.1kg, 81% yield).

Scheme 1.19. Boric acid mediated synthesis of imidazoline in kilogram scale



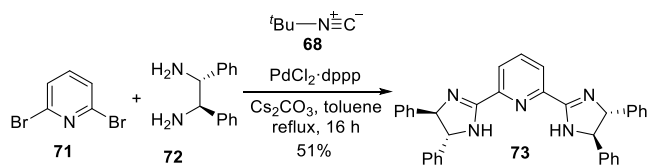
In 2013, a palladium mediated catalytic three-component reaction to synthesize 2-imidazolines (**70**) was reported by Geden *et al.* (**Scheme 1.20**).⁴¹ The three components that combined in the reaction were aryl halides (**67**), isocyanides (**68**), and diamines (**69**). Initially, phenyl iodide, ethylenediamine and *tert*-butyl isocyanide were treated with various palladium catalysts, and ligands and the authors reported two best combinations of catalyst and ligand for this reaction. These combinations were PdCl_2 with phosphine ligand dppp and $\text{dppf} \cdot \text{CH}_2\text{Cl}_2$.

Scheme 1.20. Palladium-catalyzed synthesis of imidazolines



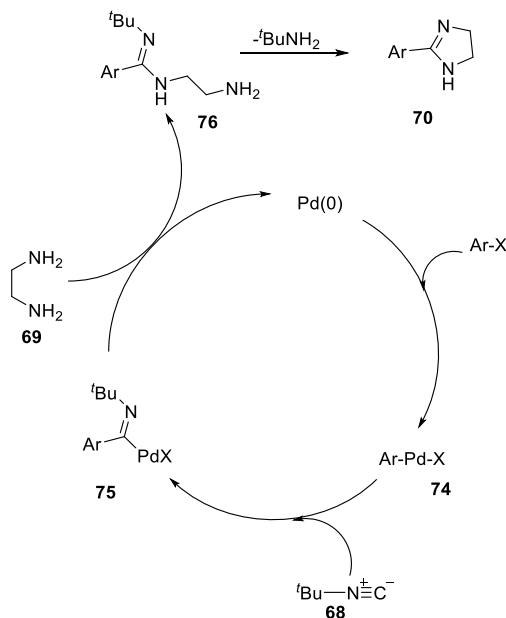
After the optimization of the reaction, various aryl and heteroaromatic halides were tested with the two catalyst/ligand combinations. Most of the halides produced the desired product (**70**) in better yields (up to 96%) with $\text{PdCl}_2 \cdot \text{dppp}$, whereas electron-rich aryl bromides provided superior yields of the 2-imidazolines (51-94%) with the combination of $\text{PdCl}_2 \cdot \text{dppf} \cdot \text{CH}_2\text{Cl}_2$. The steric effect was noticeably seen with 2-MePhI, where the isolated imidazoline yield was 32%. Besides, a five-component reaction was reported with the addition of 2,6-dibromopyridine (**71**) and (1*R*,2*R*)-(+)-1,2-diphenyl ethylenediamine (**72**) to synthesize a bis-imidazoline (chiral pybim ligand) (**73**) (**Scheme 1.21**).

Scheme 1.21. Synthesis of chiral pybim ligand



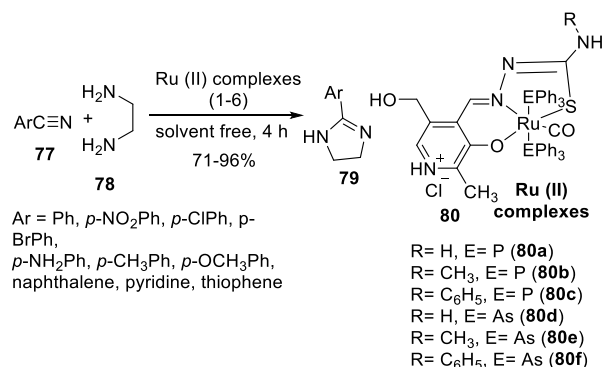
A catalytic cycle was depicted in the literature, where the reaction begins by the formation of aryl halide-palladium complex **74**, which then combines with **68** to form the intermediate **75**. Next, the intermediate **75** reacts with a diamine (**69**) to afford the amidine **76** and release palladium(0) for the next cycle. Lastly, the 2-imidazoline **70** is generated by an intermolecular cyclization of **76** with the liberation of an amine (**Scheme 1.22**).

Scheme 1.22. Mechanism of the catalytic cycle of 2-aryl-2-imidazoline (**70**) synthesis



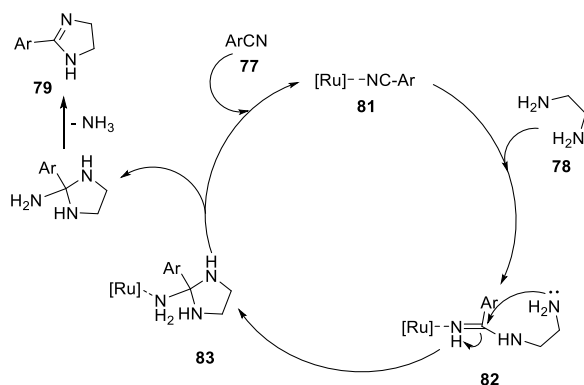
In 2015, Manikandan and co-workers described a ruthenium(II) carbonyl complexes (**80**) mediated synthesis of 2-aryl-2-imidazolines (**79**) from the reaction of ethylenediamine (**78**) and aryl nitriles (**77**) (**Scheme 1.23**).⁴² The ruthenium(II) carbonyl complexes were synthesized by reacting pyridoxal N(4)-substituted semicarbazone hydrochloride ligands with $[\text{RuHCl}(\text{CO})(\text{EPh}_3)_3]$ (E= phosphorous (P) or arsenic (As)). Among those ligands, six of those were employed with various aromatic nitriles, and **78**, and the product (**79**) were isolated in good to excellent yields (71-96%). The EWG (4-BrPh, 4-ClPh, 4-NO₂Ph) bearing nitriles exhibited superior reactivity towards the imidazoline synthesis (86-96%) then the EDG (4-NH₂Ph, 4-CH₃Ph, 4-OCH₃Ph) nitriles (73-84%). Moreover, heteroatom-containing aryl nitriles (*o*-cyanothiophene, *m*-cyanopyridine) gave 71-82% of the desired products. Among the ruthenium complexes (**80**), compound **80a** & **80d** showed a better catalytic reactivity.

Scheme 1.23. Ruthenium complex mediated synthesis of imidazolines



A catalytic reaction mechanism has been proposed in the article (**Scheme 1.24**). Initially, the nitrile (**77**) substitutes the PPh₃ group of the ruthenium (II) complex and then binds to the Ru(II) to generate the intermediate **81**. Then, by nucleophilic addition, **81** combines with the ethylenediamine (**78**) to form the intermediate **82**. After that, by intramolecular cycloaddition of **82**, imidazolidine **83** forms. Lastly, **83** produces the 2-imidazoline (**79**) and releases one equivalent of NH₃ and Ru(II), and restores the catalyst for the next catalytic cycle.

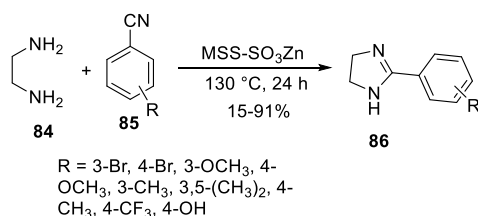
Scheme 1.24. Mechanism of ruthenium (II) catalyzed 2-imidazoline synthesis



In 2018, Chen *et al.* reported the Zn-modified magnetic Si-sphere H₂SO₄ catalyst (MSS-SO₃Zn) to synthesize 2-aryl-2-imidazoline via the condensation aromatic nitriles (**85**) and ethylenediamine (**84**) (**Scheme 1.25**).⁴³ After completion of the reaction, a magnetic force was

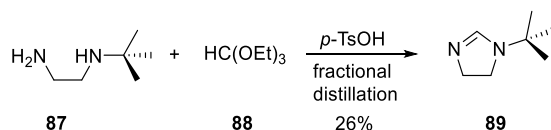
used to isolate the catalyst from the other reagents. Various aromatic nitriles (**85**) were screened with ethylenediamine (**84**), and the products (**86**) were obtained in yields up to 91%.

Scheme 1.25. Zn-modified magnetic Si-sphere H₂SO₄ mediated synthesis of imidazoles



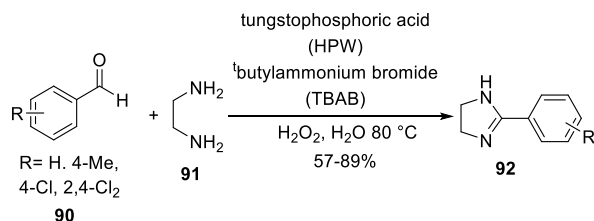
In 2019, Evans and co-workers described the first synthesis of 1-*tert*-butyl-2-imidazoline (**89**) from the reaction of N-*tert*-butyl-ethylenediamine (**87**) with triethyl orthoformate (**88**) using *p*-TSA in a fractional distillation process (**Scheme 1.26**).⁴⁴ The yield of the isolated imidazoline was low (26%).

Scheme 1.26. Synthesis of 1-*tert*-butyl-2-imidazoline



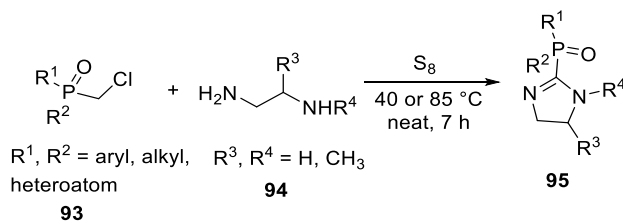
The same year, Liu *et al.* disclosed a green reaction to synthesize 2-imidazolines (**92**) from ethylenediamine (**91**) and aromatic aldehydes (**90**) by using H₂O₂ as an oxidant (**Scheme 1.27**).⁴⁵ The reaction was catalyzed by tungstophosphoric acid and TBAB in H₂O. Different catalysts were screened in the optimization step, including phosphomolybdic acid (HPMo), tungstosilicic acid (HSiW), tungstophosphoric acid (HPW) and, with or without TBAB and oxidant. It was noticed that one: one ratio of TBAB and HPW in the presence of H₂O₂ afforded superior reaction condition. A few aromatic aldehydes, including 4-MePh, 4-ClPh, 2,4-Cl₂Ph, and benzaldehyde, were screened with the diamine to generate 2-imidazoline in 57-89% yields.

Scheme 1.27. Peroxide mediated synthesis of imidazolines



Kozlov *et al.* demonstrated a sulfur-mediated synthesis of phosphoryl-substituted imidazolines (**95**) by reacting alkyl-substituted diamines (**94**) with phosphinic chlorides (**93**) (Scheme 1.28).⁴⁶ The reaction was achieved under solvent-free conditions in the presence of elemental sulfur (S_8). Initially, a concise optimization was done using different ratios of **93** and **94**, in the presence of S_8 , with or without solvent. The reaction was found to be most efficient under neat conditions. After optimizing the reaction, various substituents (aryl, alkyl, and heteroatom) at the P-group of phosphinic chlorides were treated with **94**, and both symmetrical and asymmetrical 2-imidazolines were afforded in 43-70% yield.

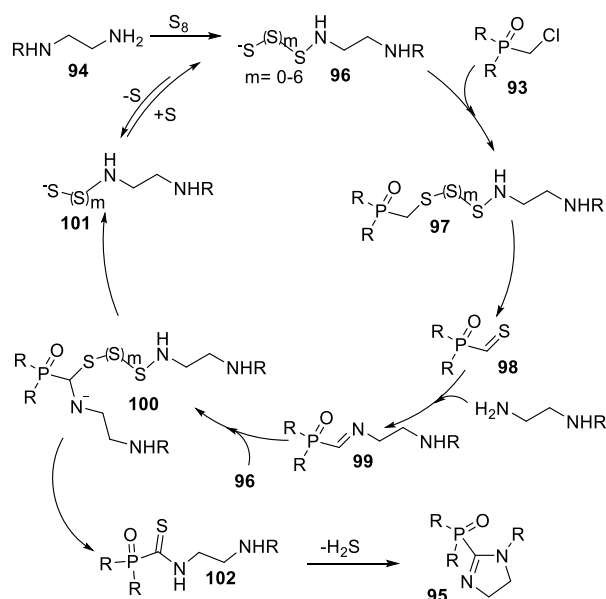
Scheme 1.28. Sulfur-mediated synthesis of phosphoryl-substituted imidazolines



A proposed mechanism of phosphoryl-substituted imidazolines (**95**) synthesis was illustrated in the article (Scheme 1.29). First, the nucleophilic ring-opening of sulfur (S_8) by ethylenediamine (**94**) forms the polysulfide intermediate **96**. This extremely nucleophilic intermediate **96** interacts with the phosphinic chlorides to form the intermediate **97**. After that, cleavage of the S-S bond of **97** and proton abstraction generates the thioaldehyde **98**, which further forms the imine intermediate **99**. Then **99** then reacts with **96** to provide the intermediate **100**. Next, the elimination

of **101** from **100** produces the thioamide **102**. Lastly, imidazoline product **95** forms by intramolecular cyclization of thioamide **102** and by removal of H₂S.

Scheme 1.29. Mechanism of phosphoryl-substituted imidazolines synthesis

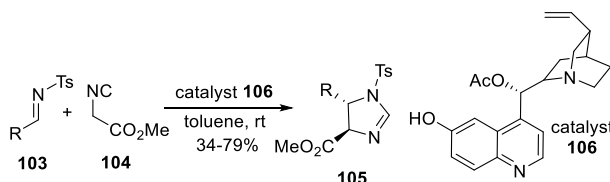


1.4.2 Method B: Synthesis of imidazolines from isocyanides

In 2010, Zhang *et al.* disclosed the first organocatalytic asymmetric Mannich-type cycloaddition reaction of *N*-sulfonylimines (**103**) with methyl isocyanoacetate (**104**) with to generate the 2-imidazolines (**105**) (**Scheme 1.30**).⁴⁷ Cinchona alkaloid-derived organocatalysts were used to form 2-imidazolines in a purely diastereoselective and enantioselective manner. Initially, the reaction was investigated by reacting *N*-*p*-toluenesulfonylimine with methyl isocyanoacetate in the presence of a base including *N,N*-diisopropylethylamine (Hünig's base), DABCO, TEA, DMAP, DBU, and (-)-sparteine. The alkaloidal base (-)-sparteine forms product **105** in 82% yield with an almost racemic mixture and later found that compound **106** is the best catalyst for this reaction. Under the optimized conditions, several aromatic and heteroaromatic (2-thienyl, 2-furyl) imines

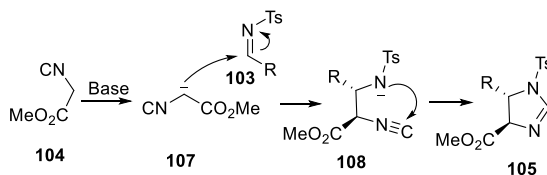
were screened with the methyl isocyanoacetate. Most of the imidazolines were isolated in more than 90% *dr*. Less sterically hindered 4-substituted imines offered better enantioselective products (up to 68% *ee*), whereas more sterically hindered imines (*o*-dimethoxy phenyl) afforded only 38% *ee*. Electronic properties directly affected the enantioselectivity of the reaction. Strong EWG 4-NO₂Ph generated 2-imidazolines in only 5% *ee*.

Scheme 1.30. Cinchona alkaloid-derived organocatalytic reaction to synthesize imidazolines



A reaction mechanism is depicted for the 2-imidazoline synthesis (**Scheme 1.31**). Initially, the chiral base (**106**) deprotonates the acidic α -carbon of the **104** and promotes the addition of the deprotonated isocyanoacetate (**107**) to the imine generates the intermediate **108**. Intramolecular cyclization of the intermediate **108** affords the 2-imidazoline (**105**) product.

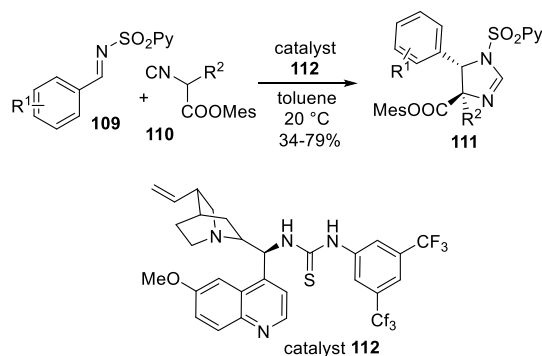
Scheme 1.31. Proposed mechanism of the reaction shown in Scheme 1.30



In 2012, Nakamura and co-workers disclosed another diastereoselective and enantioselective Mannich-type reaction by utilizing *N*-sulfonylimines (**109**) with isocyanoacetates (**110**) to synthesized 2-imidazolines (**111**) with quaternary stereocenters (**Scheme 1.32**).⁴⁸ The reactions provided the 2-imidazoline products (**111**) in up to >99:1 *dr* and 96% *ee*. Several chiral organocatalysts were screened in initial optimization, including chiral phosphoric acid derivative,

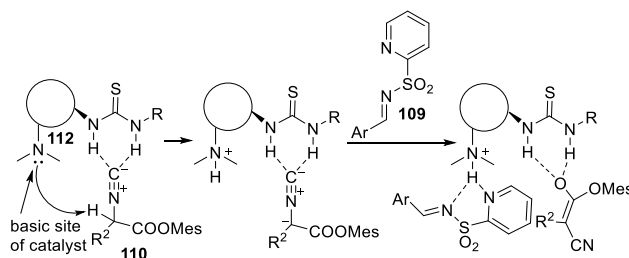
quinine, squaramide, cinchonidine, and thioureas, where thiourea catalyst **112** demonstrated as a superior catalyst in terms of yields and stereoselectivities.

Scheme 1.32. Organocatalytic diastereoselective and enantioselective Mannich-type reaction to synthesize imidazolines



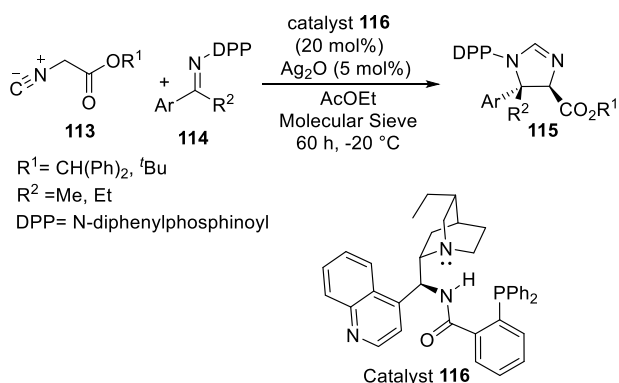
From the experimental results, a reaction mechanism was illustrated (**Scheme 1.33**). The catalyst **112** activates both imines and cyanides in a bifunctional catalyst pathway. The catalyst **112** coordinates to the isocyanide group in **110** by hydrogen bonding and increases the acidity of the α -proton. Then, the basic part of the catalyst **112** deprotonates the acidic α -proton. This newly generated carbanion then transforms into the more stable ester enolate. After that, the two N's of the *N*-(2-pyridinesulfonyl)-imine coordinate to the H of the protonated **112** and stabilize the intermediate. Lastly, α -carbanion of the isocyanide adds to the stabilized imine in the coordination sphere of **112** to generate the chiral product.

Scheme 1.33. Proposed mechanism of the reaction shown in Scheme 1.32



In 2014, Ortín and Dixon developed a high yield catalytic asymmetric Mannich-type addition/cyclization reaction to synthesize a fully β -substituted carbon atom containing 2-imidazolines (**115**) (**Scheme 1.34**).⁴⁹ The reaction utilized cinchona derived precatalyst (**116**) and a silver salt with isocyanoacetate (**113**), and *N*-diphenylphosphinoyl ketimines (**114**). The catalyst **116** contains both phosphine (RPPH₂ as Lewis base) groups and amino (R₂N-H as H-bond donor, NR₃ as Brønsted base) and situated in conjunction with chiral pocket. The *trans*-2-imidazoline product with high diastereo- and enantioselectivity. Under the optimized conditions, ketamines bearing both the aryl and alkyl (Me, Et) groups were screened with isocyanoacetate, and the *trans*-2-imidazolines were obtained in good to excellent yields (70-97%) with up to 97% *ee* and up to 99:1 *dr*.

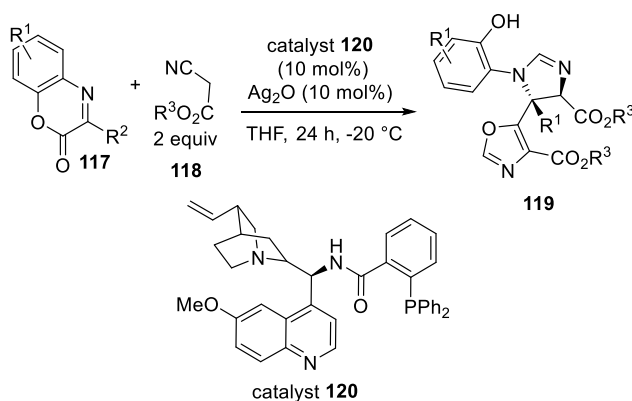
Scheme 1.34. Cinchona derived precatalyst mediated fully β -substituted imidazolines synthesis



The same year, Shao *et al.* described a new linked oxazole-imidazoline synthesis by employing the bifunctional α -imino ester (**117**) (**Scheme 1.35**).⁵⁰ The reaction was proceeded by stereoselective cyclization of the isocyanoacetate (**118**) with α -imino ester (**117**) in the presence of chiral organocatalyst and Ag₂O in an open-air. From the initial screening of metal salts, Ag₂CO₃ and Ag₂O afforded 99% of the racemic product, whereas chloride salts of gold, copper, and zinc, and strong Lewis acids such as Sc(OTf)₃ and BF₃·OEt₂ offered less than 2% product. In the case

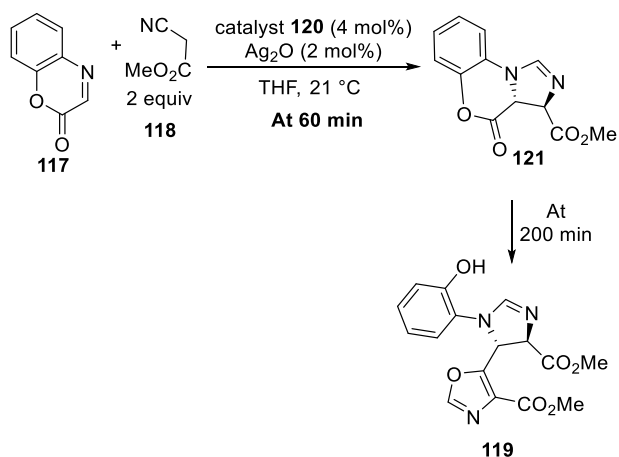
of enantioselectivity investigation, cinchona-derived amino phosphine catalysts similar to the Dixon group⁶¹ report afforded excellent enantioselectivity (99% ee) of the product using catalyst **120**. Several alkyl- and aryl- ester-containing isocyanoacetates were treated with substituted cyclic imino esters to explore the reaction's scope, and the desired substrates (**119**) were obtained in good to excellent yields (69-99%) and up to 99% ee.

Scheme 1.35. Linked oxazole-imidazoline synthesis from bifunctional α -imino ester



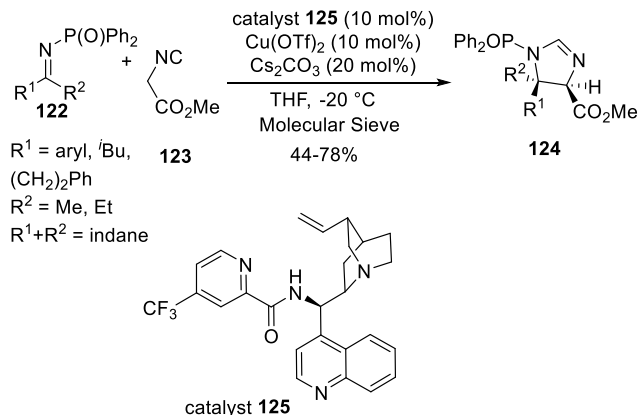
To investigate the reaction mechanism, a kinetic study test was performed (**Scheme 1.36**). The NMR spectroscopic data showed a stepwise reaction pathway between **117** and **118**. In 60 minutes reaction time, the imidazoline ring containing product **121** was noticed without any formation of **119**. Prolongation of the reaction revealed a conversion of **121** into **119**. The ratio of **119** and **121** found to be 9:1 in 200 minutes time point.

Scheme 1.36. NMR studies reaction of Scheme 1.35



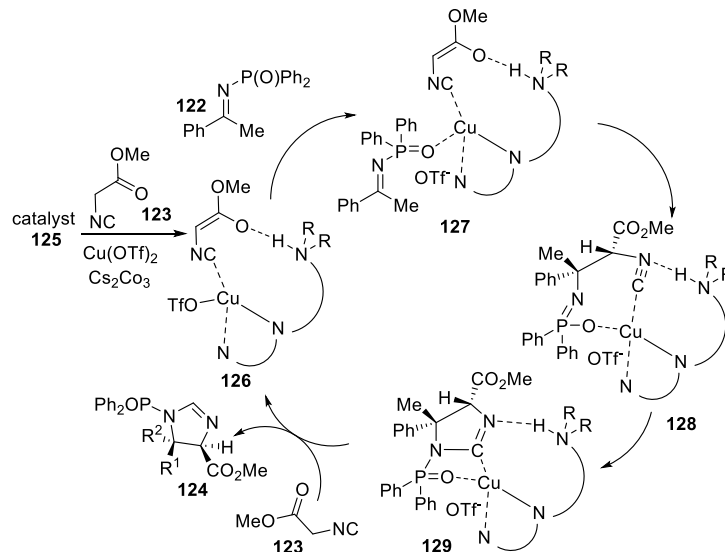
Nakamura *et al.* also described another asymmetric Mannich-type reaction to synthesize quaternary carbon center bearing *syn*-selective and enantioselective imidazoline (**124**) from the reaction of ketimines (**122**) with α -isocyanoacetates (**123**) (**Scheme 1.37**).⁵¹ Initially, the reaction of **122** and **123** was investigated in picolinamide ligands and metals salts. Solely *anti*-selective imidazoline product was isolated when the reaction was run without the metal salts, whereas metal salts such as Cu(OTf)₂, Zn(OTf)₂, Et₃Zn, Cu(OAc)₂, Ni(OTf)₂ with the combination of catalyst **125**, afforded superior yields and stereoselectivity of *syn*-products. Under the best conditions, different aromatic and aliphatic substituted ketimines were treated with **123**. The compounds containing aromatic groups (both EWG and EDG containing aryl) as R¹ of **122**, provided 44-68% of *syn*-imidazolines with more than 90% *ee*. On the other side, the dialkyl ketones derived **122** afforded 54-78% yields of *syn*-imidazolines with high enantioselectivity (93-95% *ee*). In addition, a tetrasubstituted imidazoline was isolated in 55% yield and moderate enantioselectivity by reacting methyl 2-isocyanopropanoate with **122** (R¹=Ph, R²=Me).

Scheme 1.37. Synthesis of quaternary carbon center *syn*-selective imidazolines



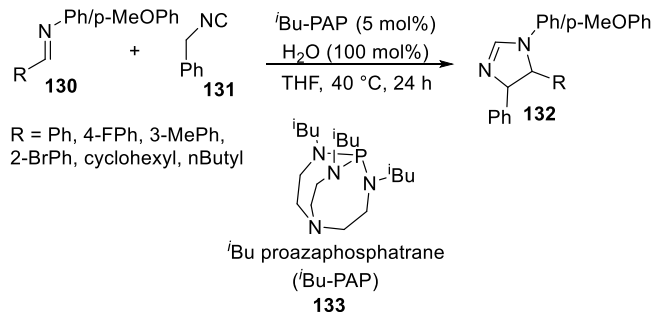
A catalytic reaction mechanism was reported in the article (**Scheme 1.38**). The α -isocyanoacetates (**123**), Cs_2CO_3 , Cu(OTf)_2 coordinates with the catalyst **125** to generate the complex **126**, which has the ketene hemiacetal configuration of **123**. Then the ketimine (**122**) coordinates to **126** and generates the new complex **127**. Then, the C-C bond formation reaction occurs between **122** and **123** within the coordination sphere of copper(II) and forms the Mannich-type complex **128**. After that, the complex **129** forms by intramolecular imidazoline formation from complex **128**. Finally, ligand exchange between α -isocyanoacetates (**123**) and the complex **129** forms the product **124**.

Scheme 1.38. Mechanism of *syn*-imidazoline synthesis



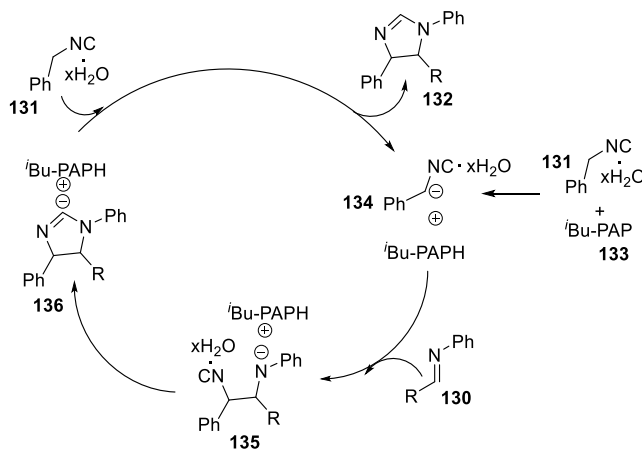
Honey and co-workers demonstrated the activation of isocyanides (**131**) with H_2O and the reaction between imines (**130**) with the activated isocyanides in the presence of superbase proazaphosphatrane (PAP) (**133**) to generate 2-imidazolines (**132**) (**Scheme 1.39**).⁵² Initial optimization was done using diphenyl imine and benzyl isocyanide with isobutyl proazaphosphatrane (*i*Bu-PAP) in different amounts of water. It was revealed that *i*Bu-PAP (5 mol%) in THF with 100 mol% of H_2O generated 80% of the imidazoline product *trans:cis* = 98:2. On the contrary, the reaction stalled under anhydrous conditions. Under these optimized conditions, the 2-imidazolines were afforded moderate to excellent yields (43-86%), with the *trans* isomer as the major compound. This report offered the first example of the water-tolerant *i*Bu-PAP system.

Scheme 1.39. Superbase proazaphosphatrane mediated imidazoline synthesis



From the mechanistic experiments and observation, a mechanism was illustrated in the report (**Scheme 1.40**). Initially, water activates the isocyanide, and after that, *t*Bu-PAP deprotonates the isocyanide and forms the stabilized intermediate **134**. Next, **134** reacts with **135** and generates the intermediate **135**. Finally, cyclization and followed by removal of *t*Bu-PAPH⁺ from the complex **136** affords the imidazoline product **132**.

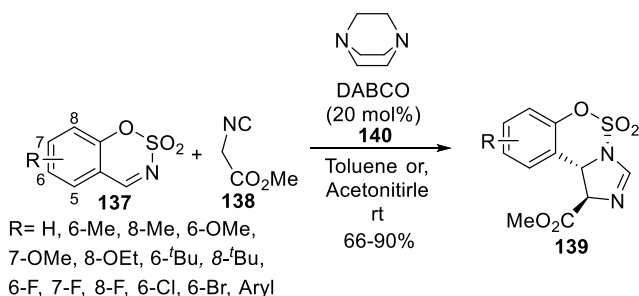
Scheme 1.40. Mechanism of water and PAP mediated imidazoline synthesis



Guo and co-workers demonstrated a new sulfamate-fused 2-imidazolines (**139**) synthesis from the reaction of isocyanoacetate (**138**) with sulfamate-derived cyclic imines (**137**) via [3+2] annulation reaction in the presence of a Lewis base DABCO (**140**) (**Scheme 1.41**).⁵³ A few Lewis bases (DABCO, DBU, TEA, and DMAP) were screened for the annulation reaction of

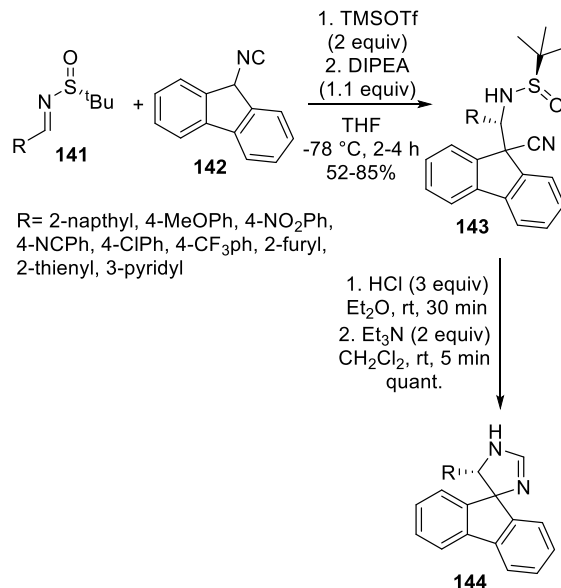
isocyanoacetate and imines. Among those bases, 20 mol% of DABCO showed the most catalytic activity in the solvent toluene with 90% of the product (**139**) formation in excellent diastereoselectivity (32:1). Regardless of the imines' electronic or steric characteristics, the cyclic imidazolines were obtained in 66-90% yields with diastereoselectivities up to 48:1.

Scheme 1.41. Synthesis of sulfamate-fused 2-imidazolines



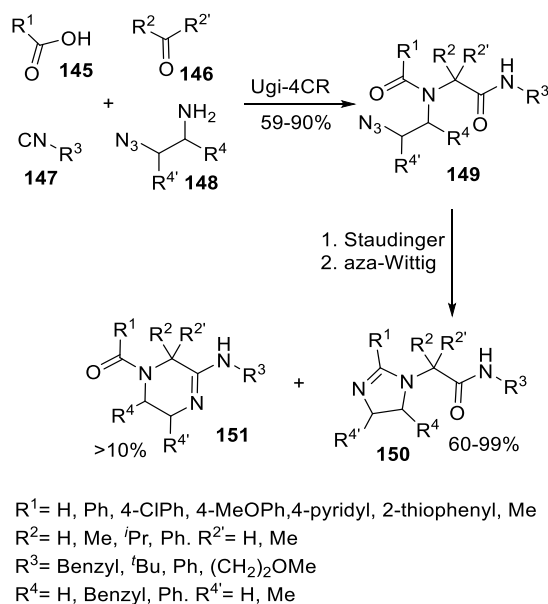
Orru and co-workers reported an asymmetric synthesis of β -sulfinylamino isocyanides (**143**), which later cyclized to 2-imidazolines (**144**) (**Scheme 1.42**).⁵⁴ The compounds **143** were synthesized from the reaction of *N-tert*-butanesulfinimines (**141**) with 9-isocyanofluorene (**142**) in the presence of DIPEA and a Lewis acid. A couple of Lewis acids were screened, including TMSOTf, Ti(O^{*i*}Pr)₄, AlCl₃, Sc(OTf)₃, BF₃·OEt₂ with DIPEA. The combination of trimethylsilyl trifluoromethanesulfonate (TMSOTF) with DIPEA in the solvent THF, superior optically pure β -sulfinylamino isocyanide was isolated. In contrast, the same combination in the solvent DCM did not afford any product. These opposite results maybe because of the stabilization of the cationic intermediate of the sulfinimine by the solvent THF. Several isocyanides (**143**) were screened, and the β -sulfinylamino isocyanides were isolated in excellent *dr* (>99:1) and *ee* (>99%). In the next step, the sulfinyl group was removed from the optically pure **143** with an excess HCl in diethyl ether and then promptly cyclized to 2-imidazolines (**144**) with the base TEA in DCM. The imidazolines were obtained in a quantitative amount with >99% *ee*.

Scheme 1.42. Synthesis of imidazolines from β -sulfinylamino isocyanides



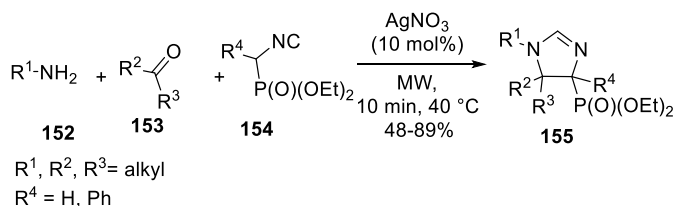
In 2015, Welsch *et al.* illustrated a Ugi–Staudinger–aza-Wittig-sequence mediated synthesis of 2-(acetamide-2-yl)-imidazolines (**150**) (**Scheme 1.43**).⁵⁵ The reaction combined an azide containing substituted amine, aldehyde/ketone, a carboxylic acid, and isocyanide, and by a Ugi 4-components reaction, the bis-amide (**149**) was formed. In the next step, the cyclized 2-imidazoline products (**150**) were obtained by implementing a Staudinger and aza-Wittig reaction. The second step was performed in MW irradiation for 20 minutes at 150 °C. Several substitutes in all four components of the Ugi reaction were tested to explore the scope of the reaction, and the imidazolines (**150**) were isolated in 60-99% yields. In the case of formaldehyde or acetone (**149**), all *in-situ* formed imidazoline (**150**) products were rapidly converted amidines (**151**) (50-80% yields).

Scheme 1.43. Ugi–Staudinger–aza-Wittig-sequence mediated synthesis of 2-(acetamide-2-yl)-imidazolines



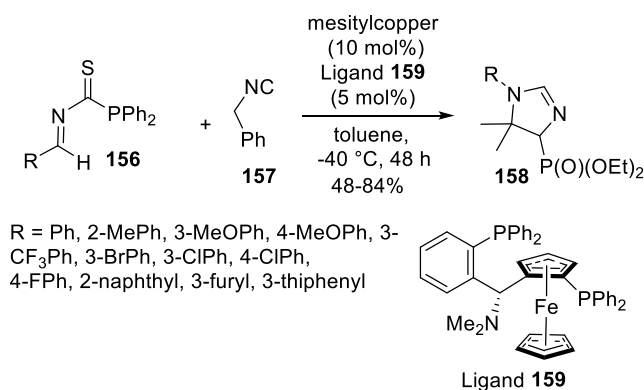
Abás *et al.* disclosed an MW-assisted silver-catalyzed multicomponent reaction to synthesize (2-imidazolin-4-yl)phosphonates (**155**) (**Scheme 1.44**).⁵⁶ The reaction employed α -isocyanophosphonates (**154**), dialkyl ketones (**153**), and aliphatic amines (**152**) in the presence of AgNO_3 , under MW at 40 °C for 10 minutes. The imidazolines were isolated in 48-89% yields where sterically hindered alkyl (1-methylbenzyl or, 1-adamantylethyl) amines (**152**) did not afford any product formation at high 40 °C or with MW irradiation, and those reactions were executed at RT to generate the imidazolines in good yields (60-71%).

Scheme 1.44. Silver-catalyzed multicomponent reaction to synthesize (2-imidazolin-4-yl)phosphonates



Tamura and co-workers described a Cu(I)-mediated enantioselective 2-imidazolines (**158**) synthesis from the reaction of *N*-(diphenylthiophosphinoyl)imines (**156**) and isocyanide (**157**) (**Scheme 1.45**).⁵⁷ Initial screening was performed by using few soft Lewis acids, including AgBF₄, CuPF₆, AgPF₆, mesitylcopper, and chiral ligands with the phenyl substituted **156** and isocyanide. Among these, the combination of (*R,R*_p)-Ph-Taniaphos (**159**) and MesCu provided 84% yield with good *ee* (*trans*:78%; *cis*:77%) and *dr* (*trans/cis*: 75/25).

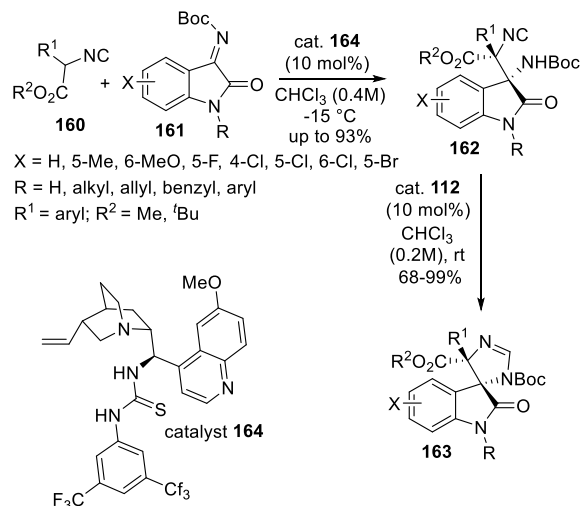
Scheme 1.45. Cu(I)-mediated enantioselective 2-imidazolines



Zhao *et al.* reported another asymmetric Mannich reaction, utilizing Cinchona alkaloid thiourea from the reaction of isocyanoacetates (**160**) and isatin-derived ketimines (**161**) and consequent organocatalyzed cyclization to synthesize spirooxindole imidazolines (**163**) (**Scheme 1.46**).⁵⁸ Initially, quinine- or quinidine-derived thioureas were screened with *N*-Boc isatinimine (**161**) (X = H, R = Me) with isocyanoacetate (**160**) (R¹ = H, R² = Me), where catalyst **164** was found to be the superior catalyst to obtain compound **162**. After the optimized conditions were identified, various substituted Mannich products (**162**) were isolated with up to 93% yields in 69-97% *ee*'s and >20:1 *dr*'s. The reaction significantly affected by the steric effects, whereas no substantial electronic effects were found. With 2-substituted (2-BrPh) isocyanoacetate, product formation was stalled entirely. In a further step, screening of organocatalysts was performed again

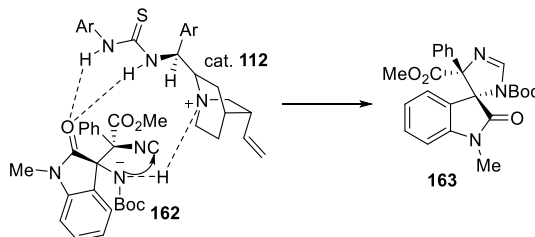
for the cyclization step to synthesize imidazolines from Mannich products. Here, the catalyst **112** was identified to be the best catalyst for the enantioselective imidazoline formation. The compounds **162** were treated with catalyst **112**, and the spirooxindole imidazolines (**163**) were isolated in 68-99% yields with *ee* 90-97% and *dr* of >20:1.

Scheme 1.46. Cinchona alkaloid thiourea mediated synthesis of spirooxindole imidazolines



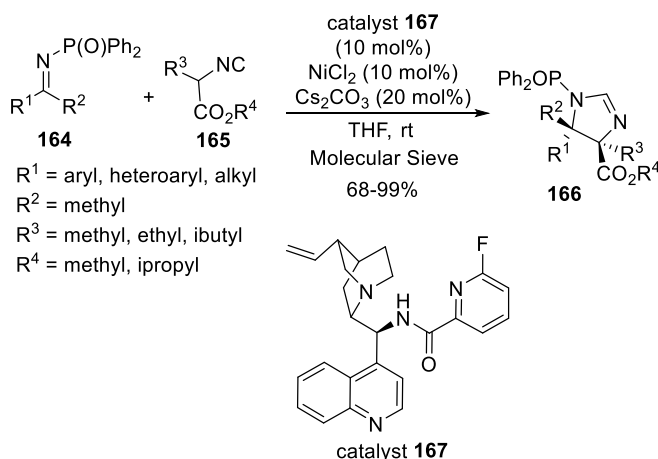
The mechanism of formation of the spirocyclic imidazoline from the Mannich adduct (**162**) was illustrated as a *5-endo-dig* cyclized process (**Scheme 1.47**). This process was commenced by the deprotonation of the Boc-protected amino group by the catalyst **112**. After that, an intramolecular cyclization reaction between the deprotonated amino group and the isocyano group forms the spirooxindole imidazolines (**163**).

Scheme 1.47. Transition-state model of the Scheme 1.46 cyclization step



In 2016, Nakamura *et al.* described another cinchona alkaloid-based amide catalyst mediated asymmetric direct Mannich-type reaction to synthesize vicinal tetra-substituted 2-imidazolines (**Scheme 1.48**).⁵⁹ The reaction utilized ketimines (**164**) and α -isocyanoacetates (**165**) in the presence of catalyst **167** with CsCO₃ and NiCl₂. In the optimization step, 10 mol% of NiCl₂ with 10 mol% of catalyst **167** afforded the best yield of the imidazoline product **166** (99%) with good enantioselectivity (*anti*=5:95) and diastereoselectivity (*anti/syn*=98:2). Several EDG and EWG containing ketimines (**164**) were treated with a series of α -isocyanoacetates (**165**), and the imidazolines were isolated in good to moderate yields (68-99%) with excellent *er* (*anti*=94-6-96:4) and *dr* (*anti/syn*=95:5-97:3).

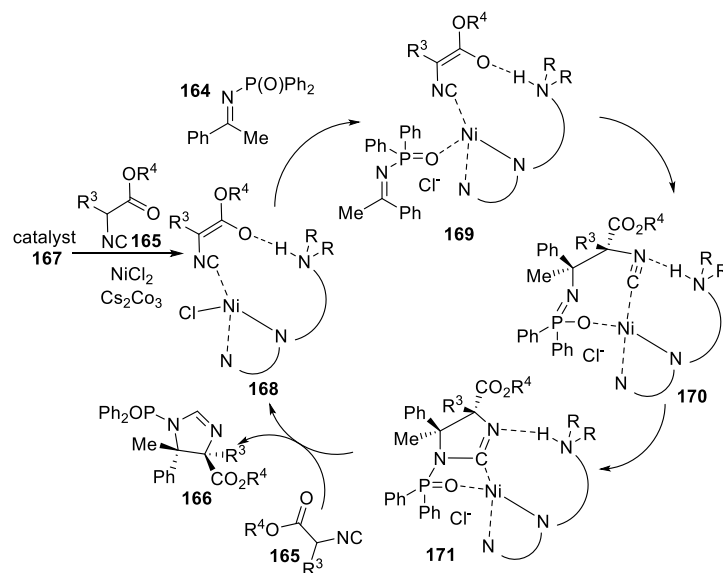
Scheme 1.48. Cinchona alkaloid-based amide catalyst mediated synthesis of vicinal tetra-substituted 2-imidazolines



The author depicted a catalytic cycle for the reaction, as shown in the proceeding scheme (**Scheme 1.49**). Initially, complex **168** forms and then converts to complex **169** by coordinating with ketimine (**164**). After that, the complex **169** generates the adduct **170** by the Mannich-reaction of the α -isocyanoacetate and the ketimine. Next, An intramolecular cyclization provides the

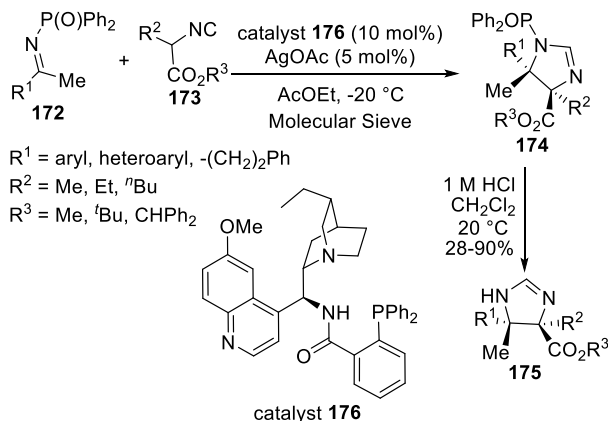
complex **171**. Lastly, an exchange reaction between **171** and **165** provides the desired imidazoline **166** and another complex **168**.

Scheme 1.49. Proposed mechanism of the reaction shown in Scheme 1.48



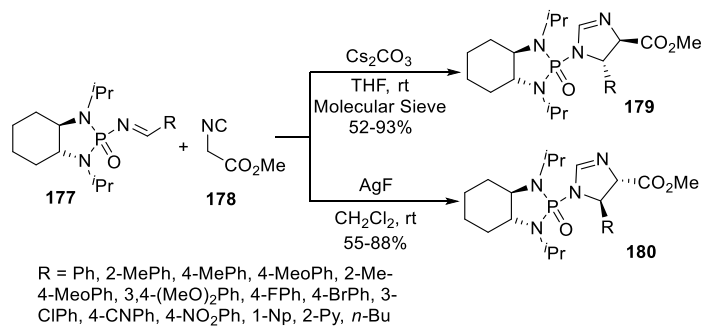
The same year, Dixon and co-workers described another enantioselective Mannich type reaction of α -substituted isocyanoacetates (**173**) with diphenylphosphinoyl protected ketimines (**172**) to synthesize the vicinal tetra-substituted 2-imidazolines (**Scheme 1.50**).⁶⁰ Similar to their previous report,⁴⁹ the reaction utilized cinchona-derived amide catalyst (**176**) and Ag(I) salt to generate the protected imidazoline (**174**) and then deprotected the by using 1 M HCl in DCM to obtain the deprotected imidazoline (**175**). The reaction was well tolerated with both EDG and EWG containing starting material, and the deprotected imidazolines (**175**) were obtained in good to excellent yields (63-89%) and enantiomeric excesses (87-95%). Dialkyl ketone ($R^1 = (CH_2)_2Ph$) containing ketimine reacted moderately, and the imidazoline was obtained in 48% yield and 87% *ee*.

Scheme 1.50. Cinchona-derived amide catalyst and Ag(I) salt mediated synthesis of vicinal tetra-substituted 2-imidazolines



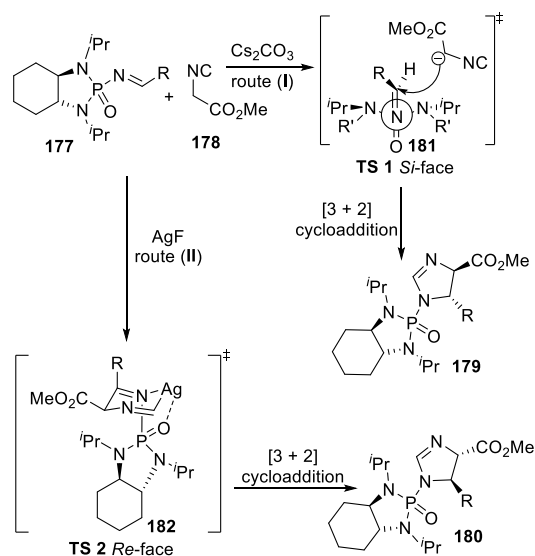
In 2017, Qiao *et al.* developed a new method to access 2-imidazolines in a diastereoselective manner, via an asymmetric [3 + 2]- cycloaddition reaction of methyl isocyanoacetate (**178**) with chiral *N*-phosponyl imines (**177**) (Scheme 1.51).⁶¹ The reaction was promoted by Cs_2CO_3 to afford one form of a diastereoselective product (**179**). In contrast, the opposite diastereoselective outcome (**180**) was obtained by using AgF instead of Cs_2CO_3 as a catalyst. From the initial optimization of bases, Cs_2CO_3 and Ag_2O , offered the imidazoline products (**179** and **180**) in high yield (99%), albeit Cs_2CO_3 afforded better stereoselectivity (**179**:**180** = 96:4). AgF also offered 99% product yield with an inverse stereoselectivity (**179**:**180** = 12:88).

Scheme 1.51. Diastereoselective synthesis of imidazolines



Based on the experimental data and observations, the authors illustrated two different mechanistic pathways to synthesize products **179** and **180** (Scheme 52). Under the basic conditions, the deprotonated isocyanoacetate prefers the *Si*-face of the auxiliary group, which is shown in the TS-1 (**181**). This transition state 1, gives a diastereo-pure intermediate followed by the intramolecular nucleophilic addition to generate the imidazoline **179**. On the other hand, the Ag(I) catalyzed reaction forms a six-member ring by the interaction of the C-atom of the isocyanide with the N-atom of the imine, as well as coordination of the Ag⁺ with the oxygen on the phosphonyl group. These interactions favor the *Re*-face, as shown in the TS-2 (**182**), and later affords **180** in a [3 + 2]- cycloaddition manner.

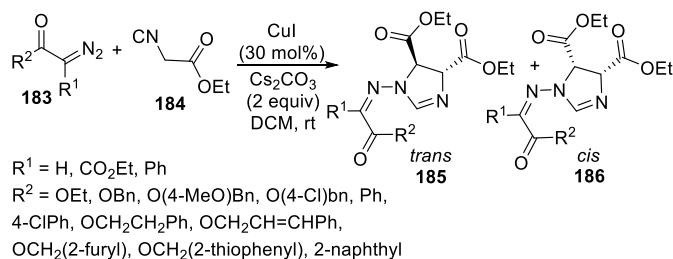
Scheme 1.52. Proposed mechanism of [3 + 2]- cycloaddition reaction of Scheme 1.51



Bu *et al.* reported a Cu-catalyzed cascade reaction of isocyanide (**184**) with α -diazocarbonyls (**183**) to synthesize 2-imidazolines (Scheme 1.53).⁶² Initial optimization showed that 30 mol% of CuI with Cs_2CO_3 in DCM afforded the *trans*-imidazoline (**185**) in 85% yield. The diazoacetates (**183**) possessing the ethyl-ester group ($\text{R}^2 = \text{OEt}$) offered the *trans*-imidazoline product (**185**) in

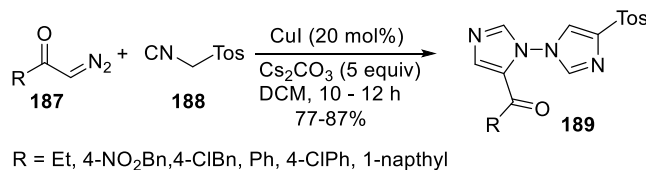
high yields (65-85%) solely. On the contrary, hetero-aromatic or benzyl group-containing diazoacetates formed a mixture of *trans*- (**185**) and *cis*-imidazolines (**186**) (*trans*: *cis* = 51:49 to 61:39) in 72-92% yields.

Scheme 1.53. Cu-catalyzed synthesis of imidazolines



In addition, TosMIC (**188**) was treated with a few α -diazocarbonyls (**187**) (**Scheme 1.54**), but surprisingly only 1,1'-biimidazole (**189**) products were obtained in high yields (77-88%).

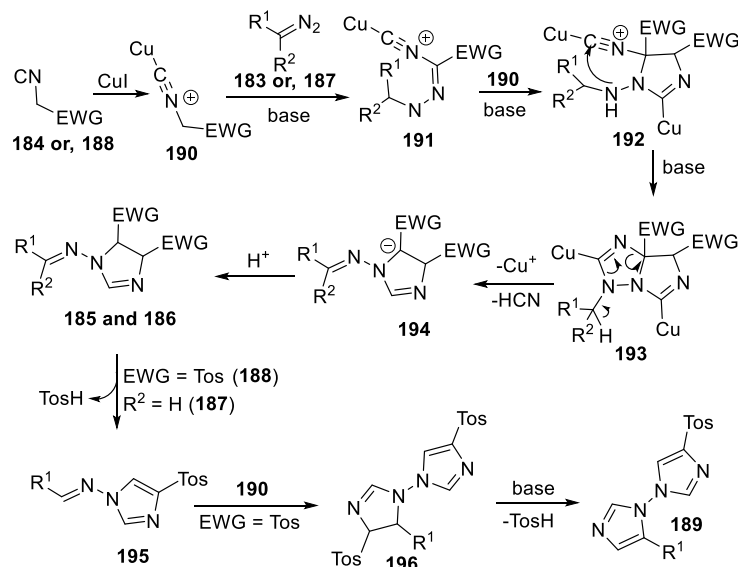
Scheme 1.54. CuI-catalyzed cascade cyclization to synthesize 1,1'-biimidazole



A mechanism for the formation of 1,1'-biimidazole and imidazoline was illustrated in the literature (Scheme 1.55). Initially, the isocyanide interacts with CuI to form the Cu^+ -isocyanide complex **190**. After that, the complex **190** undergoes an intermolecular nucleophilic addition to the α -diazocarbonyls (**183/187**) to give **191**. Then, a [3 + 2] cycloaddition reaction of intermediate **191** with complex **190** generates the intermediate **192**. This intermediate **192** will further cyclize in an intramolecular fashion to the bicyclic intermediate **193**. Finally, a sequential ring-opening, as well as elimination of HCN and protonation, affords the desired imidazoline (**185/186**). When the isocyanide (**188**) possesses an EWG (tosyl), the imidazoline (**185/186**) releases the *p*-toluenesulfinic acid and generates a new intermediate **195**. Further [3 + 2]-cycloaddition of the

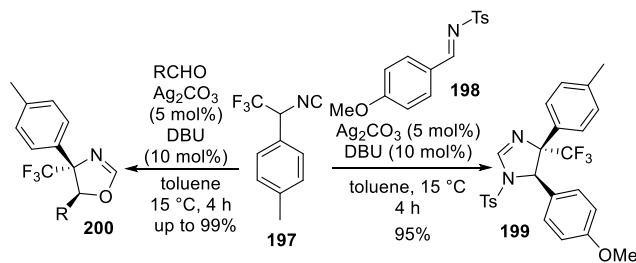
intermediate **195** with the complex **190**, forms **196**. Lastly, the elimination of another TosH offers the 1,1'-biimidazole **189**.

Scheme 1.55. Proposed mechanism of the reaction shown in Scheme 1.53 and 1.54



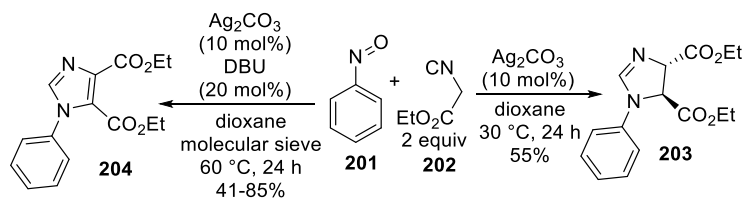
Xu and co-workers reported an example of an Ag-catalyzed [3+2]- cycloaddition reaction of an imine with α -trifluoromethylated methyl isocyanide (**197**) to synthesize a 2-imidazoline (**Scheme 1.56**).⁶³ The report concentrated on the synthesis of oxazolines (**200**) from the reaction of isocyanides and aldehydes in the presence of DBU (10 mol%) and Ag₂CO₃ (5 mol%). To extend the scope of that reaction, 2-imidazoline analog (**199**) was synthesized under the standard conditions. For that, 1-methyl-4-(2,2,2-trifluoro-1-isocyanoethyl)benzene (**197**) was treated with an imine (**198**), and the desired imidazoline (**199**) was isolated in 95% yield with a *dr* of 4.2:1.

Scheme 1.56. Ag-catalyzed [3+2]- cycloaddition reaction to synthesize imidazolines



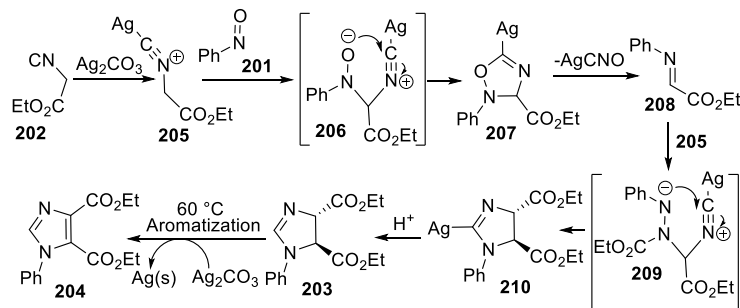
In 2018, Fang and co-workers reported an example of an Ag-mediated [3+1+1] annulation of nitrosoarene (**201**) with isocyanoacetate (**202**) to synthesize 2-imidazoline (**Scheme 1.57**).⁶⁴ Nitrosobenzene (**201**) and isocyanoacetate (**202**) was reacted in the presence of Ag₂CO₃ (10 mol%) at 30 °C to obtain the *trans*-imidazoline (**203**) in 55% yield. The article was primarily focused on the synthesis of imidazole (**204**) at high temperature (60 °C), under similar reaction conditions. The imidazoline was the intermediate of the imidazole synthesis, which undergoes aromatization at high temperatures.

Scheme 1.57. Ag-mediated [3+1+1] annulation reaction to synthesize imidazolines



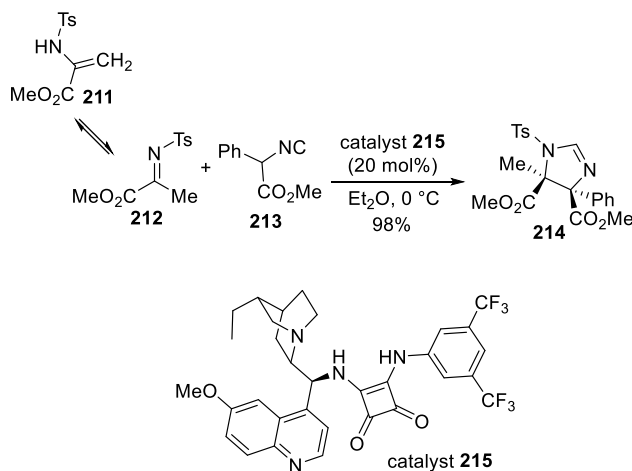
A mechanism was illustrated for the imidazole and imidazoline synthesis, as shown below (**Scheme 1.58**). Initially, the Ag-complex **205** is generated from the interaction of Ag₂CO₃ and isocyanide **202**. Then a cycloaddition reaction of the complex **205** with nitrosobenzene (**201**) generates the intermediate **207** via **206**. In the next step, AgCNO is eliminated from the intermediate **207** to generate the α -imino ester (**208**). The α -imino ester (**208**) then reacts with another Ag-complex **205** to afford the intermediate **210** via the complex **209**. Lastly, the imidazoline **203** is generated by the protonation of the intermediate **210**. Furthermore, at high temperature (60 °C) aromatization of the imidazoline (**203**) occurs, and imidazole (**204**) is formed.

Scheme 1.58. Mechanism of the silver-promoted [3+1+1] annulation



Wang *et al.* disclosed a new imidazoline (**214**) synthesis method using a new cinchona-derived bifunctional squaramide catalyst (**215**) from the reaction of the *N*-protected enamine (**211**) with isocyanoacetate (**213**) (**Scheme 1.59**).⁶⁵ *In situ* transformation of the enamine into an imine (**212**) lead to the reaction with the isocyanoacetate (**213**) in a 20 mol% of catalyst **215** loadings, and the imidazoline (**214**) was obtained in 98% yield with high stereoselectivities (*cis: trans* = 88:12; *ee* = 90%).

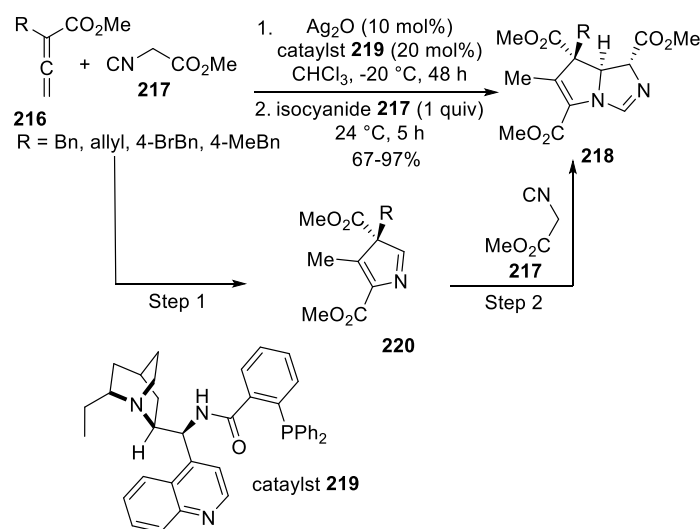
Scheme 1.59. Cinchona-derived bifunctional squaramide catalyst mediated imidazoline synthesis



The same year, Kok *et al.* reported an Ag₂O, and phosphine-based catalyst (**219**) mediated enantioselective [3+2]- cycloaddition reaction of isocyanoacetate (**217**) with allenoates (**216**) to generate 2-imidazoline (**218**) (**Scheme 1.60**).⁶⁶ The catalyst **219** was first introduced by the Dixon

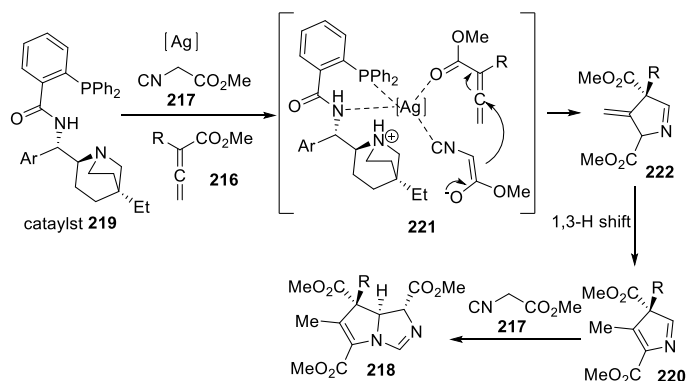
group to the synthesis of oxazolines.⁶⁷ First, the reaction was screened by reacting isocyanoacetate (**217**) with a substituted (R = benzyl) allenolate (**216**) in the presence of Ag₂O and catalyst **219** and pyrrole (**220**) was obtained from the reaction. However, with an increasing amount of isocyanoacetate, the formation of the imidazoline (**218**) was observed as the major product, and with two equivalent of isocyanoacetate, only imidazoline product was isolated in good to excellent yields (67-97%) with high enantioselectivities (*ee* = 81-91%).

Scheme 1.60. Ag₂O & phosphine-based catalyst mediated enantioselective imidazoline synthesis



A mechanism was illustrated in the report based on the experimental results (**Scheme 1.61**). Initially, the ligand **219** forms a chiral pocket by interacting with the Ag and then coordinates with the allenolate (**216**) and the enolate form of **217** to generate the complex **221**. Next, through a [3+2]-cyclization process, complex **221** converts into the intermediate **222**, and then by a 1,3-H shift generates the pyrrole **220**. Lastly, another equivalent of isocyanoacetate (**217**) reacts with the pyrrole in a second [3+2]- cyclization process and forms the bicyclic imidazoline **218**.

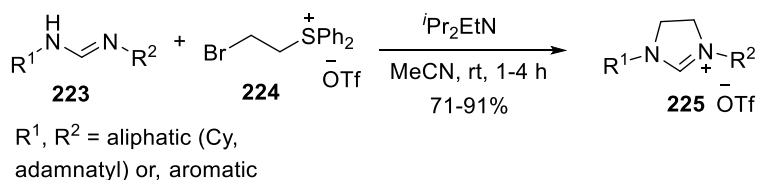
Scheme 1.61. Proposed mechanism of the reaction shown in Scheme 1.60



1.4.3 Method C: Synthesis of imidazolines from amidines

In 2011, Aggarwal and co-workers reported a new method to synthesize imidazolinium salts (**225**) from a base mediated reaction of sulfonium salt (**224**) and amidines (**223**) (**Scheme 1.62**).⁶⁸ Initial base and solvent screening showed the Hünig's base (*i*Pr₂EtN) in acetonitrile is the best condition to obtain imidazolinium salt (yield 91%). Under the suitable conditions, various symmetric and asymmetric amidines were explored with the sulfonium salt (**224**), and with the symmetrical aromatic-substituted (R¹, R² = 2-MePh) amidine, imidazoline was isolated in 95% yield. In contrast, the EWG (R¹, R² = 4-ClPh) containing or the alkyl-substituted (R¹, R² = adamantyl) amidines provided only 71% product.

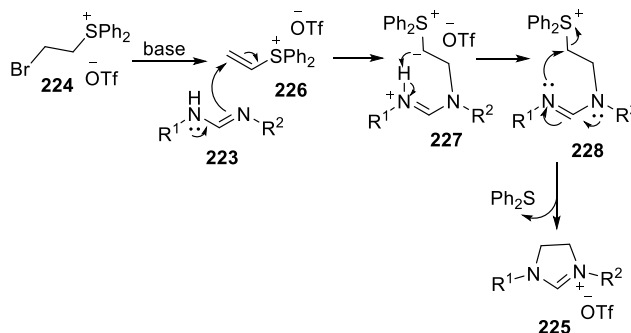
Scheme 1.62. Synthesis of imidazolines from amidines and sulfonium salts



In terms of a mechanism, as shown below (**Scheme 63**), initially, vinylsulfonium salt (**226**) was formed *in situ* by deprotonation and elimination from the bromoethylsulfonium salt (**224**) with

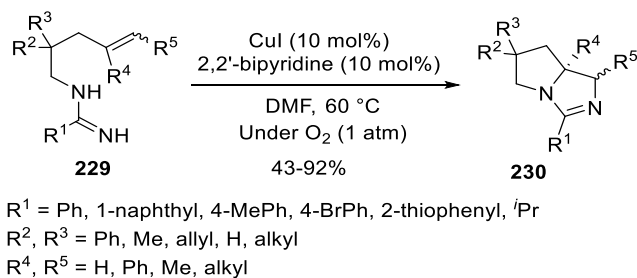
a base. The salt **226** reacts promptly with the amidine (**223**) to form the sulfur ylide (**227**), which subsequently generates the intermediate **228** by proton transfer. Lastly, an intramolecular nucleophilic attack releases the diphenyl sulfide (Ph_2S), and generates the desired imidazolinium salt (**225**).

Scheme 1.63. The mechanism for the synthesis of imidazolinium salts (**225**)



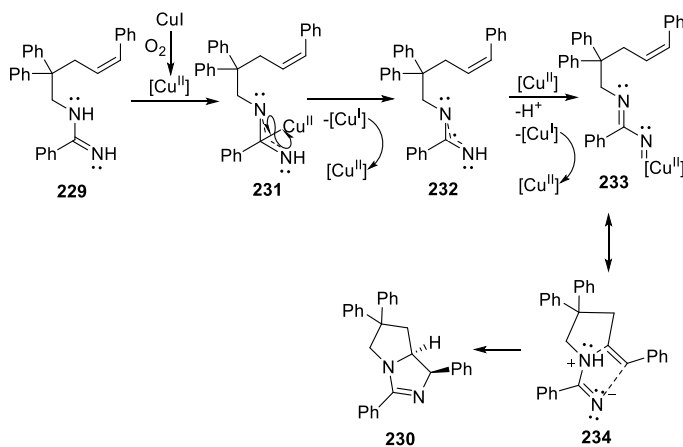
In 2012, Chiba and co-workers reported a Cu(I)-catalyzed aerobic [3+2]-annulation reaction of *N*-alkenyl amidines (**229**) to synthesize bi- and tri-cyclic imidazolines (**230**) (Scheme 1.64).⁶⁹ First, the initial screening was performed by treating an amidine ($\text{R}^1, \text{R}^2, \text{R}^3 = \text{Ph}; \text{R}^4, \text{R}^5 = \text{H}$) (**229**) with various copper salts (CuBr_2 , CuI , CuCl , $\text{CuBr} \cdot \text{SMe}_2$) and ligands. The combination of 2,2'-bipyridine (10 mol%) and CuI salt (10 mol%) under 1 atm of O_2 , afforded the bicyclic imidazoline in 87% yield, whereas under the N_2 atmosphere, product formation stalled. Next, various alkyl- and aryl-substituted amidines (**226**) were investigated under the optimized conditions. Aromatic substituted ($\text{R}^1 = \text{aryl}$) amidines provided the imidazolines in 61-85% yields, whereas aliphatic substituted ($\text{R}^1 = i\text{Pr}$) amidine offered moderate product yield (51%). Heteroaromatic ($\text{R}^1 = 2\text{-thiophenyl}$) group containing amidine provided 92% of the imidazoline product. With a phenyl-group at the R^5 position of the amidine, the yield decreased to only 43%.

Scheme 1.64. Cu(I)-catalyzed aerobic reaction to synthesize bi- and tri-cyclic imidazolines



Based on the mechanistic experiment and observed results, a mechanism was described in the report (**Scheme 1.65**). First, the Cu(I) is oxidized by oxygen (O₂) to generate a higher oxidation state species, Cu(II). One-electron oxidation of the amidine (**229**) with the resulting Cu(II) forms the 1,3-diazaallyl radical **232** via the intermediate **231**. Then, the radical **232** is further oxidized by another Cu(II) species to form the copper-nitrene complex **233**. This intermediate **233** will afford the intermediate **234**. Finally, the intramolecular concerted [3+2]- cycloaddition reaction of the **234** with the alkenyl moiety generates the product (**230**).

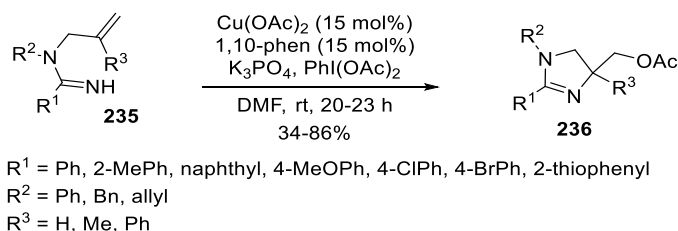
Scheme 1.65. Proposed mechanism of the [3+2]- annulation reaction of amidine



Later in 2012, Sanjaya and Chiba disclosed a Cu-catalyzed aminoacetoxylation of *N*-alkenylamidines (**235**) to synthesize 4-acetoxymethyl-2-imidazolines (**236**) (**Scheme 1.66**).⁷⁰ Initial screening of the amidine (**235**) and Cu(OAc)₂ with a few ligands and bases showed that the 1,10-phenanthroline (15 mol%) and K₃PO₄ with 15 mol% of Cu(OAc)₂, provided the best yield

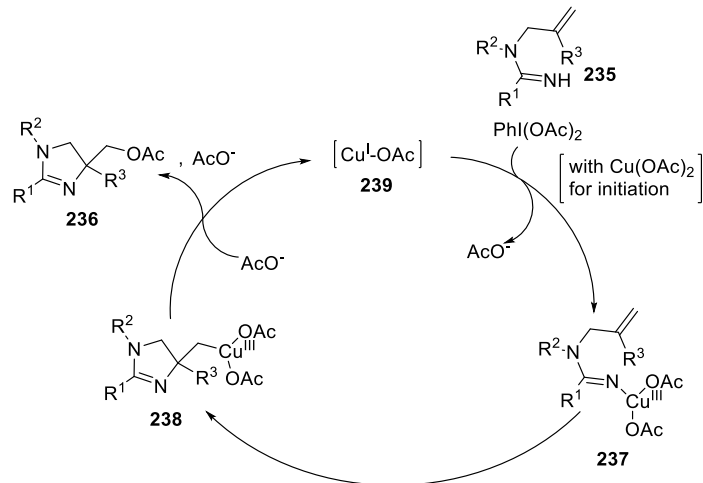
(86%) of **236**. The reaction didn't afford any product without any ligand or copper-catalyst. Under optimized condition, both EDG and EWG at the R¹ and R² positions were investigated, and the imidazolines were isolated in moderate to good yields (up to 86%). However, the aryl-group containing (at the R³ position) *N*-alkenylamidines (**235**), the imidazoline was isolated with only 34% yield.

Scheme 1.66. Cu-catalyzed synthesis of imidazolines from *N*-alkenylamidines



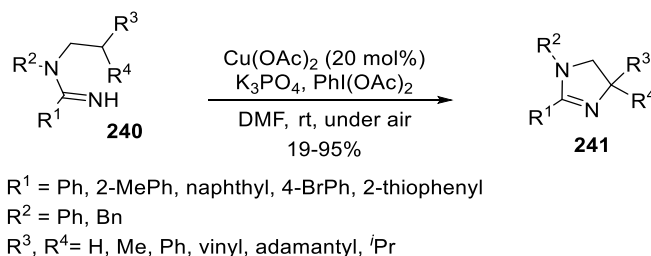
Based on the experimental data, a catalytic cycle was reported in the article (**Scheme 1.67**). The reaction starts with the formation of higher valent N-Cu(III) species **237** from the interaction among the amidine, Cu(OAc)₂, and PhI(OAc)₂. Then **237** undergoes a 5-*exo* amino-cupration onto the alkenyl moiety to generate the Cu(III) complex **238**. Subsequent S_N2 type substitution reaction with an acetate ion forms the desired 4-acetoxymethyl-2-imidazoline (**236**) along with the copper(I) complex **239** to maintain the catalytic cycle.

Scheme 1.67. Proposed mechanism of the reaction shown in Scheme 1.66



Next year in 2013, Chiba and co-workers reported subsequent Cu-mediated 2-imidazoline (**241**) synthesis, utilizing $\text{Cu}(\text{OAc})_2$, $\text{PhI}(\text{OAc})_2$, and K_3PO_4 to execute amination of the C-H bond of the amidines (**240**) (**Scheme 1.68**).⁷¹ Initial optimization showed among the copper catalysts (CuBr_2 , $\text{Cu}(\text{OAc})_2$, $\text{CuBr}\cdot\text{SMe}_2$, $\text{Cu}(\text{esp})_2\cdot 2\text{H}_2\text{O}$, CuTC) and oxidants (selectfluor, $\text{PhI}(\text{OAc})_2$, $\text{PhI}=\text{O}$, $\text{PhI}(\text{OCO}^t\text{Bu})_2$) investigated with the amidine ($\text{R}^1, \text{R}^2, \text{R}^3 = \text{Ph}$; $\text{R}^4 = \text{Me}$) (**240**), $\text{PhI}(\text{OAc})_2$ and 20 mol% $\text{Cu}(\text{OAc})_2$ afforded the product (**241**) in 80% yield. Under these optimized conditions, the imidazolines were isolated up to 95% yield with different substituted amidine where only 19% product was formed when alkyl group was inserted in both R^3, R^4 group of the amidine.

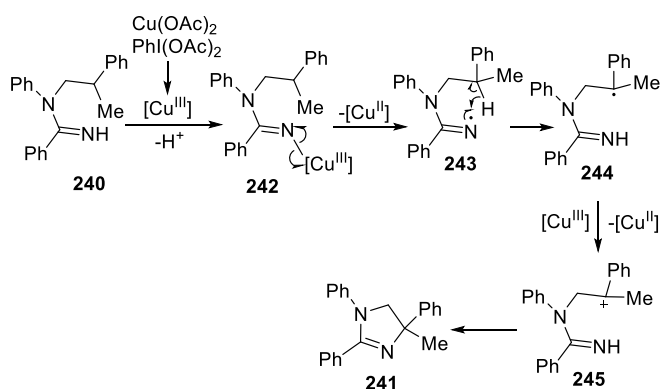
Scheme 1.68. Cu-mediated 2-imidazoline synthesis



A mechanism was depicted in the report (**Scheme 1.69**), which is similar to scheme 1.67. The reaction initiates by the formation of higher valent Nitrogen-Cu(III) complex **242** from the amidine

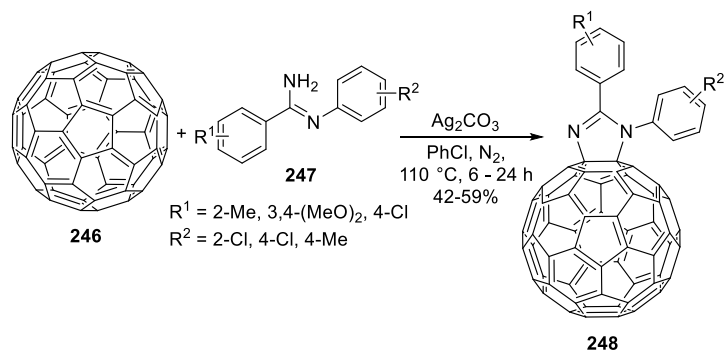
(**240**), $\text{Cu}(\text{OAc})_2$, and $\text{PhI}(\text{OAc})_2$. After that, the homolytic cleavage of the N-Cu(III) bond forms the N-radical species **243**, which consequently undergoes a 1,5-H radical shift to form the C-radical species **244**. Additionally, Cu-mediated one-electron oxidation of the **244** creates the carbocation **245**. Lastly, the product(**245**) is obtained by the intramolecular cyclization of that carbocation species **245**.

Scheme 1.69. Proposed mechanism of the reaction shown in Scheme 1.68



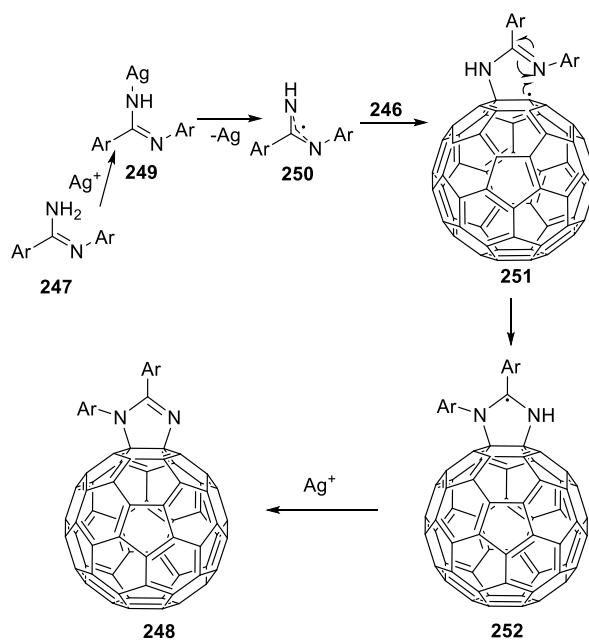
In the same year, He *et al.* developed a buckminsterfullerene fused imidazoline (**248**) synthesis by using amidine (**247**) and fullerene- C_{60} (**246**) (Scheme 1.70).⁷² Initial reaction was investigated by treating the amidine and **24** with different oxidants, and AgCO_3 found to be the best oxidant to generate the fullerene-fused imidazoline (56%) (**248**). With various substituted (Both EWG and EDG) amidines (**247**), the product yield was moderate (42-59%). Surprisingly, sterically hindered 2-substituted aromatic group ($\text{R}^2 = 2\text{-Cl}$) works better (59%) than the rest of the compounds investigated.

Scheme 1.70. Buckminsterfullerene fused imidazolines synthesis from amidines



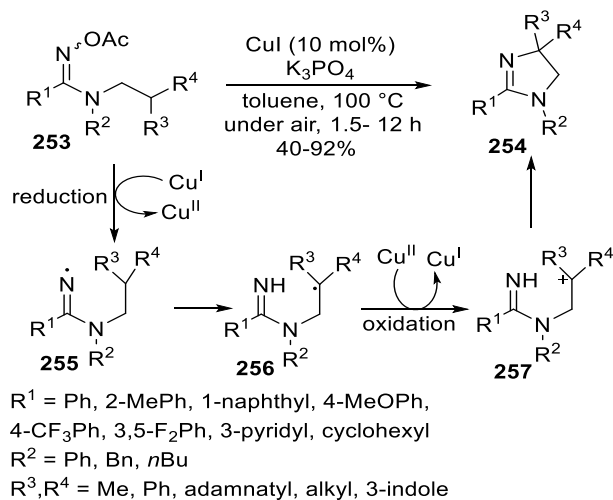
A radical-mediated mechanism was outlined in the report (**Scheme 1.71**). At first, amidine (**247**) reacts with the Ag^+ to form the intermediate **249**. Then **249** undergoes homolytic cleavage of the N-Ag bond to generate the radical species **250**. Next, radical addition of the **250** to the fullerene- C_{60} (**246**) forms the new radical **251**. Then, the radical **252** is formed by another homolytic cleavage of the radical **251**. This final radical **252** is then cyclized to the fullerene-fused imidazoline **248**.

Scheme 1.71. Mechanism of the synthesis of [60]fullerene-fused imidazolines



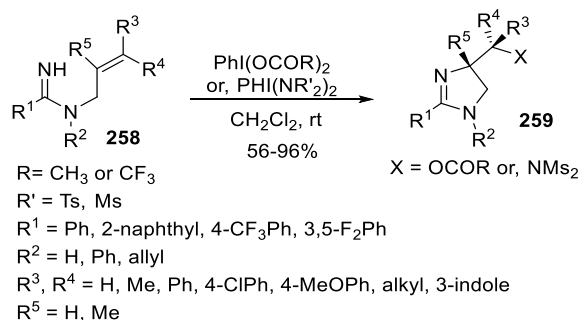
In 2014, Chen and Chiba disclosed a CuI-catalyzed redox neutral C-H amination of the amidoximes (**253**) to synthesize 2-imidazolines (**254**) (**Scheme 72**).⁷³ Compare to their previous method,⁷¹ this method was generated by a reduction of the amidine (**253**). The reduction process formed the radical species **255**, which then converted to another radical species **256**. Next, the oxidation of **256** produced the cationic intermediate **257** and consequently formed the 2-imidazoline adducts (**254**).

Scheme 1.72. CuI-catalyzed redox neutral C-H amination of the amidoximes to synthesize 2-imidazolines



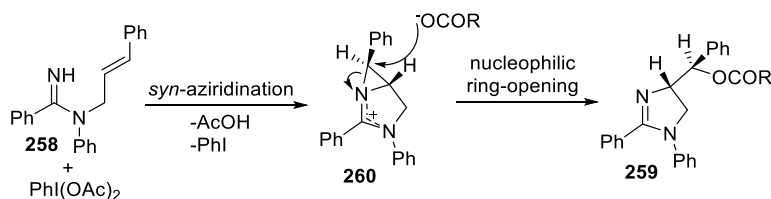
In the same year, Chen *et al.* demonstrated a hypervalent I-mediated diastereoselective *anti*-aminoxxygenation and *anti*-diamination of alkenes with amidines (**258**) to synthesize 2-imidazolines (**259**) (**Scheme 73**).⁷⁴ Initial investigations showed that $PhI(OCOCF_3)_2$ mediated reaction with amidine provided the superior yield of the product **259**. With various amidines treated with $PhI(OCOCF_3)_2$, the imidazolines were isolated in 56-96% yields with excellent diastereoselectivities (*dr* up to >20:1). Next, the investigations were expanded by treating the amidines with $PhI(NTs_2)_2$ or $PhI(NMs_2)_2$, and the diastereoselective products were obtained in 66-86% yields.

Scheme 1.73. Hypervalent Iodine-mediated diastereoselective imidazolines synthesis



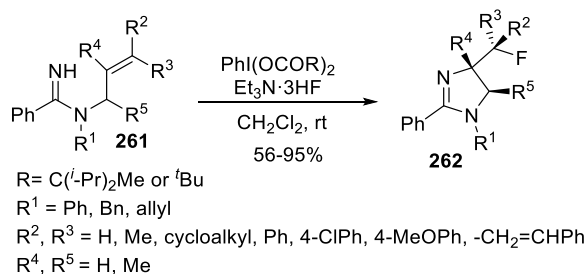
Based on the observations and experimental data, the authors depicted a mechanism shown below (**Scheme 1.74**). The reaction initiates by an intramolecular *syn*-aziridination of the alkene moiety with the amidine N to form the intermediate **260**. Then nucleophilic ring-opening of the aziridine (**260**) by the carboxylate ion (or, $-\text{NR}_2$) forms the desired imidazoline (**259**).

Scheme 1.74. Proposed mechanism of the reaction shown in Scheme 1.73



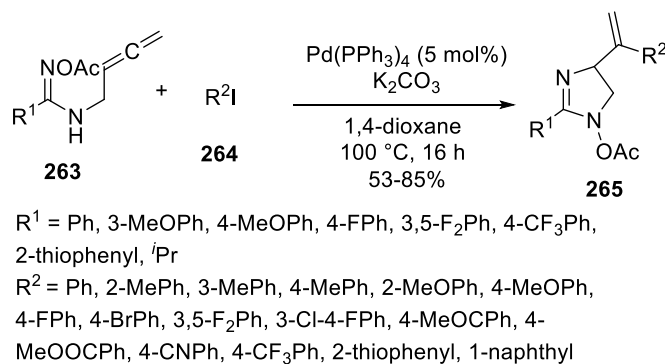
In 2016, Chen *et al.* demonstrated another hypervalent I-mediated *anti*-selective aminofluorination of alkenes with amidines (**261**) to synthesize 4-fluoroalkyl-2-imidazolines (**262**) (**Scheme 75**).⁷⁵ For aminofluorination of the di-substituted alkenes ($R^3, R^4 = \text{H}$) with the amidine moiety (**261**), the combination of $\text{Et}_3\text{N} \cdot 3\text{HF}$ with the oxidant $\text{PhI}(\text{OCOC}(i\text{Pr})_2\text{Me})_2$ was found to be the best mediators to form the desired imidazoline analogs. However, for the tri- and tetra-substituted alkenes, $\text{Et}_3\text{N} \cdot 3\text{HF}$, and the oxidant $\text{PhI}(\text{OCO}^t\text{Bu})_2$ combination was more effective.

Scheme 1.75. Hypervalent Iodine-mediated 4-fluoroalkyl-2-imidazolines synthesis



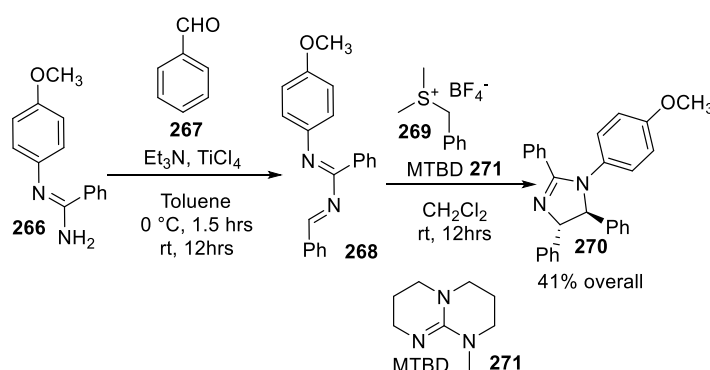
In 2018, Hu *et al.* developed a Pd-catalyzed cyclization of *N*-acetoxy-amidine (**263**) with aryl iodide (**264**) to synthesize 2-imidazoline (**265**) (**Scheme 1.76**).⁷⁶ Initial optimizations were performed by treating the amidine (**263**) with PhI (**264**) in the presence of different palladium catalysts and bases in few solvents. The best product formation (76%) was observed in the combination of $\text{Pd}(\text{PPh}_3)_4$ (5 mol%) and K_2CO_3 in 1,4-dioxane at 100 °C. Besides, a few additives ($\text{Cu}(\text{OTf})_2$, PPh_3 , $n\text{Bu}_4\text{NBr}$) were also screened with the catalysts, but none of them offers any significant improvement in product formation. Under these optimized conditions, several amidines and aryl iodide were investigated to explore the scope of the reaction. The EWG (F, Cl, Br, CF_3 , CN) containing aryl iodide (**264**) offered the imidazolines (**265**) in better yields (78-85%) than the aryl iodide (**264**) possessing the EDG (Me, MeO) (59-68%).

Scheme 1.76. Pd-catalyzed cyclization of *N*-acetoxy-amidine to synthesize imidazolines



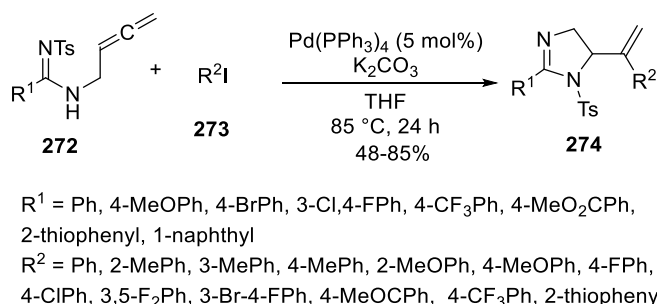
In 2019, we (Mehedi & Tepe) developed a new method to synthesize 2-imidazoline (**270**) from the reaction of sulfonium salt (**269**) and 1,3-diaza-1,3-butadiene (**268**) in the presence of a base (MTBD) (**Scheme 1.77**).⁷⁷ The 1,3-diaza-1,3-butadiene (**268**) was generated from the reaction of benzaldehyde (**267**) with amidine (**266**) in the presence of a base Et₃N and Lewis acid TiCl₄. The details of this new method are described in chapter three.

Scheme 1.77. Synthesis of 2-imidazoline from the reaction of sulfonium salt and 1,3-diaza-1,3-butadiene



Recently in 2020, Liu *et al.* described another Pd-catalyzed cyclized reaction of aryl iodide (**273**) with *N*-tosyl-amidine (**272**) to synthesize 2-imidazoline (**274**) (**Scheme 1.78**).⁷⁸ Similar to their previous report,⁷⁶ Pd(PPh₃)₄ (5 mol%) and K₂CO₃ was used, but in a different solvent THF at a lower temperature (85 °C) for a 24 h reaction, and the imidazoline analogs were isolated in 48-85% yields. When the alkyl group was incorporated in **272** or aryl iodide, only a trace amount of compound was obtained.

Scheme 1.78. Pd-catalyzed synthesis of imidazolines



1.5 Conclusion

Due to widespread application in pharmaceutical, medicinal, and agricultural sectors, the development of new methods to synthesize chiral and achiral imidazoline analogs is one of the progressing areas in organic chemistry. Although there has been significant progress in this field of research in recent years, there are still some areas that remain underexplored. *N*-substituted diamines and the multicomponent synthesis of stereoselective imidazoline analogs still needs more investigation. In addition, the utilization of renewable starting materials under mild reaction conditions and more greener methods will be the future in imidazoline synthesis.

REFERENCES

REFERENCES

- [1] K. Hofmann, in *Chemistry of Heterocyclic Compounds*, Vol. 6 (Ed.: C. Hofmann), John Wiley & Sons, Inc., Hoboken, NJ, USA, **1953**, pp. 213.
- [2] a) R. B. Kinnel, H.-P. Gehrken, R. Swali, G. Skoropowski, P. J. Scheuer, *J. Org. Chem.* **1998**, *63*, 3281; b) K. Murai, M. Morishita, R. Nakatani, O. Kubo, H. Fujioka, Y. Kita, *J. Org. Chem.* **2007**, *72*, 8947.
- [3] a) H. Stähle, *Best Pract. Res. Clin. Anaesthesiol.* **2000**, *14*, 237; b) L. T. Vassilev, *Science* **2004**, *303*, 844; c) R. W. Clarke, J. Harris, *CNS Drug Rev.* **2006**, *8*, 177; d) E. Njomen, P. A. Osmulski, C. L. Jones, M. Gaczynska, J. J. Tepe, *Biochemistry* **2018**, *57*, 4214.
- [4] P. Bousquet, J. Feldman, J. Schwartz, *J. Pharmacol. Exp. Ther.* **1984**, *230*, 232.
- [5] M. D. Brewer, R. J. J. Dorgan, B. R. Manger, P. Mamalis, R. A. B. Webster, *J. Med. Chem.* **1987**, *30*, 1848.
- [6] K. Sztanke, K. Pasternak, A. Sidor-Wójtowicz, J. Truchlińska, K. Jóźwiak, *Biorg. Med. Chem.* **2006**, *14*, 3635.
- [7] a) V. Sharma, T. A. Lansdell, S. Peddibhotla, J. J. Tepe, *Chem. Biol.* **2004**, *11*, 1689; b) V. Sharma, S. Peddibhotla, J. J. Tepe, *J. Am. Chem. Soc.* **2006**, *128*, 9137; c) V. Sharma, C. Hupp, J. Tepe, *Curr. Med. Chem.* **2007**, *14*, 1061; d) D. K. Kahlon, T. A. Lansdell, J. S. Fisk, C. D. Hupp, T. L. Friebe, S. Hovde, A. D. Jones, R. D. Dyer, R. W. Henry, J. J. Tepe, *J. Med. Chem.* **2009**, *52*, 1302; e) D. K. Kahlon, T. A. Lansdell, J. S. Fisk, J. J. Tepe, *Biorg. Med. Chem.* **2009**, *17*, 3093.
- [8] B. Szabo, *Pharmacol. Ther.* **2002**, *93*, 1.
- [9] L. Crane, M. Anastassiadou, S. E. Hage, J. L. Stigliani, G. Baziard-Mouysset, M. Payard, J. M. Leger, J.-G. Bizot-Espiard, A. Ktorza, D.-H. Caignard, P. Renard, *Biorg. Med. Chem.* **2006**, *14*, 7419.
- [10] E. Njomen, J. J. Tepe, *Cell Chem. Biol.* **2019**, *26*, 1283.
- [11] a) C. L. Jones, J. J. Tepe, *Molecules* **2019**, *24*, 2841; b) E. Njomen, J. J. Tepe, *J. Med. Chem.* **2019**, *62*, 6469.
- [12] T. Isobe, K. Fukuda, Y. Araki, T. Ishikawa, *Chem. Commun.* **2001**, 243.
- [13] C. A. Busacca, J. C. Lorenz, N. Grinberg, N. Haddad, H. Lee, Z. Li, M. Liang, D. Reeves, A. Saha, R. Varsolona, C. H. Senanayake, *Org. Lett.* **2008**, *10*, 341.
- [14] Y. Hsiao, L. S. Hegedus, *J. Org. Chem.* **1997**, *62*, 3586.

- [15] a) R. C. F. Jones, K. J. Howard, J. S. Snaith, *Tetrahedron Lett.* **1996**, 37, 1707; b) F. E. Hahn, M. C. Jahnke, *Angew. Chem. Int. Ed.* **2008**, 47, 3122.
- [16] a) K. Murai, S. Fukushima, A. Nakamura, M. Shimura, H. Fujioka, *Tetrahedron* **2011**, 67, 4862; b) A. E. Sheshenev, E. V. Boltukhina, A. J. P. White, K. K. M. Hii, *Angew. Chem. Int. Ed.* **2013**, 52, 6988.
- [17] M. Kondo, M. Sugimoto, S. Nakamura, *Chem. Commun.* **2016**, 52, 13604.
- [18] A. Barakat, M. S. Islam, A. M. A. Al Majid, Z. A. Al-Othman, *Tetrahedron* **2013**, 69, 5185.
- [19] S. Haneda, C. Ueba, K. Eda, M. Hayashi, *Adv. Synth. Catal.* **2007**, 349, 833.
- [20] A. J. Davenport, D. L. Davies, J. Fawcett, D. R. Russell, *J. Organomet. Chem.* **2006**, 691, 3445.
- [21] F. Bureš, J. Kulháněk, A. Růžicka, *Tetrahedron Lett.* **2009**, 50, 3042.
- [22] J. Ma, X. Cui, B. Zhang, M. Song, Y. Wu, *Tetrahedron* **2007**, 63, 5529.
- [23] H. Liu, D.-M. Du, *Adv. Synth. Catal.* **2009**, 351, 489.
- [24] V. Ji Ram, A. Sethi, M. Nath, R. Pratap, in *The Chemistry of Heterocycles*, Elsevier, **2019**, pp. 149.
- [25] A. W. Hofmann, *Berichte Dtsch. Chem. Ges.* **1888**, 21, 2332.
- [26] A. Shaabani, M. Seyyedhamzeh, A. Maleki, F. Rezazadeh, *Appl. Catal. A-Gen.* **2009**, 358, 146.
- [27] X. Wang, J. Xia, X. Dai, S. You, *Science in China Series B: Chemistry* **2009**, 52, 1331.
- [28] M. Weber, J. E. M. N. Klein, B. Miehlich, W. Frey, R. Peters, *Organometallics* **2013**, 32, 5810.
- [29] M. Nasr-Esfahani, M. Montazerozohori, M. Moghadam, P. Akhlaghi, *Arkivoc* **2010**, 2010, 97.
- [30] V. G. Nenajdenko, V. M. Muzalevskiy, A. V. Shastin, E. S. Balenkova, E. V. Kondrashov, I. A. Ushakov, A. Y. Rulev, *J. Org. Chem.* **2010**, 75, 5679.
- [31] Q. Zhu, Y. Lu, *Org. Lett.* **2010**, 12, 4156.
- [32] J. Zhang, X. Wang, M. Yang, K. Wan, B. Yin, Y. Wang, J. Li, Z. Shi, *Tetrahedron Lett.* **2011**, 52, 1578.
- [33] M. Nasr-Esfahani, M. Montazerozohori, S. Mehrizi, *J. Heterocycl. Chem.* **2011**, 48, 249.
- [34] F. Mohanazadeh, N. Nami, S. S. Hosseini, *Chin. J. Chem.* **2011**, 29, 1055.

- [35] G.-y. Bai, K. Xu, G.-f. Chen, Y.-h. Yang, T.-y. Li, *Synthesis* **2011**, 2011, 1599.
- [36] H. Jiang, L. Sun, S. Yuan, W. Lu, W. Wan, S. Zhu, J. Hao, *Tetrahedron* **2012**, 68, 2858.
- [37] K. A. Shaikh, V. A. Patil, P. A. Shaikh, *Chin. J. Chem.* **2012**, 30, 924.
- [38] A. M. Reverdito, I. A. Perillo, A. Salerno, *Synth. Commun.* **2012**, 42, 2083.
- [39] L. Shu, P. Wang, W. Liu, C. Gu, *Org. Process Res. Dev.* **2012**, 16, 1866.
- [40] Y. Sato, K. Okada, M. Akiyoshi, K. Tokudome, T. Matsunaga, *J. Loss Prev. Process Indust.* **2011**, 24, 656.
- [41] J. V. Geden, A. K. Pancholi, M. Shipman, *J. Org. Chem.* **2013**, 78, 4158.
- [42] R. Manikandan, P. Anitha, G. Prakash, P. Vijayan, P. Viswanathamurthi, R. J. Butcher, J. G. Malecki, *J. Mol. Catal. A: Chem.* **2015**, 398, 312.
- [43] R. Jiang, H.-B. Sun, S. Li, K. Zhan, J. Zhou, L. Liu, K. Zhang, Q. Liang, Z. Chen, *Synth. Commun.* **2018**, 48, 2652.
- [44] K. J. Evans, B. Potrykus, S. M. Mansell, *Heteroat. Chem* **2019**, 2019, 1.
- [45] S. Liu, W. Li, Y. Pang, H. Xiao, Y. Zhou, X. Wang, *J. Heterocycl. Chem.* **2019**, 56, 998.
- [46] M. Kozlov, A. Komkov, T. Losev, A. Tyurin, A. Dmitrenok, I. Zavarzin, Y. Volkova, *J. Org. Chem.* **2019**, 84, 11533.
- [47] Z.-W. Zhang, G. Lu, M.-M. Chen, N. Lin, Y.-B. Li, T. Hayashi, A. S. C. Chan, *Tetrahedron: Asymmetry* **2010**, 21, 1715.
- [48] S. Nakamura, Y. Maeno, M. Ohara, A. Yamamura, Y. Funahashi, N. Shibata, *Org. Lett.* **2012**, 14, 2960.
- [49] I. Ortín, D. J. Dixon, *Angew. Chem. Int. Ed.* **2014**, 53, 3462.
- [50] P.-L. Shao, J.-Y. Liao, Y. A. Ho, Y. Zhao, *Angew. Chem. Int. Ed.* **2014**, 53, 5435.
- [51] M. Hayashi, M. Iwanaga, N. Shiomi, D. Nakane, H. Masuda, S. Nakamura, *Angew. Chem. Int. Ed.* **2014**, 53, 8411.
- [52] M. A. Honey, Y. Yamashita, S. Kobayashi, *Chem. Commun.* **2014**, 50, 3288.
- [53] Z. Gao, L. Zhang, Z. Sun, H. Yu, Y. Xiao, H. Guo, *Org. Biomol. Chem.* **2014**, 12, 5691.
- [54] G. V. Janssen, E. Vicente-García, W. Vogel, J. C. Slootweg, E. Ruijter, K. Lammertsma, R. V. A. Orru, *Eur. J. Org. Chem.* **2014**, 2014, 3762.

- [55] S. J. Welsch, M. Umkehrer, C. Kalinski, G. Ross, C. Burdack, J. Kolb, M. Wild, A. Ehrlich, L. A. Wessjohann, *Tetrahedron Lett.* **2015**, *56*, 1025.
- [56] S. Abás, C. Estarellas, F. Javier Luque, C. Escolano, *Tetrahedron* **2015**, *71*, 2872.
- [57] K. Tamura, N. Kumagai, M. Shibasaki, *Eur. J. Org. Chem.* **2015**, *2015*, 3026.
- [58] M.-X. Zhao, L. Jing, H. Zhou, M. Shi, *RSC Advances* **2015**, *5*, 75648.
- [59] S. Nakamura, R. Yamaji, M. Iwanaga, *Chem. Commun.* **2016**, *52*, 7462.
- [60] R. de la Campa, A. D. Gammack Yamagata, I. Ortín, A. Franchino, A. L. Thompson, B. Odell, D. J. Dixon, *Chem. Commun.* **2016**, *52*, 10632.
- [61] S. Qiao, C. B. Wilcox, D. K. Unruh, B. Jiang, G. Li, *J. Org. Chem.* **2017**, *82*, 2992.
- [62] X.-B. Bu, Y. Yu, B. Li, L. Zhang, J.-J. Chen, Y.-L. Zhao, *Adv. Synth. Catal.* **2017**, *359*, 351.
- [63] X. Zhang, X. Wang, Y. Gao, X. Xu, *Chem. Commun.* **2017**, *53*, 2427.
- [64] G. Fang, H. Wang, Q. Liu, X. Cong, X. Bi, *Asian J. Org. Chem.* **2018**, *7*, 1066.
- [65] Z.-P. Wang, Q. Wu, J. Jiang, Z.-R. Li, X.-J. Peng, P.-L. Shao, Y. He, *Org. Chem. Front.* **2018**, *5*, 36.
- [66] G. P. Y. Kok, P.-L. Shao, J.-Y. Liao, S. N. F. B. S. Ismail, W. Yao, Y. Lu, Y. Zhao, *Chem. Eur. J.* **2018**, *24*, 10513.
- [67] F. Sladojevich, A. Trabocchi, A. Guarna, D. J. Dixon, *J. Am. Chem. Soc.* **2011**, *133*, 1710.
- [68] E. M. McGarrigle, S. P. Fritz, L. Favereau, M. Yar, V. K. Aggarwal, *Org. Lett.* **2011**, *13*, 3060.
- [69] Y.-F. Wang, X. Zhu, S. Chiba, *J. Am. Chem. Soc.* **2012**, *134*, 3679.
- [70] S. Sanjaya, S. Chiba, *Org. Lett.* **2012**, *14*, 5342.
- [71] H. Chen, S. Sanjaya, Y.-F. Wang, S. Chiba, *Org. Lett.* **2013**, *15*, 212.
- [72] C.-L. He, R. Liu, D.-D. Li, S.-E. Zhu, G.-W. Wang, *Org. Lett.* **2013**, *15*, 1532.
- [73] H. Chen, S. Chiba, *Org. Biomol. Chem.* **2014**, *12*, 42.
- [74] H. Chen, A. Kaga, S. Chiba, *Org. Lett.* **2014**, *16*, 6136.
- [75] H. Chen, A. Kaga, S. Chiba, *Org. Biomol. Chem.* **2016**, *14*, 5481.

- [76] J. Hu, Z. Li, X. Zhang, Y. Han, Y. Liu, Y. Zhao, Y. Liu, P. Gong, *Org. Lett.* **2018**, *20*, 2116.
- [77] M. S. A. Mehedi, J. J. Tepe, *J. Org. Chem.* **2019**, *84*, 7219.
- [78] Y. Liu, C. Zhang, X. Liang, X. Zeng, R. Lu, Z. Fang, S. Wang, Y. Liu, J. Hu, *Synthesis* **2020**, *52*, 901.

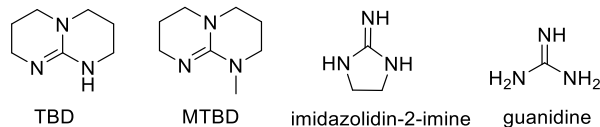
Chapter 2: Synthesis of diastereoselective 2,3-disubstituted aziridines in the presence of a guanidine base

2.1 Introduction

Aziridines are three-member nitrogen-containing heterocyclic compounds present in many biologically active natural products.¹ They are also important building blocks in many organic syntheses.² In our lab, we have developed a one-pot synthesis of 2-imidazolines from the ring expansion of aziridines with imidoyl chlorides.³ In addition, azetidines,⁴ β -lactams,⁵ pyrroles,⁶ oxazoles,⁷ imidazoles,⁸ piperidines,⁹ piperazines,¹⁰ and various other heterocyclic analogs were also synthesized by employing aziridine moieties.¹¹

Although several synthetic methods have been reported to synthesize aziridine analogs,¹ there is still an opportunity to improve the aziridine synthesis efficiently and straightforwardly by utilizing simple and cost-effective starting material. In recent years, guanidine bases (**Figure 2.1**), primarily known as superbases, were used in various synthetic and organocatalytic reactions.¹²

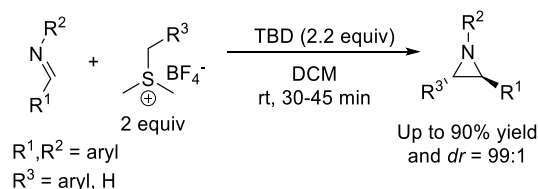
Figure 2.1. Guanidine bases



In 2010, Phillips *et al.* reported¹³ the use of guanidine bases to obtain epoxides by using the Corey-Chaykovsky epoxidation reaction.¹⁴ The reaction was performed by treating *in situ* formed aldehydes with sulfonium salts in the presence of a guanidine base (1,5,7-triazabicyclo(4.4.0)dec-5-ene (TBD) or, 7-methyl-1,5,7-triazabicyclo(4.4.0)dec-5-ene (MTBD), **Figure 2.1**) at room temperature to obtain epoxides in high yields. Considering the similarity of the Corey-Chaykovsky epoxidation reaction, we envisioned using guanidine bases in a modified Corey-Chaykovsky

aziridination reaction¹⁵ to generate diastereoselective aziridines from the reaction of an imine and a sulfonium salt (**Scheme 2.1**).

Scheme 2.1. Synthesis of aziridines



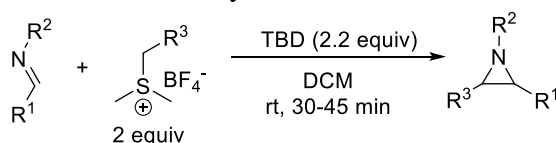
2.2 Results and discussion

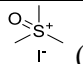
The investigation was initiated by treating different *N*-aryl (**2.1-2.3**) or alkyl (**2.4**) group-containing imines with two equivalents of sulfonium salt (**2a**) in the presence of the guanidine base TBD in dichloromethane (DCM) (**Table 2.1**). Unfortunately, no product formation was observed in any of those reactions, which provided the idea to use an electron-withdrawing group at the *N*-position of the imine to afford a more electrophilic imine carbon. At first, the tosyl group containing imine (**2.5**) was used with **2a** under the same reaction conditions. The reaction provided 90% of the aziridine product (**A1**) with a *dr* of 80:20 (*trans:cis*). Based on this reaction outcome, a few sulfonium salts (**2.10**, **2b**) were treated with the imine **2.5**. These reactions afforded good yields (73-76%) of the aziridine products (**A2**, **A3**) with poor regioselectivity. With the electron-withdrawing *p*-ClPh (R³) containing sulfonium salt, the reaction provided more *cis* aziridine product than *trans* aziridine (44:56 = *trans:cis*). The electron-donating group containing imine (*p*MeO-Ph = R²) also did not afford any better selectivity of the reaction (60:40 = *trans:cis*). Moreover, a poor yield (35%) of the aziridine (**A7**) was obtained when an alkyl containing sulfonium salt (**2.9**) was treated with the imine **2.5**.

Next, to further explore the diastereoselectivity of the reaction, a Boc (*tert*-butoxycarbonyl) group was introduced at the *N*-position of the imine (**2.7**) and screened with two sulfonium salts

(**2a**, **2.10**). Both reactions provided the aziridines (**A4**, **A5**) in moderate to good yield (57-71%) with excellent diastereoselectivity (95:5 = *trans*:*cis* with **2a**, and 99:1= *trans*:*cis* with **2.10**). Similarly, Cbz (carboxybenzyl-) group was inserted at the *N*-position of the imine (**2.8**), and the aziridine (**A6**) was isolated in moderate yield (47%) with less diastereoselectivity (85:15 = *trans*:*cis*) then the Boc reactions. In addition, a significant amount of aldehyde and amine product was isolated in the Boc-imines and Cbz-imine reactions.

Table 2.1. Synthesis of aziridines



Imine	R ²	R ¹	R ³ *	Product	Yield%	Trans: Cis
2.1	Ph	Ph	Ph (2a)	-	N/A	N/A
2.2	<i>p</i> MeO-Ph	Ph	Ph (2a)	-	N/A	N/A
2.3	<i>p</i> NO ₂ -Ph	<i>p</i> MeO-Ph	Ph (2a)	-	N/A	N/A
2.4	Ph-CH ₂	Ph	Ph (2a)	-	N/A	N/A
2.5	Tosyl	Ph	Ph (2a)	A1	90	80:20
2.5	Tosyl	Ph	<i>p</i> Cl-Ph (2.10)	A2	76	44:56
2.5	Tosyl	Ph	<i>p</i> MeO-Ph (2b)	A3	73	60:40
2.6	Tosyl	<i>p</i> MeO-Ph	Ph (2a)	A3	71	60:40
2.7	Boc	Ph	Ph (2a)	A4	71	95:5
2.7	Boc	Ph	<i>p</i> Cl-Ph (2.10)	A5	57	99:1
2.8	Cbz	Ph	Ph (2a)	A6	47	85:15
2.5	Tosyl	Ph	 (2.9)	A7	35	N/A

* 2a and 2b are from chapter three

To prevent the decomposition of the imine, a less hygroscopic guanidine base (MTBD) was introduced in the reaction of **2.8** and **2a**, whereas the TBD base was found to be extremely hygroscopic.¹⁶ The reaction afforded a better yield of the aziridine **A6** (53%). This newly found result also sparked us to introduce the MTBD base in the imidazoline synthesis (**Scheme 4.3**, Chapter 4), which significantly improved the yield of imidazoline products.

2.3 Conclusion

A guanidine base (TBD) was used to synthesize *N*-substituted aziridines in moderate to good yields with moderate to excellent diastereoselectivity. Later, to prevent the decomposition of the starting imine, a new guanidine base (MTBD) was introduced, which improved the yield of the aziridine and lead us to the imidazoline synthesis.

2.4 Experimental sections

The general methods to synthesize imines:

Method A:

To a solution of dry dichloromethane (40 mL) in a 100 mL dry round bottom flask, corresponding aldehyde (1 equiv, 10 mmol), and amine (1 equiv, 10 mmol) were added, followed by anhydrous sodium sulfate (5 grams) and the reaction was stirred for 12 hours at room temperature. After that, the solvent was evaporated, and the crude product was purified using automated CombiFlash chromatography (silica gel 20-40 microns, using ethyl acetate in hexane) or, used as crude to yield the imine.

Method B:

To a solution of dry toluene (40 mL) in a 100 mL dry round bottom flask, corresponding aldehyde (1 equiv, 10 mmol) and amine (1 equiv, 10 mmol) were added. The reaction was then refluxed with a Dean-Stark apparatus for 6 hours. After that, the solvent was evaporated, and the crude

product was purified using automated CombiFlash chromatography (silica gel 20-40 microns, using ethyl acetate in hexane) or, used as crude to obtain the imine.

Method C:

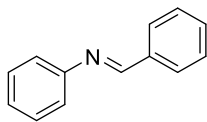
To a solution of dry toluene (40 mL) in a 100 mL dry round bottom flask, corresponding aldehyde (1 equiv, 10 mmol) and amine (1 equiv, 10 mmol) were added, followed by Amberlyst-15 (0.016 equiv). The reaction was then refluxed with a Dean-Stark apparatus for 12 hours. After that, the solvent was evaporated, and the crude mixture was recrystallized in 15% ethyl acetate in hexane to obtain the imine.

Method D:

Step-1: To a solution of methanol (10 mL) and water (20 mL) in a 100 mL dry round bottom flask, a mixture of benzaldehyde (2.00 equiv, 10 mmol), *tert*-butyl carbamate or benzyl carbamate (1.00 equiv, 5 mmol), toluenesulfinic acid sodium salt (2.50 equiv, 12.5mmol), and formic acid (2.00 equiv, 10 mmol) were stirred at room temperature for 24 h. The resulting white solid was filtered and washed with water (40 mL) and then with ether (40 mL) and then dried to get sulphone, which was then used in the next step without further purification.

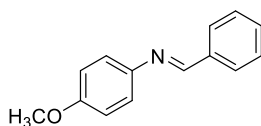
Step-2: Under an inert atmosphere, in a 100 mL flame-dried round-bottom flask, anhydrous K_2CO_3 (6 equiv, 6 mmol) was added and flame dried. Then appropriate sulphone (1 equiv, 1mmol) was added under inert condition, followed by THF and heated at reflux for 24 h. The reaction mixture was then allowed to cool to room temperature, followed by filtration through a well-pressed Celite[®] pad. Evaporation of the organic solvent was carried out under reduced pressure to give the pure desired imine essentially.

N,1-diphenylmethanimine (**2.1**)¹⁷:



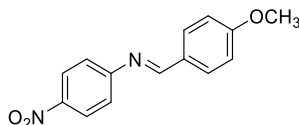
Method A, Purified as oil mixture (1.45 gm, 80% in crude). IR: 3060, 3027, 2889, 1623, 1481, 1447 cm^{-1} . ^1H NMR (500 MHz, CHCl_3 -*d*) δ 8.48 (s, 1H), 7.95 – 7.92 (m, 2H), 7.50 (dd, J = 4.1, 1.4 Hz, 3H), 7.44 – 7.40 (m, 2H), 7.27 – 7.22 (m, 3H). $^{13}\text{C}\{^1\text{H}\}$ NMR (126 MHz, CHCl_3 -*d*) δ 160.4, 152.1, 136.2, 134.5, 131.4, 129.2, 128.8, 126.0, 120.9. HRMS (ESI-TOF) m/z : $[\text{M}+\text{H}]^+$ calcd for ($\text{C}_{13}\text{H}_{12}\text{N}^+$) 182.0964; Found 182.0968.

N-(4-methoxyphenyl)-1-phenylmethanimine (**2.2**)¹⁸:



Method B, Purified as cream color solid (2 gm, 95%). Melting Point: 73-74 $^{\circ}\text{C}$. IR: 3062, 3029, 2953, 1628, 1245, 1034 cm^{-1} . ^1H NMR (500 MHz, CHCl_3 -*d*) δ 8.50 (s, 1H), 7.93 – 7.88 (m, 2H), 7.50 – 7.46 (m, 3H), 7.26 (d, J = 9 Hz, 2H), 6.95 (d, J = 9 Hz, 2H), 3.85 (s, 3H). $^{13}\text{C}\{^1\text{H}\}$ NMR (126 MHz, CHCl_3 -*d*) δ 158.5, 158.3, 144.8, 136.4, 131.1, 128.8, 128.6, 122.2, 114.4, 55.5. HRMS (ESI-TOF) m/z : $[\text{M}+\text{H}]^+$ calcd for ($\text{C}_{14}\text{H}_{14}\text{NO}^+$) 212.1070; Found 212.1097.

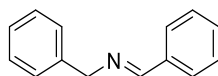
1-(4-methoxyphenyl)-*N*-(4-nitrophenyl)methanimine (**2.3**)¹⁹:



Method B, Brownish solid (2.2 gm, 86%), Melting Point: 122-124 $^{\circ}\text{C}$. IR: 3063, 2929, 1596, 1566, 1505, 1422 cm^{-1} . ^1H NMR (500 MHz, CHCl_3 -*d*) δ 8.35 (s, 1H), 8.26 (d, J = 8.9 Hz, 2H), 7.87 (d,

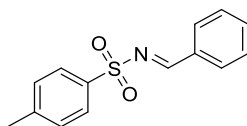
$J = 8.7$ Hz, 2H), 7.23 (d, $J = 8.9$ Hz, 2H), 7.01 (d, $J = 8.7$ Hz, 2H), 3.90 (s, 3H). $^{13}\text{C}\{^1\text{H}\}$ NMR (126 MHz, CHCl_3 - d) δ 163.1, 161.9, 158.3, 145.2, 131.2, 128.3, 125.0, 121.3, 114.4, 55.5. HRMS (ESI-TOF) m/z : $[\text{M}+\text{H}]^+$ calcd for $(\text{C}_{14}\text{H}_{13}\text{N}_2\text{O}_3^+)$ 257.0921; Found 257.0928.

N-benzyl-1-phenylmethanimine (**2.4**)¹⁸:



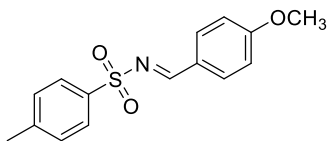
Method B, Yellowish liquid (1.86 gm, 95%). IR: 3060, 3026, 2869, 1642, 1493, 1446 cm^{-1} . ^1H NMR (500 MHz, CHCl_3 - d) δ 8.41 (s, 1H), 7.83 – 7.76 (m, 2H), 7.48 – 7.39 (m, 3H), 7.39 – 7.31 (m, 4H), 7.33 – 7.23 (m, 1H), 4.84 (d, $J = 1.2$ Hz, 2H). $^{13}\text{C}\{^1\text{H}\}$ NMR (126 MHz, CHCl_3 - d) δ 162.0, 139.3, 136.2, 130.8, 128.6, 128.5, 128.3, 128.0, 127.0, 65.1. HRMS (ESI-TOF) m/z : $[\text{M}+\text{H}]^+$ calcd for $(\text{C}_{14}\text{H}_{14}\text{NO}^+)$ 196.1121; Found 196.1135.

N-benzylidene-4-methylbenzenesulfonamide (**2.5**)²⁰:



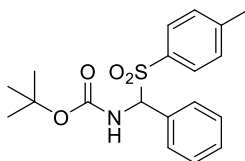
Method C. White solid (2.34 gm, 90%), Melting Point: 113-116 $^{\circ}\text{C}$. IR: 3055, 3027, 2927, 1652, 1575, 1380, 1160 cm^{-1} . ^1H NMR (500 MHz, CHCl_3 - d) δ 9.03 (s, 1H), 7.96 – 7.87 (m, 4H), 7.65 – 7.58 (m, 1H), 7.52 – 7.45 (d, $J = 8.1$ Hz, 2H), 7.35 (d, $J = 8.1$ Hz, 2H), 2.44 (s, 3H). $^{13}\text{C}\{^1\text{H}\}$ NMR (126 MHz, CHCl_3 - d) δ 170.1, 144.6, 134.9, 132.4, 131.3, 130.2, 129.8, 129.1, 128.1, 21.7. HRMS (ESI-TOF) m/z : $[\text{M}+\text{H}]^+$ calcd for $(\text{C}_{14}\text{H}_{14}\text{NO}_2\text{S}^+)$ 260.0740; Found 260.0740.

N-(4-methoxybenzylidene)-4-methylbenzenesulfonamide (**2.6**)²⁰:



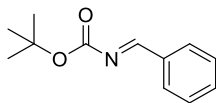
Method C. Yellowish white solid (2.87 gm, 99%), Melting Point: 127-129 °C. IR: 3060, 2955, 1665, 1561, 1374, 1325, 1165 cm⁻¹. ¹H NMR (500 MHz, CHCl₃-*d*) δ 8.93 (s, 1H), 7.92 – 7.85 (m, 4H), 7.32 (d, *J* = 8.1 Hz, 2H), 6.96 (d, *J* = 8.8 Hz, 2H), 3.87 (s, 3H), 2.42 (s, 3H). ¹³C{¹H} NMR (126 MHz, CHCl₃-*d*) δ 169.2, 165.3, 144.3, 135.7, 133.7, 129.7, 127.9, 125.2, 114.7, 55.7, 21.6. HRMS (ESI-TOF) *m/z*: [M+H]⁺ calcd for (C₁₅H₁₆NO₃S⁺) 290.0845; Found 290.0843.

tert-butyl (phenyl(tosyl)methyl)carbamate (**2.7a**)²¹:



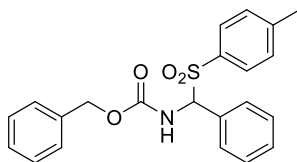
Method D, Step-1. White solid (1.8 gm, 99%), Melting Point: 160-162 °C. IR: 3363, 3262, 3066, 2981, 1692, 1506, 1496, 1304, 1139, 1065 cm⁻¹. ¹H NMR (500 MHz, CHCl₃-*d*) δ 7.79 (d, *J* = 8.0 Hz, 2H), 7.49 – 7.38 (m, 5H), 7.33 (d, *J* = 8.0 Hz, 2H), 5.91 (d, *J* = 10.7 Hz, 1H), 5.85 (d, *J* = 10.7 Hz, 1H), 2.43 (s, 3H), 1.26 (s, 9H). ¹³C{¹H} NMR (126 MHz, CHCl₃-*d*) δ 153.5, 145.0, 133.8, 130.1, 129.8, 129.7, 129.5, 129.0, 128.7, 81.1, 73.9, 28.0, 21.7. HRMS (ESI-TOF) *m/z*: [M+Na]⁺ calcd for (C₁₉H₂₃NO₄SN⁺) 384.1240; Found: 384.1249.

tert-butyl (*E*)-benzylidenecarbamate (**2.7**)²¹:



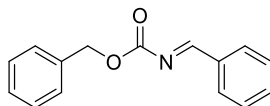
Method D, Step-2. Colorless oil (185 mg, 90%). IR: 3026, 2979, 1718, 1639, 1269 cm⁻¹. ¹H NMR (500 MHz, CHCl₃-*d*) δ 8.89 (s, 1H), 7.92 (d, *J* = 7.2 Hz, 2H), 7.57 (m, 1H), 7.48 (t, *J* = 7.6 Hz, 2H), 1.64 – 1.56 (m, 9H). ¹³C{¹H} NMR (126 MHz, CHCl₃-*d*) δ 169.8, 162.7, 134.1, 133.5, 130.2, 128.9, 82.3, 27.9. HRMS (ESI-TOF) *m/z*: [M+H]⁺ calcd for (C₁₂H₁₆NO₂⁺) 206.1176; Found 206.1176.

benzyl (*phenyl*(*tosyl*)*methyl*)carbamate (**2.8a**)²¹:



Method D, Step-1. White solid (1.6 gm, 84%), Melting Point: 158-160 °C. IR: 3365, 3064, 3032, 2973, 1698, 1508, 1316, 1304, 1146, 1038 cm⁻¹. ¹H NMR (500 MHz, DMSO-*d*₆) δ 9.13 (d, *J* = 10.7 Hz, 1H), 7.67 (d, *J* = 8.0 Hz, 2H), 7.60 (d, *J* = 6.8 Hz, 2H), 7.36 (m, 8H), 7.20 (d, *J* = 6.8 Hz, 2H), 6.03 (d, *J* = 10.7 Hz, 1H), 4.90 (d, *J* = 12.6 Hz, 1H), 4.84 (d, *J* = 12.6 Hz, 1H), 2.38 (s, 3H). ¹³C{¹H} NMR (126 MHz, DMSO-*d*₆) δ 155.7, 145.1, 136.8, 134.2, 130.9, 130.1, 130.0, 129.8, 129.6, 128.8, 128.6, 128.4, 128.1, 75.3, 66.5, 21.7. HRMS (ESI-TOF) *m/z*: [M+H]⁺ calcd for (C₂₂H₂₂NO₄S⁺) 396.1264; Found 396.1266.

benzyl (*E*)-benzylidenecarbamate (**2.8**)²¹:



Method D, Step-2. Colorless oil (216 mg, 90%). IR: 3058, 2967, 1719, 1185, 1034 cm^{-1} . ^1H NMR (500 MHz, $\text{CHCl}_3\text{-}d$) δ 8.79 (s, 1H), 7.79 – 7.75 (m, 2H), 7.44 – 7.39 (m, 1H), 7.35 – 7.29 (m, 4H), 7.26 – 7.19 (m, 3H), 5.16 (s, 2H). $^{13}\text{C}\{^1\text{H}\}$ NMR (126 MHz, $\text{CHCl}_3\text{-}d$) δ 171.7, 164.1, 138.2, 135.7, 134.3, 130.8, 129.4, 129.3, 129.0, 128.6, 69.3. HRMS (ESI-TOF) m/z : $[\text{M}+\text{H}]^+$ calcd for ($\text{C}_{15}\text{H}_{14}\text{NO}_2^+$) 240.1019; Found 240.1016.

*trimethylsulfoxonium iodide (2.9)*²²:

To a solution of dimethyl sulfoxide (4.23 mmol) in a 50 mL dry round bottom flask, methyl iodide (12.7 mmol, 3 equiv) was added and refluxed for three days. After that, the solvent was evaporated, and the crude solid was washed with acetone and dried over a vacuum to get the desired product.

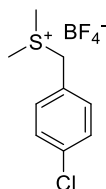


Yellowish amorphous solid (186 mg, 20%). Melting Point: 175 $^{\circ}\text{C}$. IR: 2960, 1226, 1039 cm^{-1} . ^1H NMR (500 MHz, $\text{DMSO-}d_6$) δ 3.84 (s, 9H). $^{13}\text{C}\{^1\text{H}\}$ NMR (126 MHz, $\text{DMSO-}d_6$) δ 39.4. HRMS (ESI-TOF) m/z : $[\text{M}+\text{H}]^+$ calcd for ($\text{C}_3\text{H}_9\text{OS}^+$) 93.0369; Found 93.0385.

(4-chlorobenzyl)dimethylsulfonium tetrafluoroborate (2.10):

To a solution of dry dichloromethane (30 mL) in a 100 mL dry round bottom flask, the 4-chlorobenzyl alcohol (1 equiv, 10 mmol) was added, followed by dimethyl sulfide (2 equiv, 20 mmol) and placed under nitrogen gas. A solution of tetrafluoroboric acid (tetrafluoroboric acid diethyl ether complex) (1 equiv, 10 mmol) was added dropwise for 5 minutes at 0 $^{\circ}\text{C}$. The mixture was stirred for 12 hours at room temperature. Evaporation of the solvent under reduced pressure

gave a colorless, thick oil, which was precipitated with diethyl ether to obtain the desired salt as a solid.

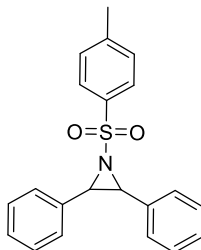


Colorless, crystalline solid (1.6 gm, 86%). Melting Point: 68-70 °C. IR: 3033, 2942, 1026, 780 cm^{-1} . ^1H NMR (500 MHz, CHCl_3 -*d*) δ 7.56 (d, J = 8.4 Hz, 2H), 7.47 (d, J = 8.4 Hz, 2H), 4.62 (s, 2H), 2.78 (s, 6H). $^{13}\text{C}\{^1\text{H}\}$ NMR (126 MHz, CHCl_3 -*d*) δ 139.7, 137.7, 134.6, 132.5, 50.1, 28.9. HRMS (ESI-TOF) m/z : $[\text{M}+\text{H}]^+$ calcd for $(\text{C}_9\text{H}_{13}\text{ClS}^+)$ 187.0343; Found 187.0349.

Synthesis of aziridines:

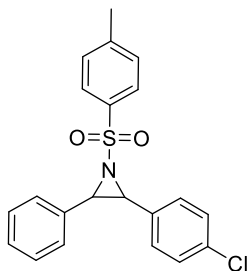
To a solution of dry dichloromethane (20 mL) in a 50 mL dry round bottom flask, different imines (0.25 mmol, 1 equivalent), and sulfonium salts (0.5 mmol, 2 equivalents) were added, followed by TBD or MTBD base (0.55 mmol, 2.2 equivalents). The reaction was stirred for 30-45 minutes at room temperature. After that, the solvent was evaporated, and the crude product was purified using automated CombiFlash chromatography (silica gel 20-40 microns, using ethyl acetate in hexane) to yield aziridines (**A1-A7**).

2,3-diphenyl-1-tosylaziridine (**A1**)²³:



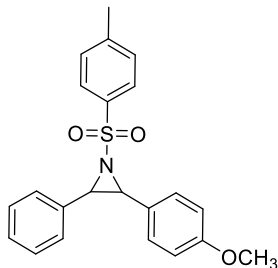
(79 mg, 90%, trans:cis=80:20). Trans- ¹H NMR (500 MHz, CHCl₃-*d*) δ 7.65 (d, *J* = 8.0 Hz, 2H), 7.47 – 7.42 (m, 4H), 7.41 – 7.34 (m, 6H), 7.21 (d, *J* = 8.0 Hz, 2H), 4.29 (s, 2H), 2.39 (s, 3H). ¹³C{¹H} NMR (126 MHz, CHCl₃-*d*) δ 144.0, 137.0, 133.0, 129.5, 128.7, 128.5, 128.3, 127.6, 50.4, 21.6. Cis- ¹H NMR (500 MHz, CHCl₃-*d*) δ 7.98 (d, *J* = 8.3 Hz, 2H), 7.37 (d, *J* = 8.3 Hz, 2H), 7.16 – 7.11 (m, 6H), 7.09 – 7.03 (m, 4H), 4.24 (s, 2H), 2.46 (s, 3H). ¹³C{¹H} NMR (126 MHz, CHCl₃-*d*) δ 144.8, 134.8, 132.0, 129.9, 128.1, 128.0, 127.8, 127.8, 47.5, 21.7. HRMS (ESI-TOF) *m/z*: [(M+H)+] calcd for (C₂₁H₂₀NO₂S⁺) 350.1209; Found 350.1208.

2-(4-chlorophenyl)-3-phenyl-1-tosylaziridine (**A2**)²⁴:



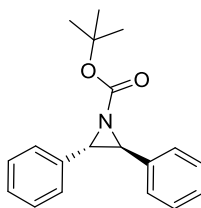
(73 mg, 76%, trans:cis=44:56). IR: 3063, 1596, 1492, 1320, 1154, 1084, 903 cm⁻¹. Cis- ¹H NMR (500 MHz, CHCl₃-*d*) δ 7.95 (d, *J* = 8.3 Hz, 2H), 7.38 – 7.32 (m, 7H), 7.09 (d, *J* = 8.3 Hz, 2H), 6.98 (d, *J* = 8.3 Hz, 2H), 4.24 (d, *J* = 4.4 Hz, 1H), 4.18 (d, *J* = 4.4 Hz, 1H), 2.44 (s, 3H). ¹³C{¹H} NMR (126 MHz, CHCl₃-*d*) δ 145.0, 136.9, 133.7, 129.9, 129.56, 129.1, 128.7, 128.5, 128.3, 128.2, 128.1, 127.7, 47.6, 46.7, 21.7. HRMS (ESI-TOF) *m/z*: [(M+H)+] calcd for (C₂₁H₁₉ClNO₂S⁺) 384.0820; Found 384.0815.

2-(4-methoxyphenyl)-3-phenyl-1-tosylaziridine (**A3**)²⁴:



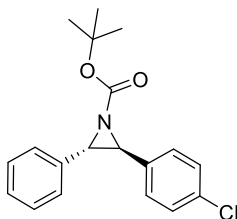
Reaction between **5.5** with **2b** (69 mg, 73%, trans:cis=60:40). Reaction between **5.6** with **2a** (68mg, 71%, trans:cis=60:40). IR: 3007, 1612, 1595, 1514, 1456, 1336, 1255 cm^{-1} . Trans- ^1H NMR (500 MHz, CHCl_3 -*d*) δ 7.65 – 7.62 (m, 2H), 7.42 – 7.31 (m, 7H), 7.22 – 7.18 (d, J = 9.0 Hz, 2H), 6.91 – 6.87 (d, J = 9.0 Hz, 2H), 4.34 (d, J = 4.5 Hz, 1H), 4.16 – 4.14 (d, J = 4.5 Hz, 1H), 3.81 (s, 3H), 2.38 (s, 3H). $^{13}\text{C}\{^1\text{H}\}$ NMR (126 MHz, CHCl_3 -*d*) δ 159.9, 143.9, 137.1911, 133.7, 130.0, 129.4, 128.6, 128.5, 127.9, 127.5, 124.3, 113.8, 55.3, 51.3, 49.3, 21.6. Cis- ^1H NMR (500 MHz, CHCl_3 -*d*) δ 7.98 – 7.94 (d, J = 8.0 Hz, 2H), 7.36 (d, J = 8.0 Hz, 2H), 7.17 – 7.12 (m, 3H), 7.09 – 7.03 (m, 2H), 6.98 – 6.93 (d, J = 9.0 Hz, 2H), 6.68 – 6.63 (d, J = 9.0 Hz, 2H), 4.19 (d, J = 7 Hz, 2H), 3.69 (s, 3H), 2.45 (s, 3H). $^{13}\text{C}\{^1\text{H}\}$ NMR (126 MHz, CHCl_3 -*d*) δ 159.1, 144.7, 134.9, 132.2, 129.8, 129.0, 128.0, 128.0, 127.8, 127.7, 124.0, 113.4, 55.1, 47.5, 47.2, 21.7. HRMS (ESI-TOF) m/z : $[(\text{M}+\text{H})^+]$ calcd for $(\text{C}_{22}\text{H}_{22}\text{NO}_3\text{S}^+)$ 380.1315; Found 380.1311.

tert-butyl 2,3-diphenylaziridine-1-carboxylate (**A4**)²³:



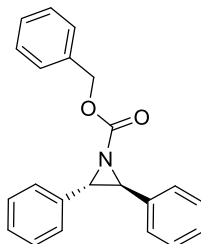
(53mg, 71%, trans:cis=95:5). ¹H NMR (500 MHz, CHCl₃-d) δ 7.41 – 7.31 (m, 10H), 3.80 (s, 2H), 1.21 (s, 9H). ¹³C{¹H} NMR (126 MHz, CHCl₃-d) δ 159.4, 135.6, 128.5, 128.1, 127.0, 81.5, 47.6, 27.7. HRMS (ESI-TOF) m/z: [(M+H)+] calcd for (C₁₉H₂₂NO₂⁺-Boc) 196.1121; Found: 196.1130.

tert-butyl 2-(4-chlorophenyl)-3-phenylaziridine-1-carboxylate (**A5**):



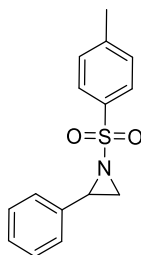
(47mg, 57%). IR: 2963, 1710, 1493, 1456, 1308, 1257, 1227 cm⁻¹. Trans- ¹H NMR (500 MHz, CHCl₃-d) δ 7.32 (m, 9H), 3.84 – 3.76 (d, *J* = 3.0 Hz, 1H), 3.71 – 3.62 (d, *J* = 3.0 Hz, 1H), 1.20 (s, 9H). ¹³C{¹H} NMR (126 MHz, CHCl₃-d) δ 159.2, 134.9, 134.4, 133.9, 128.7, 128.5, 128.3, 128.2, 127.1, 81.7, 48.4, 46.2, 27.6. HRMS (ESI-TOF) m/z: [(M+H)+] calcd for (C₁₉H₂₁ClNO₂⁺-Boc) 230.0731; Found: 230.0739.

benzyl 2,3-diphenylaziridine-1-carboxylate (**A6**)²⁵:



(39mg, 47%, trans:cis=85:15 with TBD base). (44 mg, 53% with MTBD base). Trans- ¹H NMR (500 MHz, CHCl₃-d) δ 7.37 – 7.23 (m, 13H), 7.00 (dd, *J* = 7.5, 1.4 Hz, 2H), 5.03 (d, *J* = 12.1 Hz, 1H), 4.92 (d, *J* = 12.1 Hz, 1H), 3.78 (s, 2H). ¹³C{¹H} NMR (126 MHz, CHCl₃-d) δ 160.4, 135.4, 128.7, 128.6, 128.4, 128.3, 128.2, 128.1, 126.6, 68.2, 48.4. m/z: [M+H]⁺ calcd for (C₂₂H₂₀NO₂)⁺ 330.1489; Found 330.1485.

2-phenyl-1-tosylaziridine (**A7**)²⁶:



White solid (24 mg, 35%). Melting Point: 90-92 °C. IR: 3039, 1594, 1494, 1456, 1385, 1156, 1091, 905 cm⁻¹. ¹H NMR (500 MHz, CHCl₃-d) δ 7.87 (d, *J* = 8.2 Hz, 2H), 7.31 (m, 5H), 7.24 – 7.20 (m, 2H), 3.78 (dd, *J* = 7.1, 4.4 Hz, 1H), 2.99 (d, *J* = 7.1 Hz, 1H), 2.43 (s, 3H), 2.39 (d, *J* = 4.4 Hz, 1H). ¹³C{¹H} NMR (126 MHz, CHCl₃-d) δ 144.7, 135.0, 129.8, 128.6, 128.3, 128.0, 126.6, 41.0, 36.0, 21.7. HRMS (ESI-TOF) m/z: [M+H]⁺ calcd for (C₁₅H₁₆NO₂)⁺ 274.0896; Found 274.0899.

APPENDIX

APPENDIX

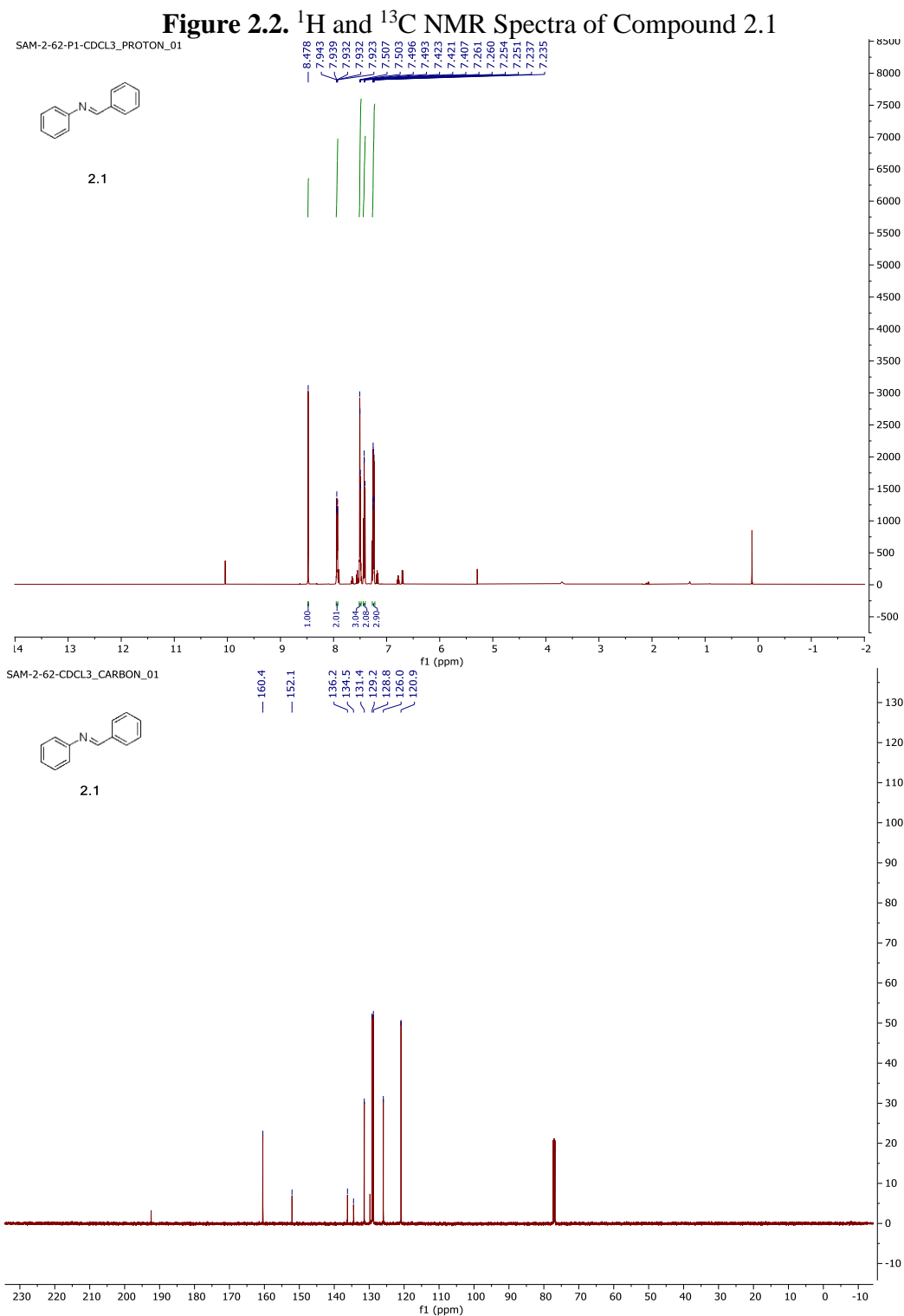


Figure 2.3. ^1H and ^{13}C NMR Spectra of Compound 2.2

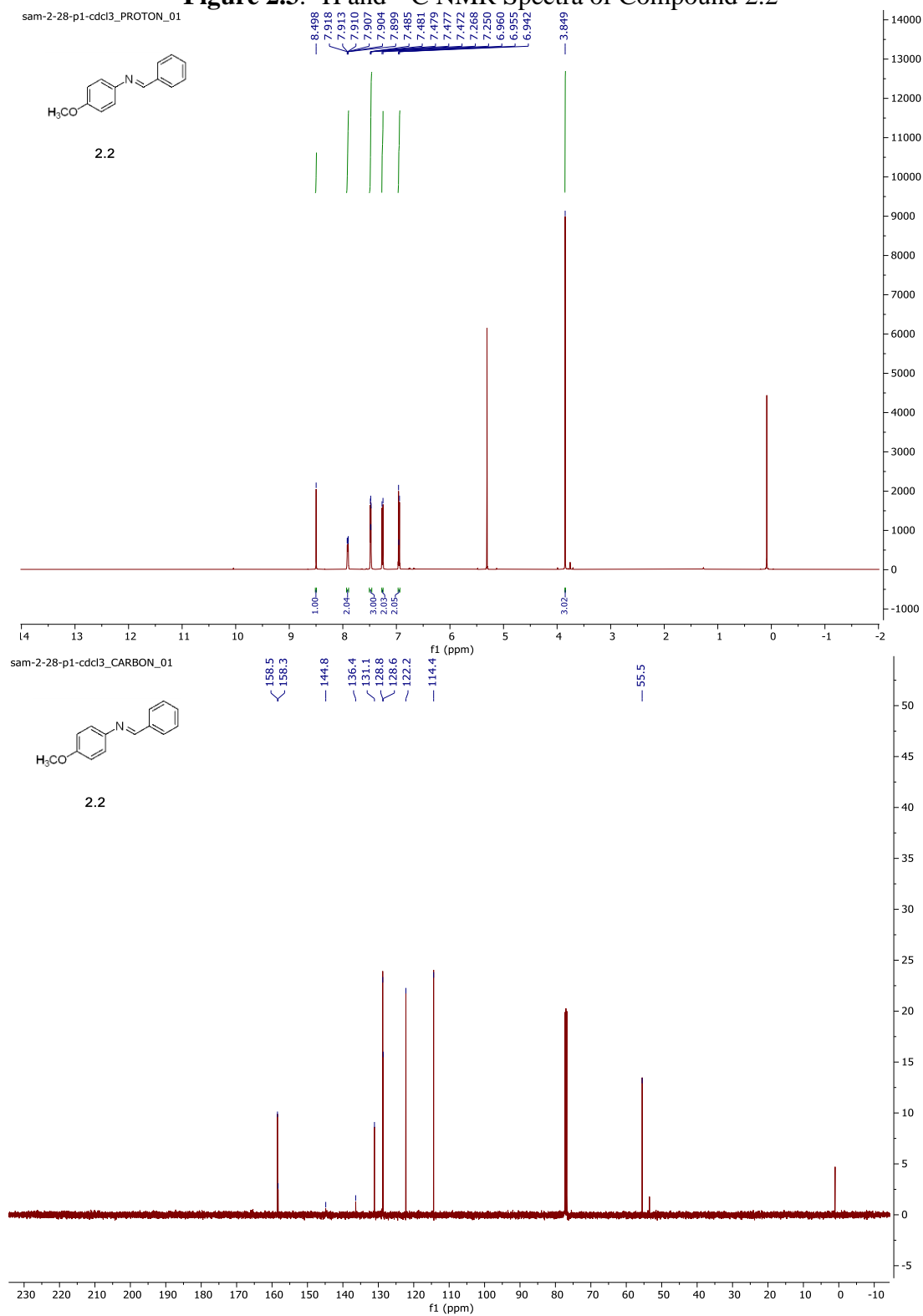


Figure 2.4. ^1H and ^{13}C NMR Spectra of Compound 2.3

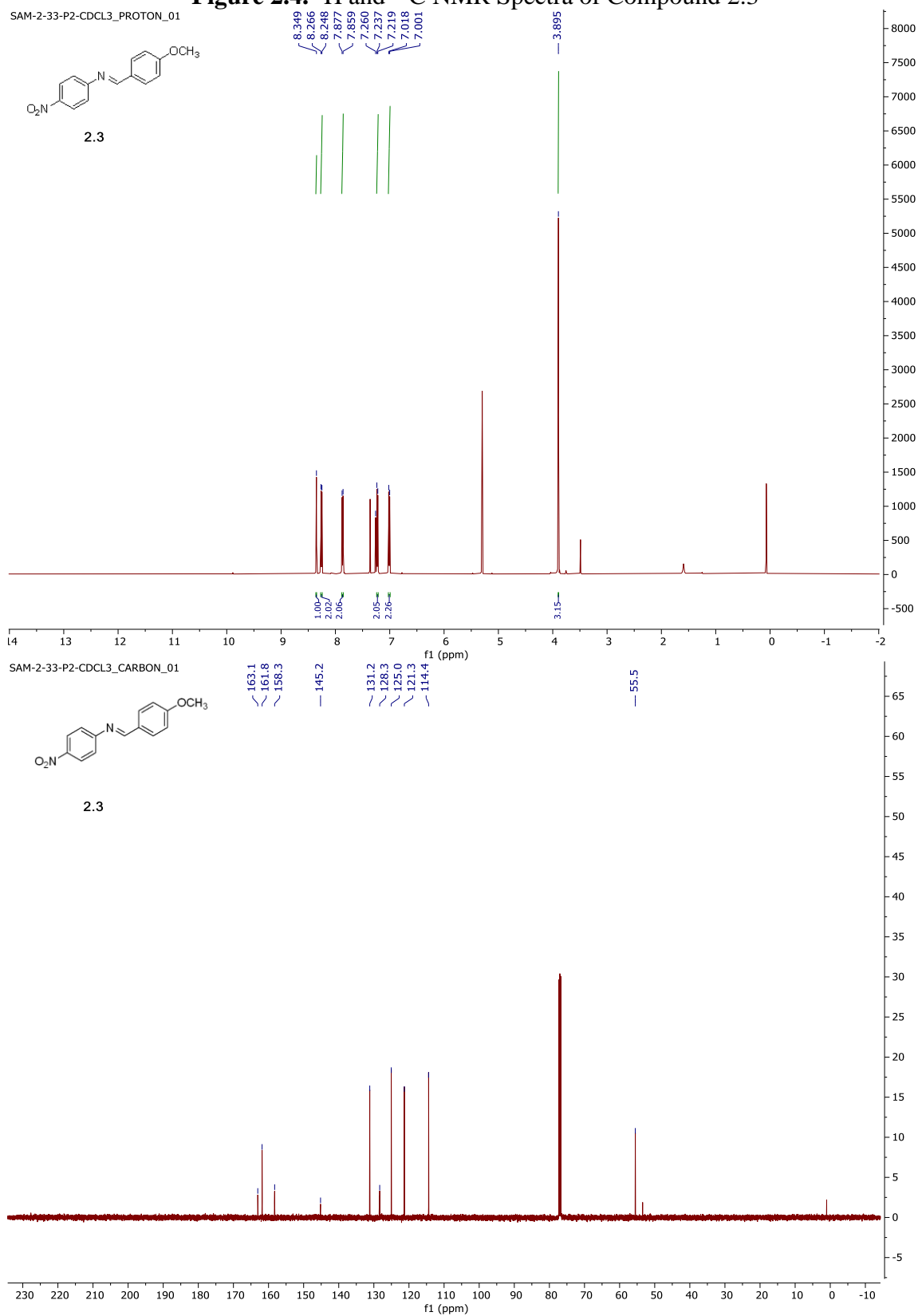


Figure 2.5. ^1H and ^{13}C NMR Spectra of Compound 2.4

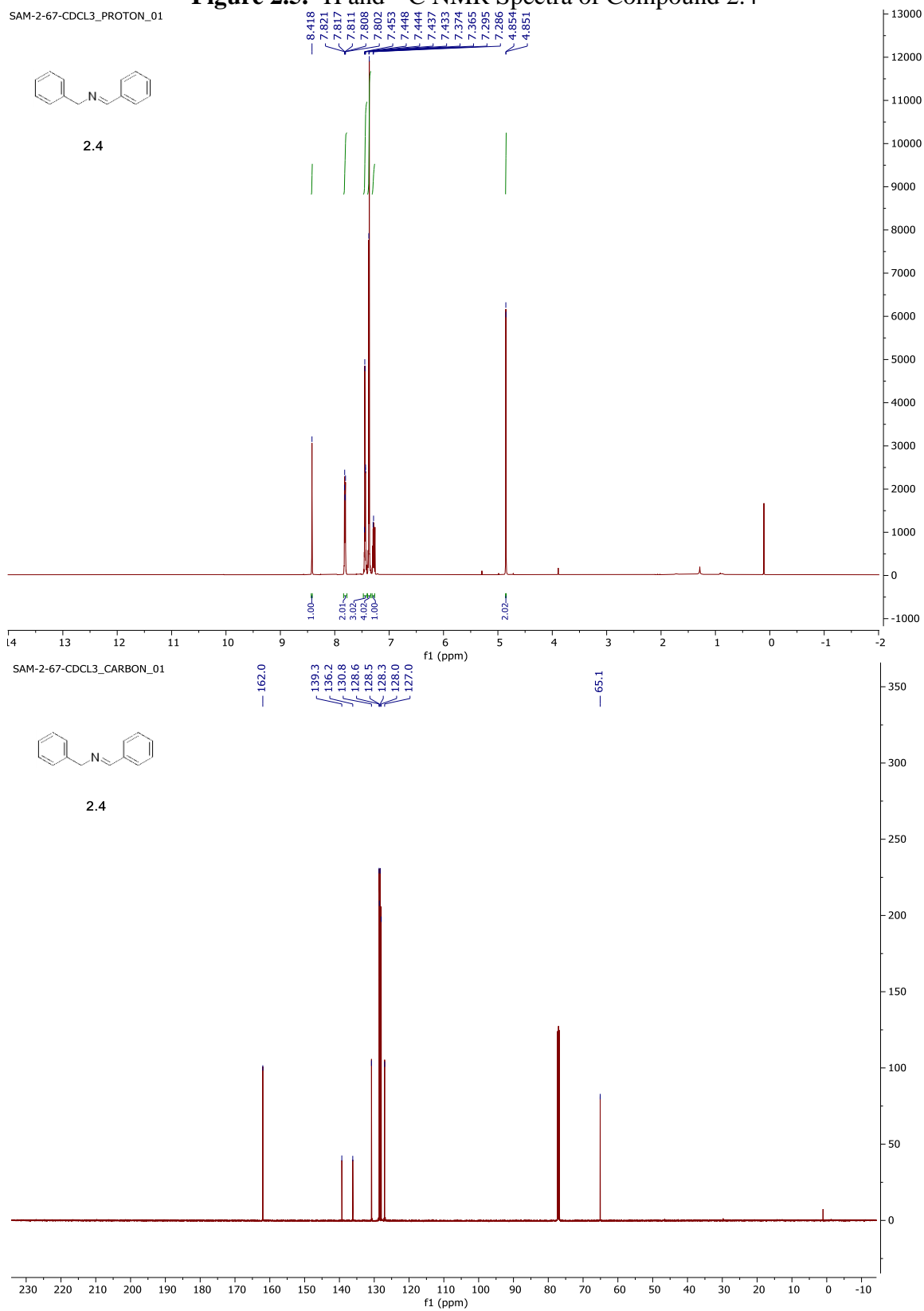


Figure 2.6. ^1H and ^{13}C NMR Spectra of Compound 2.5

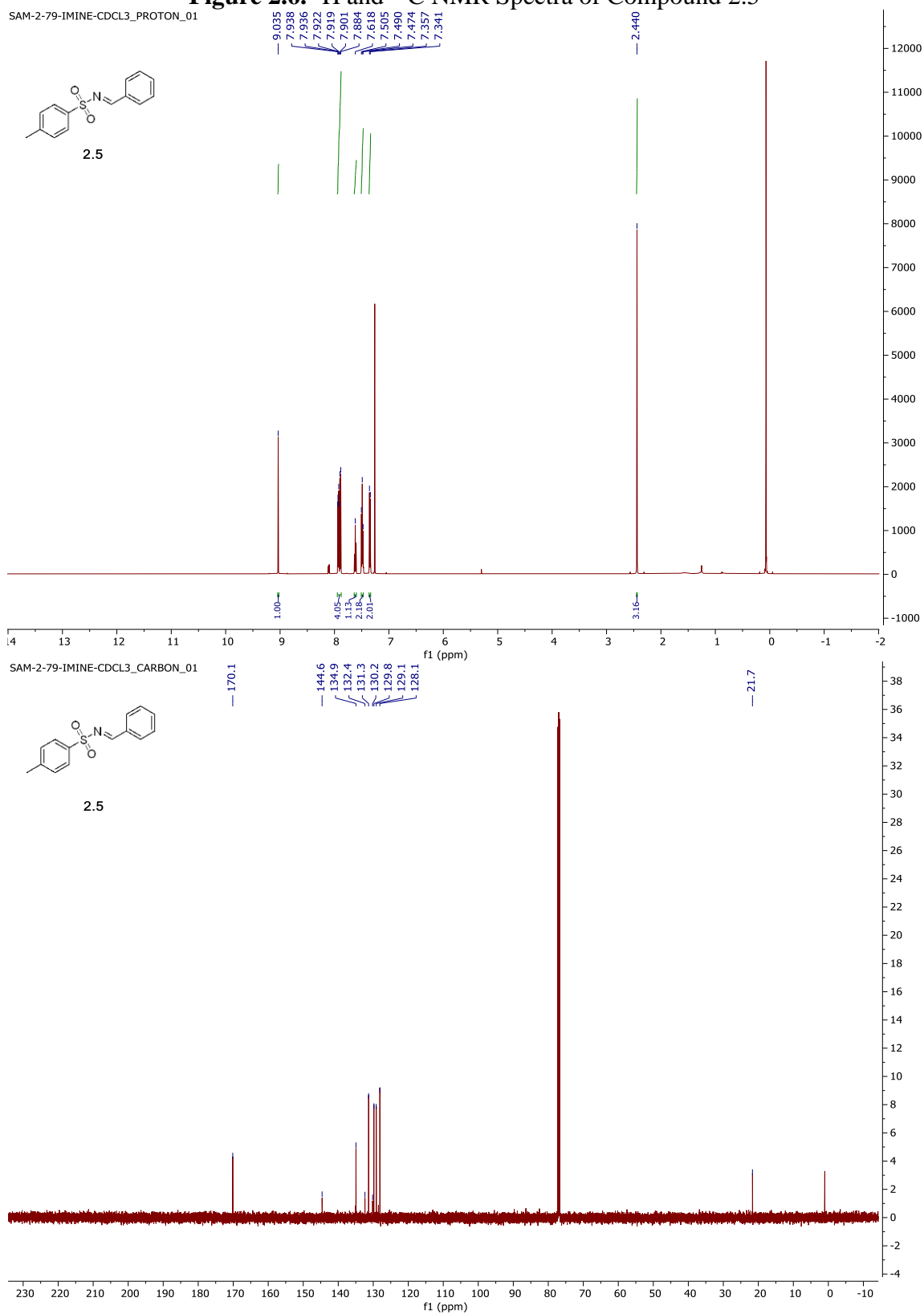


Figure 2.7. ^1H and ^{13}C NMR Spectra of Compound 2.6

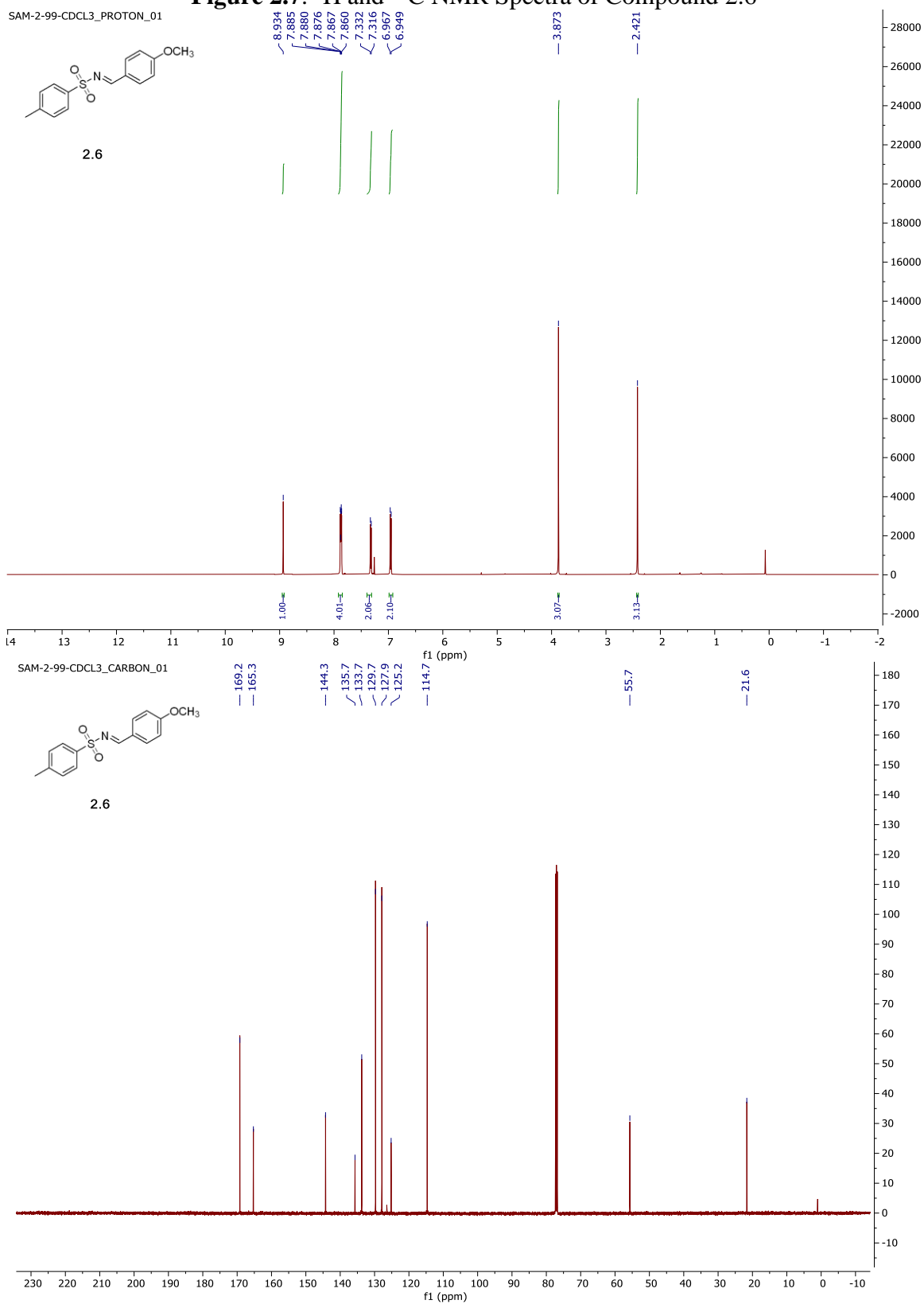


Figure 2.8. ^1H and ^{13}C NMR Spectra of Compound 2.7a

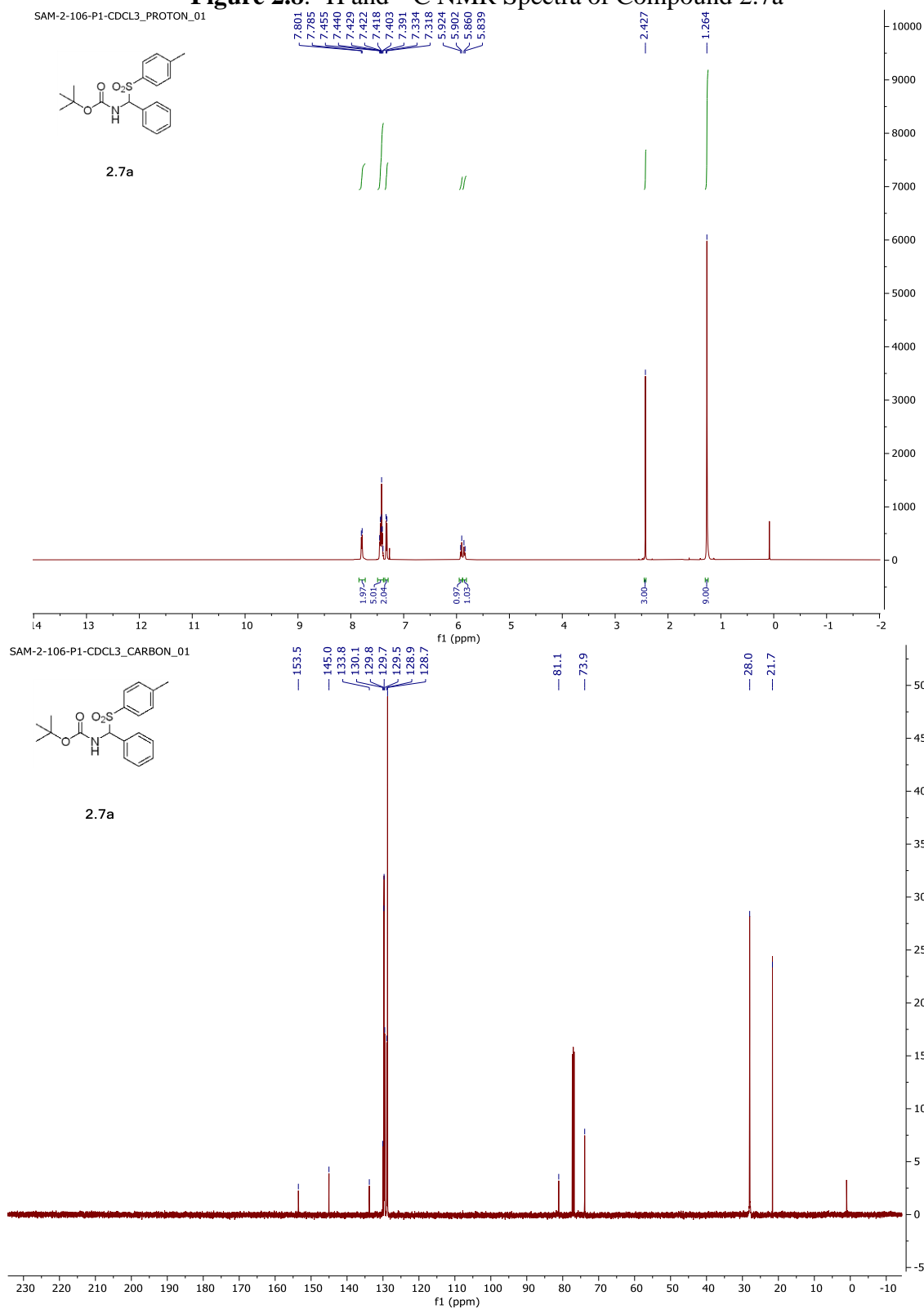


Figure 2.9. ^1H and ^{13}C NMR Spectra of Compound 2.7

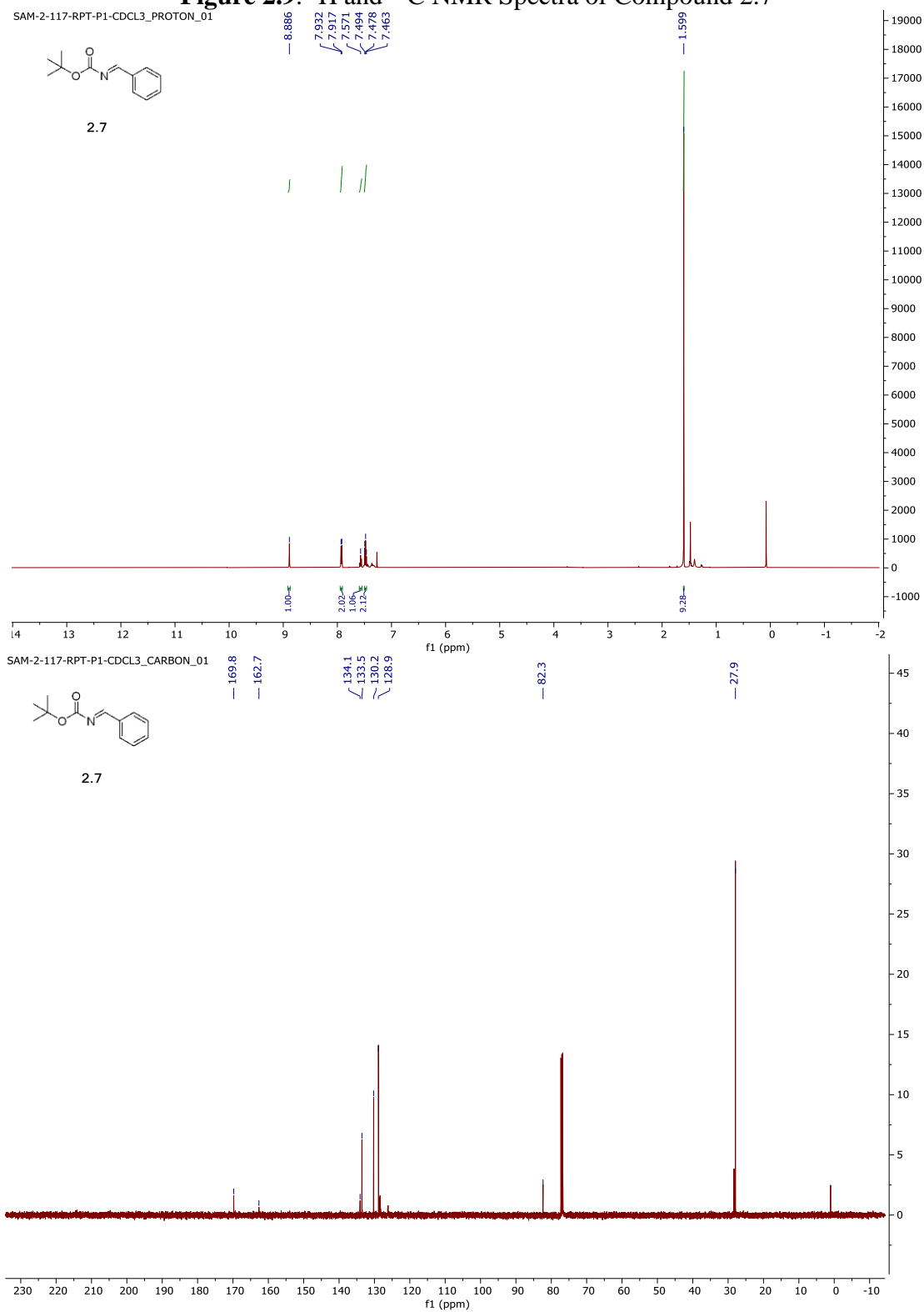


Figure 2.10. ^1H and ^{13}C NMR Spectra of Compound 2.8a

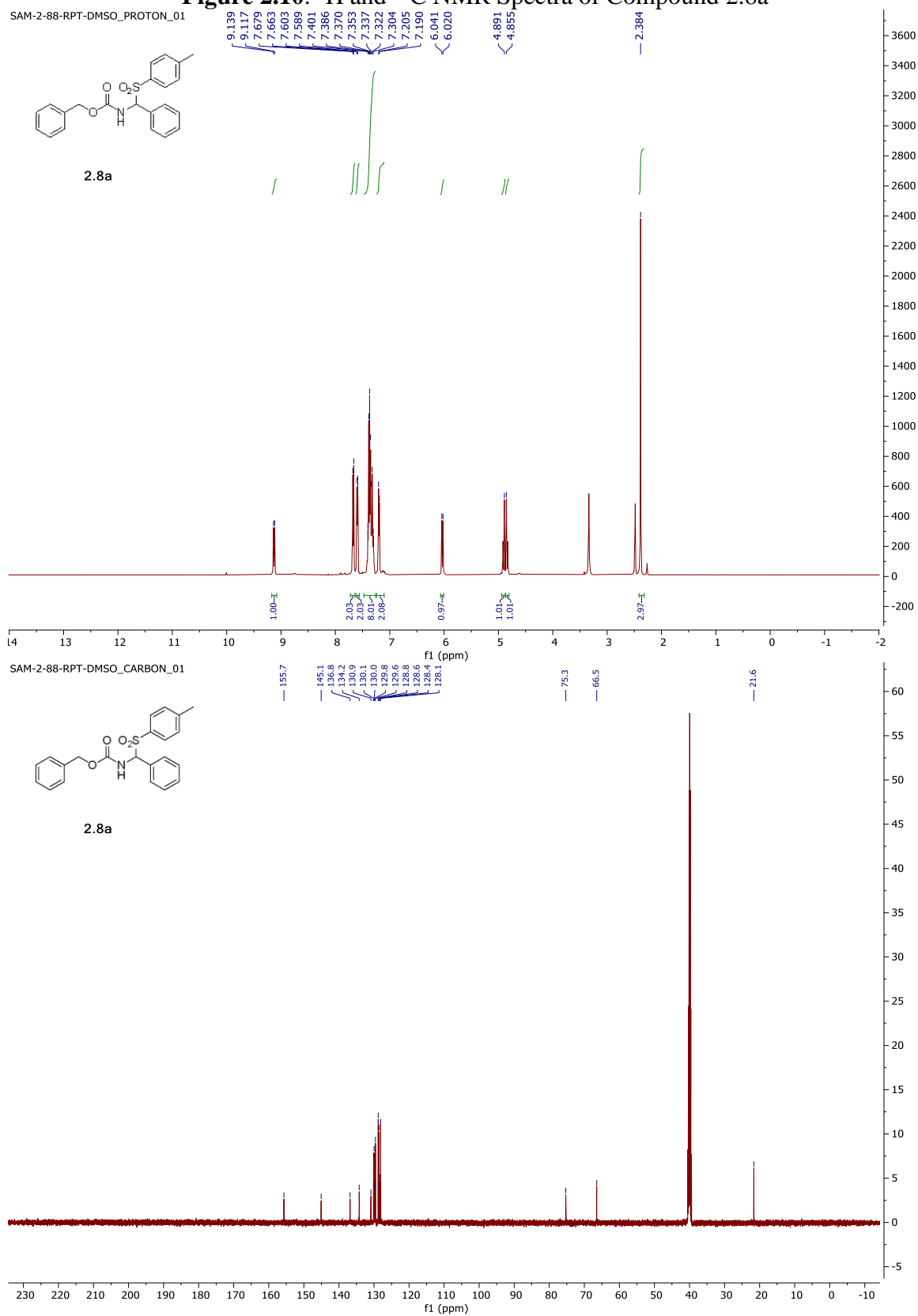


Figure 2.11. ^1H and ^{13}C NMR Spectra of Compound 2.8

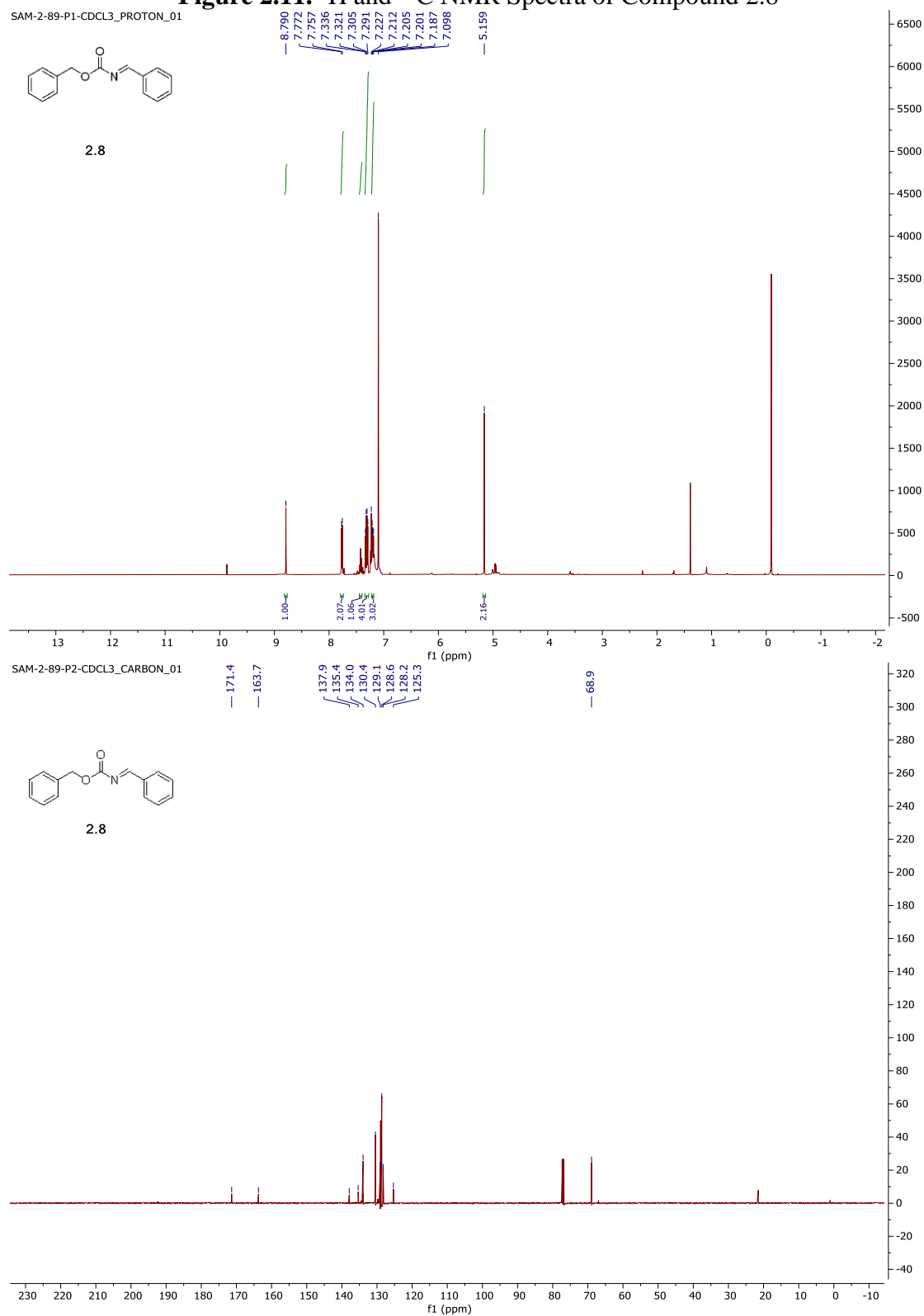


Figure 2.12. ^1H and ^{13}C NMR Spectra of Compound 2.9

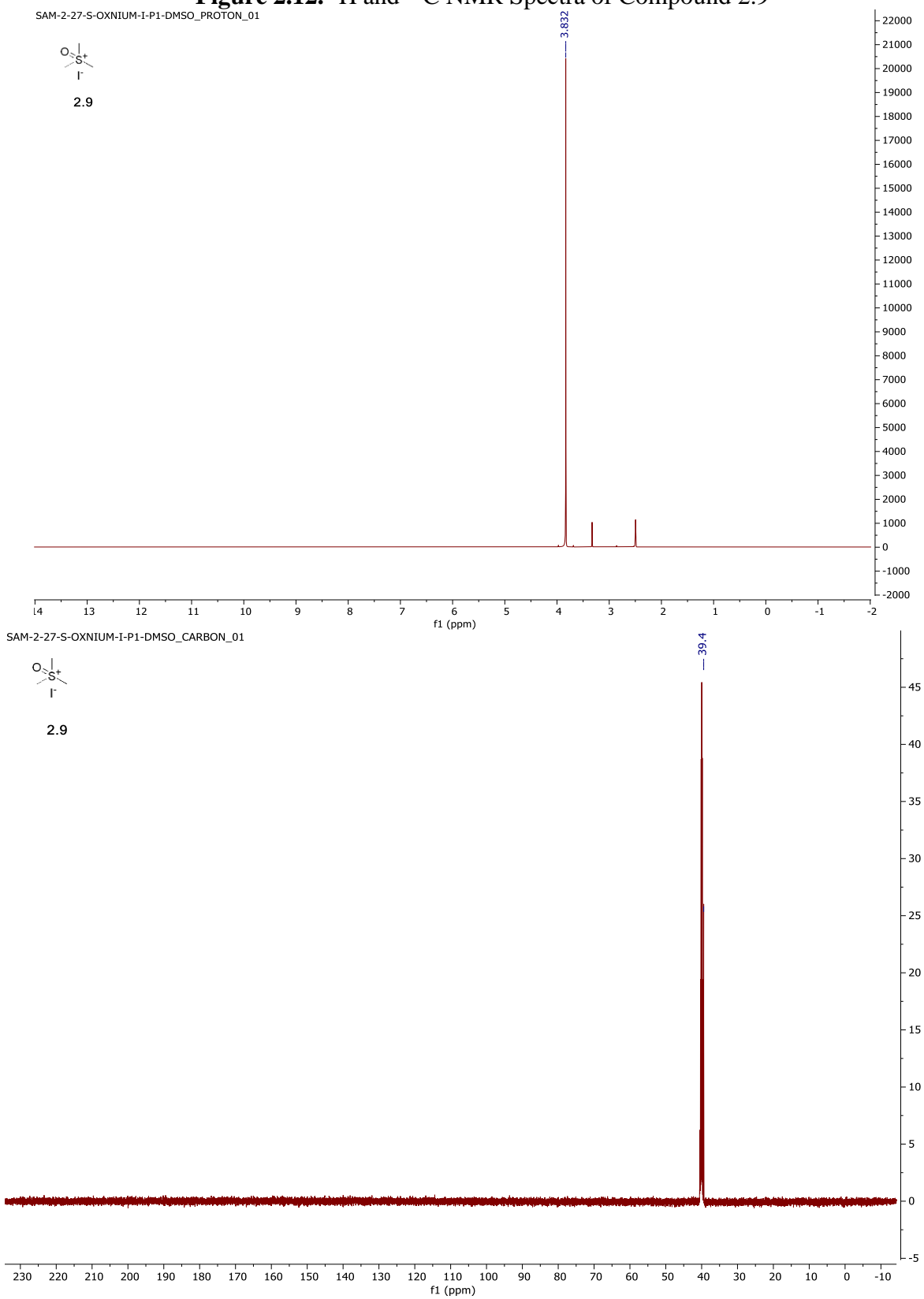


Figure 2.13. ^1H and ^{13}C NMR Spectra of Compound 2.10

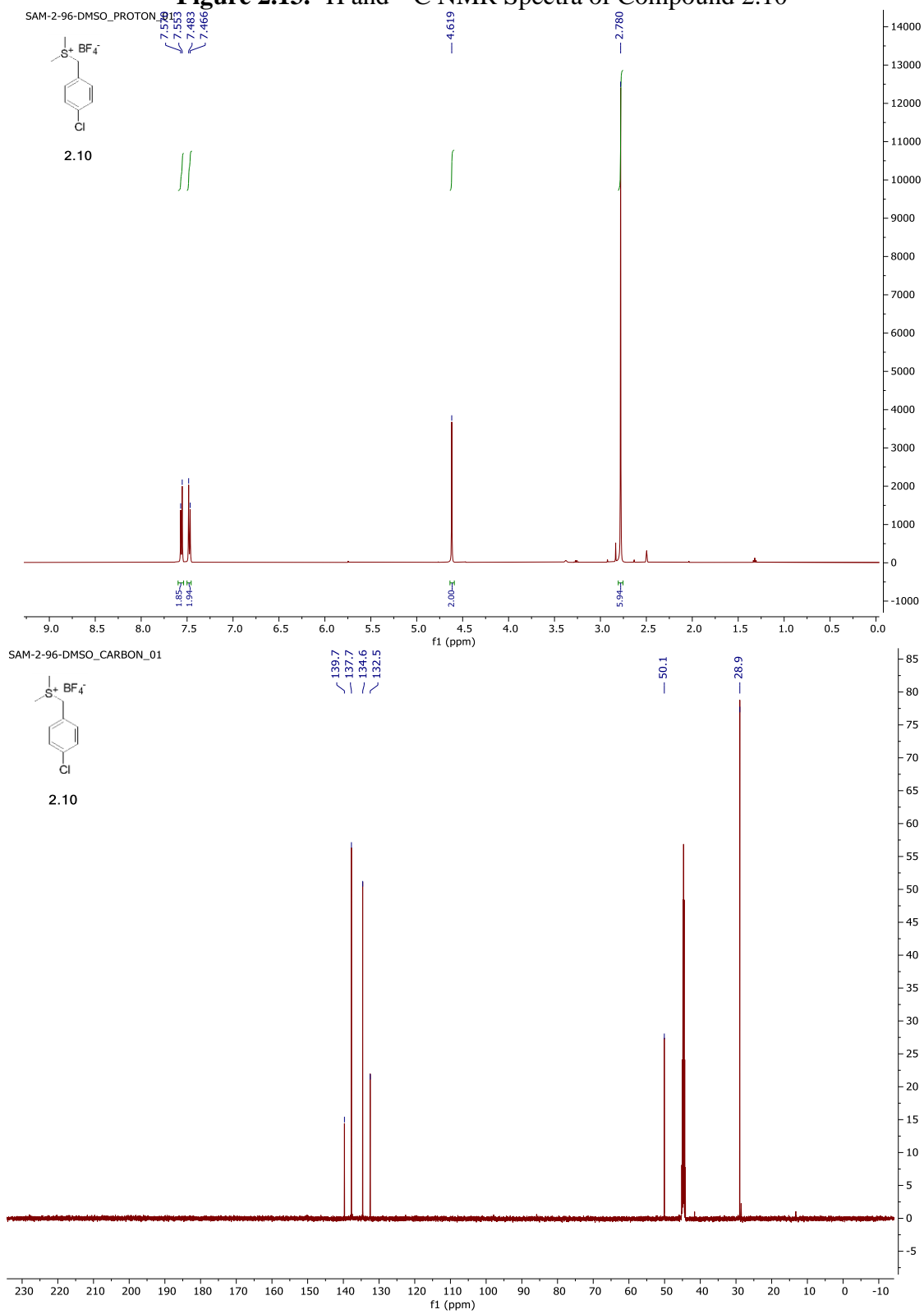


Figure 2.14. ^1H and ^{13}C NMR Spectra of Compound A1 (trans)

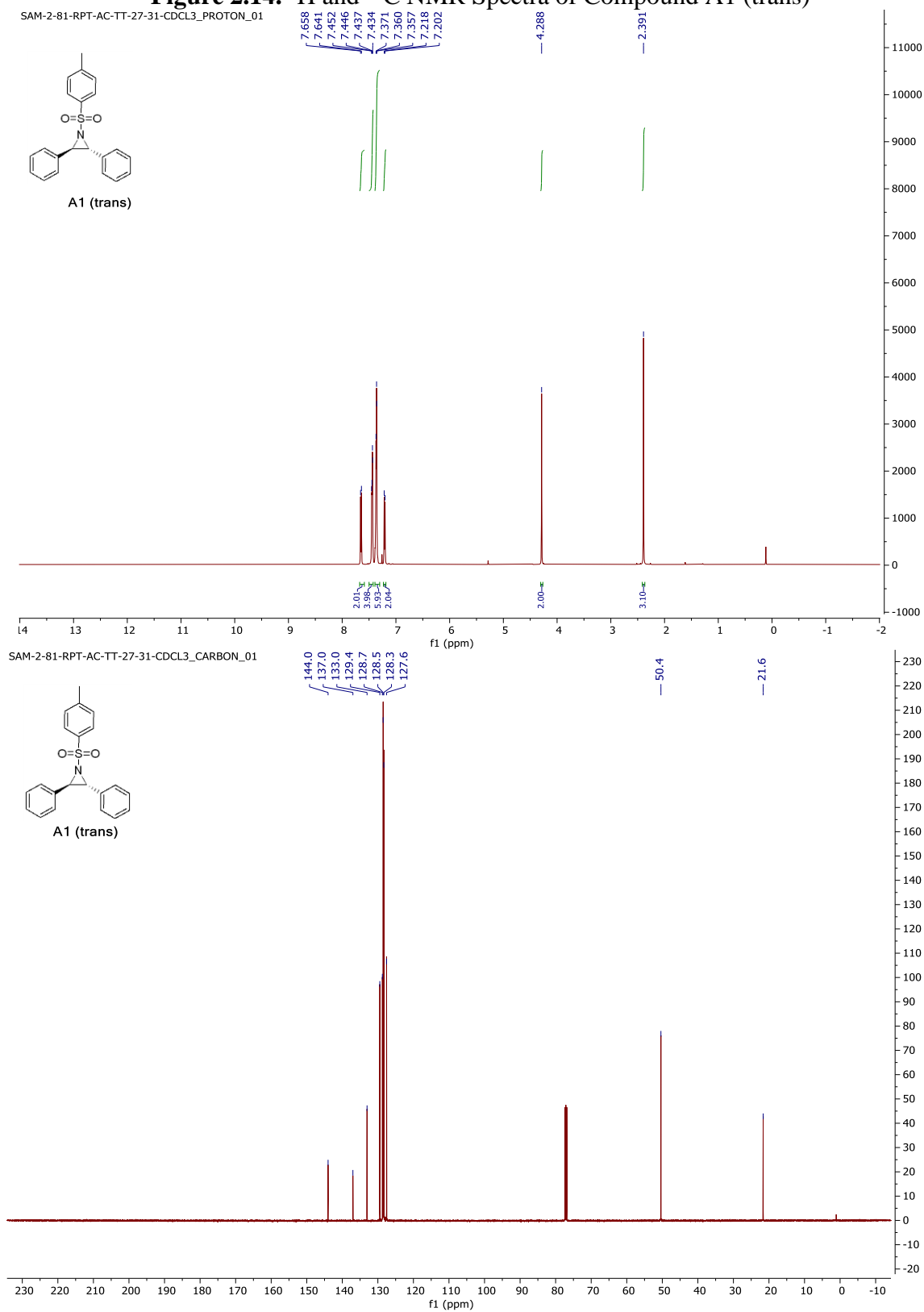


Figure 2.15. ^1H and ^{13}C NMR Spectra of Compound A1 (cis)

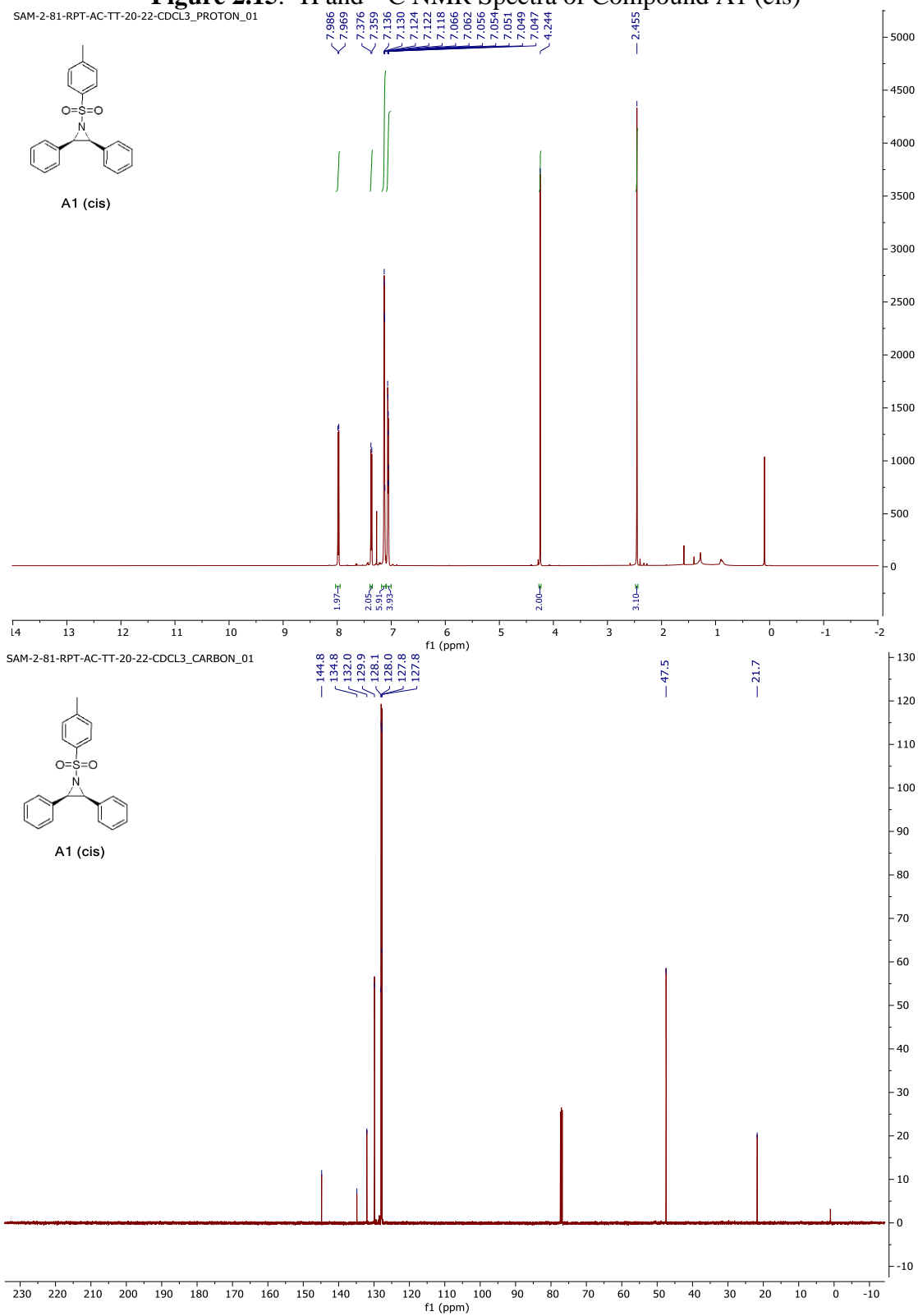
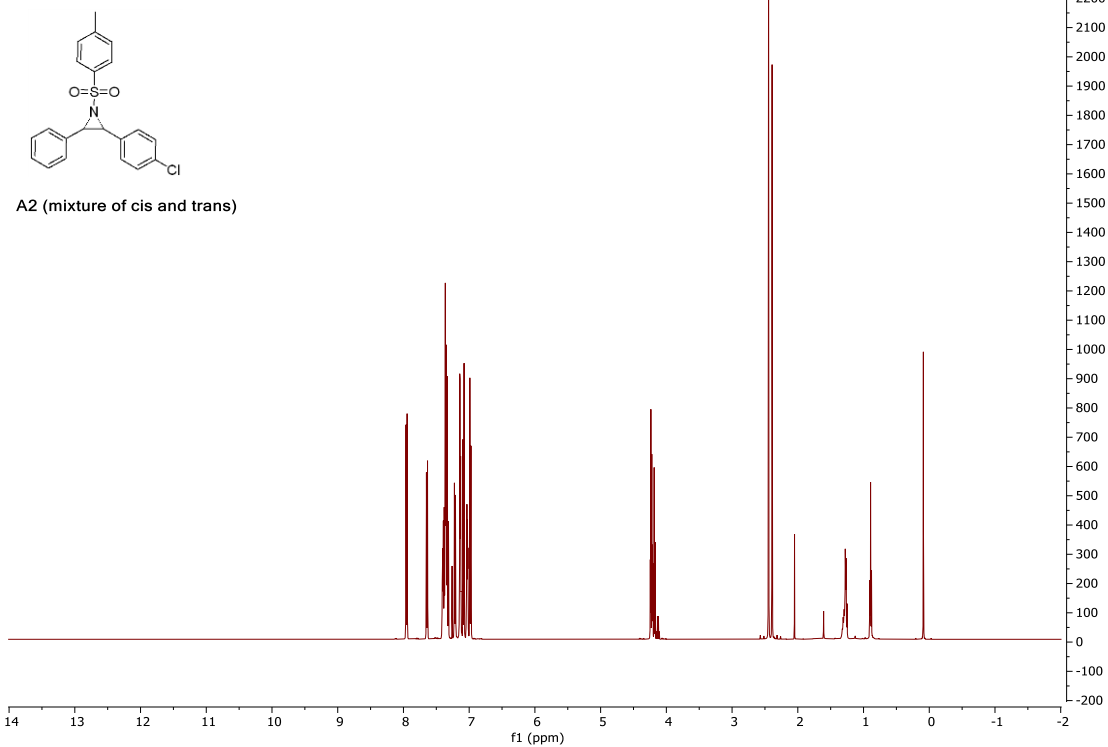


Figure 2.16. ^1H and ^{13}C NMR Spectra of Compound A2 (mixture)

SAM-2-103-AC-TT-14-CDCL3_PROTON_01



SAM-2-103-AC-TT-14-CDCL3_CARBON_01

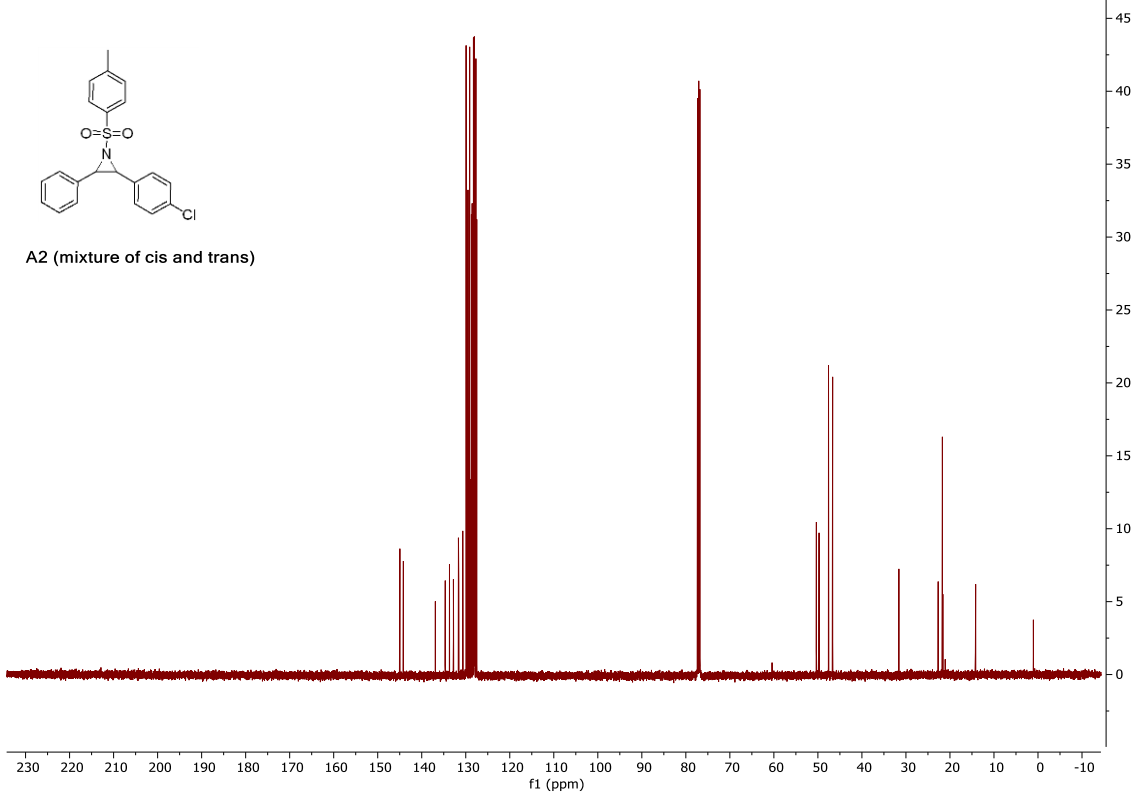


Figure 2.17. ^1H and ^{13}C NMR Spectra of Compound A3 (trans)

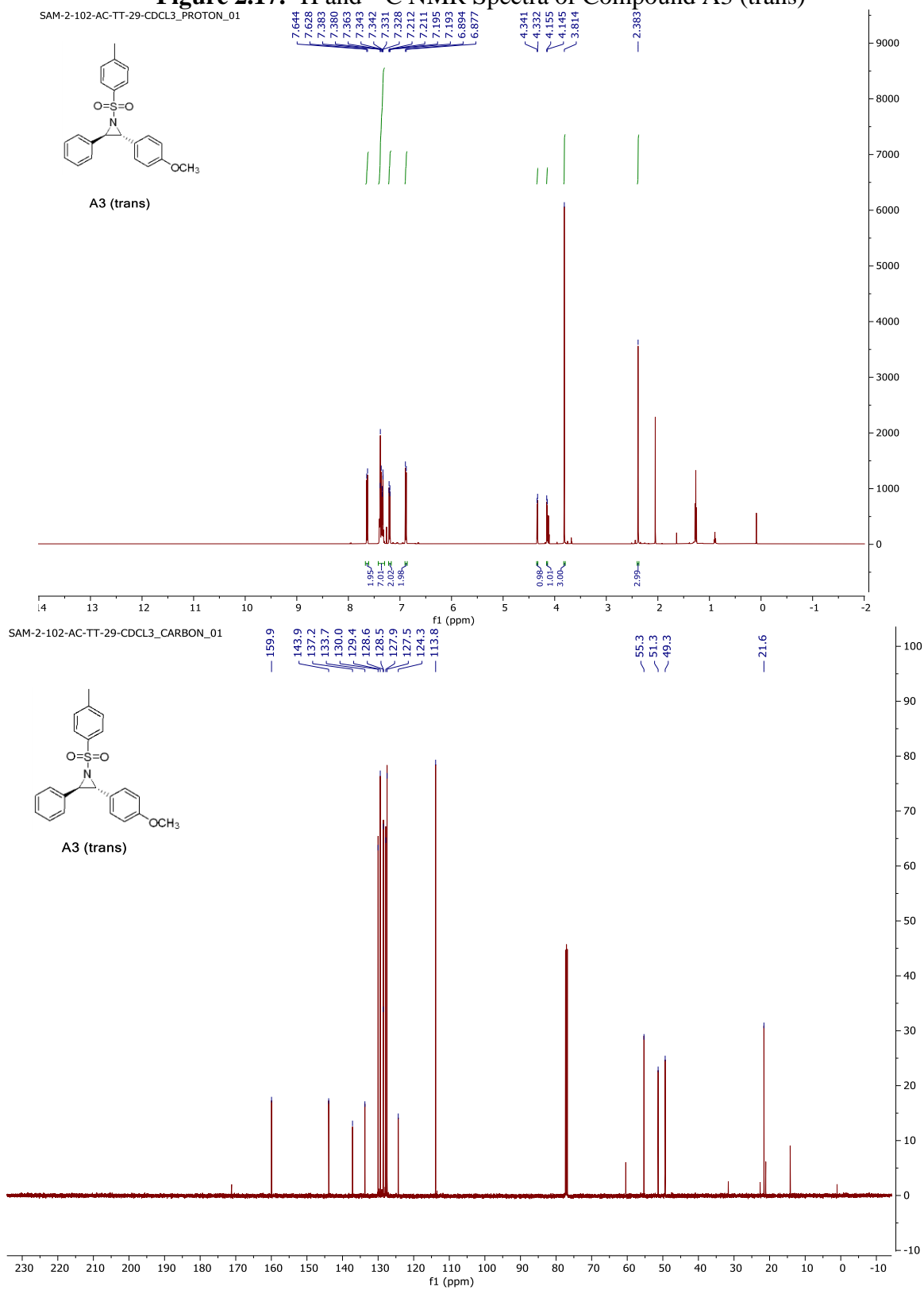


Figure 2.18. ^1H and ^{13}C NMR Spectra of Compound A3 (cis)

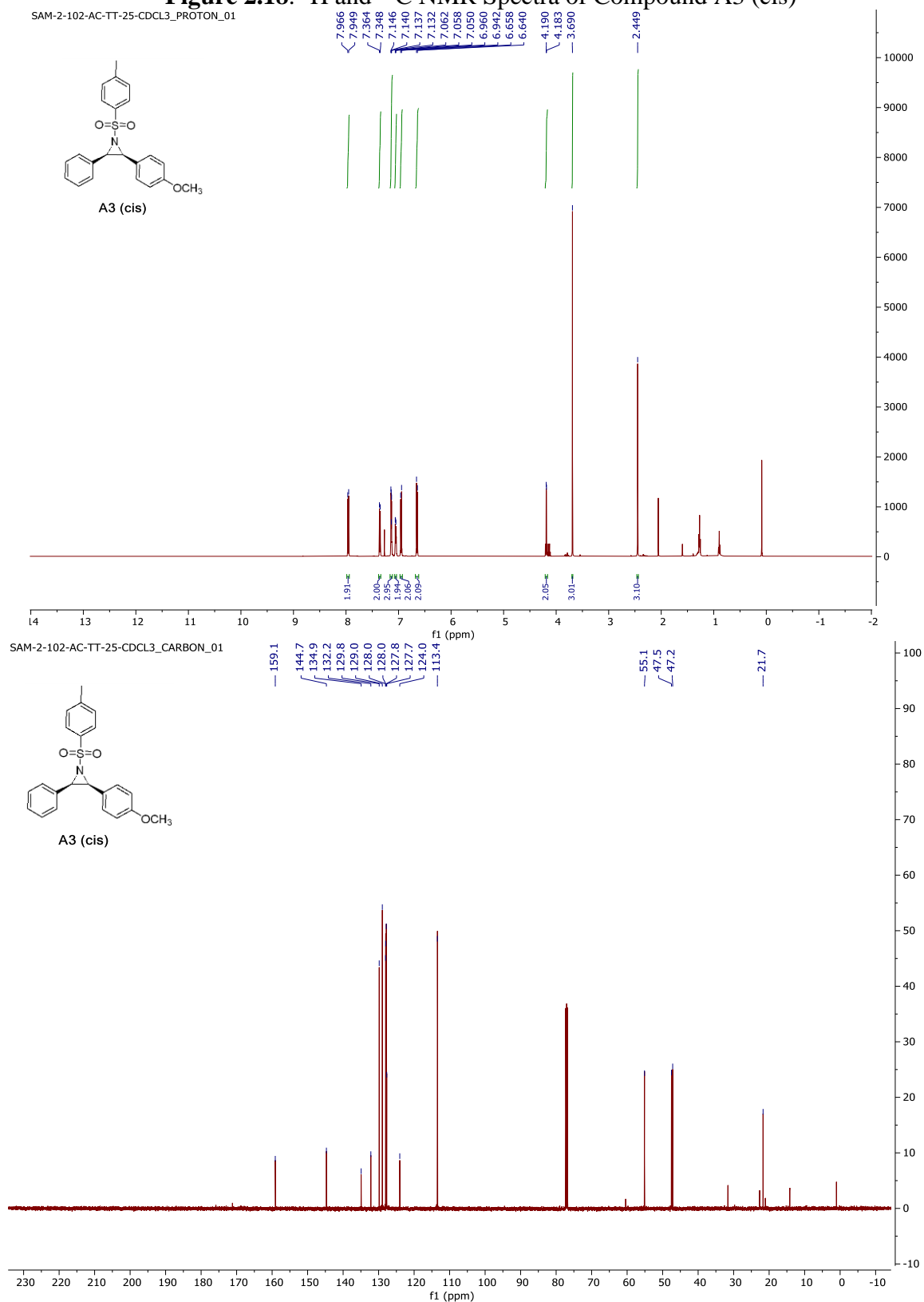


Figure 2.19. ^1H and ^{13}C NMR Spectra of Compound A4

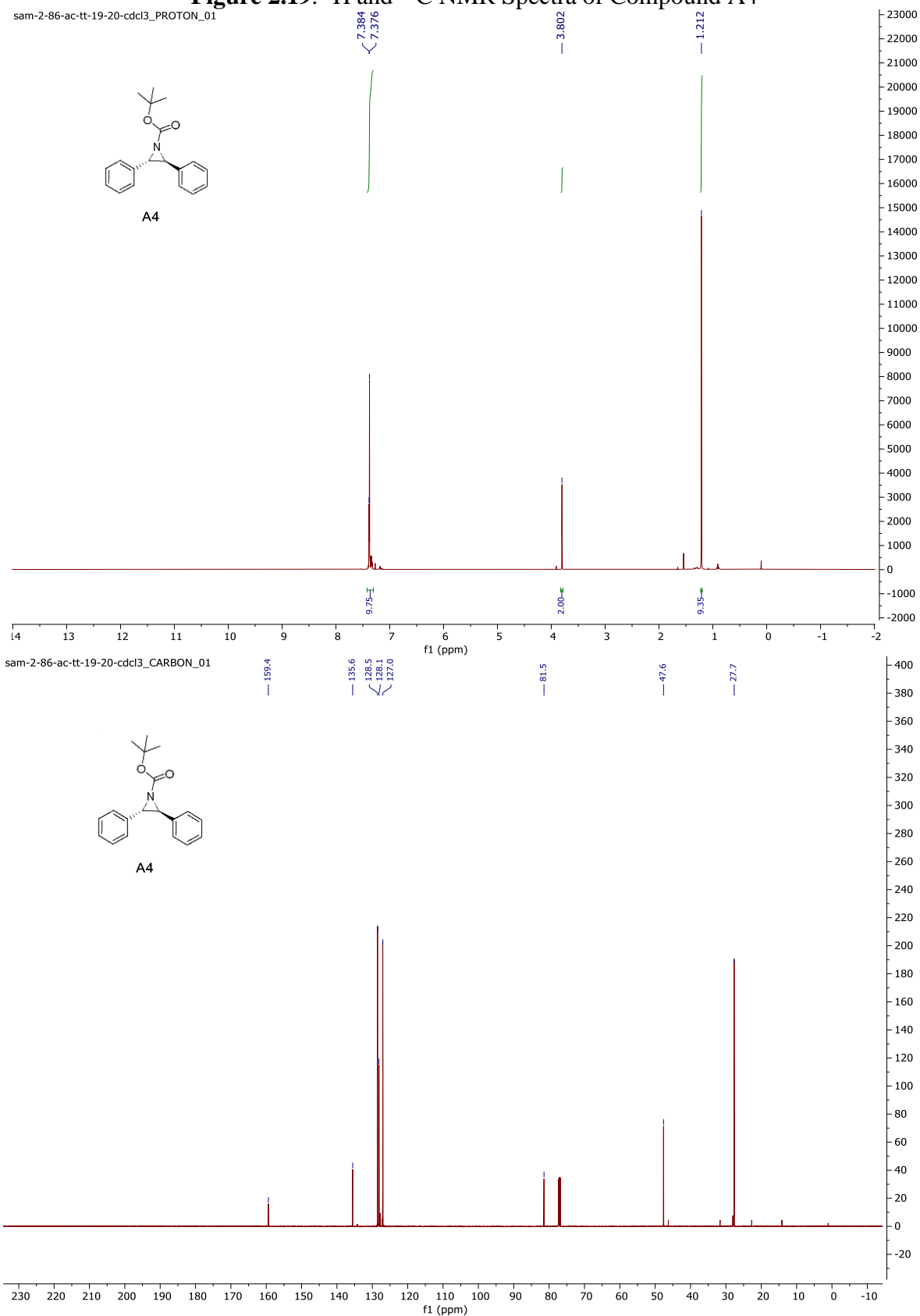


Figure 2.20. ^1H and ^{13}C NMR Spectra of Compound A5

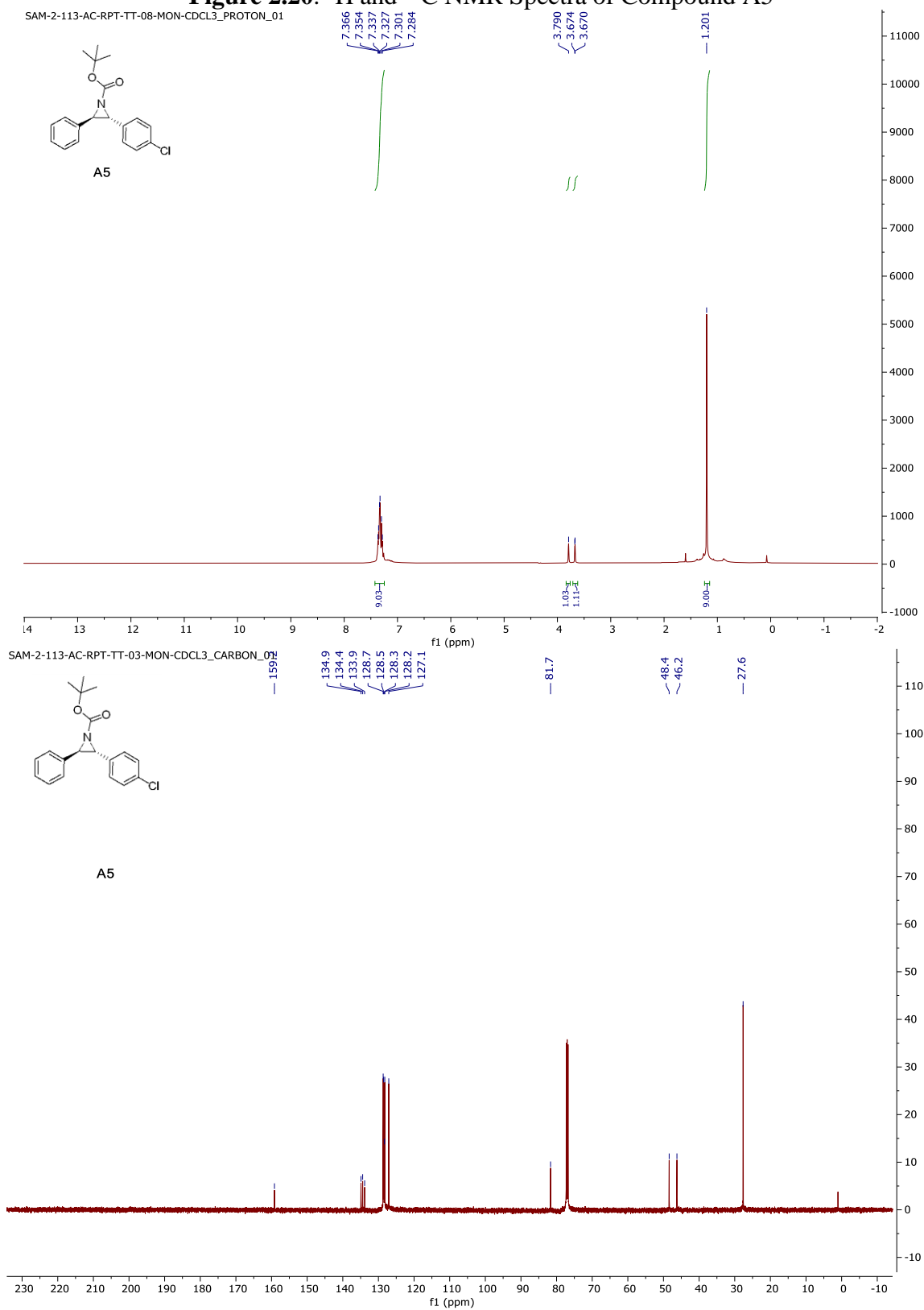


Figure 2.21. ^1H and ^{13}C NMR Spectra of Compound A6

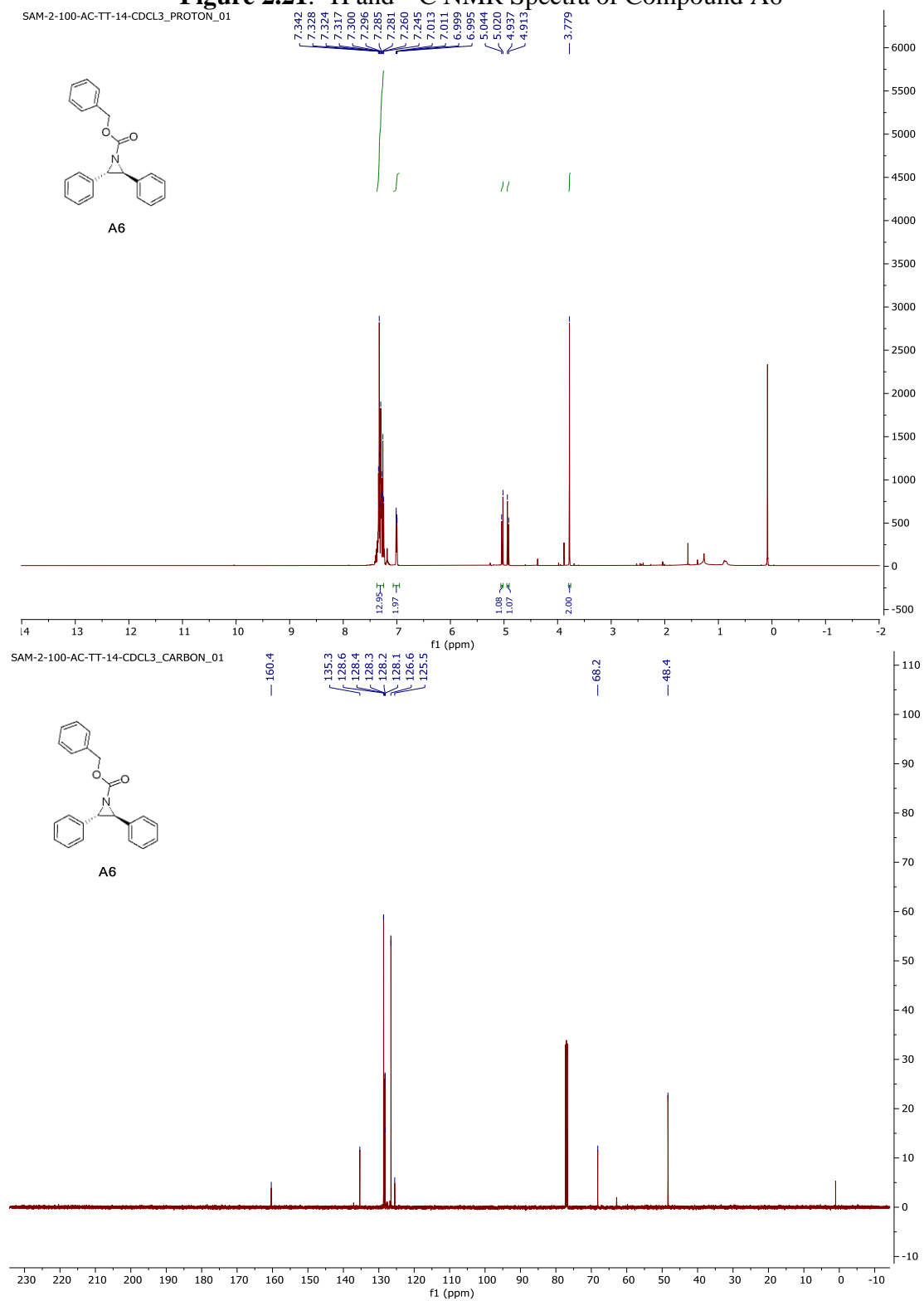
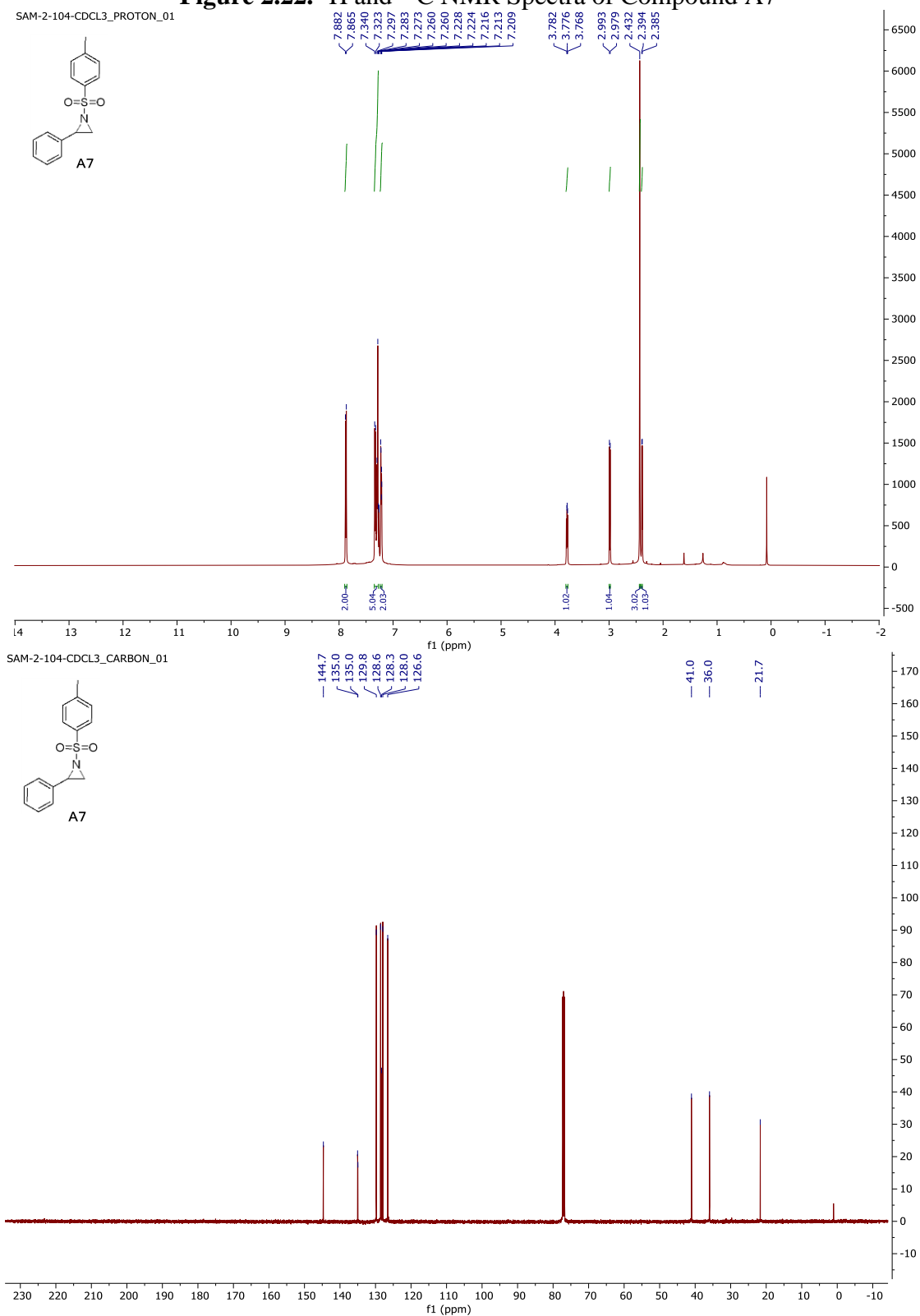


Figure 2.22. ^1H and ^{13}C NMR Spectra of Compound A7



REFERENCES

REFERENCES

- [1] Degennaro, L.; Trinchera, P.; Luisi, R. *Chem. Rev.* **2014**, *114*, 7881.
- [2] Padwa, A. In *Comprehensive Heterocyclic Chemistry III*; Elsevier, 2008; pp 1.
- [3] Kuszpit, M. R.; Wulff, W. D.; Tepe, J. J. *J. Org. Chem.* **2011**, *76*, 2913.
- [4] Stanković, S.; Catak, S.; D'hooghe, M.; Goossens, H.; Abbaspour Tehrani, K.; Bogaert, P.; Waroquier, M.; Van Speybroeck, V.; De Kimpe, N. *J. Org. Chem.* **2011**, *76*, 2157.
- [5] Huang, L.; Zhao, W.; Staples, R. J.; Wulff, W. D. *Chem. Sci.* **2013**, *4*, 622.
- [6] Wang, S.; Zhu, X.; Chai, Z.; Wang, S. *Org. Biomol. Chem.* **2014**, *12*, 1351.
- [7] Samimi, H.; Dadvar, F. *Synthesis* **2015**, *47*, 1899.
- [8] Colpaert, F.; Mangelinckx, S.; Giubellina, N.; De Kimpe, N. *Tetrahedron* **2011**, *67*, 1258.
- [9] Dolfen, J.; Vervisch, K.; De Kimpe, N.; D'hooghe, M. *Chem. - Eur. J.* **2016**, *22*, 4945.
- [10] Samanta, K.; Panda, G. *Chem. - Asian J.* **2011**, *6*, 189.
- [11] Singh, G. S.; Sudheesh, S.; Keroletswe, N. *Arkivoc* **2017**, *2018*, 50.
- [12] Selig, P. Guanidine Organocatalysis. *Synthesis* **2013**, *45*, 703.
- [13] Phillips, D. J.; Graham, A. E. *Synlett* **2010**, *2010*, 769.
- [14] Corey, E. J.; Chaykovsky, M. *J. Am. Chem. Soc.* **1962**, *84*, 867.
- [15] (a) Aggarwal, V. K.; Winn, C. L. *Acc. Chem. Res.* **2004**, *37*, 611; (b) Corey, E. J.; Chaykovsky, M. *J. Am. Chem. Soc.* **1965**, *87*, 1353.
- [16] Huczynski, A.; Brzezinski, B.; Furukawa, T. In *Encyclopedia of Reagents for Organic Synthesis*; John Wiley & Sons, Ltd: Chichester, UK, 2014; pp 1.
- [17] Montalvo-González, R.; Ariza-Castolo, A. J. *Mol. Struct.* 2003, *655*, 375–389.
- [18] Bowman, R. K.; Johnson, J. S. *J. Org. Chem.* 2004, *69*, 8537–8540.
- [19] Chakraborti, A. K.; Bhagat, S.; Rudrawar, S. *Tetrahedron Lett.* 2004, *45*, 7641–7644.
- [20] Cai, H.; Zhou, Y.; Zhang, D.; Xu, J.; Liu, H. *Chem Commun* 2014, *50*, 14771–14774.

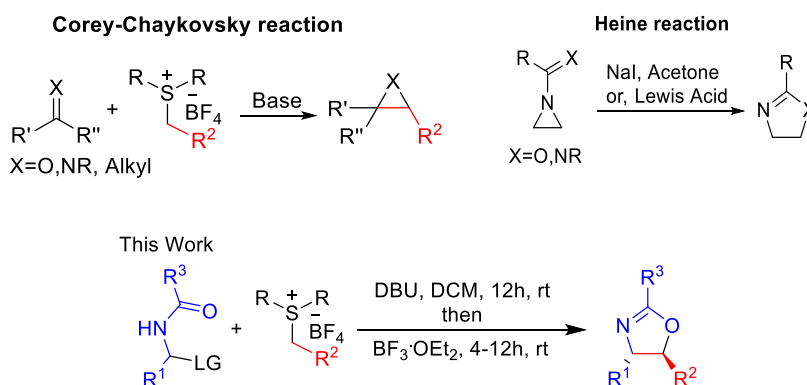
- [21] Tillman, A. L.; Ye, J.; Dixon, D. J. *Chem. Commun.* 2006, 11, 1191–1193.
- [22] Forrester, J.; Jones, R. V. H.; Newton, L.; Preston, P. N. *Tetrahedron* 2001, 57, 2871–2884.
- [23] Huang, M.-T.; Wu, H.-Y.; Chein, R.-J. *Chem Commun* 2014, 50, 1101–1103.
- [24] Illa, O.; Arshad, M.; Ros, A.; McGarrigle, E. M.; Aggarwal, V. K. *J. Am. Chem. Soc.* 2010, 132, 1828–1830.
- [25] Aggarwal, V. K.; Ferrara, M.; O'Brien, C. J.; Thompson, A.; Jones, R. V. H.; Fieldhouse, R. J. *Chem. Soc. [Perkin 1]* 2001, No. 14, 1635–1643.
- [26] Kishore Kumar, G. D.; Baskaran, S. *Chem. Commun.* 2004, 1026–1027.

Chapter 3: Synthesis of oxazolines via reaction of acyl imines with sulfur ylides

3.1 Introduction

The oxazoline scaffolds are an important group of molecules present in numerous natural and synthetic bioactive products.¹ Moreover, oxazolines are key components in chiral ligands used in many asymmetric catalytic reactions.² Due to the significance of this versatile scaffold, several synthetic methods have been developed, but mainly focused on cyclodehydration,³ aldol condensations⁴ or condensation reactions with amino alcohols.⁵ In these methods, the formation of the C4-C5 bond is a less commonly used strategy but denotes a facile approach to incorporate functionalities in the C-2, C-4, and C-5 positions of the oxazoline. This chapter will discuss a one-pot procedure to obtain highly substituted oxazoline analogs by utilizing a modified Corey-Chaykovsky-type reaction, followed by an *in situ* Heine type ring expansion reaction of aziridine (Scheme 3.1).

Scheme 3.1. Synthesis of oxazolines via expansion of modified Corey-Chaykovsky-type reaction and Heine reaction



In the Corey-Chaykovsky reactions,⁶ various aldehydes, imines, or olefines are treated with different sulfur ylides in the presence of a base to form epoxides, aziridines, and cycloalkanes, respectively (**Scheme 3.1**).⁷ In the Heine reaction, ring expansion of benzoylated aziridines or imidoyl aziridines generate the 2-substituted oxazolines or imidazolines, respectively.⁸ Here, we

treated stable acyl imines containing a leaving group (LG) with sulfonium salts in the presence of a base to generate solely *trans*-selective oxazolines in a one-pot sequence (**Scheme 3.1**).

Aggarwal *et al.* previously showed an example of an *N*-benzoylimine reaction with a 3-furyl sulfonium salt to obtain an expected aziridine, along with a low yield oxazoline as a side product.⁹ Due to the instability of the acylimine starting material, the isolation of the oxazoline was limited and resulting low yielding product mixture. However, this result inspired us to further explore a new method for oxazoline synthesis by investigating stable precursors of acylimine, and later an *in situ* Heine-type ring expansion of the aziridine to access *trans*-oxazolines.

3.2 Results and discussion

At first, 1-benzotriazolyl-*N*-benzoyl-1-phenyl methylamine (**1**) was introduced as a stable precursor to obtain the *N*-benzoylbenzaldimine *in situ*.¹⁰ The acylimine precursor **1**, was treated with benzyldimethylsulfonium tetrafluoroborate salt (**2a**) in a few solvents (dichloromethane (DCM), CH₃CN, and tetrahydrofuran (THF)), and several bases (1,8-diazabicyclo(5.4.0)undec-7-ene (DBU), 1,1,3,3-tetramethylguanidine (TMG), 7-Methyl-1,5,7-triazabicyclo(4.4.0)dec-5-ene (MTBD), imidazoline, K₂CO₃, KH, and lithium hexamethyldisilazane (LiHMDS)) were tested for product formation (**Table 3.1**). Among the bases screened, DBU, MTBD, K₂CO₃, and KH provided the known aziridines (both *cis* and *trans*) and *trans*-oxazoline (**3a**) as a 1:2 mixture of products by NMR.¹¹ Assured that we could effortlessly transform the aziridine to the oxazoline product at a later stage with a Lewis acid (**Scheme 3.1**),^{8d} our initial goal was to increase the conversion of starting material to the aziridine/oxazoline products, with the least number of variables. Therefore, the reaction was further optimized with the most promising bases of our initial screen. From this stage of the optimization, five equivalents of sulfonium salt (**2a**) and ten

equivalents of DBU base offered a 76% conversion (**Table 3.1**, Entry 11) to a 1:2 mixture of the aziridine/oxazoline products.

In the next step, we investigated the stable acylimine precursor, 1-methoxy-*N*-benzoyl-1-phenyl-methylamine (**4**), with the methoxide (-OMe) as a leaving group.¹² Unfortunately, all optimization efforts provided inferior product yields compared to precursor **1**. Afterward, *N*-(phenyl(tosyl)-methyl)benzamide (**5a**) was evaluated, where *p*-toluene sulfinate (*p*Ts) acts as the *in situ* leaving group.¹³ We assumed that the Ts would provide a better leaving group (pKa ~1.99)¹⁴ than the previously screened precursors, thus forming a rapid acylimine formation. Various conditions were tested with this precursor (Table 1), including Cs₂CO₃ as a base according to the previous reports.¹⁵ Gratifyingly, 3.5 equivalents of sulfonium salt (**2a**), and five equivalents of DBU in DCM, afforded 85% conversion (**Table 3.1**, Entry 27) to the aziridine/oxazoline product mixture (1:2). Further, the ideal loading amount of starting material was established by varying the equivalents of base and sulfonium salt. Lowering the amounts of the base to three equivalents and sulfonium salt to 1.5 equivalents did not significantly reduce product formation (84% conversion, **Table 3.1**, Entry 35) and were hence considered as the best conditions for our future studies.

Table 3.1. Optimization of oxazoline synthesis with different as a leaving group in compound **X**

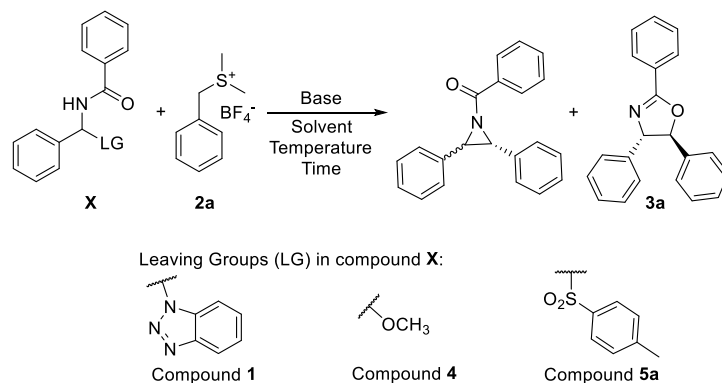


Table 3.1. (cont'd)

Entry	2a Equiv.	Base	Base Equiv.	Solvent	Temp.	Time (hrs)	% Yield ^a
Reactions with Compound 1							
1	1.5	MTBD	2.5	DCM	RT	2.5	48
2	2.5	MTBD	4	DCM	RT	2.5	73
3	2.5	MTBD	4	CH ₃ CN	RT	2.5	57
4	2.5	MTBD	4	THF	RT	4	48
5	2.5	MTBD	5	THF	RT	4	52
6	2.5	DBU	4	THF	RT	4	60
7	2.5	DBU	5	THF	RT	4	63
8	3.5	DBU	5	THF	RT	4	69
9	3.5	DBU	5	THF	reflux	7	48
10	3.5	DBU	5	THF	0 °C	7	52
11	5	DBU	10	THF	RT	7	76
12	2.5	K ₂ CO ₃	4	THF	RT	4	5
13	2.5	KH	4	THF	RT	4	21
14	2.5	KH	15	THF	RT	4	31
15	3.5	KH	15	THF	reflux	7	0
16	3.5	KH	15	THF	0 °C	7	0
17	7	KH	15	THF	RT	7	41
Reactions with Compound 4							
19	3.5	DBU	5	THF	RT	8	20

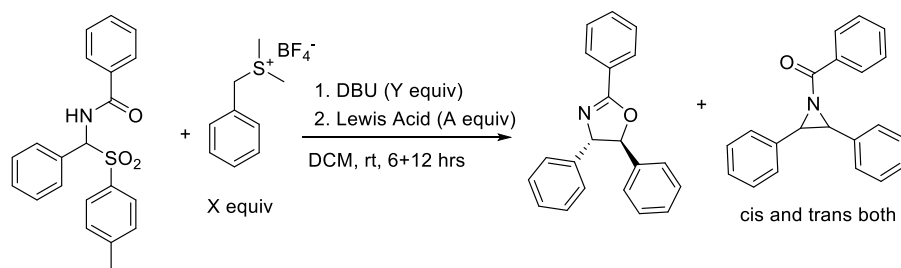
Table 3.1. (cont'd)

20	3.5	DBU	5	THF	reflux	8	32
21	3.5	DBU	10	THF	reflux	8	29
22	5	DBU	5	THF	reflux	8	28
23	3.5	DBU	10	THF	reflux	8	29
24	3.5	KH	5	THF	RT	8	0
Reactions with Compound 5a							
25	5	Cs ₂ CO ₃	10	DCM	RT	12	69
26	5	DBU	10	DCM	RT	12	84
27	3.5	DBU	5	DCM	RT	12	85
28	5	DBU	10	THF	RT	12	60
29	3.5	DBU	5	THF	RT	12	48
30	1	DBU	1	DCM	RT	12	11
31	1	DBU	2	DCM	RT	12	72
32	1.2	DBU	2	DCM	RT	12	65
33	1.2	DBU	2.5	DCM	RT	12	77
34	1.5	DBU	2	DCM	RT	12	79
35	1.5	DBU	3	DCM	RT	12	84
36	1.5	DBU	4	DCM	RT	12	82
37	2	DBU	2.5	DCM	RT	12	79
38	2	DBU	4	DCM	RT	12	86
39	2	DBU	5	DCM	RT	12	85

^aMixture of *trans/cis* aziridine and *trans*-oxazoline. RT = room temperature.

In the next stage of our investigations, we explored the conversion of the aziridine to oxazoline under mildly acidic conditions.^{8d} For these, we screened several Lewis acids, including CuCl₂, ZnCl₂, TMSCl, BF₃.OEt₂, AlCl₃, and TiCl₄ (**Table 3.2**), following the optimized reaction conditions reported in **Table 3.1** (Entry 35). Among those, BF₃.OEt₂ afforded a complete conversion of *cis*- and *trans*- aziridine solely to *trans*- oxazoline in 12 hours (**Table 3.2**, Entry 5).

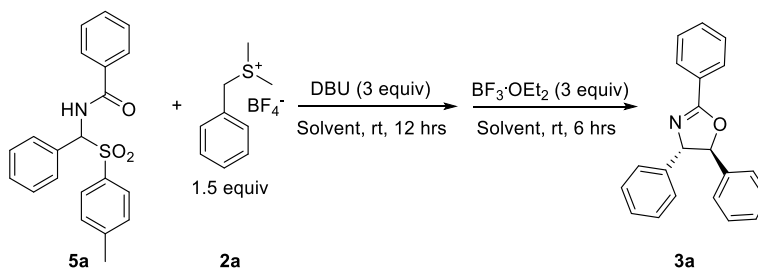
Table 3.2. Lewis acid optimization



Entry	L. A. (A)	(X) S. Ylides	DBU (Y)	% Yield (Mixture)	Trans Oxazoline: Cis Aziridine: Trans Aziridine
1	BF ₃ .OEt ₂ (5)	3.5	5	41	1:0:0
2	BF ₃ .OEt ₂ (2)	3.5	5	84	2.4:0.8:1
3	BF ₃ .OEt ₂ (10)	3.5	5	51	1:0:0
4	BF ₃ .OEt ₂ (10)	5	10	33	1:0:0
5	BF₃.OEt₂ (3)	1.5	3	60	1:0:0
6	CuCl ₂ (5)	3.5	5	70	1:0.3:0.03 (2days)
7	ZnCl ₂ (1)	5	5	45	2.2:0.6:1
8	AlCl ₃ (5)	3.5	5	56	2.3:0.5:1
9	TMSCl (5)	3.5	5	57	3.2:0.7:1
10	TiCl ₄ (5)	3.5	5	52	1:0.15:0.02

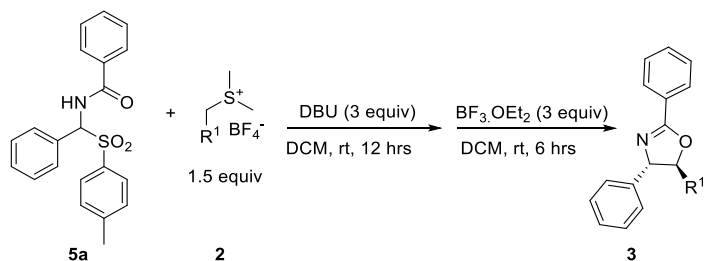
After the Lewis acid optimization studies, a few solvents (DCM, DME, DMSO, CH₃CN, THF, and toluene) were screened with BF₃.OEt₂ and among them, DME and DCM produced an overall yield of 61% and 60%, respectively, of only the *trans*-oxazoline, whereas the most inferior yield was obtained in toluene (**Table 3.3**). Considering the similarity in overall yields, DCM was determined as our optimum solvent to avoid a solvent exchange procedural step.

Table 3.3. Solvent screening for the synthesis of oxazoline **3a** from compound **5a**



Entry	Solvent (20 mL)	% Yield
1	DCM	60
2	DME	61
3	THF	55
4	CH ₃ CN	53
5	DMSO	55
6	Toluene	23

After identifying the optimal reaction conditions, we explored the substrate scope by reacting compound **5a** with various sulfonium salts. As shown in **Table 3.4**, sulfonium salts bearing either electron-withdrawing or electron-donating groups underwent the reaction in moderate to good yield (37-70%) over the two consecutive steps.

Table 3.4. Scope of oxazoline synthesis with different sulfonium salts (**2**)

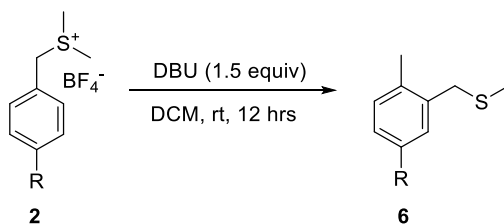
Entry	2 with R ¹	R ²	Product	% Yield
1a		H	3a	60
1b		OCH ₃	3b	51 ^a
1c		NO ₂	3c	37 ^b
2			3e	70
3			3f	52
4			3g	64

^{a,b} Reaction was stirred for 12 h^a or 4 h^b after the addition of BF₃·OEt₂

Surprisingly, the NO₂-substituted product **3c** was formed in a relatively low yield, although a sulfonium salt containing an electron-withdrawing (EW) group is more reactive than the one containing an electron-donating (ED) group. To studied further these data, four sulfonium salts (**Table 3.5**) were treated with the DBU base, and we observed that the EW group containing sulfonium salts converted to Stevens rearranged products.¹⁶ with up to 82% yield (**Table 3.5**, Entry 2,3). In contrast, EDG containing sulfonium salt did not undergo this rearrangement (**Table 3.5**,

Entry 1). We hypothesize that using a tetrahydrothiophene instead of dimethyl sulfide with EW group having sulfonium salt might reduce this undesired rearrangement from the outcome of this experiment.

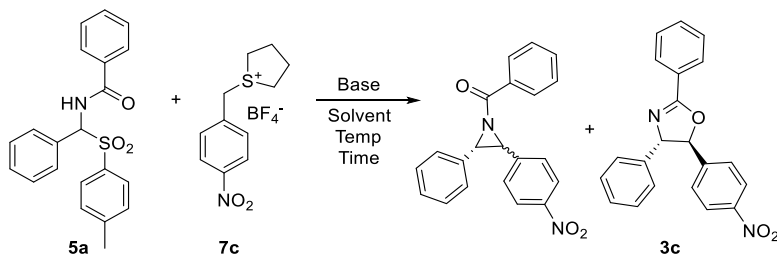
Table 3.5. Stevens rearrangement of sulfur ylides



Entry	R	Product	% Yield
1	H	6c	28
2	OCH ₃	-	N/A
3	NO ₂	6a	82
4	CF ₃	6b	73

Subsequently, 1-(4-nitrobenzyl)tetrahydrothiophenium tetrafluoroborate (**7c**) was treated with compound **5a** and further optimized to obtain 75% of the aziridine/oxazoline product mixture, when using four equivalents of DBU base (**Table 3.6**, Entry 6).

Table 3.6. Optimization of oxazoline synthesis with tetrahydrothiophene containing sulfonium salt (**7c**)

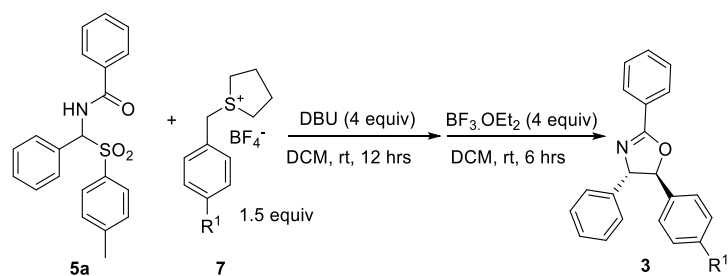


Entry	7c Equiv.	Base	Base Equiv.	Solvent	Temp.	Time (hrs)	Yield ^a %
1	1.5	MTBD	3	DCM	RT	12	39
2	1.2	DBU	3	DCM	RT	12	28
3	1.2	DBU	4	DCM	RT	12	56
4	1.5	DBU	3	DCM	RT	12	66
5	1.5	DBU	3	DCM	0 °C	12	55
6	1.5	DBU	4	DCM	RT	12	75
7	2	DBU	4	DCM	RT	12	74
8	2	DBU	5	DCM	RT	12	72
9 ^b	1.5	DBU	3	DCM	RT	12	49

^a Mixture with *trans*, *cis* aziridines, and *trans* oxazoline, ^b With dimethyl sulfonium salt (**2c**)

Under these newly optimized conditions, the same reaction was executed with the addition of $\text{BF}_3\cdot\text{OEt}_2$, which boost the yields of the NO_2 -substituted *trans*-oxazoline from 37% to 57% (**Table 3.7**, Entry 1b). A few other tetrahydrothiophene containing sulfonium salts with an electron-neutral or, electron-withdrawing group (**7**) were screened with compound **5a** (**Table 3.7**), and the *trans*-oxazolines were isolated in 51-66% yields.

Table 3.7. Scope of oxazoline synthesis with different sulfonium salts (**7**)



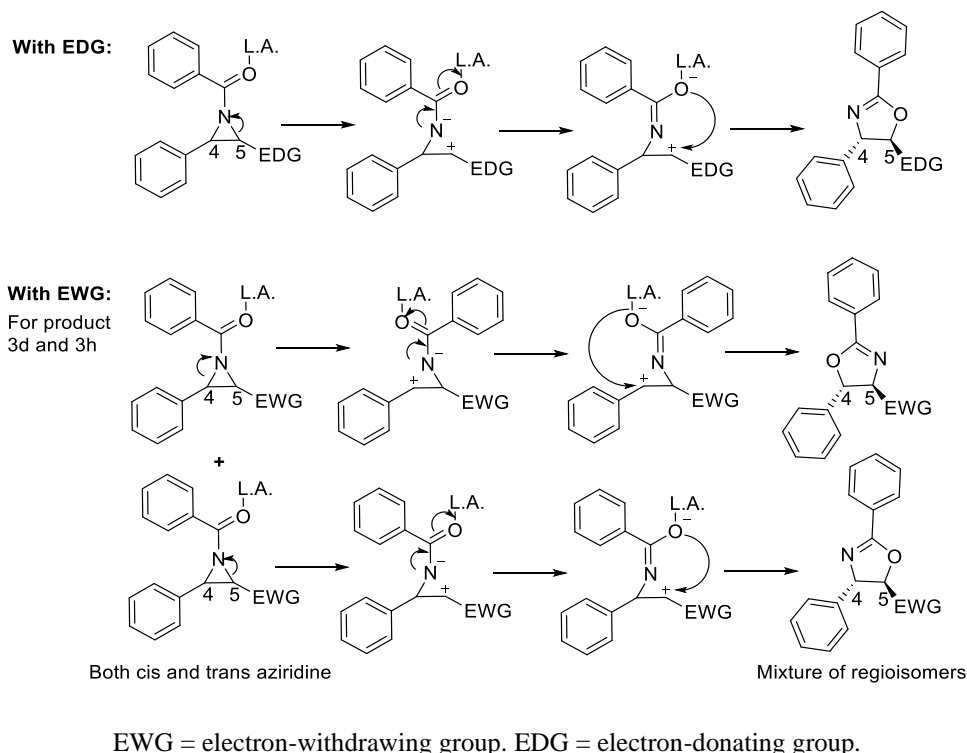
Entry	R ¹	Product	% Yield
1a	H (7a)	3a	51
1b	NO_2 (7c)	3c	57 ^b
1c	F (7d)	3d	66 ^a
1d	CF_3 (7h)	3h	55 ^a

^aMixture of regioisomer of *trans*-oxazoline, ^bThe reaction was stirred for 4 h after the addition of $\text{BF}_3\cdot\text{OEt}_2$

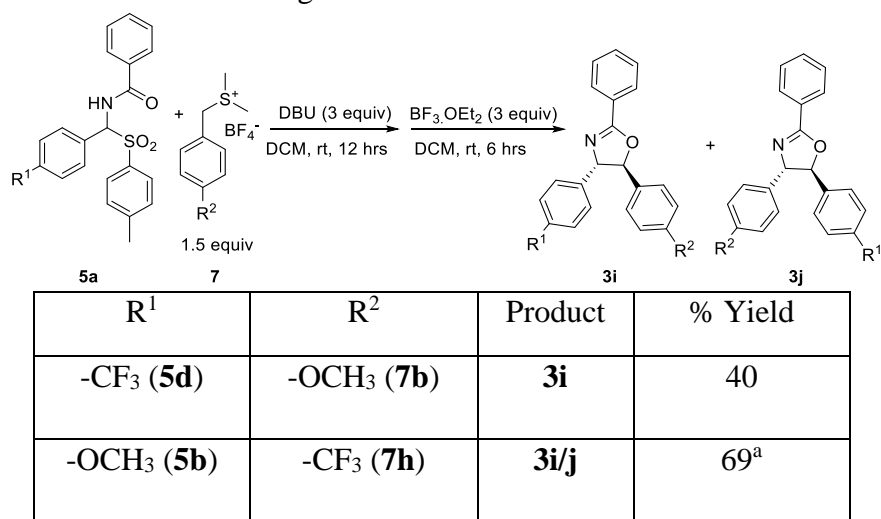
Interestingly, with the electron-withdrawing groups (F, $-\text{CF}_3$) (**Table 3.7**, entry 1c and 1d, sulfonium salt **7d** or **7h**), a mixture of regioisomers of the oxazoline products (**3**) was formed, due to the intermediate aziridine-ring can open both at the C-4 position or C-5 position (**Scheme 3.2**). However, when an electron-donating group ($-\text{OCH}_3$) was used, only one regioisomer was formed, as the aziridines primarily opened at the C-5 position, as anticipated. However, the regioisomer of the nitro-containing oxazoline **3c** was not detected (**Table 3.9**, Entry 12, **3v**), instead a substantial

amount of the corresponding oxazole product was observed. The ease of *in situ* oxidation of this nitro-substituted regioisomer could account for its depletion.¹⁷

Scheme 3.2. Proposed ring-opening mechanism of aziridine to oxazoline providing two regioisomers



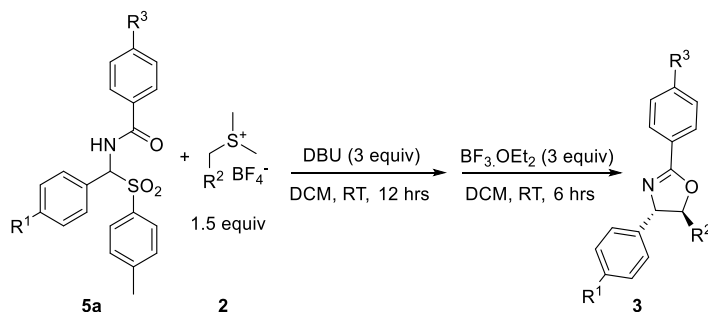
To investigate the mechanism of the reaction, an electron-withdrawing group (EWG) containing acylimine precursor (**Table 3.8, 5d**) was treated with an electron-donating group (EDG) containing sulfonium salt (**Table 3.8, 7b**). Simultaneously, an EDG containing acylimine precursor (**Table 3.8, 5b**) was treated with an EWG containing sulfonium salt (**Table 3.8, 7h**). As expected, 40% of only *trans*-oxazoline (**3i**) was isolated from the reaction between **5d** and **7b**, whereas 69% of a 1:1 mixture of the two regioisomers of the *trans*-oxazoline **3i/j** were isolated from the reaction between **5b** and **7h**. The outcomes of these reactions ratified the proposed ring-opening mechanism shown in **Scheme 3.2**.

Table 3.8. Regioselective formation of oxazolines

^a1:1 Mixture of *trans*-oxazoline regioisomer (**3i** and **3j**)

Next, we explored the scope of this reaction to synthesize *trans*-oxazolines containing electron-donating and withdrawing groups, using the imine precursor **5a** and sulfur ylide **2** (Table 3.9). The addition of electron-withdrawing groups on both starting material afforded the *trans* oxazoline **3k** in 72% yield and **3w** in 58% yield, whereas fragments containing an electron-donating group offered only 34% of the *trans* oxazoline (**3m**). To further investigate the synthetic utility of this methodology, we chose two sulfonium salts (Table 3.9, R² = **2e** and **2a**) and varied the acylimine precursor **5a**. The electron-rich sulfur ylide **2e** rendered good yields (51-74%) with the substrate **5a** containing both electron-donating and withdrawing groups in the R¹ or R³ position of **5a**. However, the aryl sulfur ylide **2a** provided moderate product formation (41-69%) using a range of electron-poor imine precursors (**5c-5f**, entry 10-13). Similar to our previous results (Table 3.7, Entry 1b), the product **3v** was obtained in low yields (30%) with a substantial amount of its corresponding oxazole as a side product. A gram scale reaction was performed to synthesize **3w**, and the *trans*-oxazoline product was isolated in a slightly lower yield of 49% (6 mmol of **5f** was used).

Table 3.9. Scope of oxazoline synthesis with different substitutions in the R¹, R², and R³ positions

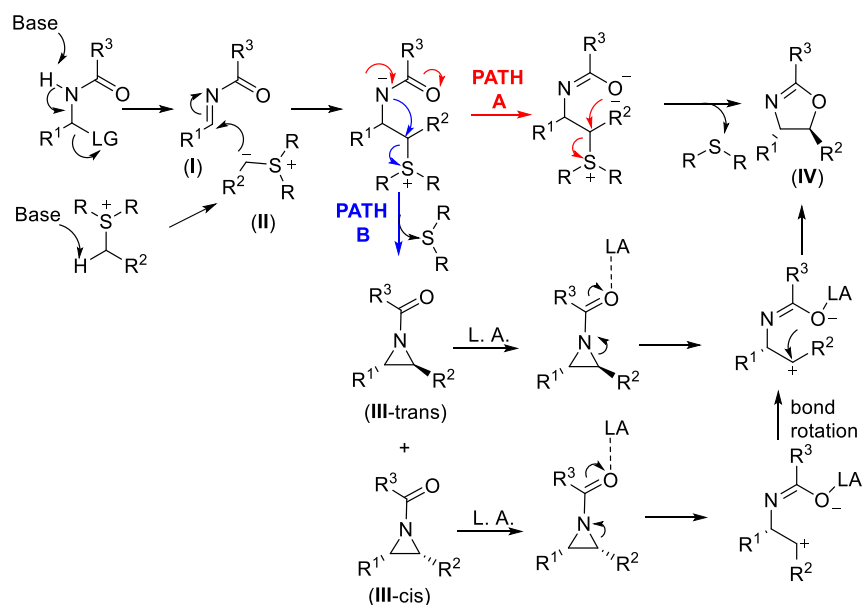


Entry	R ¹	R ²	R ³	Product	% Yield
1	CF ₃ (5d)	Ar- CF ₃ (7h)	H	3k	72 ^a
2	F (5e)	Ar-F (2d)	H	3l	57
3	OCH ₃ (5b)	Ar-OCH ₃ (2b)	H	3m	34 ^b
4	CN (5f)	Ar-CN (7i)	H	3w	58 ^a
5	F (5e)	 2e	H	3n	57
6	CF ₃ (5d)		H	3o	62
7	CN (5f)		H	3p	77
8	H (5g)		-OCH ₃	3q	74
9	H (5h)		-NO ₂	3r	51
10	-F (5e)	 2a	H	3s	41 ^c
11	-CF ₃ (5d)		H	3t	61
12	-CN (5f)		H	3u	69
13	-NO ₂ (5c)		H	3v	30

^aReaction was ran for 9 h after 4 equiv of DBU, ^bAdditional 1 equiv of BF₃.OEt₂ was added and ran for another 6 hrs. ^c3:1 Mixture of *trans*- oxazoline regioisomers (**3s** : **3d**)

Based on the experimental results and findings, a mechanism is described in **Scheme 3.3**. At first, the reaction initiates by deprotonation of the acyl imine precursor by a base to form the acylimine (**I**). Similarly, deprotonation of the sulfonium salt generates a sulfur ylide (**II**). Next, a nucleophilic addition sulfur ylide to the imine and subsequent nucleophilic substitution by oxygen releases the sulfide to generate a mixture of the *cis/trans*-aziridines (**III**) (Path B) and/or *trans*-oxazoline (**IV**) (Path A), respectively. After that, $\text{BF}_3 \cdot \text{OEt}_2$ interacts with the oxygen and facilitates the ring-opening reaction of the aziridine. The intermediate cationic form of the *cis/trans* aziridines can isomerize, and ring closure affords solely the more thermodynamically stable *trans*-oxazoline (**IV**).

Scheme 3.3. Proposed mechanism of the reaction



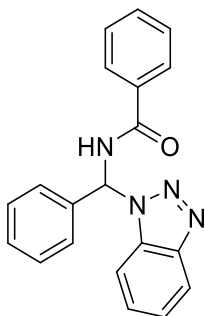
3.3 Conclusion

A modified Corey-Chaykovsky-Heine type reaction was utilized to synthesize oxazolines in good to moderate yield, using stable precursors of acyl imines and sulfur sulfonium salts in the presence of a base. The reaction involved a one-pot two steps reaction where the first step comprised of the formation of both aziridines and oxazolines, wherein the second step involved the *in situ* conversion of the aziridines to the *trans*-oxazolines by using a Lewis acid. The reaction suffered from a competing Steven rearrangement reaction when electron-deficient dimethyl sulfur ylides were used, which was solved by utilizing tetrahydrothiophene in the sulfonium salt.

3.4 Experimental sections

General Information. All commercially accessible chemicals were used without additional purification. All reactions were performed under an argon or nitrogen atmosphere with commercial-grade reagents. Dichloromethane (CH_2Cl_2) was purified through a column packed with dry alumina and was dispensed by a nitrogen pressure delivery system. All flasks were oven-dried overnight and cooled under nitrogen. All NMR spectra were performed on a 500 MHz spectrometer. The mass spectrometer ionization method was ESI with a Quadrupole detector. Infrared spectra were performed on a Jasco Series 6600 FTIR spectrometer, and melting points (mp) were taken on a MEL-TEMP[®] capillary apparatus.

*Synthesis of 1-benzotriazolyl-N-benzoyl-1-phenyl methylamine (1)*¹⁸



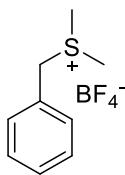
To a 40 mL solution of dry toluene in a 100 mL dry round bottom flask benzotriazole (5.45 g, 0.05 mol) was added, followed by benzaldehyde (0.05 mol, 5.31 g) and benzamide (0.05 mol, 6.05 g). The solution was refluxed for 24 hours in a Dean-Stark apparatus. Then, the reaction mixture was cooled to room temperature (RT) and the resulting white solid was filtered off. Finally, the solid was washed with Et₂O and subsequently toluene to give 1-benzotriazolyl-N-benzoyl-1-phenyl-methylamine as a white solid (83%, 13.6gm). Melting point (M.P.): 163-167 °C. IR: 3329, 3280, 3062, 2963, 1651, 1636, 1517, 1487, 1337 cm⁻¹. ¹H NMR (500 MHz, DMSO-*d*₆) δ 10.30 (d, *J* = 8.2 Hz, 1H), 8.26 (d, *J* = 8.2 Hz, 1H), 8.11 (d, *J* = 8.4 Hz, 1H), 8.02 – 7.97 (m, 3H), 7.55 (d, *J* = 7.5 Hz, 2H), 7.48 (d, *J* = 7.8 Hz, 2H), 7.44 – 7.38 (m, 6H). ¹³C{¹H} NMR (126 MHz, DMSO-*d*₆) δ 167.4, 145.8, 136.7, 133.4, 132.6, 132.5, 129.3, 129.1, 128.8, 128.5, 128.1, 127.5, 124.7, 119.8, 111.7, 66.6. HRMS (ESI-TOF) *m/z*: [M-Benzotriazole] calcd for (C₁₄H₁₂NO⁺) 210.0913; Found 210.0917.

The general method to synthesize substituted benzyldimethylsulfonium tetrafluoroborate salts (2)

To a solution of dry dichloromethane (30 mL) in a 100 mL dry round bottom flask, the appropriate alcohol (1 equiv, 10 mmol) was added, followed by dimethyl sulfide (2 equiv, 20 mmol) and placed under nitrogen gas. A solution of tetrafluoroboric acid (tetrafluoroboric acid diethyl ether complex) (1 equiv, 10 mmol) was added dropwise for 5 minutes at 0 °C. The mixture was stirred for 12

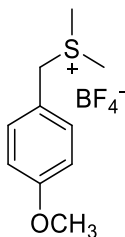
hours at room temperature. Evaporation of the solvent under reduced pressure gave a colorless, thick oil, which was precipitated with diethyl ether to obtain the desired salt as a solid.

2a



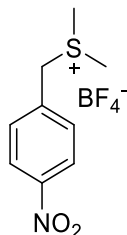
Colorless solid (2.28 gm, 95%). Melting point: 101-103 °C (Lit. value 103-104 °C).⁴ IR: 3029, 2946, 1433, 1027, 1008 cm⁻¹. ¹H NMR (500 MHz, DMSO-*d*₆) δ 7.53 – 7.42 (m, 5H), 4.62 (s, 2H), 2.77 (s, 6H). ¹³C{¹H} NMR (126 MHz, DMSO-*d*₆) δ 131.1, 130.1, 129.8, 128.7, 46.2, 24.2. HRMS (ESI-TOF) m/z: [M-BF₄⁻] calcd for (C₉H₁₃S⁺) 153.0732; Found 153.0745.

2b



Colorless solid (2.67 gm, 99%). Melting point: 58-59 °C. IR: 3030, 2975, 1434, 1216, 1030 cm⁻¹. ¹H NMR (500 MHz, DMSO-*d*₆) δ 7.36 (d, *J* = 8.7 Hz, 2H), 7.06 – 7.00 (d, *J* = 8.7 Hz, 2H), 4.56 (s, 2H), 3.77 (s, 3H), 2.72 (s, 6H). ¹³C{¹H} NMR (126 MHz, DMSO-*d*₆) δ 160.6, 132.6, 120.0, 115.2, 55.7, 45.9, 23.9. HRMS (ESI-TOF) m/z: [M-BF₄⁻-S(CH₃)₂] calcd for (C₈H₉O⁺) 121.0648; Found 121.0654.

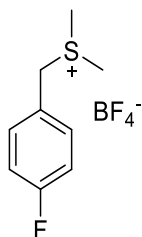
2c



Yellow solid (0.43 gm, 15%). Melting point: 135-137 °C. IR: 3031, 2943, 1525, 1354, 1026 cm^{-1} .

^1H NMR (500 MHz, $\text{DMSO}-d_6$) δ 8.32 (d, $J = 8.6$ Hz, 2H), 7.72 (d, $J = 8.6$ Hz, 2H), 4.75 (s, 2H), 2.81 (s, 6H). $^{13}\text{C}\{^1\text{H}\}$ NMR (126 MHz, $\text{DMSO}-d_6$) δ 148.6, 136.4, 132.6, 124.7, 45.2, 24.5. HRMS (ESI-TOF) m/z : $[\text{M}-\text{BF}_4^-]$ calcd for ($\text{C}_9\text{H}_{12}\text{NO}_2\text{S}^+$) 198.0583; Found 198.0591.

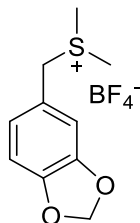
2d



White solid (1.78 gm, 69%). Melting point: 105-108 °C. IR: 3033, 2942, 1512, 1226, 1026 cm^{-1} .

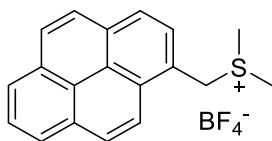
^1H NMR (500 MHz, $\text{DMSO}-d_6$) δ 7.50 (dd, $J = 8.8, 5.4$ Hz, 2H), 7.32 (t, $J = 8.8$ Hz, 2H), 4.61 (s, 2H), 2.76 (s, 6H). $^{13}\text{C}\{^1\text{H}\}$ NMR (126 MHz, $\text{DMSO}-d_6$) δ 164.2 (d, $J = 246$ Hz), 133.5 (d, $J = 8$ Hz), 125.0 (d, $J = 3$ Hz), 116.7 (d, $J = 22$ Hz), 45.4, 24.1. HRMS (ESI-TOF) m/z : $[\text{M}-\text{BF}_4^-]$ calcd for ($\text{C}_9\text{H}_{12}\text{FS}^+$) 171.0638; Found 171.0644.

2e



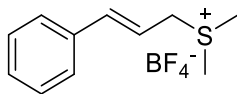
Light grey solid (2.69 gm, 95%). Melting point: 115-118 °C. IR: 3034, 2970, 1421, 1054, 1039, 1016 cm⁻¹. ¹H NMR (500 MHz, DMSO-*d*₆) δ 7.06 – 6.98 (m, 2H), 6.93 (dd, *J* = 8.0, 1.6 Hz, 1H), 6.07 (s, 2H), 4.53 (s, 2H), 2.75 (s, 6H). ¹³C{¹H} NMR (126 MHz, DMSO-*d*₆) δ 148.9, 148.3, 125.3, 121.7, 110.9, 109.4, 102.1, 46.4, 24.0. HRMS (ESI-TOF) *m/z*: [M-BF₄⁻-S(CH₃)₂] calcd for (C₈H₇O₂⁺) 135.0441; Found 135.0448.

2f



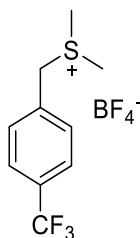
Greenish brown solid (3.28 gm, 90%). Melting point: 135-139 °C. IR: 3038, 2964, 1603, 1421, 1039 cm⁻¹. ¹H NMR (500 MHz, DMSO-*d*₆) δ 8.65 (dd, *J* = 9.3, 2.8 Hz, 1H), 8.39 (ddd, *J* = 11.6, 9.3, 4.3 Hz, 4H), 8.28 (dd, *J* = 8.9, 6.4 Hz, 1H), 8.25 – 8.21 (m, 1H), 8.19 – 8.12 (m, 2H), 5.42 (s, 2H), 2.90 (s, 6H). ¹³C{¹H} NMR (126 MHz, DMSO-*d*₆) δ 132.5, 131.1, 130.6, 130.4, 130.3, 129.3, 129.0, 127.7, 127.3, 126.7, 126.5, 125.6, 124.7, 124.0, 123.3, 122.1, 44.8, 24.8. HRMS (ESI-TOF) *m/z*: [M-BF₄⁻-S(CH₃)₂] calcd for (C₁₇H₁₁⁺) 215.0861; Found 215.0865.

2g



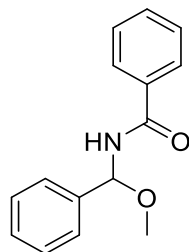
Brownish solid (2.45 gm, 92%). Melting point: 48-52 °C. IR: 3035, 2942, 1650, 1428, 1047, 1022 cm^{-1} . ^1H NMR (500 MHz, $\text{DMSO-}d_6$) δ 7.55 (d, $J = 7.3$ Hz, 2H), 7.38 (t, $J = 7.3$ Hz, 2H), 7.32 (t, $J = 7.3$ Hz, 1H), 6.86 (d, $J = 15.6$ Hz, 1H), 6.34 (dt, $J = 15.6, 7.7$ Hz, 1H), 4.18 (d, $J = 7.7$ Hz, 2H), 2.82 (s, 6H). $^{13}\text{C}\{^1\text{H}\}$ NMR (126 MHz, $\text{DMSO-}d_6$) δ 140.6, 135.7, 129.3, 129.2, 127.5, 115.7, 44.4, 23.6. HRMS (ESI-TOF) m/z : $[\text{M-BF}_4^- \cdot \text{S}(\text{CH}_3)_2]$ calcd for (C_9H_9^+) 117.0699; Found 117.0705.

2h



White solid (1.93 gm, 63%). Melting point: 112-116 °C. IR: 3028, 2941, 1423, 1323, 1022 cm^{-1} . ^1H NMR (500 MHz, $\text{DMSO-}d_6$) δ 7.86 (d, $J = 8.0$ Hz, 2H), 7.67 (d, $J = 8.0$ Hz, 2H), 4.70 (s, 2H), 2.81 (s, 6H). $^{13}\text{C}\{^1\text{H}\}$ NMR (126 MHz, $\text{DMSO-}d_6$) δ 133.6, 132.0, 130.2 (q, $J = 32$ Hz), 126.7 (q, $J = 3.5$ Hz), 123.3, 45.4, 24.4. HRMS (ESI-TOF) m/z : $[\text{M-BF}_4^-]$ calcd for $(\text{C}_{10}\text{H}_{12}\text{F}_3\text{S}^+)$ 221.0606; Found 221.0616.

*Synthesis of 1-methoxy-N-benzoyl-1-phenyl-methylamine (4)*¹⁹



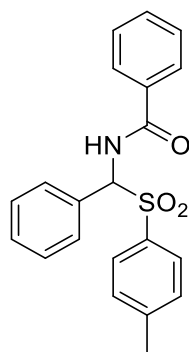
1-Benzotriazolyl-N-benzoyl-1-phenyl-methylamine (7.54 mmol, 2.47 g) was added in one portion to a solution of sodium methoxide in methanol (9.04 mmol) at room temperature (RT). The mixture was stirred at room temperature for 12 hours and poured into water (80 mL). The resulting precipitate was collected by filtration and dried to give pure 1-methoxy-N-benzoyl-1-phenyl-methylamine as an off-white solid (66%, 1.2 gm). Melting point: 96-97 °C. IR: 3290, 3031, 2942, 1650, 1088 cm⁻¹. ¹H NMR (500 MHz, DMSO-*d*₆) δ 9.17 (d, *J* = 9.0 Hz, 1H), 7.97 – 7.91 (m, 2H), 7.56 – 7.52 (m, 1H), 7.50 – 7.44 (m, 4H), 7.37 (t, *J* = 7.4 Hz, 2H), 7.32 (dd, *J* = 8.3, 6.2 Hz, 1H), 6.25 (d, *J* = 9.0 Hz, 1H), 3.38 (s, 3H). ¹³C{¹H} NMR (126 MHz, DMSO-*d*₆) δ 167.4, 140.2, 134.1, 132.1, 128.8, 128.6, 128.5, 128.1, 126.8, 82.3, 55.7. HRMS (ESI-TOF) *m/z*: [M+Na⁺] calcd for (C₁₅H₁₅NNaO₂⁺) 264.0995; Found 264.1000.

*General method to synthesize tosyl containing amide (5)*²⁰

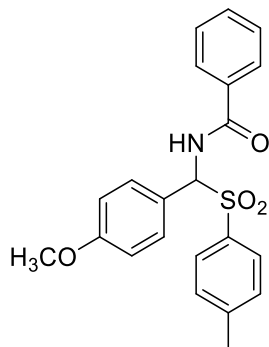
To a solution of dry acetonitrile (300 mL) in a 500 mL dry round bottom flask was added *p*-toluenesulfinic acid, sodium salt (1.5 equiv, 25 mmol) and the appropriate amide (1.5 equiv, 25 mmol). The reaction mixture was placed under nitrogen gas. To this resulting slurry, the appropriate aldehyde (1.0 equiv, 16.7 mmol) was added in one portion. The mixture was cooled to 10 °C using an ice bath. Then, chlorotrimethylsilane (TMSCl) (2.0 equiv, 33.3 mmol) was slowly

added to the reaction mixture to maintain an internal temperature below 25 °C (addition time 15 min). After complete addition of the TMSCl, the reaction was warmed to room temperature and stirred for 24hrs. After that, water (300 mL) was added and the resulting suspension was stirred for 30 min. The solid was isolated by filtration and the filter cake was washed with water (100 mL) and dried under vacuum for 24 hours to give the white powder.

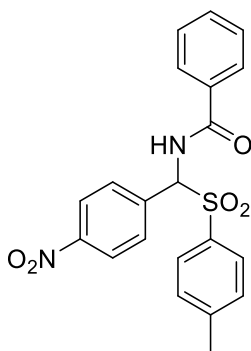
5a



Fine white solid (5.28 gm, 87%). IR: 3378, 3056, 2960, 1650, 1317, 1135 cm^{-1} . ^1H NMR (500 MHz, $\text{DMSO-}d_6$) δ 9.73 (d, $J = 10.3$ Hz, 1H), 7.82 – 7.74 (m, 4H), 7.69 – 7.62 (m, 2H), 7.55 – 7.51 (m, 1H), 7.43 (m, 5H), 7.38 (d, $J = 8.0$ Hz, 2H), 6.60 (d, $J = 10.3$ Hz, 1H), 2.35 (s, 3H). $^{13}\text{C}\{^1\text{H}\}$ NMR (126 MHz, $\text{DMSO-}d_6$) δ 167.2, 145.2, 134.4, 133.7, 132.2, 130.9, 130.5, 130.1, 129.9, 129.5, 128.7, 128.6, 128.3, 73.1, 21.6. HRMS (ESI-TOF) m/z : $[\text{M}+\text{Na}^+]$ calcd for $(\text{C}_{21}\text{H}_{19}\text{NNaO}_3\text{S}^+)$ 388.0978; Found 388.0979.

5b

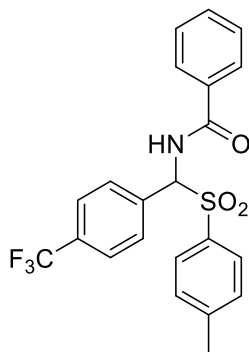
Fine white solid (5.65 gm, 86%). IR: 3353, 3054, 2952, 1670, 1509, 1434, 1305, 1250, 1140 cm^{-1} . ^1H NMR (500 MHz, $\text{DMSO-}d_6$) δ 9.65 (d, $J = 10.3$ Hz, 1H), 7.73 (d, $J = 8.0$ Hz, 2H), 7.68 (d, $J = 8.8$ Hz, 2H), 7.66 – 7.62 (m, 2H), 7.51 (t, $J = 7.6$ Hz, 1H), 7.42 (t, $J = 7.6$ Hz, 2H), 7.36 (d, $J = 8.0$ Hz, 2H), 6.97 (d, $J = 8.8$ Hz, 2H), 6.51 (d, $J = 10.3$ Hz, 1H), 3.76 (s, 3H), 2.34 (s, 3H). $^{13}\text{C}\{^1\text{H}\}$ NMR (126 MHz, $\text{DMSO-}d_6$) δ 167.1, 160.6, 145.0, 134.5, 133.7, 132.2, 131.9, 130.0, 129.4, 128.6, 128.3, 122.6, 114.1, 72.7, 55.7, 21.6. HRMS (ESI-TOF) m/z : $[\text{M-Tosyl}+\text{OCH}_3+\text{Na}^+]$ calcd for ($\text{C}_{16}\text{H}_{17}\text{NNaO}_3^+$) 294.1101; Found 294.1103.

5c

Fine white solid (5.1 gm, 75%). IR: 3254, 3057, 2980, 1650, 1519, 1344, 1322, 1146, 1083 cm^{-1} . ^1H NMR (500 MHz, $\text{DMSO-}d_6$) δ 9.89 (d, $J = 10.3$ Hz, 1H), 8.31 (d, $J = 8.8$ Hz, 2H), 8.13 (d, $J = 8.8$ Hz, 2H), 7.82 (d, $J = 8.2$ Hz, 2H), 7.67 (d, $J = 7.4$ Hz, 2H), 7.54 (t, $J = 7.4$ Hz, 1H), 7.46 –

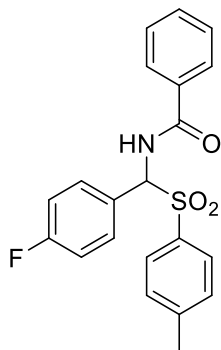
7.38 (m, 4H), 6.87 (d, $J = 10.3$ Hz, 1H). $^{13}\text{C}\{^1\text{H}\}$ NMR (126 MHz, DMSO- d_6) δ 167.3, 148.6, 145.6, 138.2, 133.9, 133.5, 132.4, 131.9, 130.2, 129.6, 128.6, 128.3, 123.7, 72.4, 21.6. HRMS (ESI-TOF) m/z : $[\text{M}+\text{Na}^+]$ calcd for ($\text{C}_{21}\text{H}_{18}\text{N}_2\text{NaO}_5\text{S}^+$) 433.0829; Found 433.0832.

5d



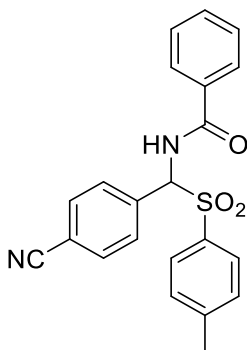
Fine white solid (5.61 gm, 78%). IR: 3281, 3061, 2941, 1649, 1526, 1322, 1145, 1065 cm^{-1} . ^1H NMR (500 MHz, DMSO- d_6) δ 9.84 (d, $J = 10.3$ Hz, 1H), 8.05 (d, $J = 8.1$ Hz, 2H), 7.82 (t, $J = 8.6$ Hz, 4H), 7.65 (d, $J = 8.1$ Hz, 2H), 7.52 (t, $J = 7.4$ Hz, 1H), 7.47 – 7.35 (m, 4H), 6.78 (d, $J = 10.3$ Hz, 1H), 2.34 (s, 3H). $^{13}\text{C}\{^1\text{H}\}$ NMR (126 MHz, DMSO- d_6) δ 167.3, 145.5, 135.6, 134.1, 133.5, 132.3, 131.4, 130.3 (q, $J = 31.8$ Hz), 130.1, 129.6, 128.6, 128.3, 125.6 (q, $J = 3.4$ Hz), 123.4, 72.5, 21.6. HRMS (ESI-TOF) m/z : $[\text{M}+\text{Na}^+]$ calcd for ($\text{C}_{22}\text{H}_{18}\text{F}_3\text{NNaO}_3\text{S}^+$) 456.0852; Found 456.0855.

5e



Fine white solid (4.93 gm, 77%). IR: 3329, 3054, 2964, 1657, 1504, 1308, 1084 cm^{-1} . ^1H NMR (500 MHz, $\text{DMSO-}d_6$) δ 9.72 (d, $J = 10.3$ Hz, 1H), 7.85 (d, $J = 8.9$ Hz, 2H), 7.76 (d, $J = 8.2$ Hz, 2H), 7.65 (d, $J = 8.4$ Hz, 2H), 7.53 (t, $J = 7.4$ Hz, 1H), 7.43 (t, $J = 7.4$ Hz, 2H), 7.38 (d, $J = 8.2$ Hz, 2H), 7.28 (t, $J = 8.9$ Hz, 2H), 6.64 (d, $J = 10.3$ Hz, 1H), 2.35 (s, 3H). $^{13}\text{C}\{^1\text{H}\}$ NMR (126 MHz, $\text{DMSO-}d_6$) δ 167.2, 162.3 (d, $J = 246$ Hz), 145.2, 134.2, 133.6, 132.8 (d, $J = 8$ Hz), 132.3, 130.1, 129.5, 128.6, 128.3, 127.3 (d, $J = 3$ Hz), 115.7 (d, $J = 22$ Hz), 72.3, 21.6. HRMS (ESI-TOF) m/z : $[\text{M}+\text{Na}^+]$ calcd for $(\text{C}_{21}\text{H}_{18}\text{FNNaO}_3\text{S}^+)$ 406.0884; Found 406.0885.

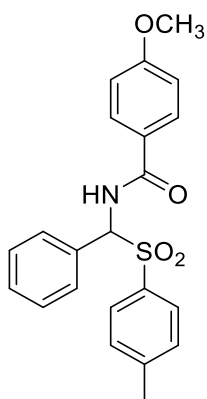
5f



Fine white solid (5.35 gm, 82%). IR: 3316, 3063, 2921, 2228, 1661, 1519, 1320, 1146 cm^{-1} . ^1H NMR (500 MHz, $\text{DMSO-}d_6$) δ 9.79 (d, $J = 10.3$ Hz, 1H), 8.02 (d, $J = 8.3$ Hz, 2H), 7.94 (d, $J = 8.3$

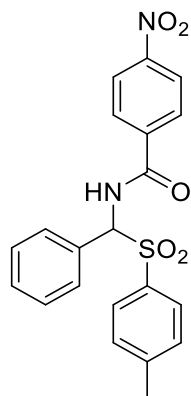
Hz, 2H), 7.79 (d, $J = 8.1$ Hz, 2H), 7.65 (d, $J = 7.4$ Hz, 2H), 7.53 (t, $J = 7.4$ Hz, 1H), 7.43 (t, $J = 7.6$ Hz, 2H), 7.39 (d, $J = 8.1$ Hz, 2H), 6.79 (d, $J = 10.3$ Hz, 1H), 2.34 (s, 3H). $^{13}\text{C}\{^1\text{H}\}$ NMR (126 MHz, DMSO- d_6) δ 167.3, 145.5, 136.3, 134.0, 133.5, 132.6, 132.3, 131.4, 130.2, 129.6, 128.6, 128.3, 119.0, 112.6, 72.5, 21.6. HRMS (ESI-TOF) m/z : $[\text{M}+\text{Na}^+]$ calcd for ($\text{C}_{22}\text{H}_{18}\text{N}_2\text{NaO}_3\text{S}^+$) 413.0930; Found 413.0930.

5g



Fine white solid (6.54 gm, 99%). IR: 3345, 3063, 2951, 1645, 1605, 1492, 1456, 1314, 1259 cm^{-1} . ^1H NMR (500 MHz, DMSO- d_6) δ 9.51 (d, $J = 10.3$ Hz, 1H), 7.79 – 7.68 (m, 6H), 7.41 (m, 3H), 7.35 (d, $J = 8.2$ Hz, 2H), 6.96 (d, $J = 8.8$ Hz, 2H), 6.57 (d, $J = 10.3$ Hz, 1H), 3.78 (s, 3H), 2.33 (s, 3H). $^{13}\text{C}\{^1\text{H}\}$ NMR (126 MHz, DMSO- d_6) δ 166.4, 162.5, 145.1, 134.4, 131.1, 130.5, 130.3, 130.0, 129.8, 129.4, 128.6, 125.6, 113.8, 73.1, 55.9, 21.6. HRMS (ESI-TOF) m/z : $[\text{M-Tosyl}+\text{OCH}_3+\text{Na}^+]$ calcd for ($\text{C}_{16}\text{H}_{17}\text{NNaO}_3^+$) 294.1101; Found 294.1104.

5h

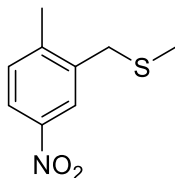


Fine white solid (5.61 gm, 82%). IR: 3309, 3061, 2963, 1667, 1514, 1308, 1141, 1084 cm^{-1} . ^1H NMR (500 MHz, $\text{DMSO-}d_6$) δ 10.11 (d, $J = 10.3$ Hz, 1H), 8.28 (d, $J = 8.7$ Hz, 2H), 7.85 (d, $J = 8.8$ Hz, 2H), 7.77 (dd, $J = 8.8, 4.3$ Hz, 4H), 7.46 – 7.41 (m, 3H), 7.38 (d, $J = 8.2$ Hz, 2H), 6.60 (d, $J = 10.3$ Hz, 1H), 2.35 (s, 3H). $^{13}\text{C}\{^1\text{H}\}$ NMR (126 MHz, $\text{DMSO-}d_6$) δ 165.8, 149.7, 145.4, 139.3, 134.1, 130.5, 130.4, 130.1, 130.0, 129.8, 129.6, 128.7, 123.8, 73.1, 21.6. HRMS (ESI-TOF) m/z : $[\text{M}+\text{Na}^+]$ calcd for ($\text{C}_{21}\text{H}_{18}\text{N}_2\text{NaO}_5\text{S}^+$) 433.0829; Found 433.0834.

Synthesis of Stevens rearrangement product (6)

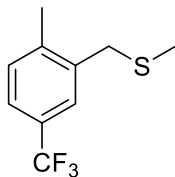
To a solution of dry dichloromethane (15 mL) in a 50 mL dry round bottom flask, different substituted benzyldimethylsulfonium tetrafluoroborate salts (1 equiv, 0.25mmol) were added, followed by DBU base (1.5 equiv, 0.38 mmol) at room temperature. The reaction was placed under nitrogen gas and stirred for 12 hours. Then the solvent was evaporated, and crude products were purified using automated CombiFlash chromatography (silica gel, 20-40 microns, gradient 2-5% ethyl acetate in hexane).

6a



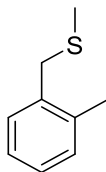
Oil (40 mg, 82%). IR: 3068, 2921, 1582, 1501, 1483, 1346, 1314, 734 cm^{-1} . ^1H NMR (500 MHz, CHCl_3 -*d*) δ 8.08 – 7.97 (m, 2H), 7.32 (d, J = 8.3 Hz, 1H), 3.72 (s, 2H), 2.48 (s, 3H), 2.05 (s, 3H). $^{13}\text{C}\{^1\text{H}\}$ NMR (126 MHz, CHCl_3 -*d*) δ 146.1, 144.8, 137.7, 131.4, 124.1, 122.2, 36.0, 19.5, 15.3. HRMS (ESI-TOF) m/z : [M-SCH₃] calcd for ($\text{C}_8\text{H}_8\text{NO}_2^+$) 150.0550; Found 150.0555.

6b



Oil (40 mg, 73%). IR: 3037, 2918, 1619, 1438, 1320, 1286, 1074 cm^{-1} . ^1H NMR (500 MHz, CHCl_3 -*d*) δ 7.42 (m, 2H), 7.28 (d, J = 7.9 Hz, 1H), 3.70 (s, 2H), 2.45 (s, 3H), 2.04 (s, 3H). $^{13}\text{C}\{^1\text{H}\}$ NMR (126 MHz, CHCl_3 -*d*) δ 140.9, 136.8, 131.0, 128.0 (q, J = 32.3 Hz), 126.1 (q, J = 3.7 Hz), 125.3, 123.9, 36.1, 19.2, 15.2. HRMS (ESI-TOF) m/z : [M-SCH₃] calcd for ($\text{C}_9\text{H}_8\text{F}_3^+$) 173.0573; Found 173.0575.

6c

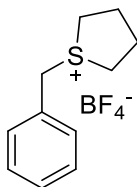


Oil (11 mg, 28%)²¹ (mixture with another compound). IR: 3017, 2913, 1492, 1239, 1049 cm^{-1} . ^1H NMR (500 MHz, CHCl_3 -*d*) δ 7.34 (d, J = 6.5 Hz, 1H), 7.21 – 7.17 (m, 3H), 3.70 (s, 2H), 2.42 (s, 3H), 2.05 (s, 3H). $^{13}\text{C}\{^1\text{H}\}$ NMR (126 MHz, CHCl_3 -*d*) δ 136.7, 135.9, 130.7, 129.7, 127.3, 125.7, 36.3, 19.2, 15.2. HRMS (ESI-TOF) m/z : $[\text{M}-\text{SCH}_3]$ calcd for (C_8H_9^+) 105.0699; Found 105.0704.

General method to synthesize substituted benzyltetrahydrothiophenium tetrafluoroborate salts (7)

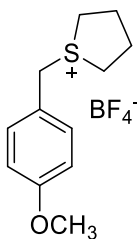
To a solution of dry dichloromethane (30mL) in a 100 mL dry round bottom flask was added the appropriate alcohol (1 equiv, 10 mmol) followed by tetrahydrothiophene (1 equiv, 10 mmol). A solution of tetrafluoroboric acid (tetrafluoroboric acid diethyl ether complex) (1 equiv, 10 mmol) was added dropwise for 10 minutes at 0 °C. The mixture was stirred for 12 hours at room temperature. Evaporation of solvent under reduced pressure gave a colorless, thick oil which was precipitated with diethyl ether to obtain the desired salt as a solid.

7a



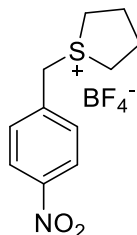
Colorless solid (2.01 gm, 76%). Melting point: 78-80 °C (Lit. value 77-79 °C).²² IR: 3011, 2958, 1497, 1263, 1046, 1013 cm⁻¹. ¹H NMR (500 MHz, CHCl₃-*d*) δ 7.48 – 7.36 (m, 5H), 4.54 (s, 2H), 3.54 (dt, *J* = 13.6, 6.6 Hz, 2H), 3.42 (dt, *J* = 12.2, 5.7 Hz, 2H), 2.29 (qq, *J* = 13.6, 6.6, 5.7 Hz, 4H). ¹³C{¹H} NMR (126 MHz, CHCl₃-*d*) δ 130.6, 130.2, 129.8, 128.0, 46.0, 42.2, 28.4. HRMS (ESI-TOF) *m/z*: [M-BF₄⁻] calcd for (C₁₁H₁₅S⁺) 179.0889; Found 179.0900.

7b



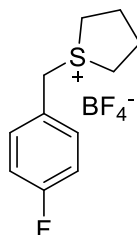
White solid (2.11 gm, 71%). Melting point: 96-99 °C (Lit. value 99-101 °C).²³ IR: 3030, 2955, 1608, 1515, 1459, 1254, 1049 cm⁻¹. ¹H NMR (500 MHz, DMSO-*d*₆) δ 7.48 (d, *J* = 8.6 Hz, 2H), 7.02 (d, *J* = 8.6 Hz, 2H), 4.47 (s, 2H), 3.76 (s, 3H), 3.38 (m, 4H), 2.17 (m, 4H). ¹³C{¹H} NMR (126 MHz, DMSO-*d*₆) δ 160.6, 132.3, 121.7, 115.3, 55.7, 45.3, 42.6, 28.6. HRMS (ESI-TOF) *m/z*: [M-BF₄⁻-SC₄H₈] calcd for (C₈H₉O⁺) 121.0648; Found 121.0655.

7c



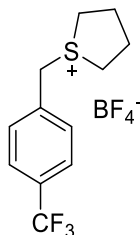
Yellow solid (1.77 gm, 57%). Melting point: 101-105 °C. IR: 3029, 2951, 1515, 1353, 1024 cm^{-1} . ^1H NMR (500 MHz, $\text{DMSO-}d_6$) δ 8.31 (d, $J = 8.5$ Hz, 2H), 7.85 (d, $J = 8.5$ Hz, 2H), 4.65 (s, 2H), 3.46 (m, 4H), 2.31 – 2.14 (m, 4H). $^{13}\text{C}\{^1\text{H}\}$ NMR (126 MHz, $\text{DMSO-}d_6$) δ 148.5, 138.0, 132.3, 124.8, 44.5, 43.6, 28.7. HRMS (ESI-TOF) m/z : $[\text{M-BF}_4^-]$ calcd for $(\text{C}_{11}\text{H}_{14}\text{NO}_2\text{S}^+)$ 224.0745; Found 224.0747.

7d



White solid (2.12 gm, 75%). Melting point: 107-110 °C (Lit. value 109 °C).²⁴ IR: 3012, 2960, 1511, 1423, 1227, 1022 cm^{-1} . ^1H NMR (500 MHz, $\text{DMSO-}d_6$) δ 7.62 (dd, $J = 8.5, 5.5$ Hz, 2H), 7.31 (t, $J = 8.8$ Hz, 2H), 4.51 (s, 2H), 3.41 (m, 4H), 2.31 – 2.08 (m, 4H). $^{13}\text{C}\{^1\text{H}\}$ NMR (126 MHz, $\text{DMSO-}d_6$) δ 162.2 (d, $J = 246$ Hz), 133.2 (d, $J = 8$ Hz), 126.7 (d, $J = 3$ Hz), 116.9 (d, $J = 22$ Hz), 44.7, 43.0, 28.6. HRMS (ESI-TOF) m/z : $[\text{M-BF}_4^-]$ calcd for $(\text{C}_{11}\text{H}_{14}\text{FS}^+)$ 197.0800; Found 197.0804.

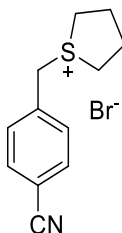
7h



White Solid (1.51 gm, 45%). Melting point: 95-98 °C. IR: 3076, 2963, 1421, 1326, 1046, 1026 cm^{-1} . ^1H NMR (500 MHz, $\text{DMSO-}d_6$) δ 7.85 (d, $J = 8.2$ Hz, 2H), 7.80 (d, $J = 8.2$ Hz, 2H), 4.61 (s, 2H), 3.49 (m, 2H), 3.40 (m, 2H), 2.31 – 2.13 (m, 4H). $^{13}\text{C}\{^1\text{H}\}$ NMR (126 MHz, $\text{DMSO-}d_6$) δ 135.3, 131.8, 130.4 (q, $J = 32.0$ Hz), 126.7 (q, $J = 3.7$ Hz), 125.5, 44.7, 43.5, 28.6. HRMS (ESI-TOF) m/z : $[\text{M-BF}_4^-]$ calcd for $(\text{C}_{12}\text{H}_{14}\text{F}_3\text{S}^+)$ 247.0763; Found 247.0769.

*Synthesis of 1-(4-cyanobenzyl) tetrahydrothiophenium bromide salts (7i)*²⁵

To a solution of dry dichloromethane (30mL) in a 100 mL dry round bottom flask was added the 4-cyanobenzyl bromide (1 equiv, 20mmol) followed by tetrahydrothiophene (2 equiv, 40 mmol) for 30 minutes at 0 °C. The mixture was stirred for 24 hours at room temperature. Evaporation of the solvent under reduced pressure gave a colorless, thick oil which was precipitated with acetone to obtain the desired salt as a solid.



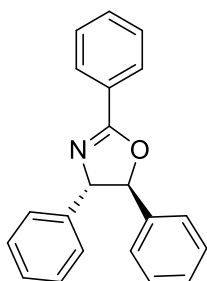
White Solid (2.67 gm, 47%). Melting point: 103-105 °C. ^1H NMR (500 MHz, $\text{DMSO-}d_6$) δ 7.96 (d, $J = 8.3$ Hz, 2H), 7.83 (d, $J = 8.3$ Hz, 2H), 4.70 (s, 2H), 3.48 (m, 4H), 2.32 – 2.13 (m, 4H).

$^{13}\text{C}\{^1\text{H}\}$ NMR (126 MHz, $\text{DMSO-}d_6$) 136.3, 133.6, 131.9, 118.8, 112.6, 44.7, 43.6, 28.7. HRMS (ESI-TOF) m/z : $[\text{M-Br}^-]$ calcd for $(\text{C}_{12}\text{H}_{14}\text{NS}^+)$ 204.0841; Found 204.0848.

The general method to synthesize oxazolines (3)

To a solution of dry dichloromethane (20 mL) in a 50 mL dry round bottom flask, sulfonium salt (1.5 equivalents, 0.38mmol) was added, followed by DBU (3 or 4 equivalents) and the appropriate amide (1 equivalent, 0.25mmol) at room temperature. The reaction was stirred for a total of 12 hours under argon. After that, $\text{BF}_3\cdot\text{OEt}_2$ (3 equivalents, unless otherwise indicated) was added by syringe through the rubber septum dropwise for 5 minutes and stirred for an additional 6 hours. After that, 20mL of 1M NaOH solution was added, and the mixture was extracted with 2×15 mL of dichloromethane, using a separatory funnel. The organic layers were combined, dried over Na_2SO_4 , and concentrated using a rotary evaporator. The desired compound was purified and isolated using automated CombiFlash chromatography (silica gel, 20-40 microns, gradient 2-20% ethyl acetate in hexane).

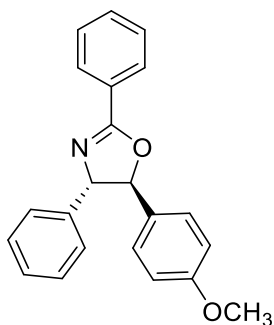
*2,4,5-triphenyl-4,5-dihydrooxazole (3a).*²⁶



Isolated as a solid (45 mg, 60%). mp: 98-100 °C. IR: 3031, 2918, 1648, 1493, 1448, 1324, 1062 cm^{-1} . ^1H NMR (500 MHz, $\text{CHCl}_3\text{-}d$) δ 8.26 – 8.10 (m, 2H), 7.60 – 7.55 (m, 1H), 7.52 – 7.48 (m, 2H), 7.48 – 7.29 (m, 10H), 5.45 (d, $J = 7.6$ Hz, 1H), 5.26 (d, $J = 7.6$ Hz, 1H). $^{13}\text{C}\{^1\text{H}\}$ NMR (126 MHz, $\text{CHCl}_3\text{-}d$) δ 164.1, 142.0, 140.5, 131.8, 129.0, 128.9, 128.7, 128.5, 128.5, 127.8, 127.5,

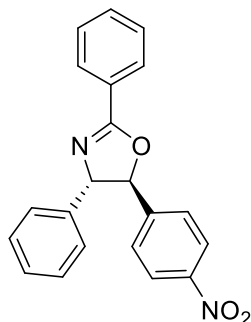
126.8, 125.7, 89.0, 79.0. HRMS (ESI-TOF) m/z : $[M+H]^+$ calcd for $(C_{21}H_{18}NO^+)$ 300.1383; Found 300.1387.

5-(4-methoxyphenyl)-2,4-diphenyl-4,5-dihydrooxazole (3b)



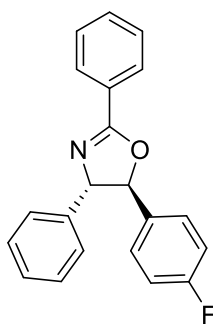
Isolated as a colorless solid (42 mg, 51%). mp: 118-121 °C. IR: 3030, 2956, 1645, 1513, 1449, 1246, 1063, 1024 cm^{-1} . 1H NMR (500 MHz, $CHCl_3-d$) δ 8.16 (d, $J = 7.3$ Hz, 2H), 7.56 (t, $J = 7.6$ Hz, 1H), 7.48 (t, $J = 7.6$ Hz, 2H), 7.38 (t, $J = 7.3$ Hz, 2H), 7.34 – 7.27 (m, 5H), 7.00 – 6.91 (m, 2H), 5.39 (d, $J = 7.8$ Hz, 1H), 5.26 (d, $J = 7.8$ Hz, 1H), 3.83 (s, 3H). $^{13}C\{^1H\}$ NMR (126 MHz, $CHCl_3-d$) δ 164.1, 159.8, 142.0, 132.3, 131.8, 128.8, 128.7, 128.5, 127.8, 127.5, 127.4, 126.7, 114.3, 89.1, 78.6, 55.4. HRMS (ESI-TOF) m/z : $[M+H]^+$ calcd for $(C_{22}H_{20}NO_2^+)$ 330.1489; Found 330.1495.

5-(4-nitrophenyl)-2,4-diphenyl-4,5-dihydrooxazole (**3c**).



Isolated as a yellowish solid (32 mg, 37%). mp: 101-104 °C. IR: 3028, 2921, 1649, 1522, 1340, 1060 cm^{-1} . ^1H NMR (500 MHz, CHCl_3 -*d*) δ 8.27 (d, J = 8.8 Hz, 2H), 8.19 – 8.09 (m, 2H), 7.58 (t, J = 7.4 Hz, 1H), 7.51 (t, J = 7.8 Hz, 4H), 7.41 (t, J = 7.3 Hz, 2H), 7.36 (t, J = 7.3 Hz, 1H), 7.32 – 7.28 (m, 2H), 5.52 (d, J = 7.7 Hz, 1H), 5.16 (d, J = 7.7 Hz, 1H). $^{13}\text{C}\{^1\text{H}\}$ NMR (126 MHz, CHCl_3 -*d*) δ 163.9, 147.9, 147.6, 141.1, 132.1, 129.1, 128.7, 128.6, 128.3, 126.9, 126.8, 126.2, 124.3, 87.7, 79.4. HRMS (ESI-TOF) m/z : $[\text{M}+\text{H}]^+$ calcd for $(\text{C}_{21}\text{H}_{17}\text{N}_2\text{O}_3)^+$ 345.1234; Found 345.1241.

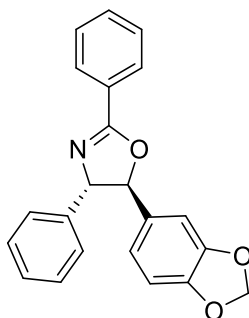
5-(4-fluorophenyl)-2,4-diphenyl-4,5-dihydrooxazole (**3d**).



Isolated as a white solid (53 mg, 66% with regioisomer). mp: 53-56 °C. IR: 3032, 2923, 1648, 1508, 1322 1223, 1062 cm^{-1} . ^1H NMR (500 MHz, CHCl_3 -*d*) δ 8.13 (d, J = 7.2 Hz, 2H), 7.56 (t, J = 7.4 Hz, 1H), 7.50 – 7.46 (m, 2H), 7.42 – 7.28 (m, 7H), 7.10 (t, J = 8.6 Hz, 2H), 5.40 (d, J = 7.7

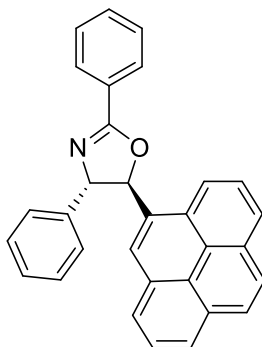
Hz, 1H), 5.20 (d, $J = 7.7$ Hz, 1H). $^{13}\text{C}\{^1\text{H}\}$ NMR (126 MHz, CHCl_3-d) δ 164.0, 163.7 (d, $J = 246$ Hz), 141.7, 136.2, 131.8, 128.9, 128.5, 127.9, 127.5 (d, $J = 8$ Hz), 127.3, 126.7, 125.7, 116.0 (d, $J = 21.5$ Hz), 88.4, 79.0. HRMS (ESI-TOF) m/z : $[\text{M}+\text{H}]^+$ calcd for ($\text{C}_{21}\text{H}_{17}\text{FNO}^+$) 318.1289; Found 318.1293.

5-(benzo[d][1,3]dioxol-5-yl)-2,4-diphenyl-4,5-dihydro oxazole (3e).



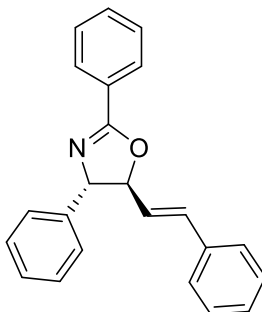
Isolated as a white solid (60 mg, 70%). mp: 121-122 °C. IR: 3033, 2980, 1636, 1491, 1444, 1248, 1063, 1020 cm^{-1} . ^1H NMR (500 MHz, CHCl_3-d) δ 8.18 – 8.10 (m, 2H), 7.58 – 7.53 (m, 1H), 7.48 (t, $J = 7.5$ Hz, 2H), 7.39 (t, $J = 7.2$ Hz, 2H), 7.35 – 7.28 (m, 3H), 6.89 (s, 1H), 6.82 (s, 2H), 5.98 (s, 2H), 5.33 (d, $J = 7.7$ Hz, 1H), 5.23 (d, $J = 7.7$ Hz, 1H). $^{13}\text{C}\{^1\text{H}\}$ NMR (126 MHz, CHCl_3-d) δ 164.0, 148.3, 147.8, 142.0, 134.2, 131.7, 128.9, 128.6, 128.5, 127.8, 127.5, 126.7, 119.7, 108.5, 106.2, 101.3, 89.1, 78.9. HRMS (ESI-TOF) m/z : $[\text{M}+\text{H}]^+$ calcd for ($\text{C}_{22}\text{H}_{18}\text{NO}_3^+$) 344.1281; Found 344.1284.

2,4-diphenyl-5-(pyren-4-yl)-4,5-dihydrooxazole (3f).



Isolated as a white solid (55 mg, 52%). mp: 131-135 °C. IR: 3028, 2980, 1648, 1600, 1577, 1448, 1317, 1240, 1061 cm^{-1} . ^1H NMR (500 MHz, CHCl_3 -*d*) δ 8.39 – 8.29 (m, 2H), 8.23 – 7.98 (m, 8H), 7.89 (d, J = 9.3 Hz, 1H), 7.61 (m, 3H), 7.53 – 7.35 (m, 5H), 6.53 (d, J = 7.2 Hz, 1H), 5.46 (d, J = 7.2 Hz, 1H). $^{13}\text{C}\{^1\text{H}\}$ NMR (126 MHz, CHCl_3 -*d*) δ 164.3, 142.0, 133.7, 131.9, 131.4, 131.3, 130.6, 129.0, 128.9, 128.7, 128.1, 128.1, 127.7, 127.6, 127.5, 127.5, 127.3, 126.2, 125.6, 125.4, 125.2, 125.1, 124.8, 122.9, 122.5, 86.9, 79.6. HRMS (ESI-TOF) m/z : $[\text{M}+\text{H}]^+$ calcd for $(\text{C}_{22}\text{H}_{20}\text{NO}_2)^+$ 424.1696; Found 424.1699.

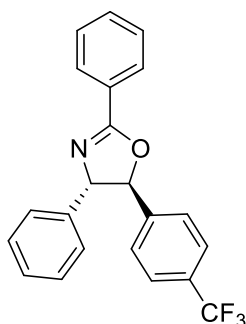
2,4-diphenyl-5-((E)-styryl)-4,5-dihydrooxazole (3g).



Isolated as a white solid (52 mg, 64%). mp: 105-108 °C. IR: 3025, 2924, 1646, 1601, 1578, 1449, 1324, 1059 cm^{-1} . ^1H NMR (500 MHz, CHCl_3 -*d*) δ 8.12 (dd, J = 8.3, 1.2 Hz, 2H), 7.57 – 7.53 (m, 1H), 7.50 – 7.43 (m, 4H), 7.43 – 7.27 (m, 8H), 6.68 (d, J = 15.8 Hz, 1H), 6.44 (dd, J = 15.8, 7.9

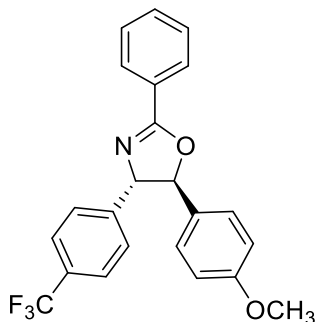
Hz, 1H), 5.17 (d, $J = 7.9$ Hz, 1H), 5.05 (m, 1H). $^{13}\text{C}\{^1\text{H}\}$ NMR (126 MHz, CHCl_3 - d) δ 164.0, 141.6, 135.9, 133.6, 131.7, 128.8, 128.7, 128.6, 128.5, 128.4, 127.8, 127.6, 126.8, 126.8, 126.6, 88.8, 76.4. HRMS (ESI-TOF) m/z : $[\text{M}+\text{H}]^+$ calcd for $(\text{C}_{23}\text{H}_{20}\text{NO}^+)$ 326.1539; Found 326.1544.

2,4-diphenyl-5-(4-(trifluoromethyl)phenyl)-4,5-dihydro oxazole (3h).



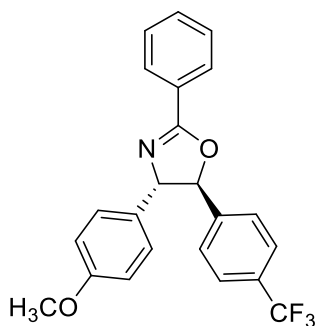
Isolated as a mixture (51 mg, 55% yield) with its regioisomer (**3t**). IR: 3032, 2988, 1675, 1650, 1320, 1281, 1063 cm^{-1} . ^1H NMR (500 MHz, CHCl_3 - d) δ 8.18 – 8.13 (m, 2H), 7.67 (m, 2H), 7.59 (t, $J = 7.4$ Hz, 1H), 7.52 – 7.31 (m, 9H), 5.49 (d, $J = 7.7$ Hz, 1H), 5.20 (d, $J = 7.7$ Hz, 1H). $^{13}\text{C}\{^1\text{H}\}$ NMR (126 MHz, CHCl_3 - d) δ 164.0, 144.4, 141.4, 132.0, 130.5 (q, $J = 32.4$ Hz), 129.0, 128.7, 128.6, 128.1, 127.1, 126.8, 125.9 (q, $J = 3.7$ Hz), 125.9, 122.9, 88.1, 79.2. HRMS (ESI-TOF) m/z : $[\text{M}+\text{H}]^+$ calcd for $(\text{C}_{22}\text{H}_{17}\text{F}_3\text{NO}^+)$ 368.1257; Found 368.1258.

5-(4-methoxyphenyl)-2-phenyl-4-(4-(trifluoromethyl) phenyl)-4,5-dihydrooxazole (**3i**).



Isolated as a white solid (40 mg, 40%). mp: 99-101 °C. IR: 3062, 2925, 1647, 1513, 1322, 1247, 1064 cm^{-1} . ^1H NMR (500 MHz, CHCl_3 -*d*) δ 8.18 – 8.09 (m, 2H), 7.64 (d, J = 8.1 Hz, 2H), 7.59 – 7.55 (m, 1H), 7.49 (t, J = 7.6 Hz, 2H), 7.42 (d, J = 8.1 Hz, 2H), 7.33 – 7.30 (m, 2H), 6.98 – 6.95 (m, 2H), 5.32 (s, 2H), 3.85 (s, 3H). $^{13}\text{C}\{^1\text{H}\}$ NMR (126 MHz, CHCl_3 -*d*) δ 164.7, 160.0, 146.0, 131.9, 131.7, 129.9 (q, J = 32.4 Hz), 128.7, 128.5, 127.5, 127.3, 127.1, 125.8 (q, J = 3.7 Hz), 123.1, 114.4, 88.9, 78.3, 55.4. HRMS (ESI-TOF) m/z : $[\text{M}+\text{H}]^+$ calcd for $(\text{C}_{23}\text{H}_{19}\text{F}_3\text{NO}_2)^+$ 398.1362; Found 398.1367.

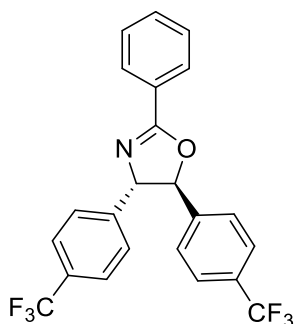
4-(4-methoxyphenyl)-2-phenyl-5-(4-(trifluoromethyl) phenyl)-4,5-dihydrooxazole (**3j**).



Isolated as a white solid (combined yield **3i/3j** (1:1) as poorly separable mixture (69mg, 69%). A small amount of pure **3j** was used for complete characterization. mp: 95-97 °C. IR: 3063, 2926, 1646, 1514, 1322, 1248, 1065 cm^{-1} . ^1H NMR (500 MHz, CHCl_3 -*d*) δ 8.12 (d, J = 7.6 Hz, 2H), 7.66

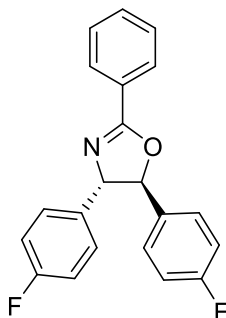
(d, $J = 8.1$ Hz, 2H), 7.57 (t, $J = 7.3$ Hz, 1H), 7.53 – 7.41 (m, 4H), 7.22 (d, $J = 8.5$ Hz, 2H), 6.92 (d, $J = 8.5$ Hz, 2H), 5.44 (d, $J = 7.7$ Hz, 1H), 5.12 (d, $J = 7.7$ Hz, 1H), 3.82 (s, 3H). $^{13}\text{C}\{^1\text{H}\}$ NMR (126 MHz, CHCl_3 -d) δ 163.7, 159.4, 144.5, 133.5, 131.9, 130.7 (q, $J = 32.4$ Hz), 128.6, 128.6, 128.0, 127.2, 125.9 (q, $J = 3.7$ Hz), 125.8, 125.1, 114.4, 88.2, 78.8, 55.4. HRMS (ESI-TOF) m/z : $[\text{M}+\text{H}]^+$ calcd for $(\text{C}_{23}\text{H}_{19}\text{F}_3\text{NO}_2^+)$ 398.1362; Found 398.1365.

4,5-bis(4-(trifluoromethyl)phenyl)-2-phenyl-4,5-dihydrooxazole (3k).



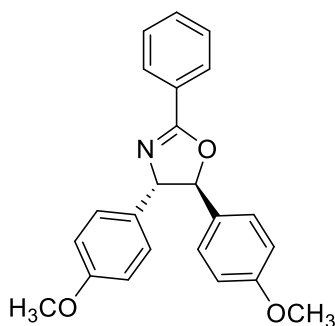
Isolated as a white solid (79 mg, 72%). mp: 98-101 °C. IR: 3058, 2924, 1694, 1322, 1109, 1062 cm^{-1} . ^1H NMR (500 MHz, CHCl_3 -d) δ 8.14 (dd, $J = 8.2, 1.0$ Hz, 2H), 7.69 (dd, $J = 14.7, 8.2$ Hz, 4H), 7.62 – 7.58 (m, 1H), 7.53 – 7.47 (m, 4H), 7.43 (d, $J = 8.2$ Hz, 2H), 5.44 (d, $J = 7.8$ Hz, 1H), 5.26 (d, $J = 7.8$ Hz, 1H). $^{13}\text{C}\{^1\text{H}\}$ NMR (126 MHz, CHCl_3 -d) δ 164.7, 145.3, 143.8, 132.2, 130.8 (q, $J = 32.7$ Hz), 130.5 (q, $J = 32.5$ Hz), 128.7, 128.7, 127.2, 126.8, 126.1 (q, $J = 3.4$ Hz), 126.0 (q, $J = 3.4$ Hz), 126.0, 125.1, 122.8, 88.0, 78.7. HRMS (ESI-TOF) m/z : $[\text{M}+\text{H}]^+$ calcd for $(\text{C}_{23}\text{H}_{16}\text{F}_6\text{NO}^+)$ 436.1131; Found 436.1134.

4,5-bis(4-fluorophenyl)-2-phenyl-4,5-dihydrooxazole (3l).



Isolated as a white solid (48 mg, 57%). mp: 85-88 °C. IR: 3053, 2923, 1650, 1604, 1507, 1319, 1219, 1063 cm⁻¹. ¹H NMR (500 MHz, CHCl₃-*d*) δ 8.17 – 8.06 (m, 2H), 7.59 – 7.53 (m, 1H), 7.48 (t, *J* = 7.6 Hz, 2H), 7.32 (m, 2H), 7.27 – 7.24 (m, 2H), 7.16 – 6.99 (m, 4H), 5.34 (d, *J* = 7.8 Hz, 1H), 5.17 (d, *J* = 7.8 Hz, 1H). ¹³C{¹H} NMR (126 MHz, CHCl₃-*d*) δ 164.1, 163.8 (d, *J* = 246 Hz), 163.4 (d, *J* = 245 Hz), 137.5 (d, *J* = 3 Hz), 135.9 (d, *J* = 3 Hz), 131.9, 128.6, 128.6, 128.4 (d, *J* = 8 Hz), 127.5 (d, *J* = 8 Hz), 127.2, 116.0 (d, *J* = 21.5 Hz), 115.7 (d, *J* = 21.5 Hz), 88.5, 78.4. HRMS (ESI-TOF) *m/z*: [M+H]⁺ calcd for (C₂₁H₁₆F₂NO⁺) 336.1194; Found 336.1200.

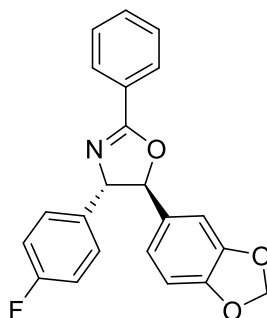
4,5-bis(4-methoxyphenyl)-2-phenyl-4,5-dihydrooxazole (3m).



Isolated as a white solid (31 mg, 34%). mp: 93-95 °C. IR: 3063, 2927, 1645, 1609, 1509, 1241, 1146, 1029 cm⁻¹. ¹H NMR (500 MHz, CHCl₃-*d*) δ 8.17 – 8.08 (m, 2H), 7.54 (t, *J* = 7.6 Hz, 1H), 7.47 (t, *J* = 7.6 Hz, 2H), 7.29 (d, *J* = 8.7 Hz, 2H), 7.22 (d, *J* = 8.7 Hz, 2H), 6.92 (dd, *J* = 14.1, 8.7

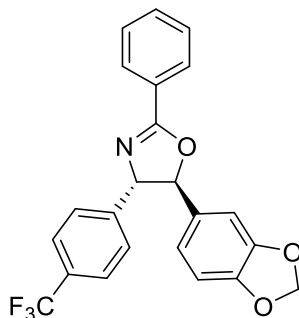
Hz, 4H), 5.34 (d, $J = 7.8$ Hz, 1H), 5.18 (d, $J = 7.8$ Hz, 1H), 3.83 (s, 3H), 3.82 (s, 3H). $^{13}\text{C}\{^1\text{H}\}$ NMR (126 MHz, CHCl_3 - d) δ 163.8, 159.8, 159.2, 134.2, 132.4, 131.6, 128.6, 128.4, 127.9, 127.7, 127.3, 114.3, 114.2, 89.1, 78.3, 55.3, 55.3. HRMS (ESI-TOF) m/z : $[\text{M}+\text{H}]^+$ calcd for $(\text{C}_{23}\text{H}_{22}\text{NO}_3^+)$ 360.1594; Found 360.1599.

5-(benzo[d][1,3]dioxol-5-yl)-4-(4-fluorophenyl)-2-phenyl -4,5-dihydrooxazole (3n).



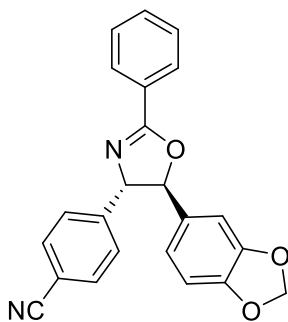
Isolated as a yellowish solid (52 mg, 57%). mp: 80-83 °C. IR: 3038, 2922, 1638, 1504, 1492, 1444, 1336, 1248, 1227, 1062, 1032 cm^{-1} . ^1H NMR (500 MHz, CHCl_3 - d) δ 8.14 – 8.08 (m, 2H), 7.55 (d, $J = 7.5$ Hz, 1H), 7.49 (d, $J = 7.8$ Hz, 2H), 7.27 – 7.23 (m, 2H), 7.07 (t, $J = 8.7$ Hz, 2H), 6.86 (d, $J = 1.6$ Hz, 1H), 6.84 – 6.78 (m, 2H), 6.00 (s, 2H), 5.26 (d, $J = 7.8$ Hz, 1H), 5.18 (d, $J = 7.8$ Hz, 1H). $^{13}\text{C}\{^1\text{H}\}$ NMR (126 MHz, CHCl_3 - d) δ 164.1, 163.4 (d, $J = 246$ Hz), 148.3, 147.9, 137.7, 133.9, 131.8, 128.6, 128.5, 128.3 (d, $J = 8$ Hz), 127.3, 119.7, 115.8 (d, $J = 21.5$ Hz), 108.5, 106.1, 101.3, 89.2, 78.2. HRMS (ESI-TOF) m/z : $[\text{M}+\text{H}]^+$ calcd for $(\text{C}_{22}\text{H}_{17}\text{FNO}_3^+)$ 362.1187; Found 362.1187.

5-(benzo[d][1,3]dioxol-5-yl)-2-phenyl-4-(4-(trifluoro methyl)phenyl)-4,5-dihydrooxazole (**3o**).



Isolated as a pink solid (64 mg, 62%). mp: 87-90 °C. IR: 3067, 2904, 1638, 1487, 1447, 1319, 1247, 1127, 1065, 1038 cm⁻¹. ¹H NMR (500 MHz, CHCl₃-d) δ 8.14 – 8.08 (m, 2H), 7.63 (d, *J* = 8.1 Hz, 2H), 7.56 (t, *J* = 7.4 Hz, 1H), 7.48 (t, *J* = 7.6 Hz, 2H), 7.41 (d, *J* = 8.1 Hz, 2H), 6.87 (d, *J* = 1.4 Hz, 1H), 6.84 – 6.77 (m, 2H), 6.00 (s, 2H), 5.27 (s, 2H). ¹³C{¹H} NMR (126 MHz, CHCl₃-d) δ 164.6, 148.4, 148.1, 145.8, 133.6, 132.0, 129.9 (q, *J* = 32.4 Hz), 128.6, 128.6, 127.2, 127.0, 125.8 (q, *J* = 3.7 Hz), 123.0, 119.9, 108.5, 106.2, 101.4, 89.0, 78.4. HRMS (ESI-TOF) *m/z*: [M+H]⁺ calcd for (C₂₃H₁₇F₃NO₃⁺) 412.1155; Found 412.1157.

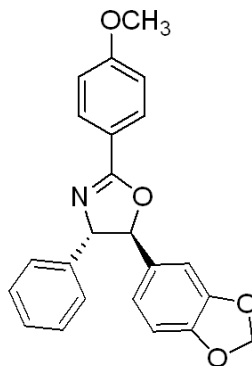
4-(5-(benzo[d][1,3]dioxol-5-yl)-2-phenyl-4,5-dihydro oxazol-4-yl)benzonitrile (**3p**).



Isolated as a colorless solid (71 mg, 77%). mp: 112-114 °C. IR: 3062, 2978, 2227, 1643, 1489, 1445, 1210, 1037 cm⁻¹. ¹H NMR (500 MHz, CHCl₃-d) δ 8.10 (d, *J* = 8.3 Hz, 2H), 7.68 (d, *J* = 8.3 Hz, 2H), 7.58 (t, *J* = 7.4 Hz, 1H), 7.49 (t, *J* = 7.6 Hz, 2H), 7.41 (d, *J* = 8.3 Hz, 2H), 6.88 – 6.82 (m, 2H), 6.80 (dd, *J* = 8.0, 1.7 Hz, 1H), 6.01 (s, 2H), 5.27 (d, *J* = 8.0 Hz, 1H), 5.23 (d, *J* = 8.0 Hz,

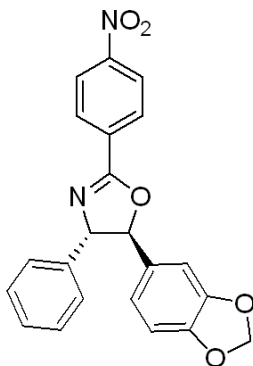
¹H). ¹³C{¹H} NMR (126 MHz, CHCl₃-*d*) δ 164.9, 148.5, 148.2, 147.1, 133.2, 132.7, 132.1, 128.7, 128.6, 127.4, 126.9, 120.0, 118.7, 111.7, 108.6, 106.2, 101.4, 88.9, 78.3. HRMS (ESI-TOF) *m/z*: [M+H]⁺ calcd for (C₂₃H₁₇N₂O₃⁺) 369.1234; Found 369.1234.

*5-(benzo[d][1,3]dioxol-5-yl)-2-(4-methoxyphenyl)-4-phenyl-4,5-dihydrooxazole (3q).*²⁷



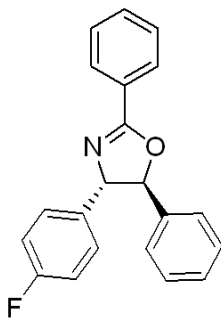
Isolated as a white solid (69 mg, 74%). mp: 93-95 °C. IR: 3029, 2979, 1643, 1608, 1501, 1488, 1446, 1339, 1243, 1146, 1038 cm⁻¹. ¹H NMR (500 MHz, CHCl₃-*d*) δ 8.06 (d, *J* = 8.8 Hz, 2H), 7.39 – 7.27 (m, 5H), 6.98 (d, *J* = 8.8 Hz, 2H), 6.87 (s, 1H), 6.83 – 6.78 (m, 2H), 5.99 (s, 2H), 5.29 (d, *J* = 7.6 Hz, 1H), 5.17 (d, *J* = 7.6 Hz, 1H), 3.89 (s, 3H). ¹³C{¹H} NMR (126 MHz, CHCl₃-*d*) δ 163.8, 162.4, 148.2, 147.8, 142.1, 134.3, 130.4, 128.8, 127.7, 126.7, 119.9, 119.7, 113.8, 108.4, 106.2, 101.3, 89.0, 78.8, 55.5. HRMS (ESI-TOF) *m/z*: [M+H]⁺ calcd for (C₂₃H₂₀NO₄⁺) 374.1387; Found 374.1387.

5-(benzo[d][1,3]dioxol-5-yl)-2-(4-nitrophenyl)-4-phenyl-4,5-dihydrooxazole (**3r**).²⁸



Isolated as a yellowish solid (50 mg, 51%). mp: 118-120 °C. IR: 3068, 2919, 1641, 1594, 1511, 1491, 1335, 1253, 1072, 1040 cm⁻¹. ¹H NMR (500 MHz, CHCl₃-d) δ 8.37 – 8.25 (m, 4H), 7.39 (t, *J* = 7.3 Hz, 2H), 7.34 (t, *J* = 7.3 Hz, 1H), 7.29 – 7.26 (m, 2H), 6.88 – 6.77 (m, 3H), 6.00 (s, 2H), 5.38 (d, *J* = 8.1 Hz, 1H), 5.26 (d, *J* = 8.1 Hz, 1H). ¹³C{¹H} NMR (126 MHz, CHCl₃-d) δ 162.1, 149.7, 148.4, 148.1, 141.1, 133.3, 133.3, 129.6, 129.0, 128.1, 126.6, 123.7, 120.0, 108.5, 106.2, 101.4, 89.8, 78.9. HRMS (ESI-TOF) *m/z*: [M+H]⁺ calcd for (C₂₂H₁₇N₂O₅)⁺ 389.1132; Found 389.1133.

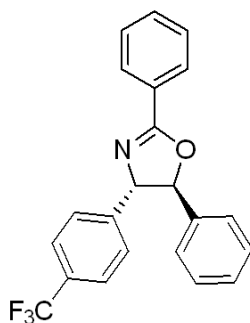
4-(4-fluorophenyl)-2,5-diphenyl-4,5-dihydrooxazole (**3s**).



Isolated as a white solid (33 mg, 41% with its regioisomer). mp: 89-93 °C. IR: 3032, 2980, 1651, 1507, 1319, 1222, 1063 cm⁻¹. ¹H NMR (500 MHz, CHCl₃-d) δ 8.19 – 8.07 (m, 2H), 7.56 (t, *J* = 7.4 Hz, 1H), 7.48 (t, *J* = 7.7 Hz, 2H), 7.43 – 7.34 (m, 5H), 7.28 (dd, *J* = 6.0, 2.7 Hz, 2H), 7.11 –

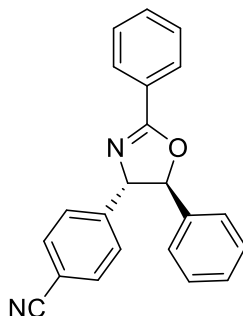
7.02 (m, 2H), 5.36 (d, $J = 7.8$ Hz, 1H), 5.21 (d, $J = 7.8$ Hz, 1H). $^{13}\text{C}\{^1\text{H}\}$ NMR (126 MHz, CHCl_3 - d) δ 164.2, 163.4 (d, $J = 246$ Hz), 140.2, 137.7, 131.8, 129.0, 128.6, 128.6, 128.5, 128.5 (d, $J = 8$ Hz), 127.3, 125.7, 115.8 (d, $J = 21.5$ Hz), 89.1, 78.4. HRMS (ESI-TOF) m/z : $[\text{M}+\text{H}]^+$ calcd for ($\text{C}_{21}\text{H}_{17}\text{FNO}^+$) 318.1289; Found 318.1292.

2,5-diphenyl-4-(4-(trifluoromethyl)phenyl)-4,5-dihydro oxazole (3t).



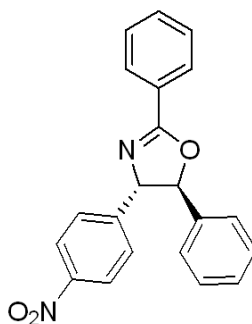
Isolated as a white solid (56 mg, 61%). mp: 92-95 °C. IR: 3031, 2923, 1645, 1619, 1321, 1120, 1065, 1019 cm^{-1} . ^1H NMR (500 MHz, CHCl_3 - d) δ 8.22 – 8.11 (m, 2H), 7.66 (d, $J = 8.1$ Hz, 2H), 7.58 (t, $J = 7.5$ Hz, 1H), 7.51 (t, $J = 7.5$ Hz, 2H), 7.47 – 7.35 (m, 7H), 5.39 (d, $J = 7.9$ Hz, 1H), 5.32 (d, $J = 7.9$ Hz, 1H). $^{13}\text{C}\{^1\text{H}\}$ NMR (126 MHz, CHCl_3 - d) δ 164.7, 145.9, 139.9, 132.0, 130.2 (q, $J = 32.4$ Hz), 129.1, 128.8, 128.7, 128.6, 127.2, 127.1, 125.9 (q, $J = 3.7$ Hz), 125.8, 123.0, 88.9, 78.5. HRMS (ESI-TOF) m/z : $[\text{M}+\text{H}]^+$ calcd for ($\text{C}_{22}\text{H}_{17}\text{F}_3\text{NO}^+$) 368.1257; Found 368.1261.

4-(2,5-diphenyl-4,5-dihydrooxazol-4-yl)benzonitrile (**3u**).



Isolated as a colorless solid (56 mg, 69%). mp: 116-118 °C. IR: 3065, 2923, 2225, 1643, 1323, 1278, 1088, 1065 cm⁻¹. ¹H NMR (500 MHz, CHCl₃-*d*) δ 8.13 (d, *J* = 7.4 Hz, 2H), 7.69 (d, *J* = 8.3 Hz, 2H), 7.59 (t, *J* = 7.4 Hz, 1H), 7.50 (t, *J* = 7.6 Hz, 2H), 7.47 – 7.39 (m, 5H), 7.36 (d, *J* = 6.8 Hz, 2H), 5.34 (d, *J* = 7.9 Hz, 1H), 5.30 (d, *J* = 7.9 Hz, 1H). ¹³C{¹H}NMR (126 MHz, CHCl₃-*d*) δ 165.0, 147.1, 139.6, 132.7, 132.1, 129.2, 128.9, 128.7, 128.6, 127.5, 127.0, 125.8, 118.7, 111.7, 88.8, 78.5. HRMS (ESI-TOF) *m/z*: [M+H]⁺ calcd for (C₂₂H₁₇N₂O⁺) 325.1335; Found 325.1338.

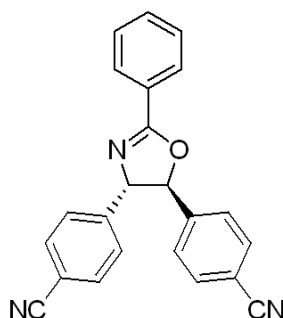
4-(4-nitrophenyl)-2,5-diphenyl-4,5-dihydrooxazole (**3v**).



Isolated as a yellowish solid (26 mg, 30%). mp: 82-85 °C. IR: 3031, 2923, 1678, 1601, 1518, 1343, 1316, 1064 cm⁻¹. ¹H NMR (500 MHz, CHCl₃-*d*) δ 8.24 (d, *J* = 8.8 Hz, 2H), 8.13 (d, *J* = 7.1 Hz, 2H), 7.58 (t, *J* = 7.4 Hz, 1H), 7.52 – 7.41 (m, 7H), 7.38 – 7.34 (m, 2H), 5.37 – 5.32 (m, 2H). ¹³C{¹H} NMR (126 MHz, CHCl₃-*d*) δ 165.1, 149.1, 147.6, 139.5, 132.2, 129.2, 129.0, 128.7,

128.6, 127.6, 127.0, 125.9, 124.1, 88.8, 78.3. HRMS (ESI-TOF) m/z : $[M+H]^+$ calcd for $(C_{21}H_{17}N_2O_3^+)$ 345.1234; Found 345.1239.

4,4'-(2-phenyl-4,5-dihydrooxazole-4,5-diyl) dibenzonitrile (3w).



Isolated as a white solid (50 mg, 58%). mp: 146-148 °C. 1H NMR (500 MHz, $CHCl_3-d$) 8.12 (dd, $J = 8.3, 1.3$ Hz, 2H), 7.73 (dd, $J = 14.2, 8.3$ Hz, 4H), 7.63 – 7.59 (m, 1H), 7.52 (t, $J = 7.6$ Hz, 2H), 7.46 (d, $J = 8.1$ Hz, 2H), 7.42 (d, $J = 8.1$ Hz, 2H), 5.40 (d, $J = 7.7$ Hz, 1H), 5.23 (d, $J = 7.7$ Hz, 1H). $^{13}C\{^1H\}$ NMR (126 MHz, $CHCl_3-d$) δ 164.9, 146.3, 144.8, 133.0, 132.9, 132.4, 128.7, 128.7, 127.5, 126.4, 126.2, 118.5, 118.3, 112.8, 112.2, 87.6, 78.7. HRMS (ESI-TOF) m/z : $[M+H]^+$ calcd for $(C_{23}H_{16}N_3O^+)$ 350.1288; Found 350.1291.

APPENDIX

151

Figure 3.1. ^1H and ^{13}C NMR Spectra of Compound 1

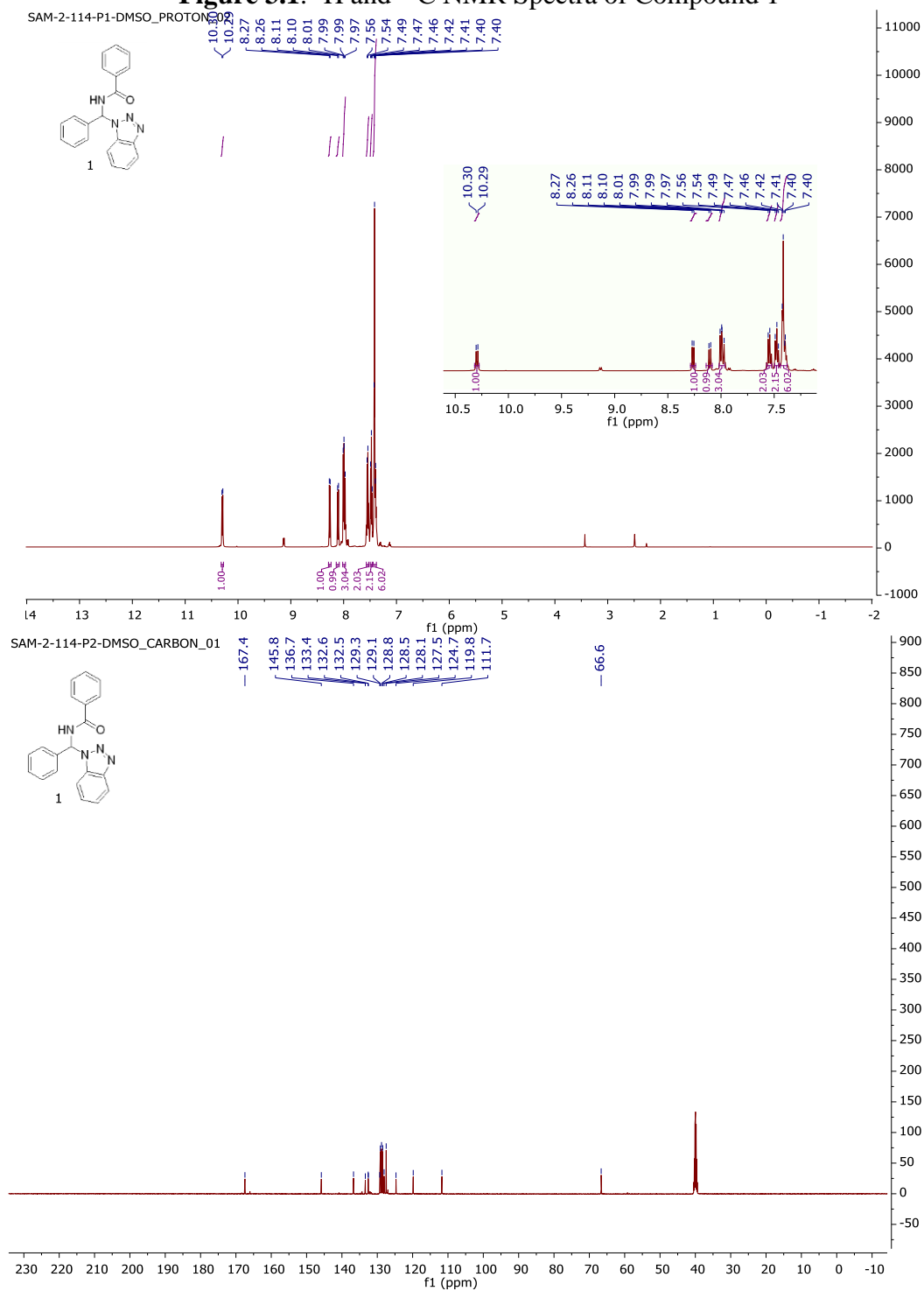


Figure 3.2. ^1H and ^{13}C NMR Spectra of Compound 2a

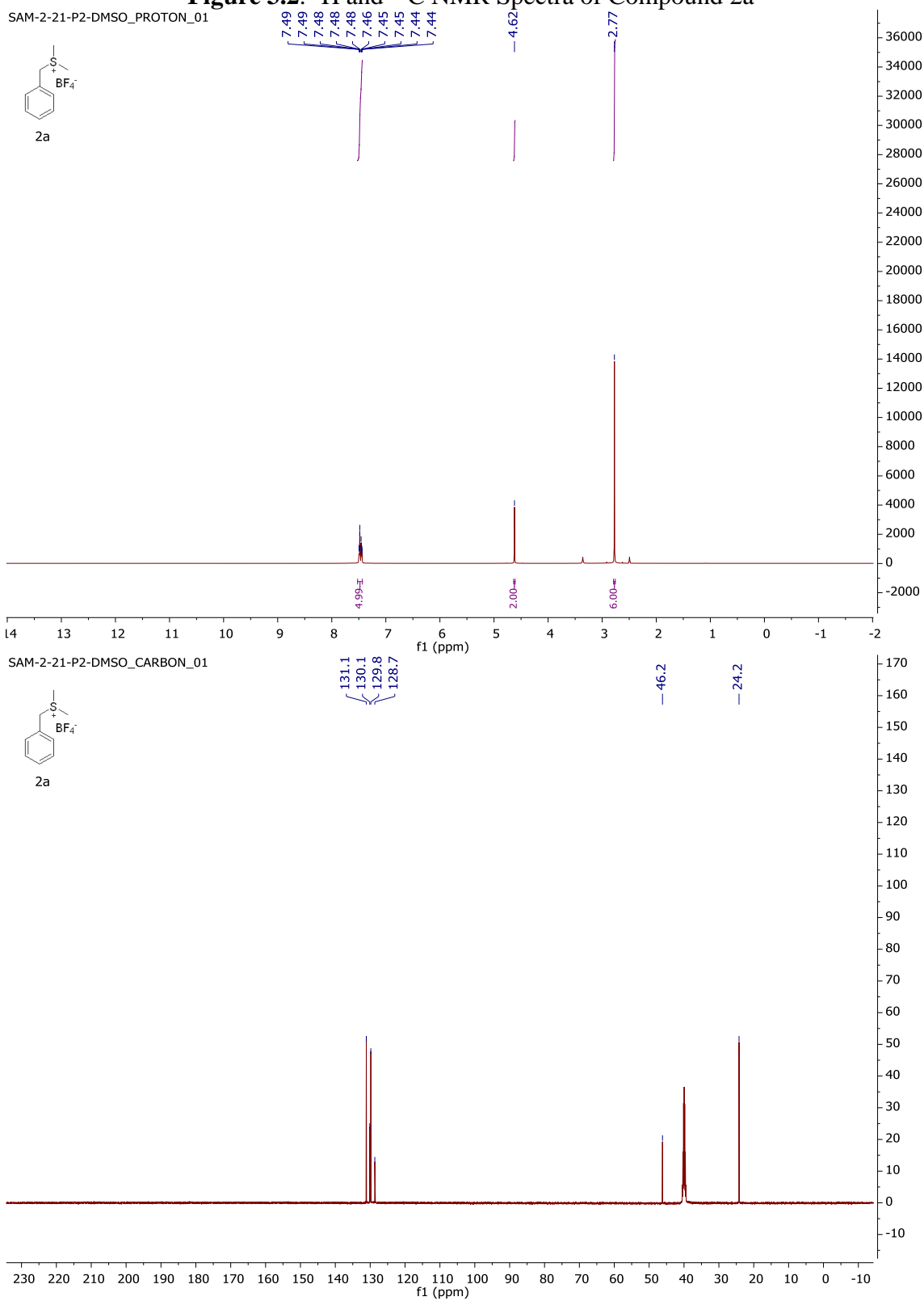


Figure 3.3. ^1H and ^{13}C NMR Spectra of Compound 2b

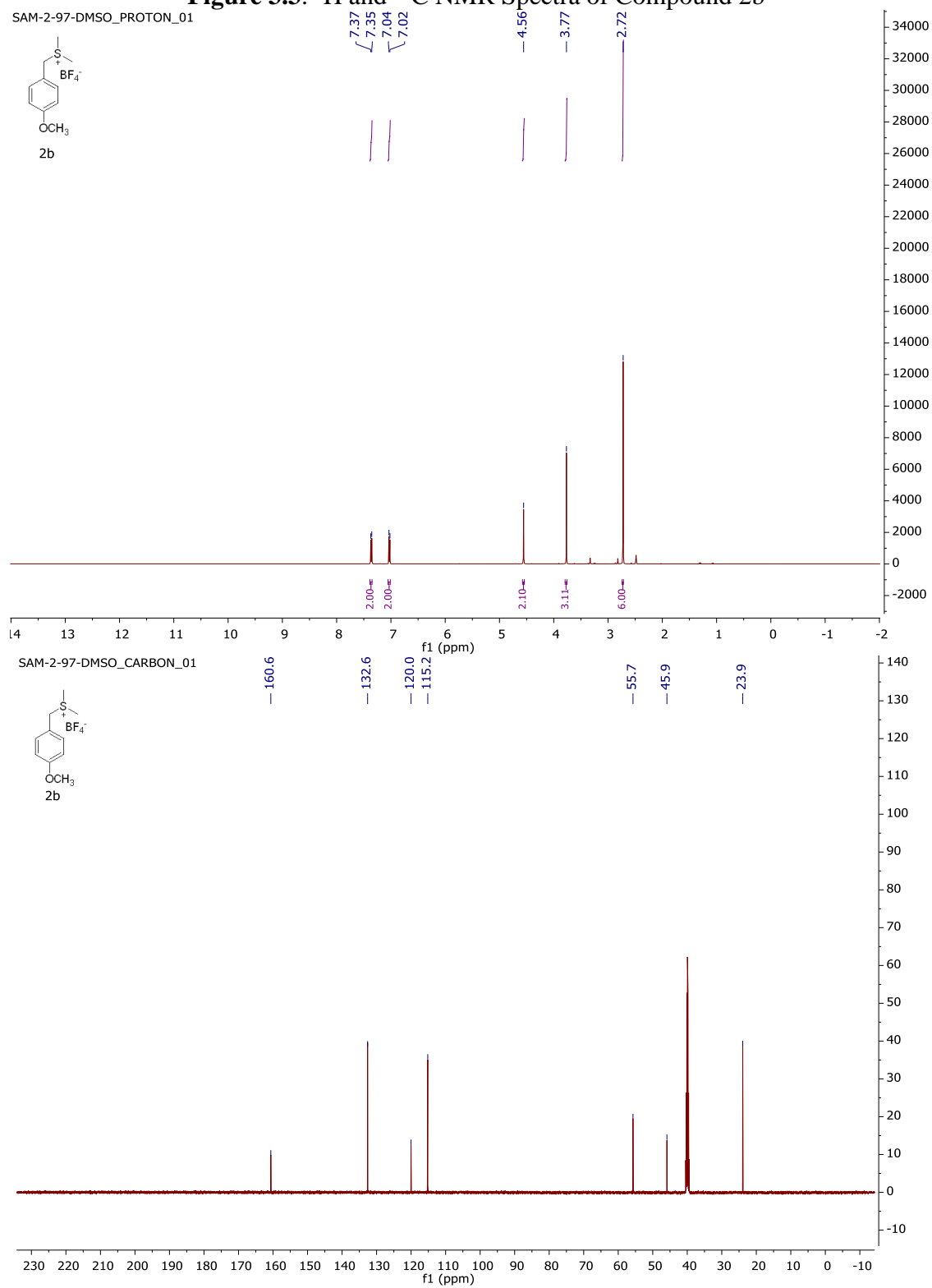


Figure 3.4. ^1H and ^{13}C NMR Spectra of Compound 2c

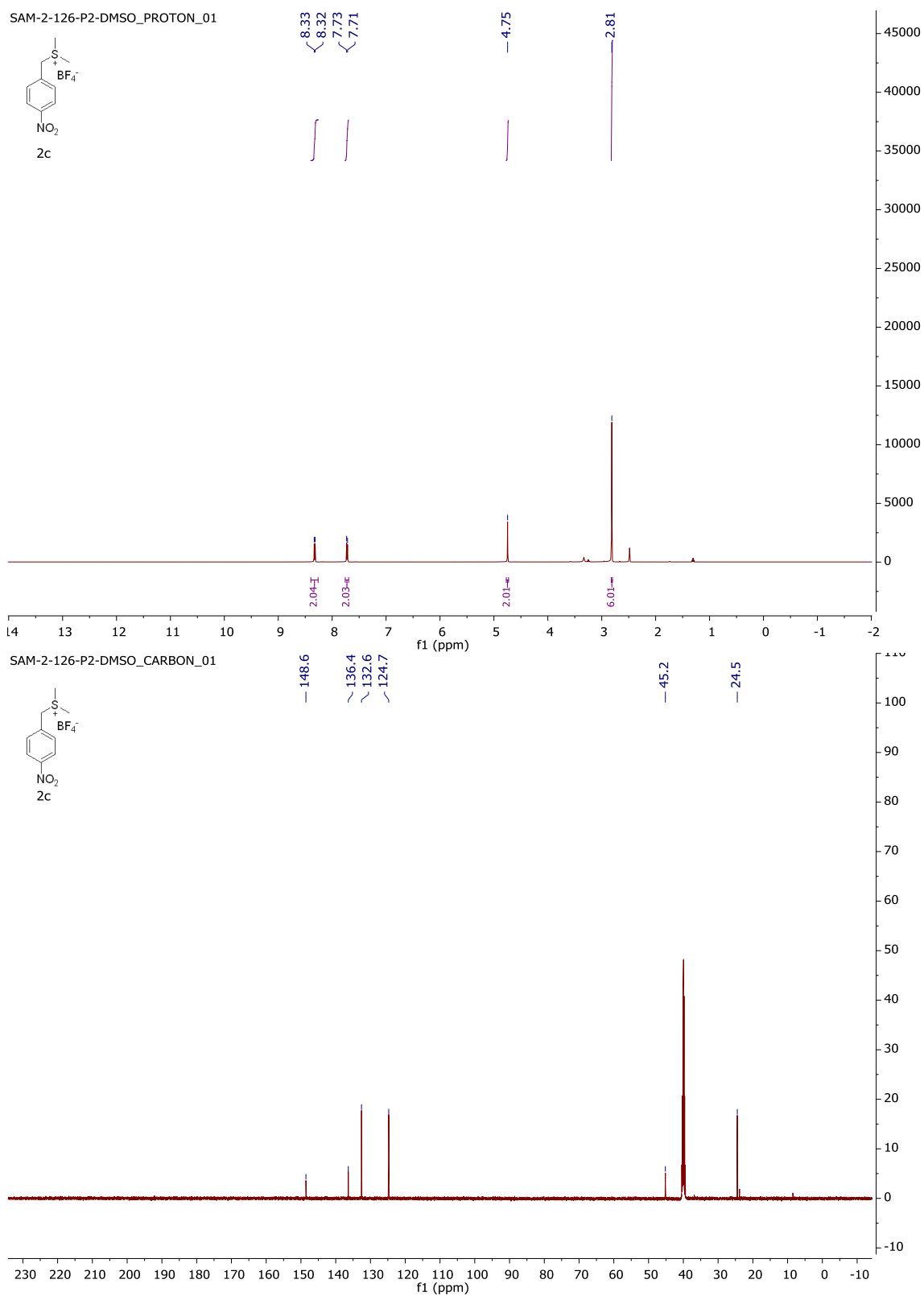


Figure 3.5. ^1H and ^{13}C NMR Spectra of Compound 2d

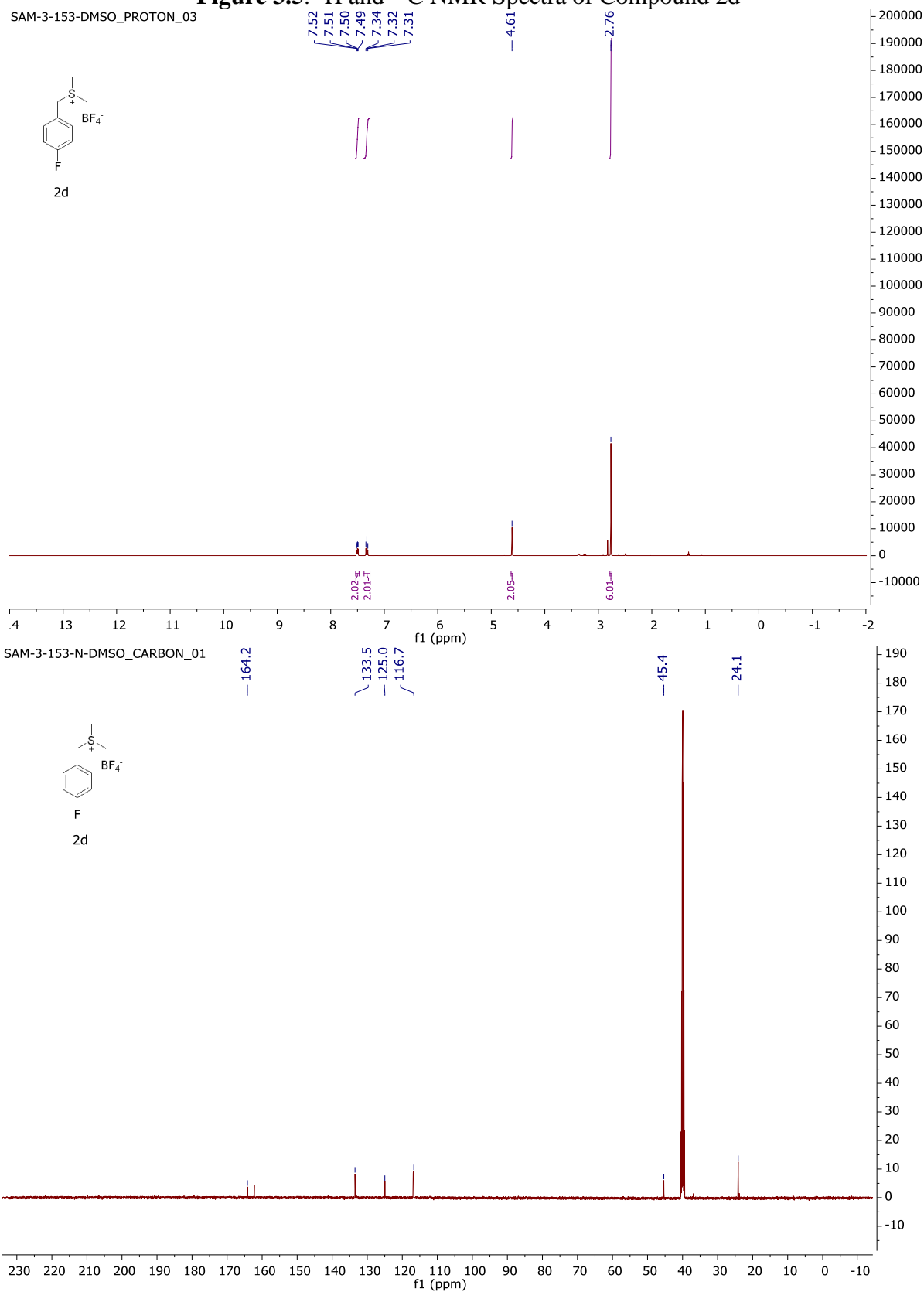


Figure 3.6. ^1H and ^{13}C NMR Spectra of Compound 2e

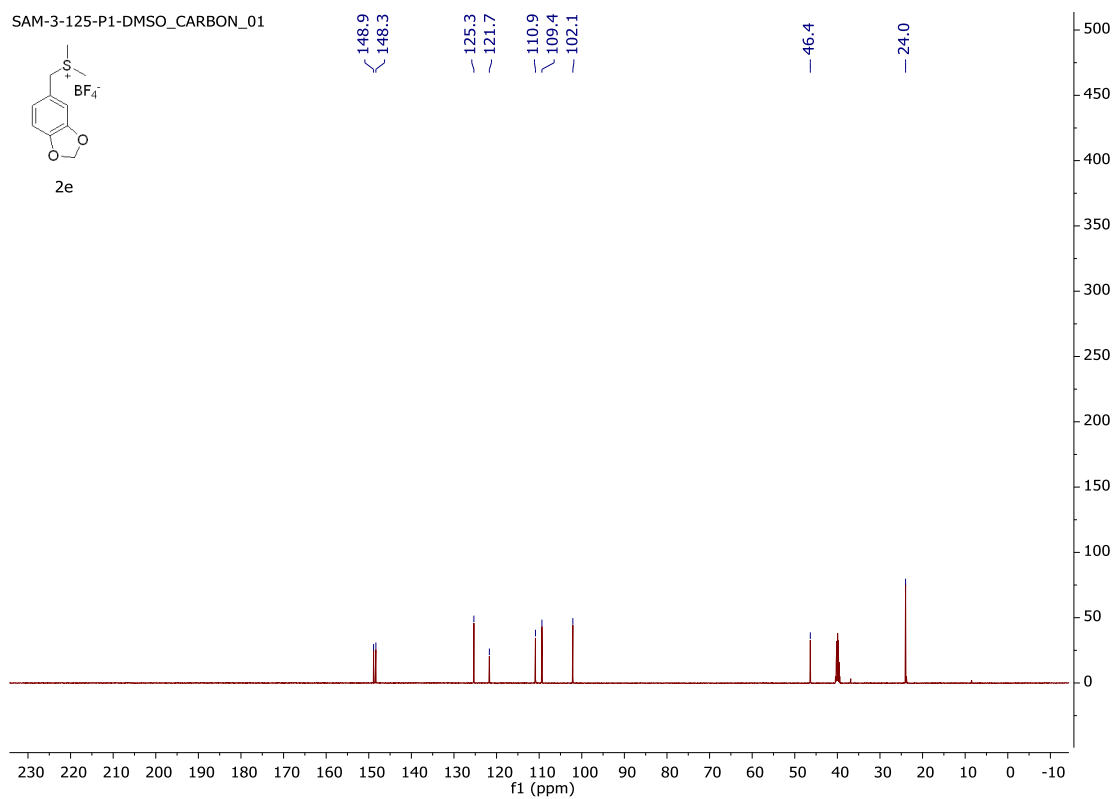
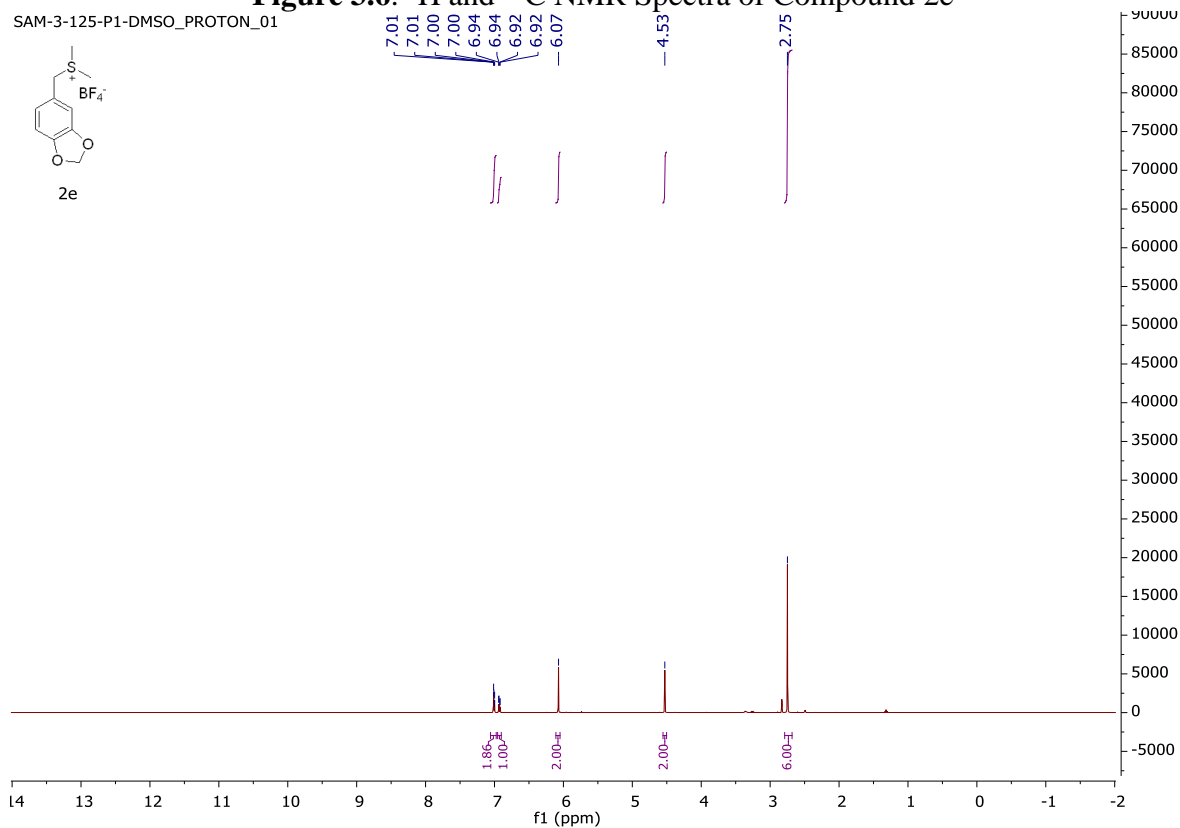


Figure 3.7. ^1H and ^{13}C NMR Spectra of Compound 2f

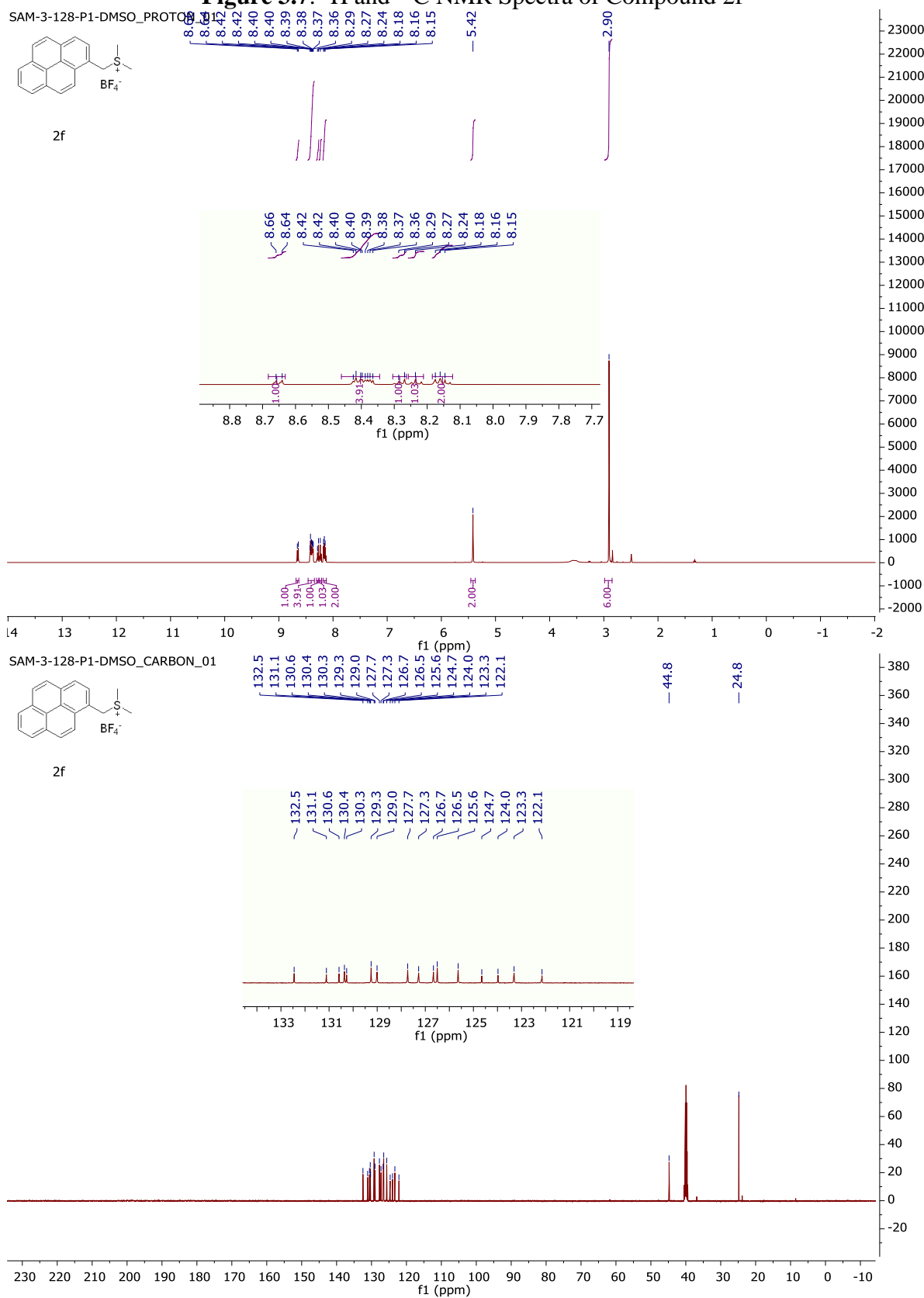


Figure 3.8. ^1H and ^{13}C NMR Spectra of Compound 2g

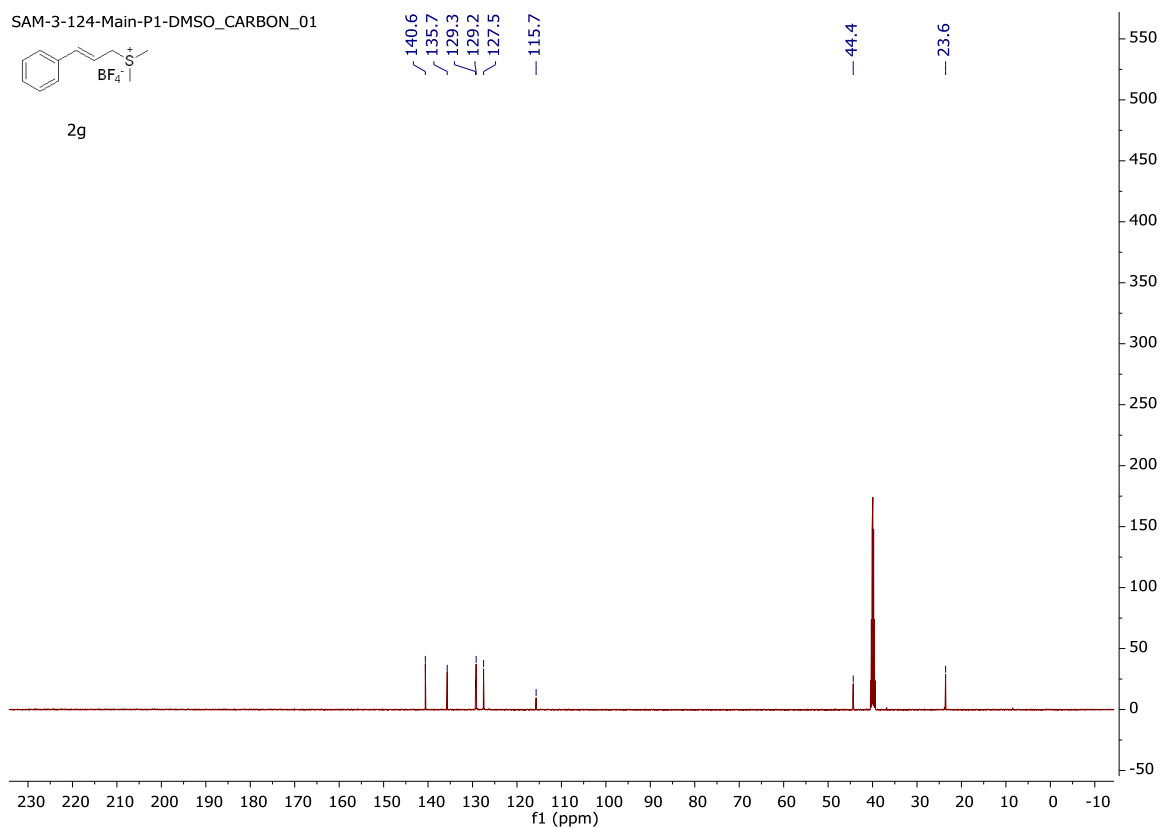
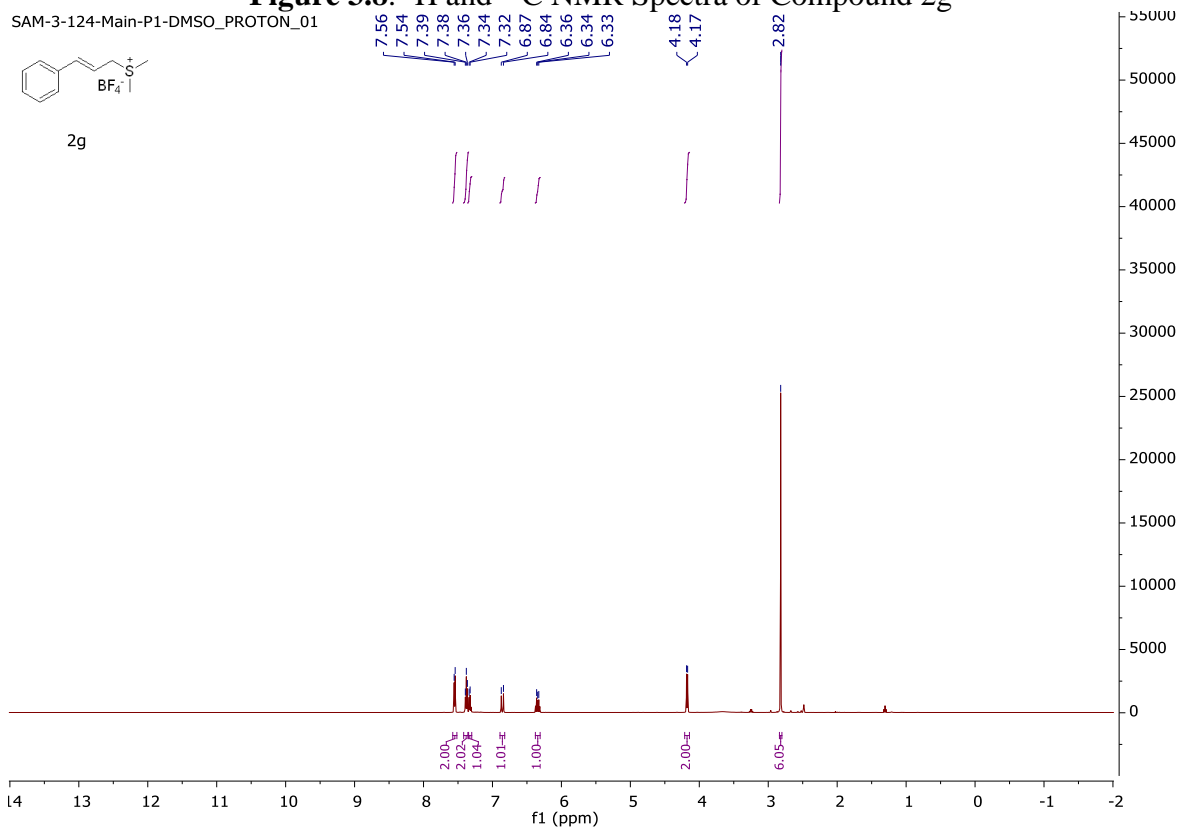


Figure 3.9. ^1H and ^{13}C NMR Spectra of Compound 2h

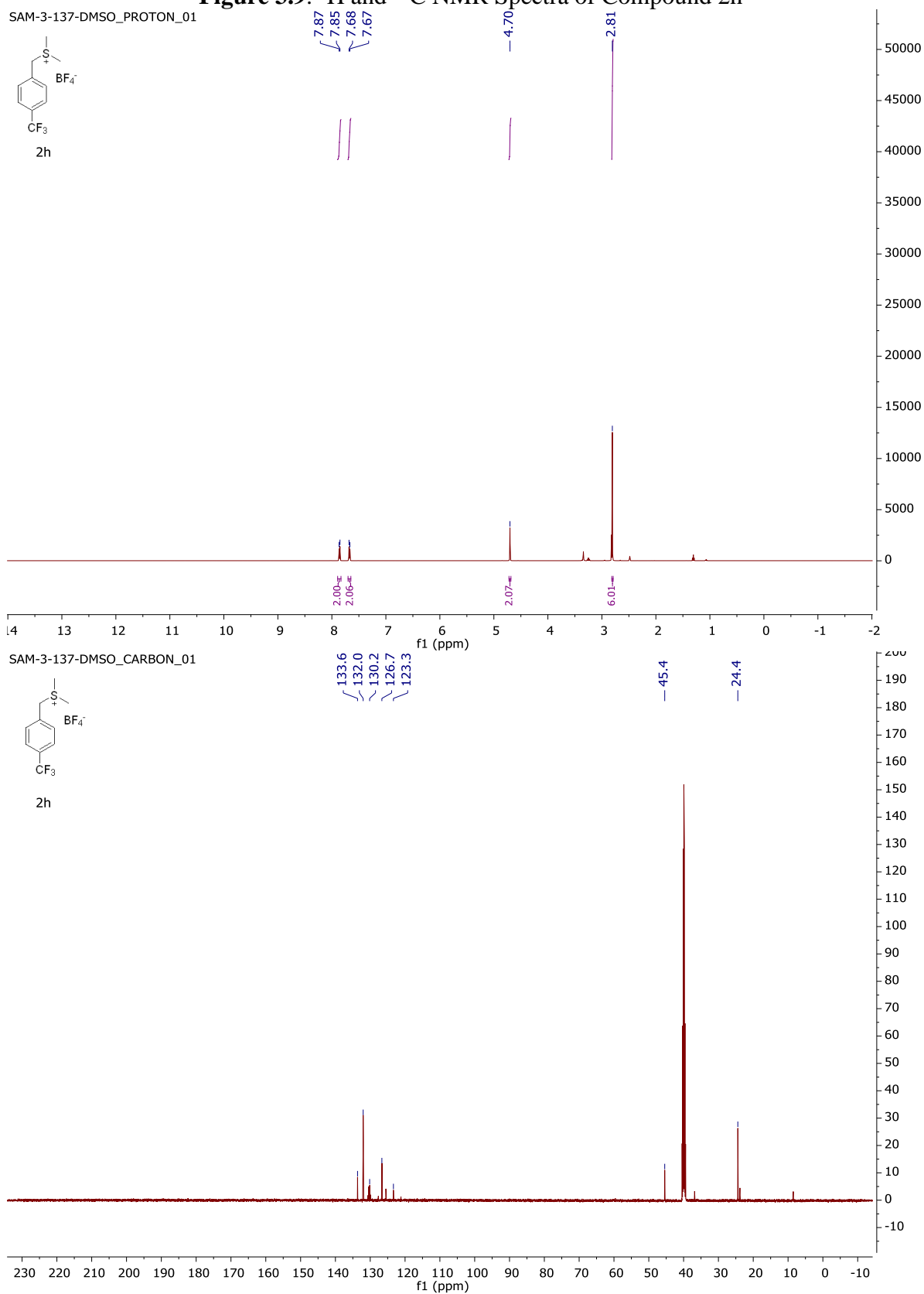


Figure 3.10. ^1H and ^{13}C NMR Spectra of Compound 3a

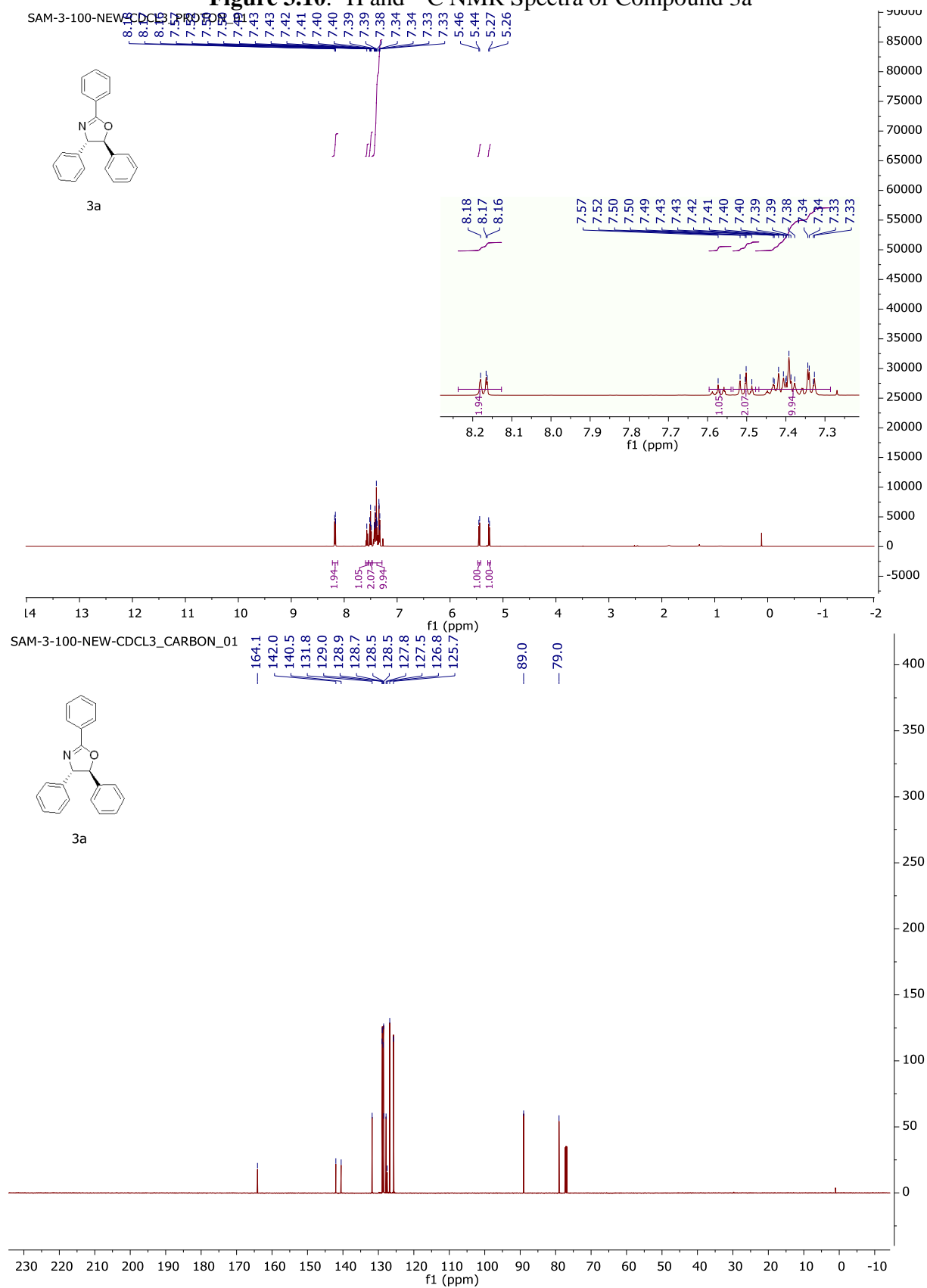


Figure 3.11. ^1H and ^{13}C NMR Spectra of Compound 3b

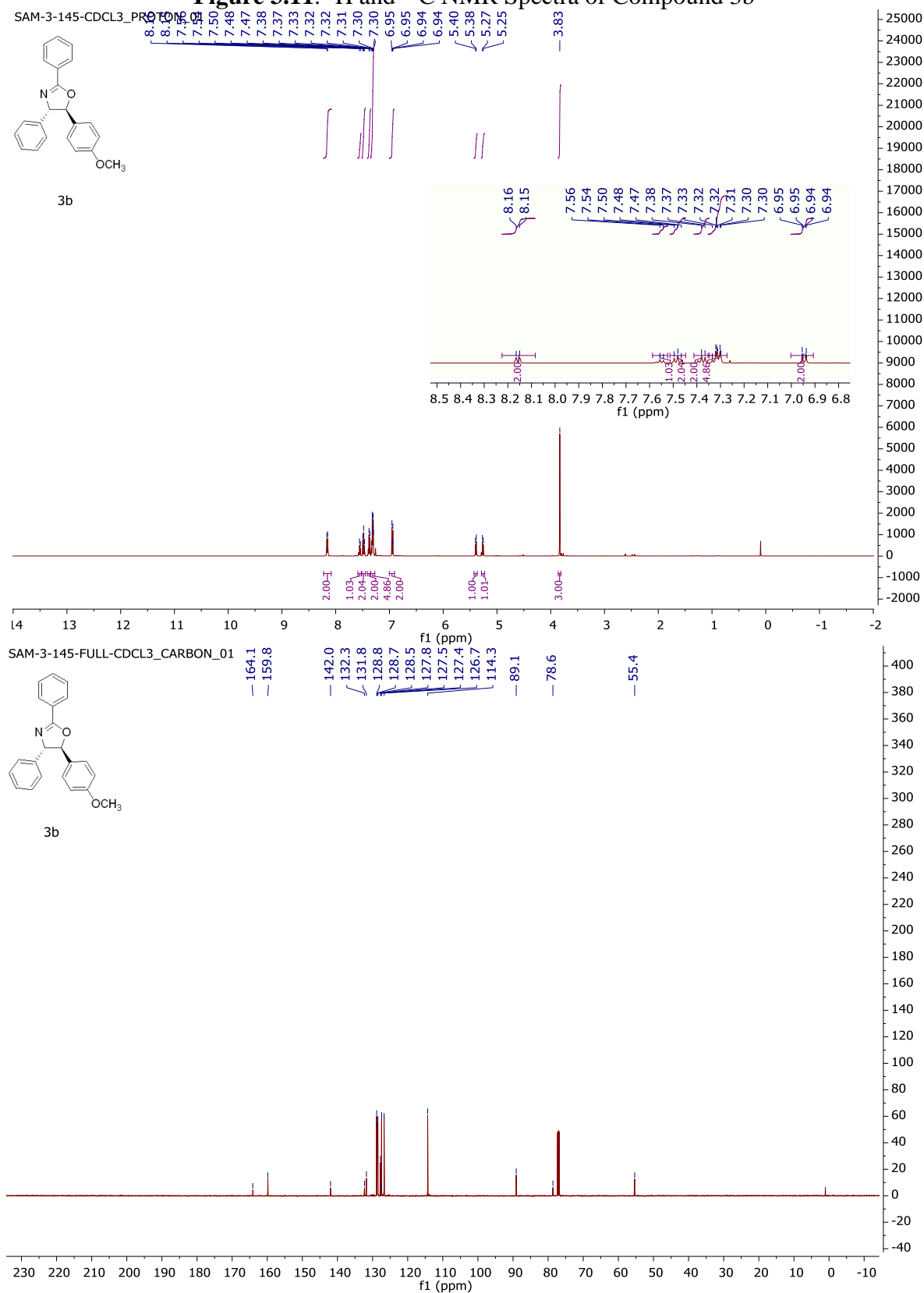


Figure 3.12. ^1H and ^{13}C NMR Spectra of Compound 3c

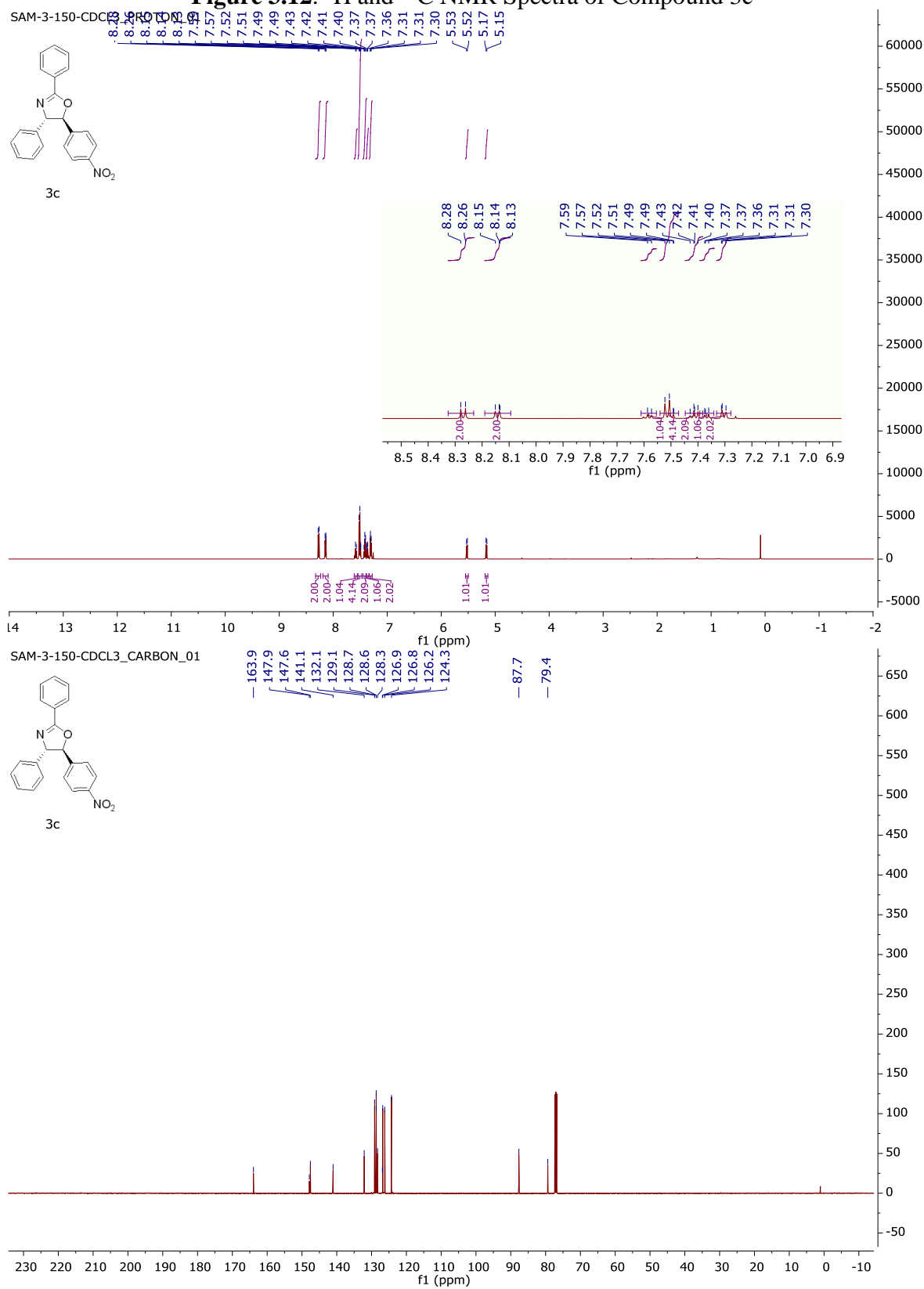


Figure 3.13. ^1H and ^{13}C NMR Spectra of Compound 3d

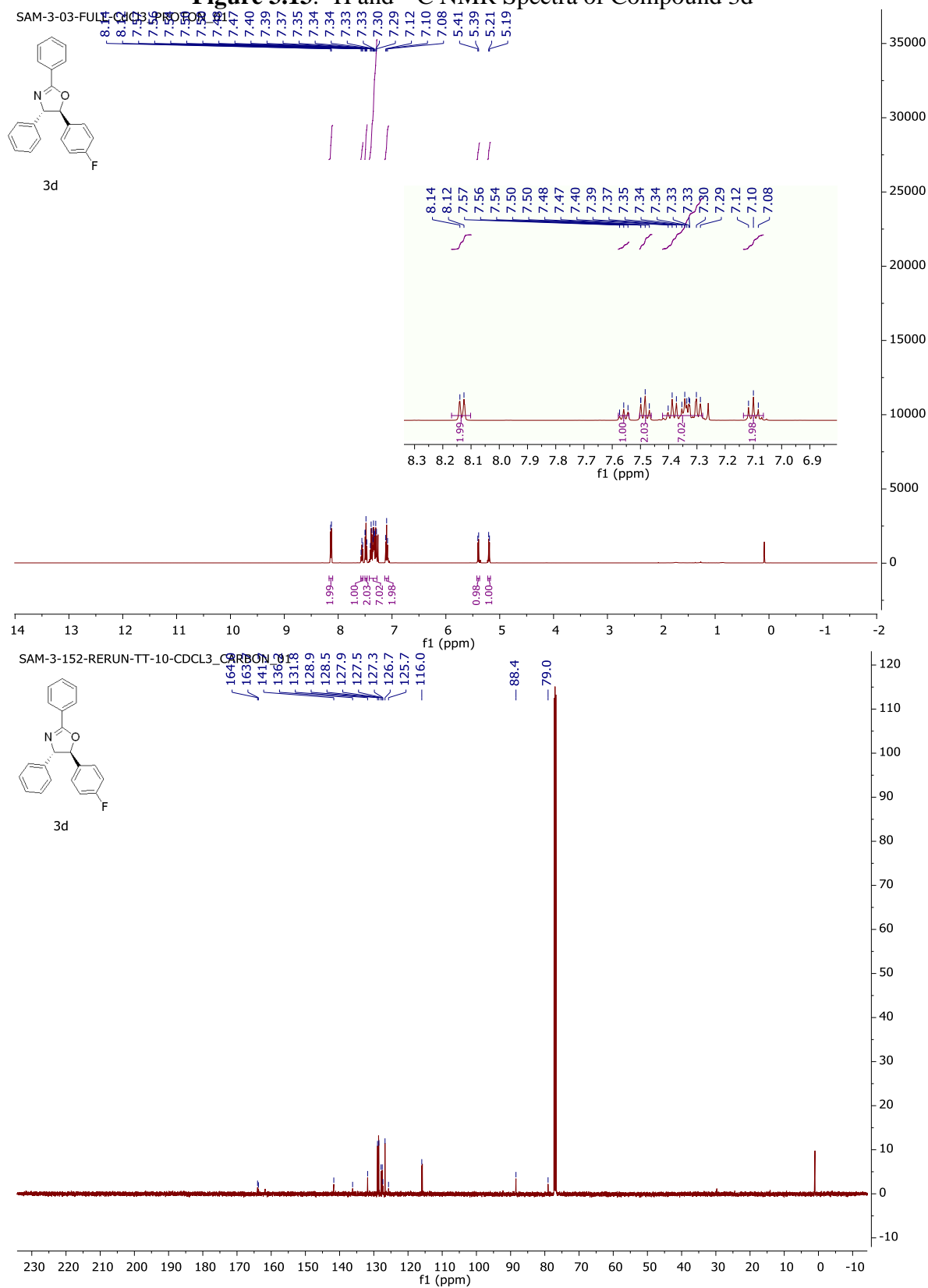


Figure 3.14. ^1H and ^{13}C NMR Spectra of Compound 3e

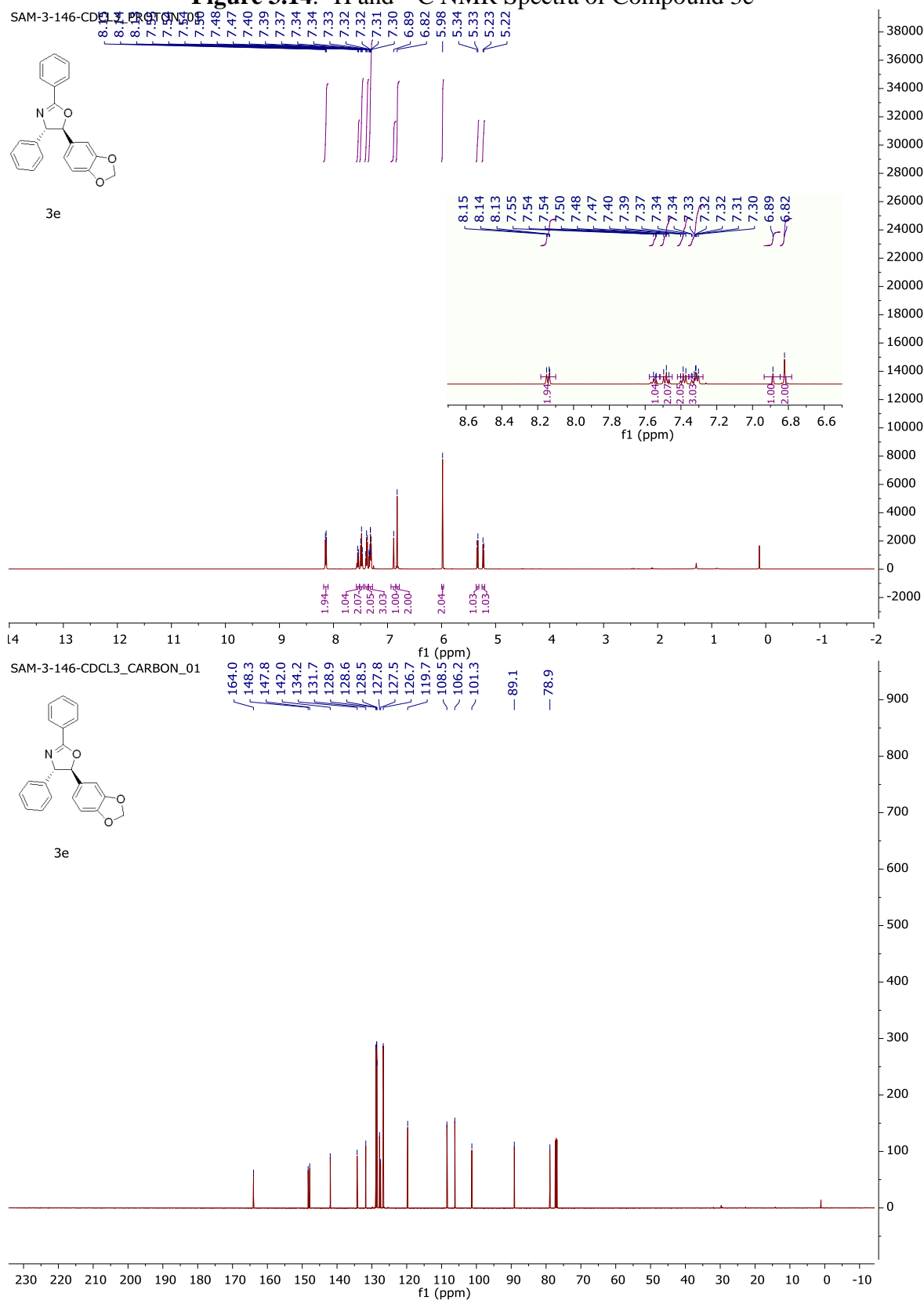
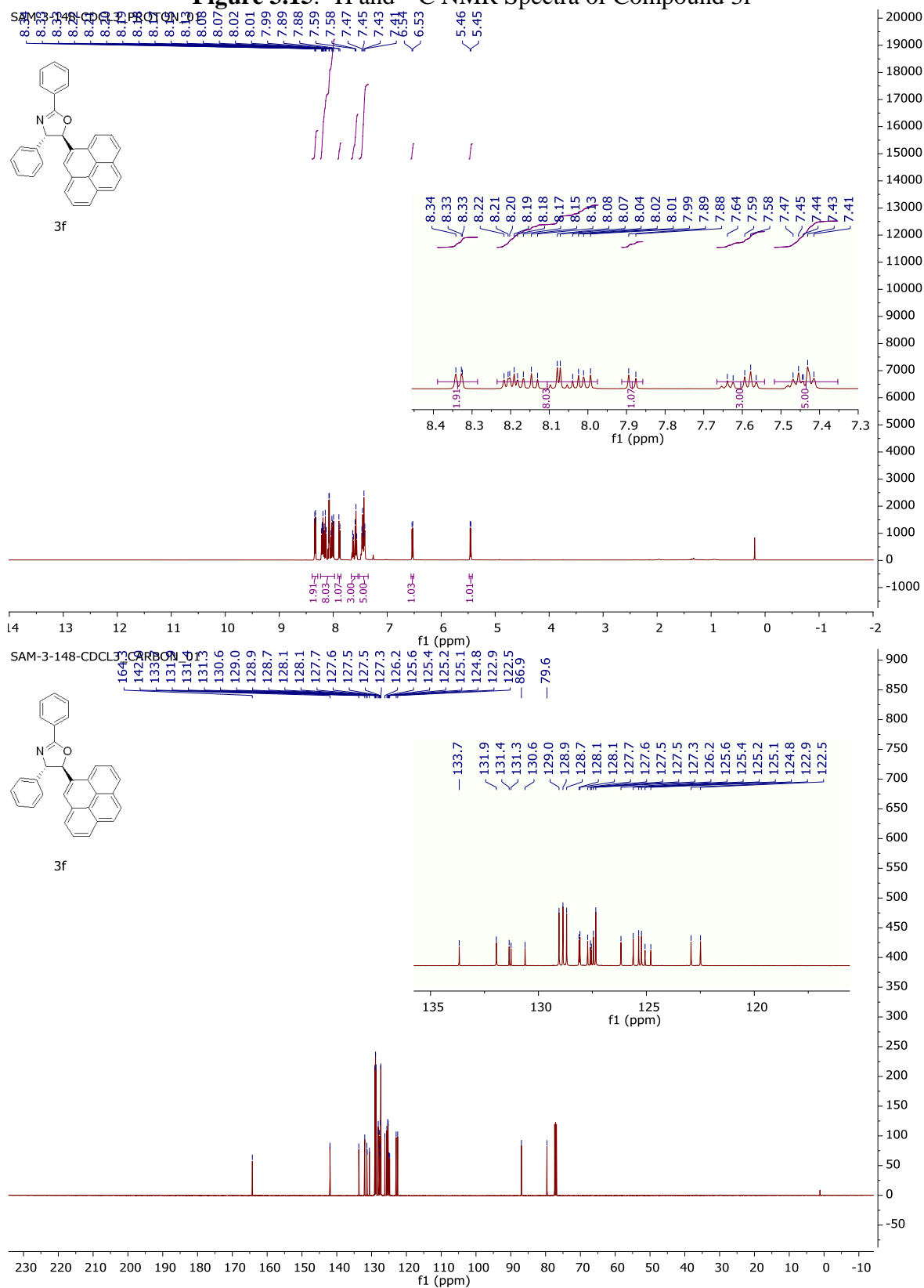


Figure 3.15. ^1H and ^{13}C NMR Spectra of Compound 3f



¹H NMR (400 MHz, CDCl₃)

Chemical structure of **3g**: c1ccc(cc1)/C=C/[C@H]2O=C(N2)c3ccccc3

Peak list (ppm): 8.13, 8.11, 8.11, 8.11, 7.55, 7.53, 7.49, 7.48, 7.46, 7.46, 7.44, 7.39, 7.38, 7.36, 7.35, 7.34, 7.34, 7.32, 7.32, 7.30, 6.66, 6.47, 6.45, 6.44, 6.42, 5.18, 5.16, 5.07, 5.07, 5.06, 5.05, 5.04.

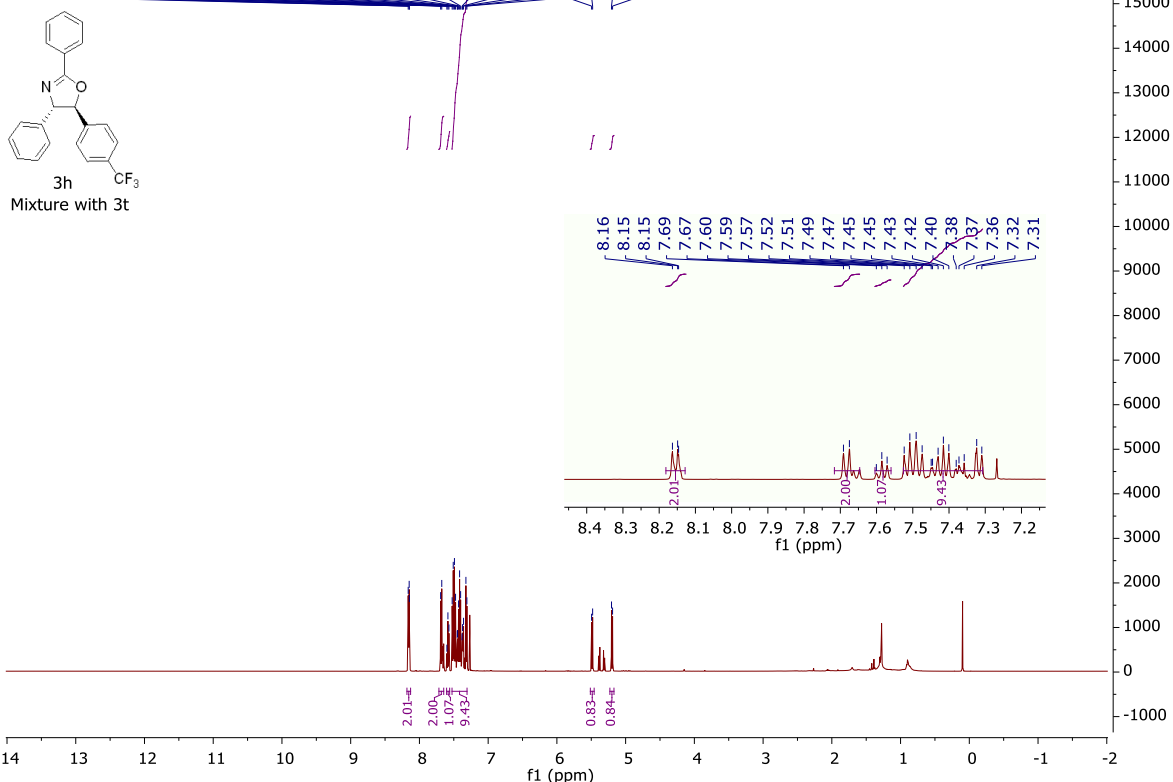
Integration values: 2.00, 1.03, 4.00, 7.95, 1.06, 1.09, 1.03, 1.05.


¹³C NMR (100 MHz, CDCl₃)

Chemical structure of **3g**: c1ccc(cc1)/C=C/[C@H]2O=C(N2)c3ccccc3

Peak list (ppm): 164.0, 141.6, 135.9, 133.6, 131.7, 128.8, 128.7, 128.6, 128.5, 128.4, 127.8, 127.6, 126.8, 126.8, 126.6, 88.8, 76.4.

Peak #	Time (min)	Area	Height	Area%	Height%
1	8.18	17667	1732	1.73	17.32
2	8.24	17667	1732	1.73	17.32
3	8.30	17667	1732	1.73	17.32
4	8.36	17667	1732	1.73	17.32
5	8.42	17667	1732	1.73	17.32
6	8.48	17667	1732	1.73	17.32
7	8.54	17667	1732	1.73	17.32
8	8.60	17667	1732	1.73	17.32
9	8.66	17667	1732	1.73	17.32
10	8.72	17667	1732	1.73	17.32
11	8.78	17667	1732	1.73	17.32
12	8.84	17667	1732	1.73	17.32
13	8.90	17667	1732	1.73	17.32
14	8.96	17667	1732	1.73	17.32
15	9.02	17667	1732	1.73	17.32
16	9.08	17667	1732	1.73	17.32
17	9.14	17667	1732	1.73	17.32
18	9.20	17667	1732	1.73	17.32
19	9.26	17667	1732	1.73	17.32
20	9.32	17667	1732	1.73	17.32
21	9.38	17667	1732	1.73	17.32
22	9.44	17667	1732	1.73	17.32
23	9.50	17667	1732	1.73	17.32
24	9.56	17667	1732	1.73	17.32
25	9.62	17667	1732	1.73	17.32
26	9.68	17667	1732	1.73	17.32
27	9.74	17667	1732	1.73	17.32
28	9.80	17667	1732	1.73	17.32
29	9.86	17667	1732	1.73	17.32
30	9.92	17667	1732	1.73	17.32
31	9.98	17667	1732	1.73	17.32
32	10.04	17667	1732	1.73	17.32
33	10.10	17667	1732	1.73	17.32
34	10.16	17667	1732	1.73	17.32
35	10.22	17667	1732	1.73	17.32
36	10.28	17667	1732	1.73	17.32
37	10.34	17667	1732	1.73	17.32
38	10.40	17667	1732	1.73	17.32
39	10.46	17667	1732	1.73	17.32
40	10.52	17667	1732	1.73	17.32
41	10.58	17667	1732	1.73	17.32
42	10.64	17667	1732	1.73	17.32
43	10.70	17667	1732	1.73	17.32
44	10.76	17667	1732	1.73	17.32
45	10.82	17667	1732	1.73	17.32
46	10.88	17667	1732	1.73	17.32
47	10.94	17667	1732	1.73	17.32
48	11.00	17667	1732	1.73	17.32
49	11.06	17667	1732	1.73	17.32
50	11.12	17667	1732	1.73	17.32
51	11.18	17667	1732	1.73	17.32
52	11.24	17667	1732	1.73	17.32
53	11.30	17667	1732	1.73	17.32
54	11.36	17667	1732	1.73	17.32
55	11.42	17667	1732	1.73	17.32
56	11.48	17667	1732	1.73	17.32
57	11.54	17667	1732	1.73	17.32
58	11.60	17667	1732	1.73	17.32
59	11.66	17667	1732	1.73	17.32
60	11.72	17667	1732	1.73	1




3h
Mixture with 3t

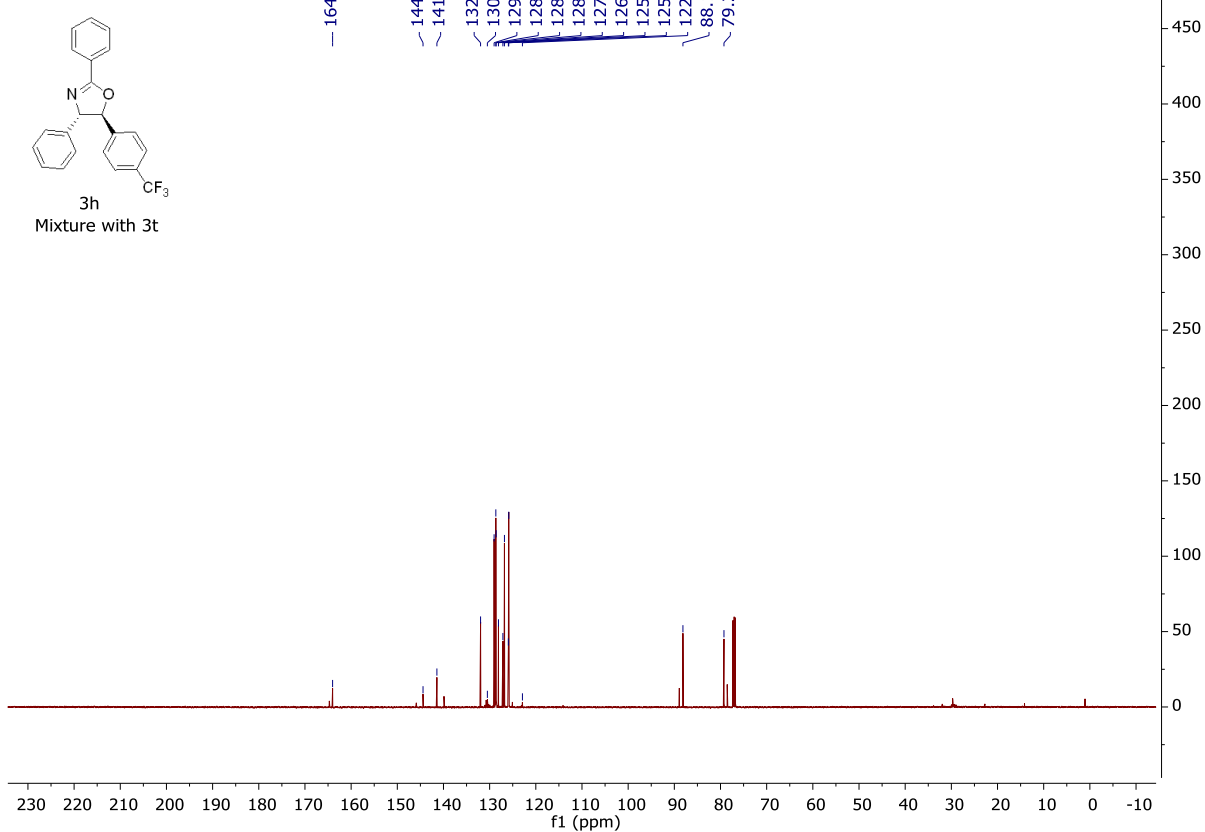


Figure 3.18. ^1H and ^{13}C NMR Spectra of Compound 3i

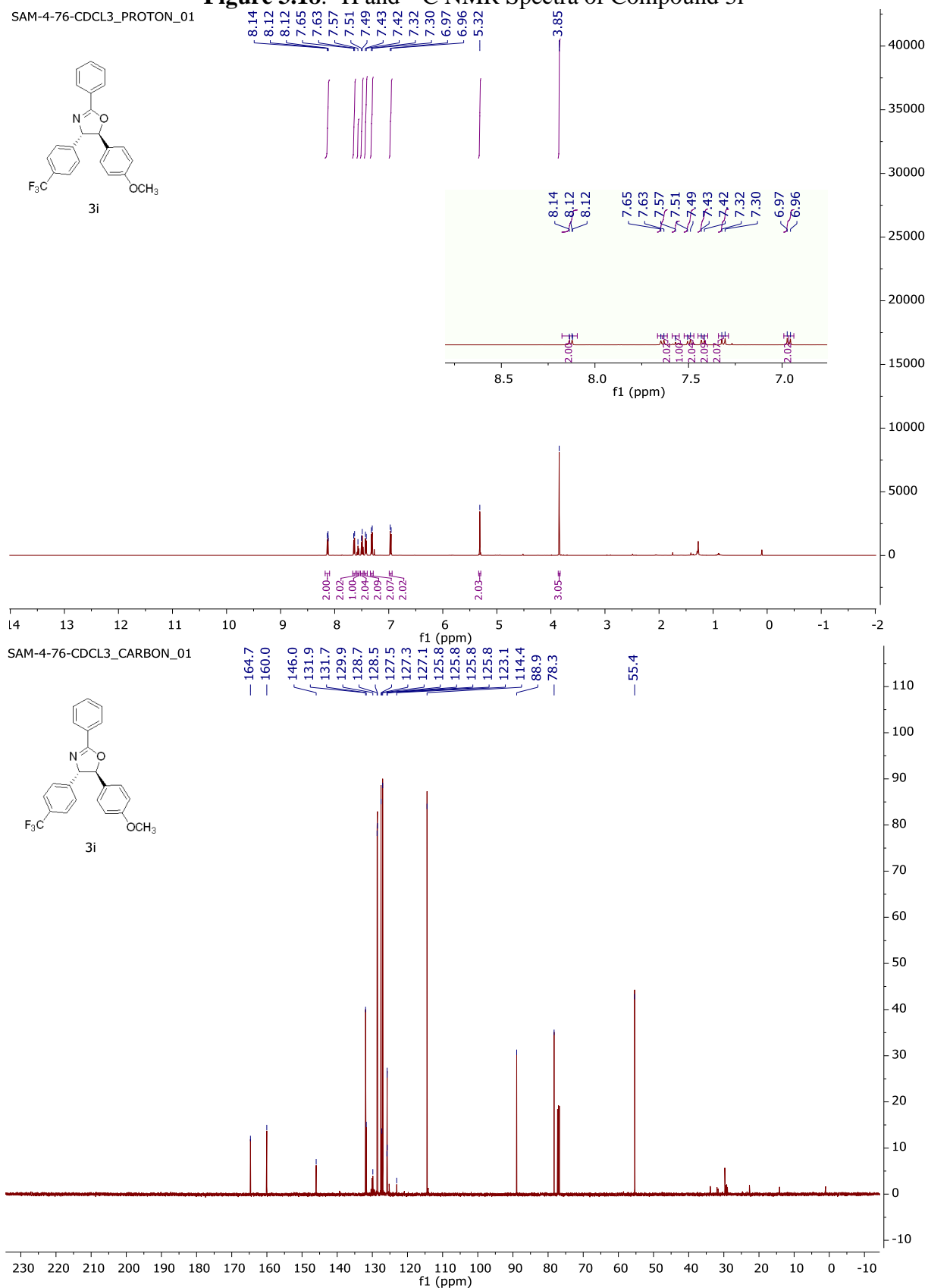
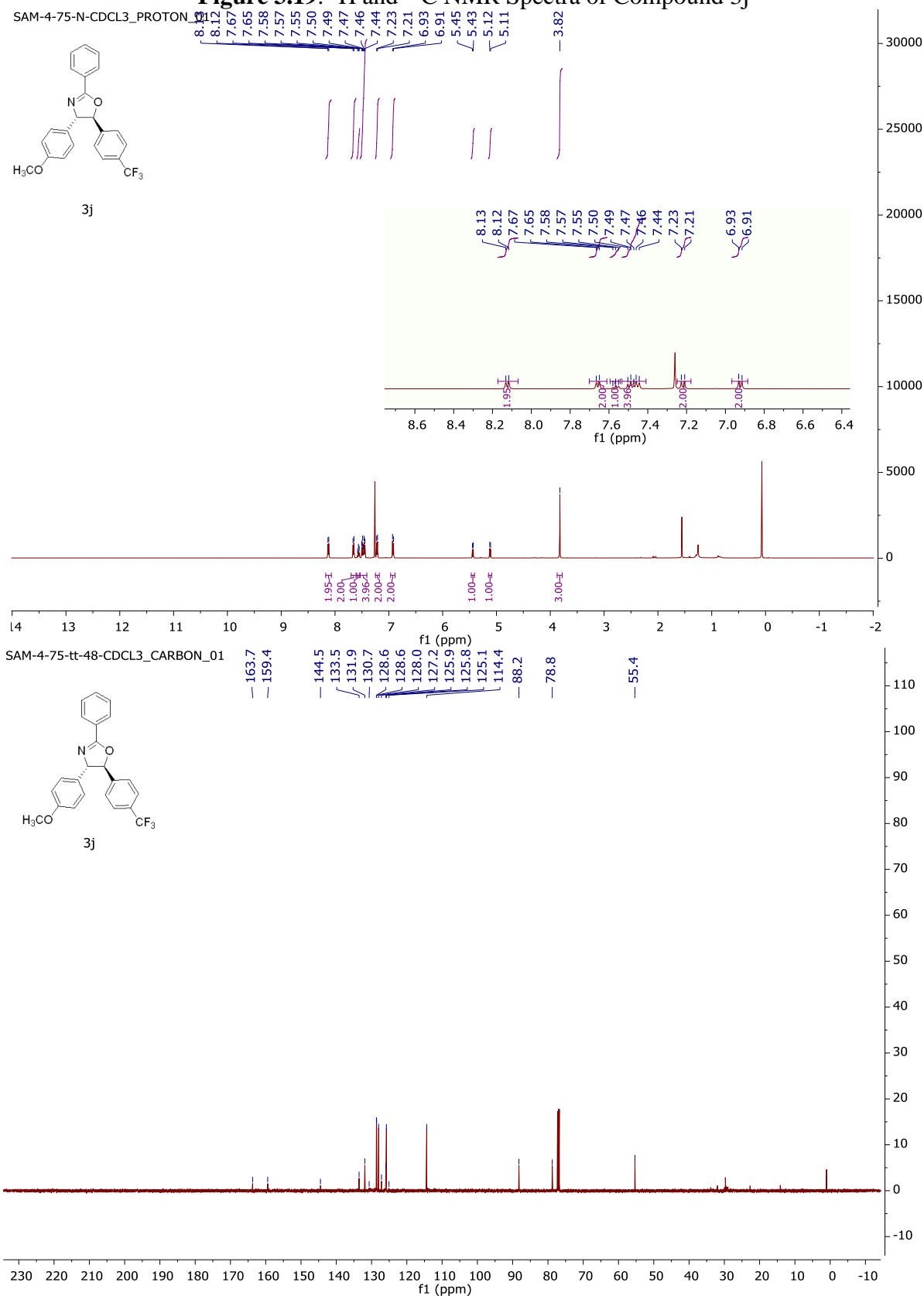


Figure 3.19. ^1H and ^{13}C NMR Spectra of Compound 3j



SAM-4-63-CDCL3_PROTON_01

Chemical structure of compound 3k is shown. The structure is a 4,5-disubstituted isoxazole ring with a phenyl group at position 3, a (4-(trifluoromethyl)phenyl) group at position 4, and a (4-(trifluoromethyl)phenyl) group at position 5. The stereochemistry is (R,S).

¹H NMR spectrum (CDCl₃) of compound 3k. The x-axis represents the chemical shift in ppm, ranging from 10 to 6.9. The y-axis represents the intensity. The spectrum shows several peaks, with the following chemical shifts (ppm) labeled: 8.15, 8.13, 8.11, 7.71, 7.69, 7.68, 7.66, 7.60, 7.59, 7.53, 7.52, 7.50, 7.49, 7.47, 7.44, 7.43, 5.44, 5.43, 5.27, 5.25. Integration values are provided for several peaks: 1.96, 4.00, 1.05, 4.00, 2.00, 1.00, 1.00.

SAM-4-63-AC-tt04-CDCL3_CARBO_01

Chemical structure of compound 3k is shown. The structure is a 4,5-disubstituted isoxazole ring with a phenyl group at position 3, a (4-(trifluoromethyl)phenyl) group at position 4, and a (4-(trifluoromethyl)phenyl) group at position 5. The stereochemistry is (R,S).

¹³C NMR spectrum (CDCl₃) of compound 3k. The x-axis represents the chemical shift in ppm, ranging from 230 to -10. The y-axis represents the intensity. The spectrum shows several peaks, with the following chemical shifts (ppm) labeled: 164.7, 145.3, 143.8, 132.2, 130.8, 130.5, 128.7, 128.7, 127.2, 126.8, 126.1, 126.0, 126.0, 125.1, 122.8, 88.0, 78.7.

Figure 3.21. ^1H and ^{13}C NMR Spectra of Compound 3l

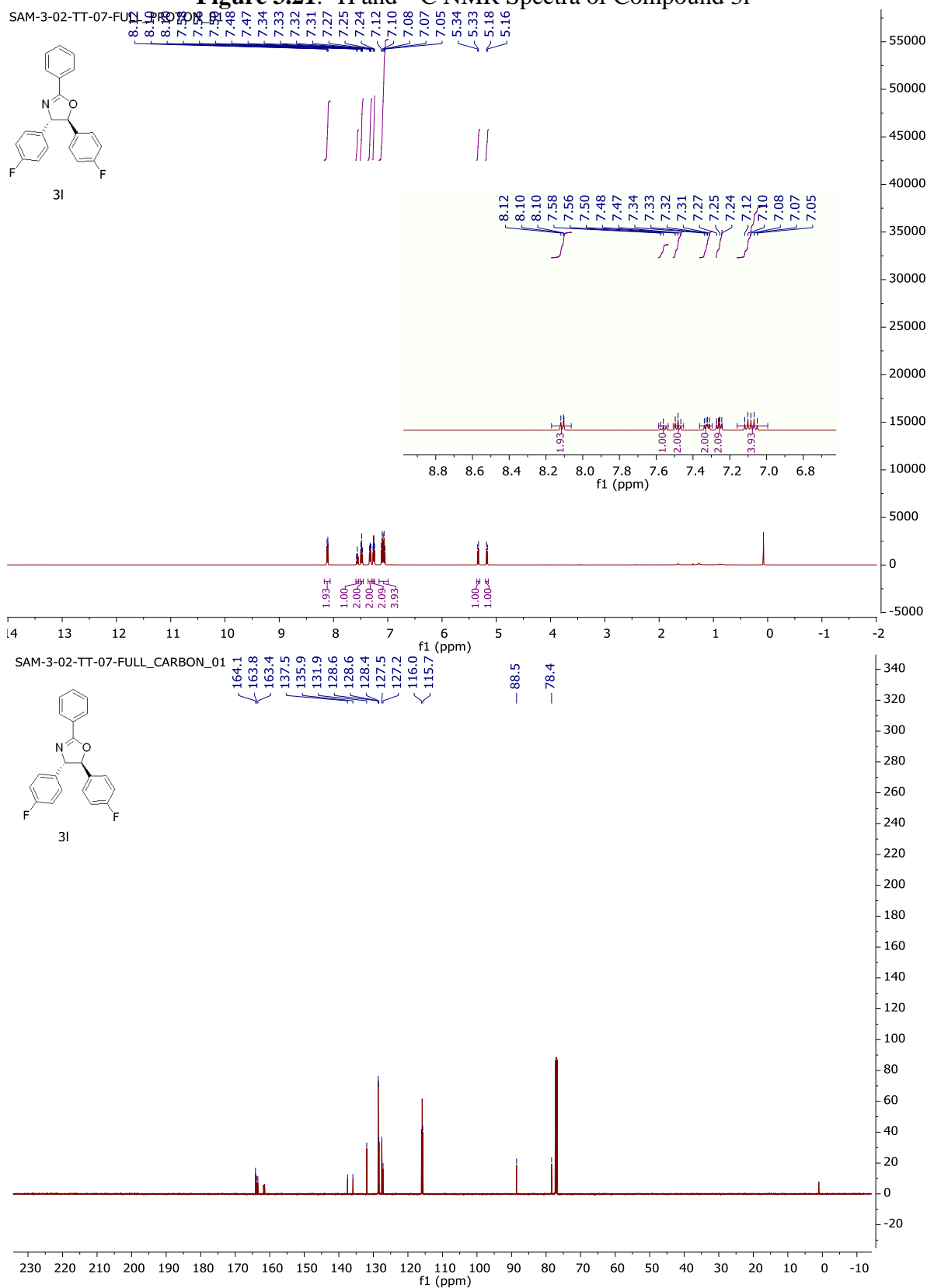
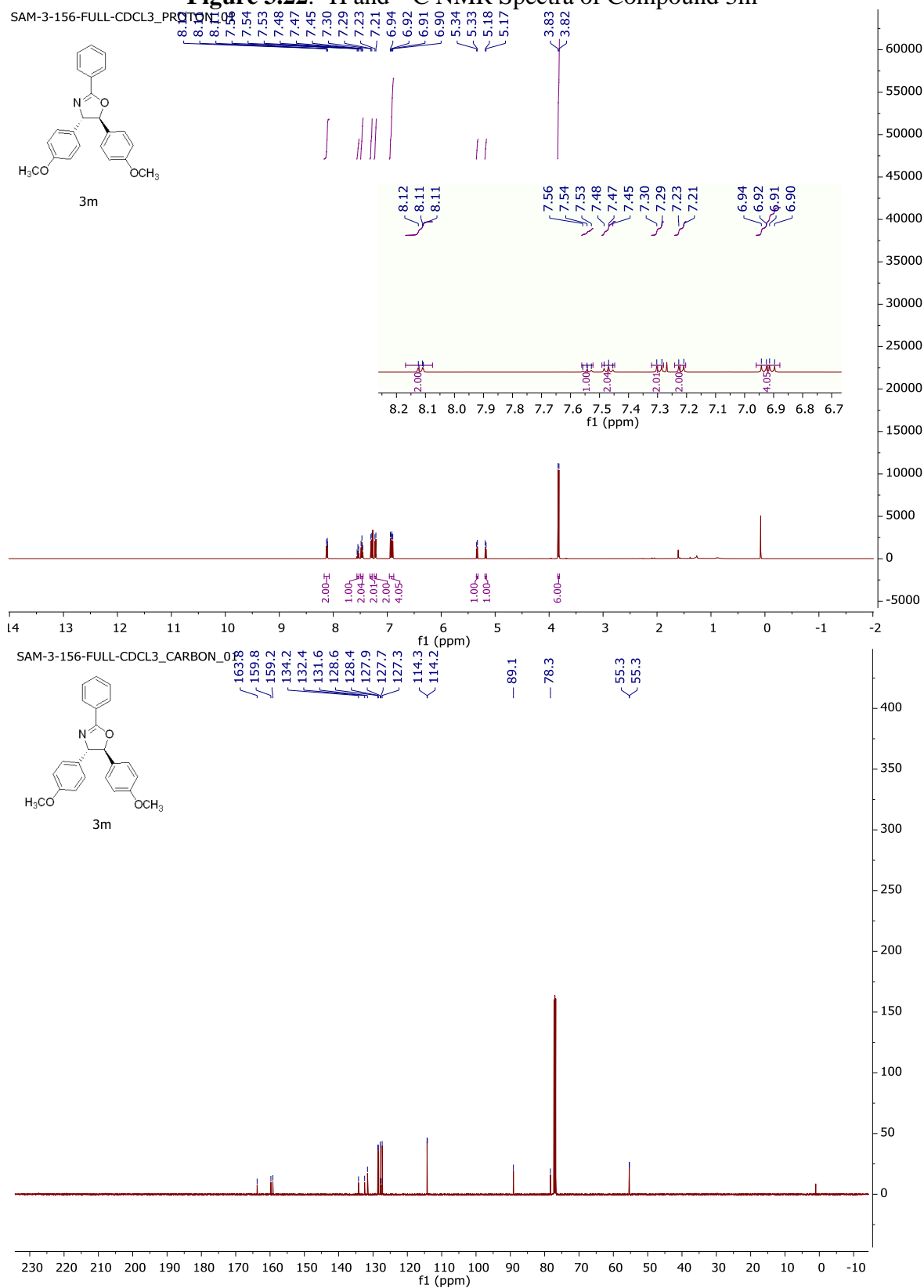


Figure 3.22. ^1H and ^{13}C NMR Spectra of Compound 3m



SAM-4-82-CDCL3_PROTON_01

Chemical structure of compound 3n is shown. The structure is a 2-phenyl-2-(4-fluorophenyl)-2H-benzofuran derivative.

¹H NMR spectrum (CDCl₃) of compound 3n is displayed. The x-axis represents the chemical shift in ppm (f1), ranging from -2 to 14. The y-axis represents the intensity. The spectrum shows several peaks, with the following chemical shifts (ppm) labeled: 8.12, 8.10, 8.10, 7.56, 7.55, 7.50, 7.48, 7.27, 7.26, 7.25, 7.07, 7.05, 6.86, 6.86, 6.82, 6.81, 6.80, 6.00, 5.27, 5.26, 5.19, 5.18.

SAM-4-82-CDCL3_CARBON_01

Chemical structure of compound 3n is shown. The structure is a 2-phenyl-2-(4-fluorophenyl)-2H-benzofuran derivative.

¹³C NMR spectrum (CDCl₃) of compound 3n is displayed. The x-axis represents the chemical shift in ppm (f1), ranging from -10 to 230. The y-axis represents the intensity. The spectrum shows several peaks, with the following chemical shifts (ppm) labeled: 164.1, 163.4, 148.3, 147.9, 137.7, 133.9, 131.8, 128.6, 128.5, 128.3, 127.3, 119.7, 115.8, 108.5, 106.1, 101.3, 89.2, 78.2.

SAM-4-86-TT-45_46-CDCL3_PROTON_03

Chemical structure of compound 3o is shown. The structure is a 2,2-diphenyl-1,3-dioxolane derivative, specifically 2,2-bis(4-(trifluoromethyl)phenyl)-1,3-dioxolane.

¹H NMR spectrum (CDCl₃) of compound 3o is displayed. The x-axis represents the chemical shift in ppm (f1), ranging from 8.3 to 7.4. The y-axis represents the intensity in arbitrary units, ranging from -2000 to 26000. The spectrum shows several peaks, with integration values provided for each peak. The peaks are labeled with their chemical shifts (ppm): 8.12, 8.10, 8.10, 7.64, 7.62, 7.56, 7.50, 7.48, 7.42, 7.40, 6.87, 6.87, 6.82, 6.81, 6.80, 6.00, and 5.27.

SAM-4-86-TT-45_46-CDCL3_CARBON_03

Chemical structure of compound 3o is shown. The structure is a 2,2-diphenyl-1,3-dioxolane derivative, specifically 2,2-bis(4-(trifluoromethyl)phenyl)-1,3-dioxolane.

¹³C NMR spectrum (CDCl₃) of compound 3o is displayed. The x-axis represents the chemical shift in ppm (f1), ranging from 230 to -10. The y-axis represents the intensity in arbitrary units, ranging from -40 to 400. The spectrum shows several peaks, with chemical shifts (ppm) labeled: 164.4, 148.4, 148.1, 145.8, 133.6, 132.0, 129.9, 128.6, 128.6, 127.2, 127.0, 125.8, 123.0, 119.9, 108.5, 106.2, 101.4, 89.0, and 78.4.

Figure 3.25. ^1H and ^{13}C NMR Spectra of Compound 3p

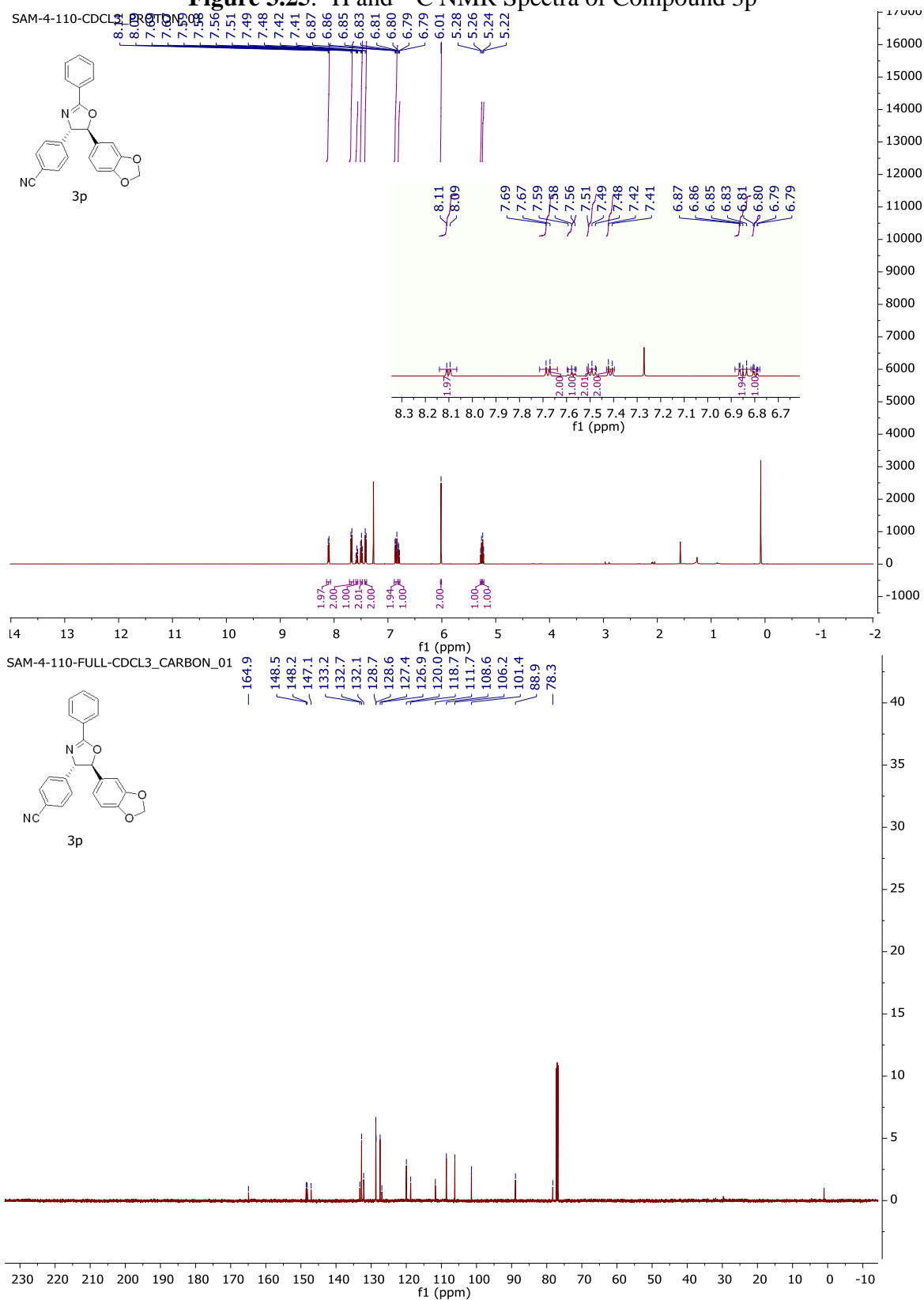


Figure 3.26. ^1H and ^{13}C NMR Spectra of Compound 3q

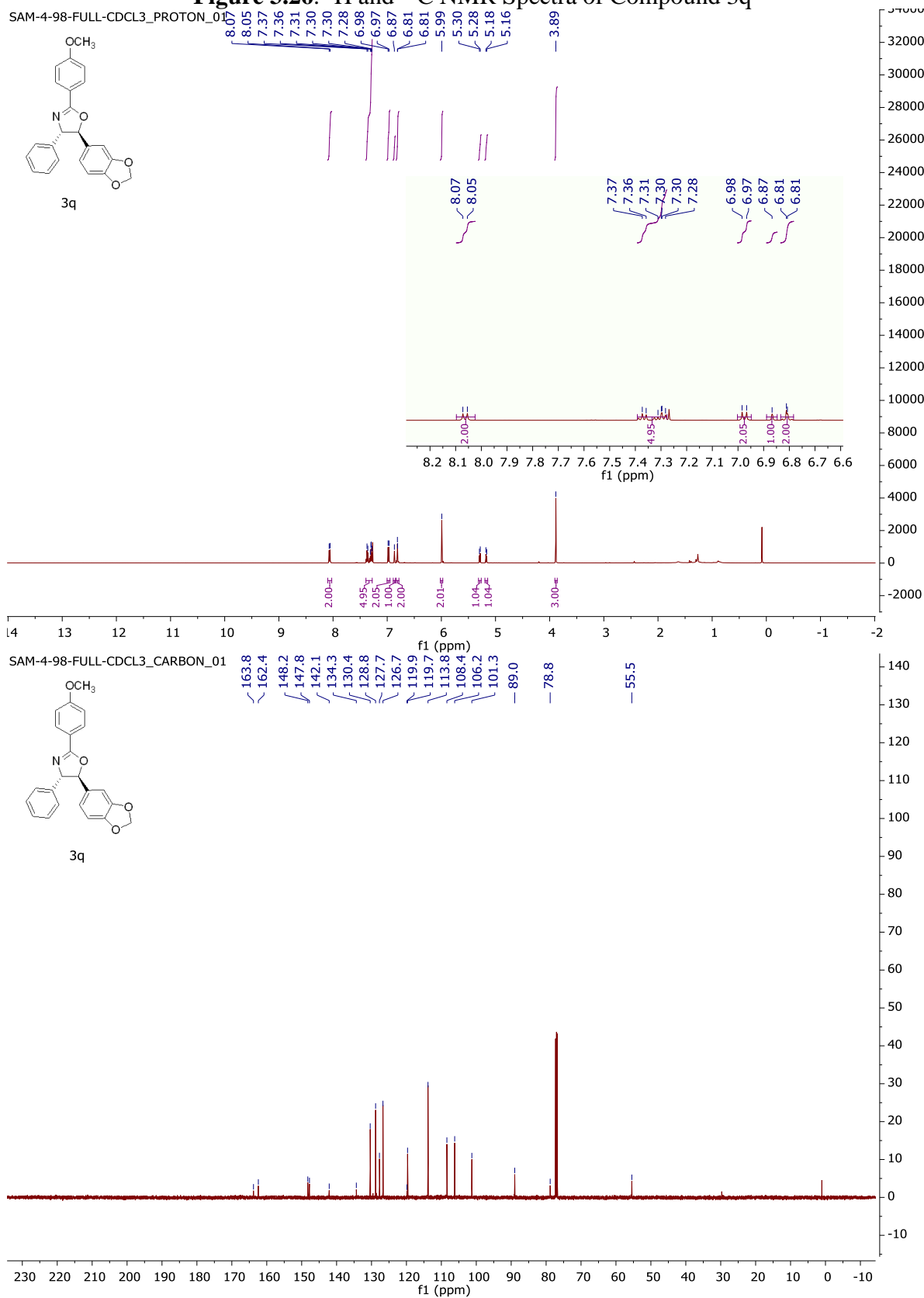


Figure 3.27. ^1H and ^{13}C NMR Spectra of Compound 3r

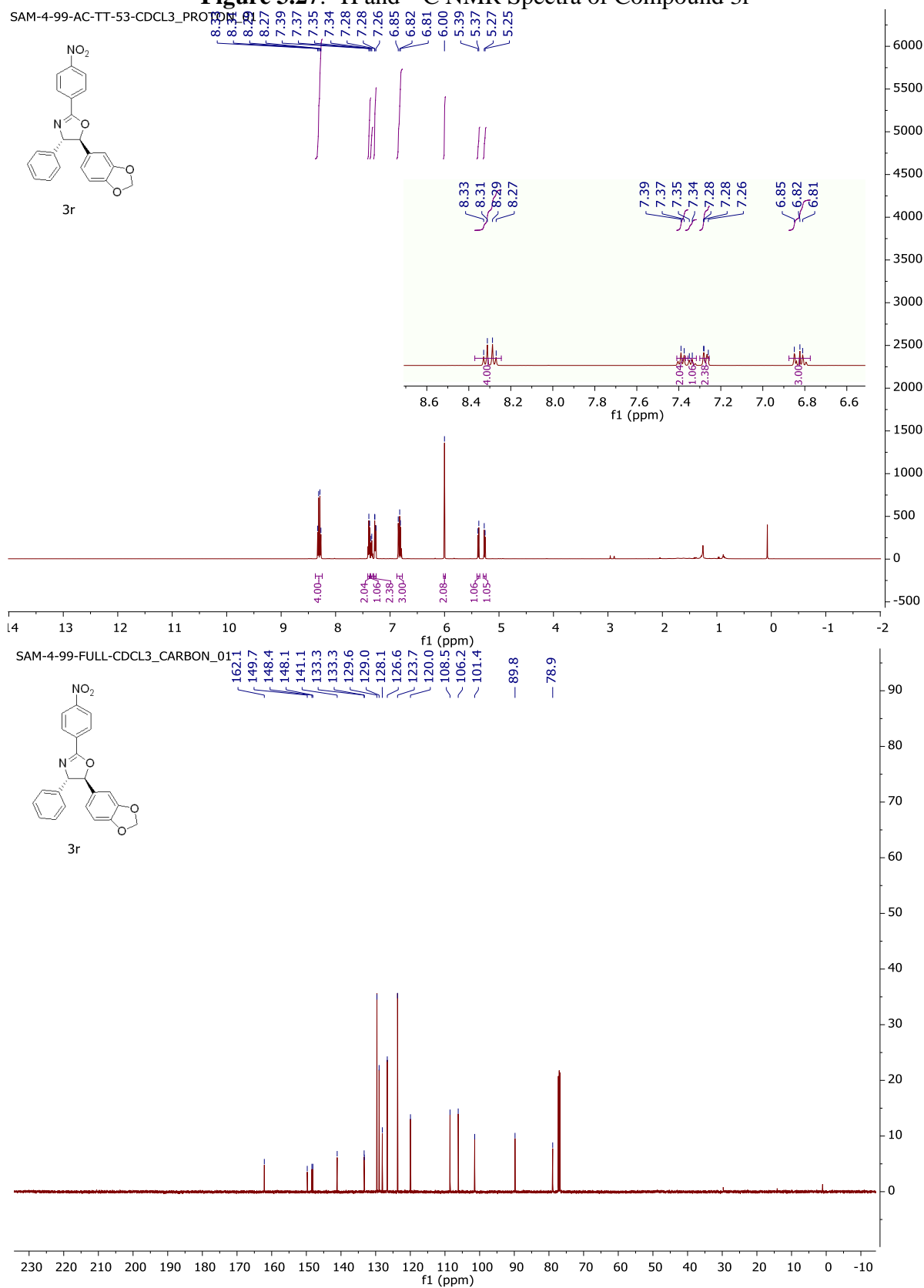


Figure 3.28. ^1H and ^{13}C NMR Spectra of Compound 3s

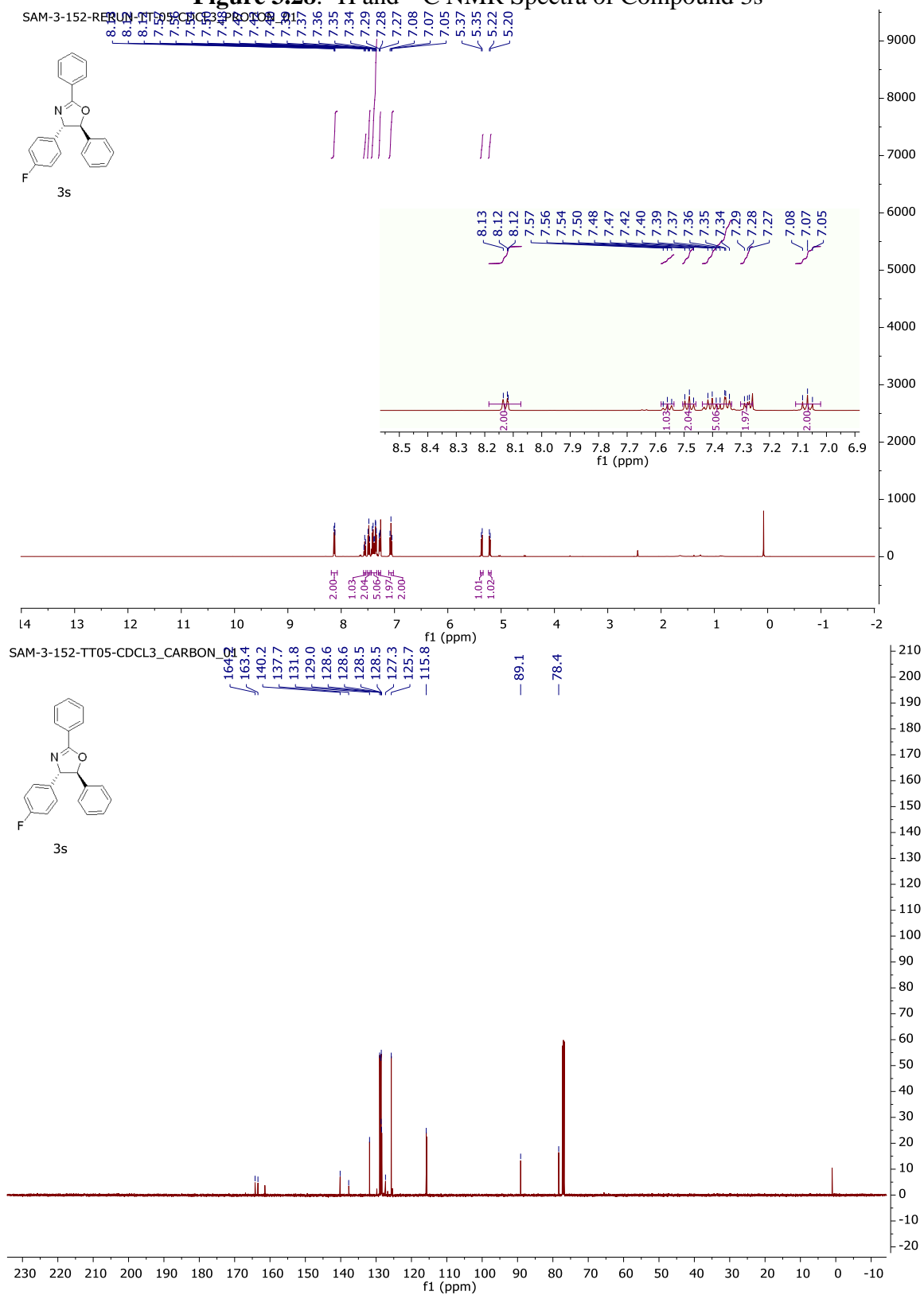


Figure 3.29. ^1H and ^{13}C NMR Spectra of Compound 3t

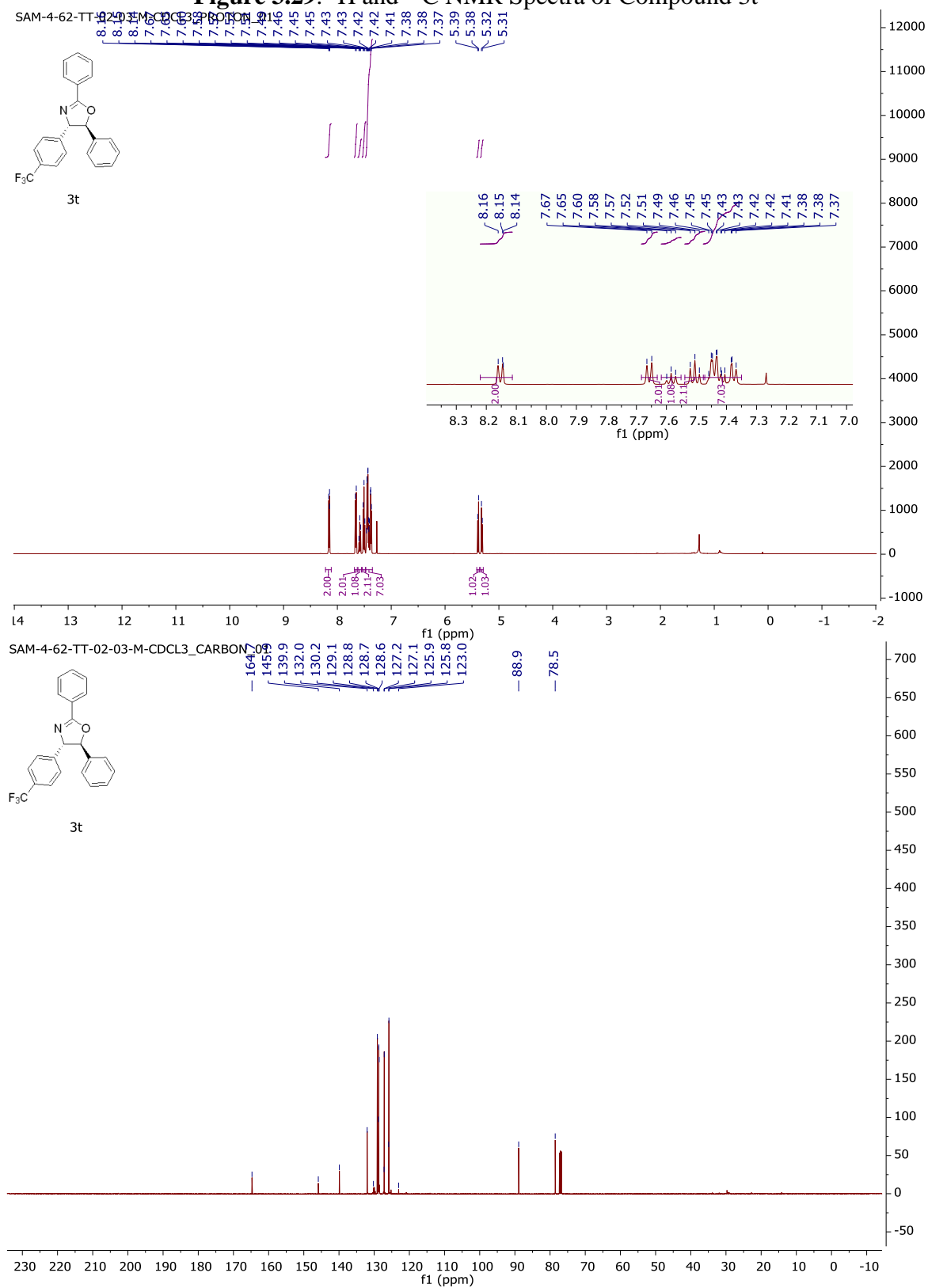


Figure 3.30. ^1H and ^{13}C NMR Spectra of Compound 3u

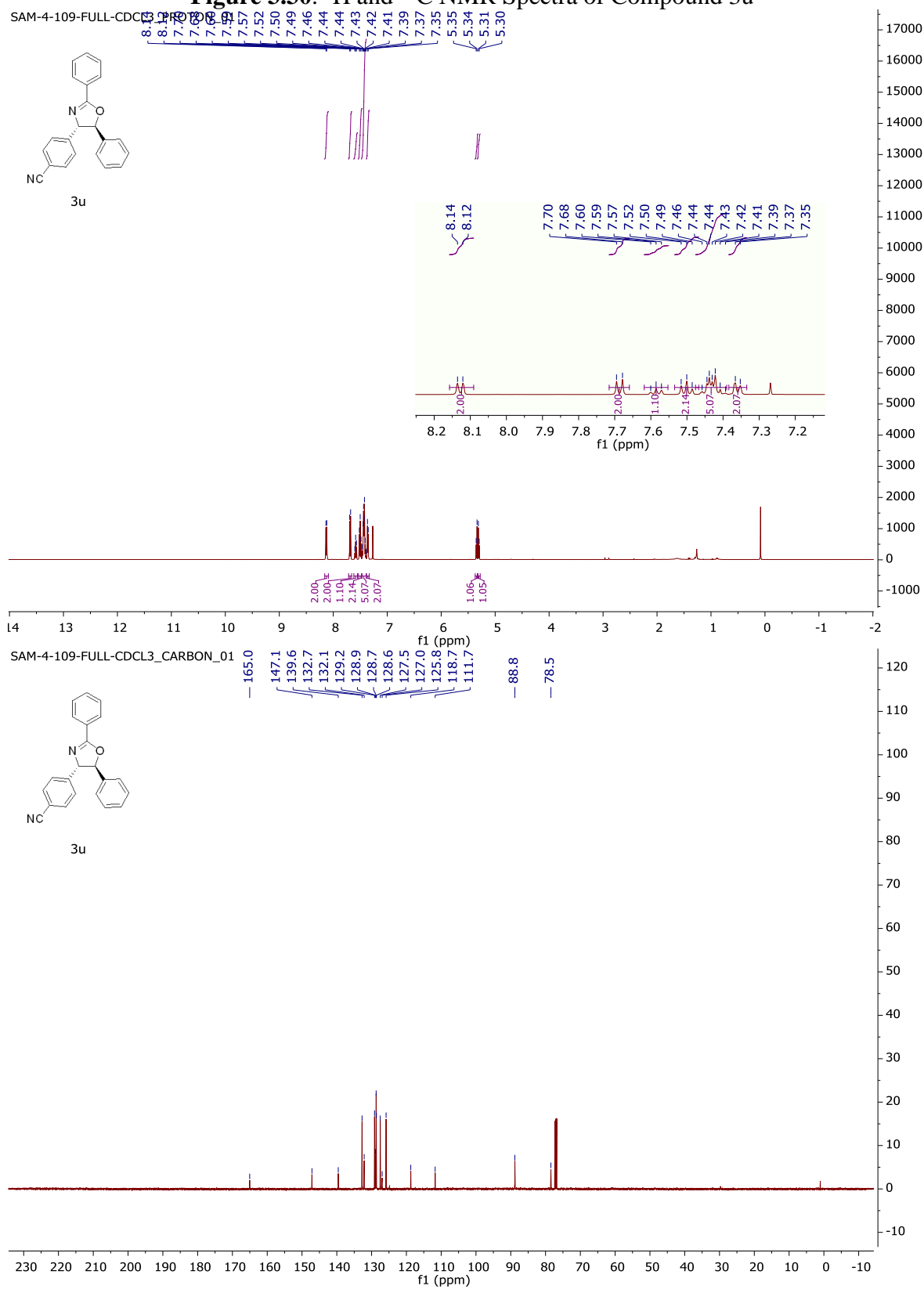


Figure 3.31. ^1H and ^{13}C NMR Spectra of Compound 3v

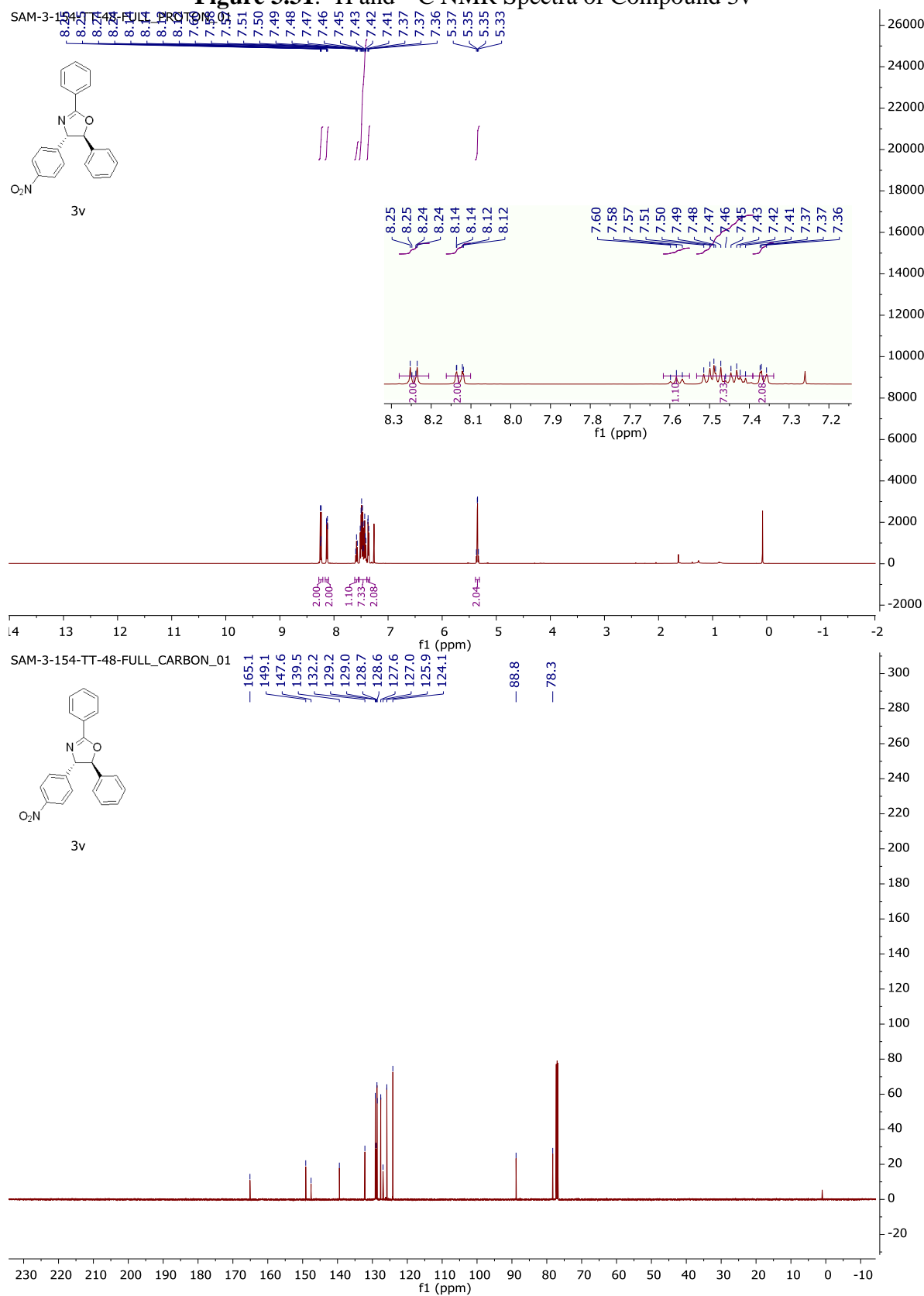


Figure 3.32. ^1H and ^{13}C NMR Spectra of Compound 3w

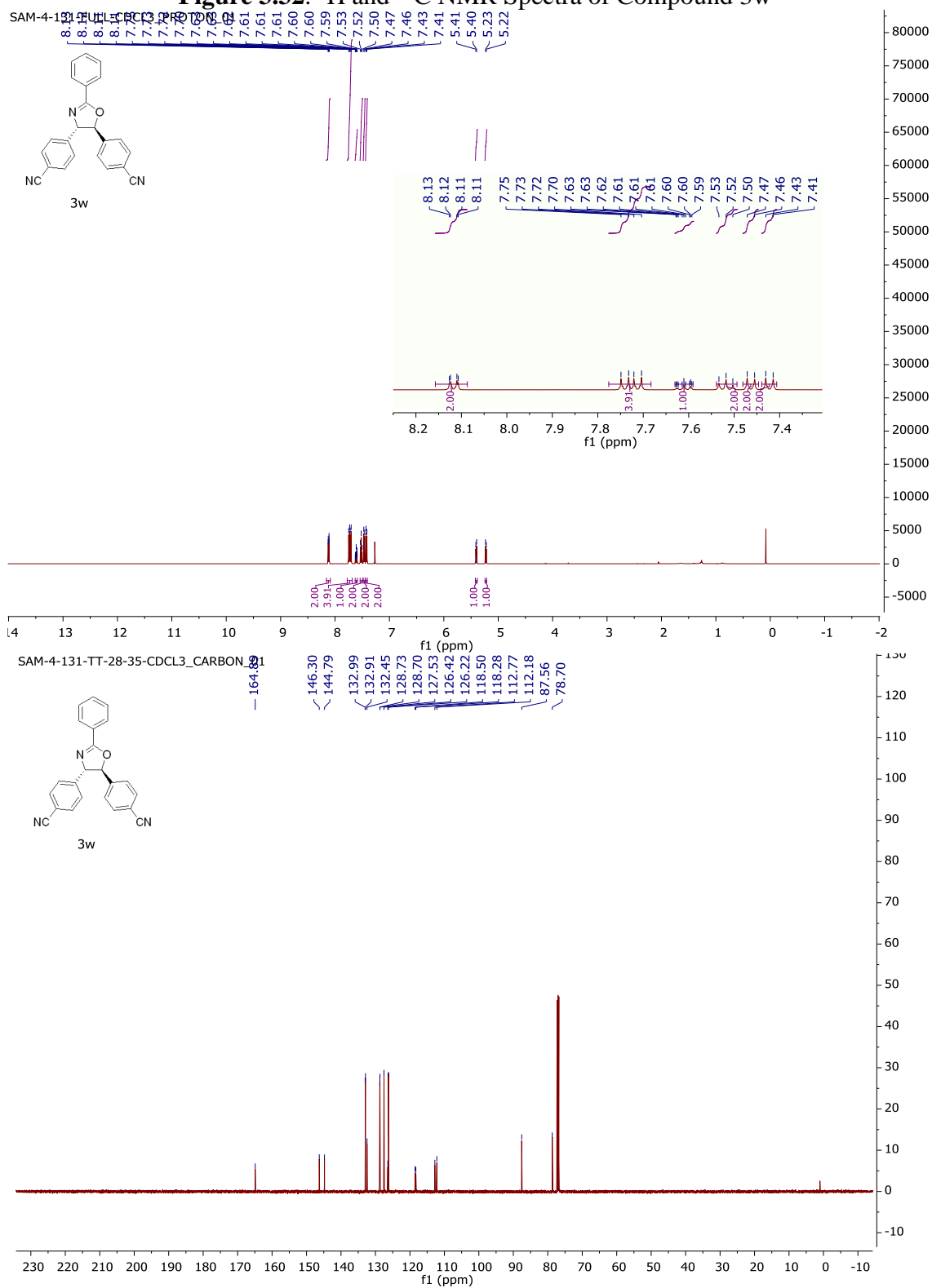


Figure S33: ¹H and ¹³C NMR spectra of Compound 4

¹H NMR spectrum (top): The spectrum shows peaks in the aromatic region (6.24–9.18 ppm) and a methoxy singlet (3.38 ppm). The x-axis represents chemical shift in ppm, ranging from -2 to 14. The y-axis represents intensity, ranging from -1000 to 13000. Integration values are provided below the peaks: 1.00, 2.00, 4.03, 2.05, 1.00, 1.00, and 3.00.

¹³C NMR spectrum (bottom): The spectrum shows peaks in the aromatic region (126.8–167.4 ppm) and a methoxy singlet (55.7 ppm). The x-axis represents chemical shift in ppm, ranging from -10 to 230. The y-axis represents intensity, ranging from -20 to 240.

Chemical structure of Compound 4: COc1ccccc1C(=O)Nc2ccccc2

Figure 3.34. ^1H and ^{13}C NMR Spectra of Compound 5a

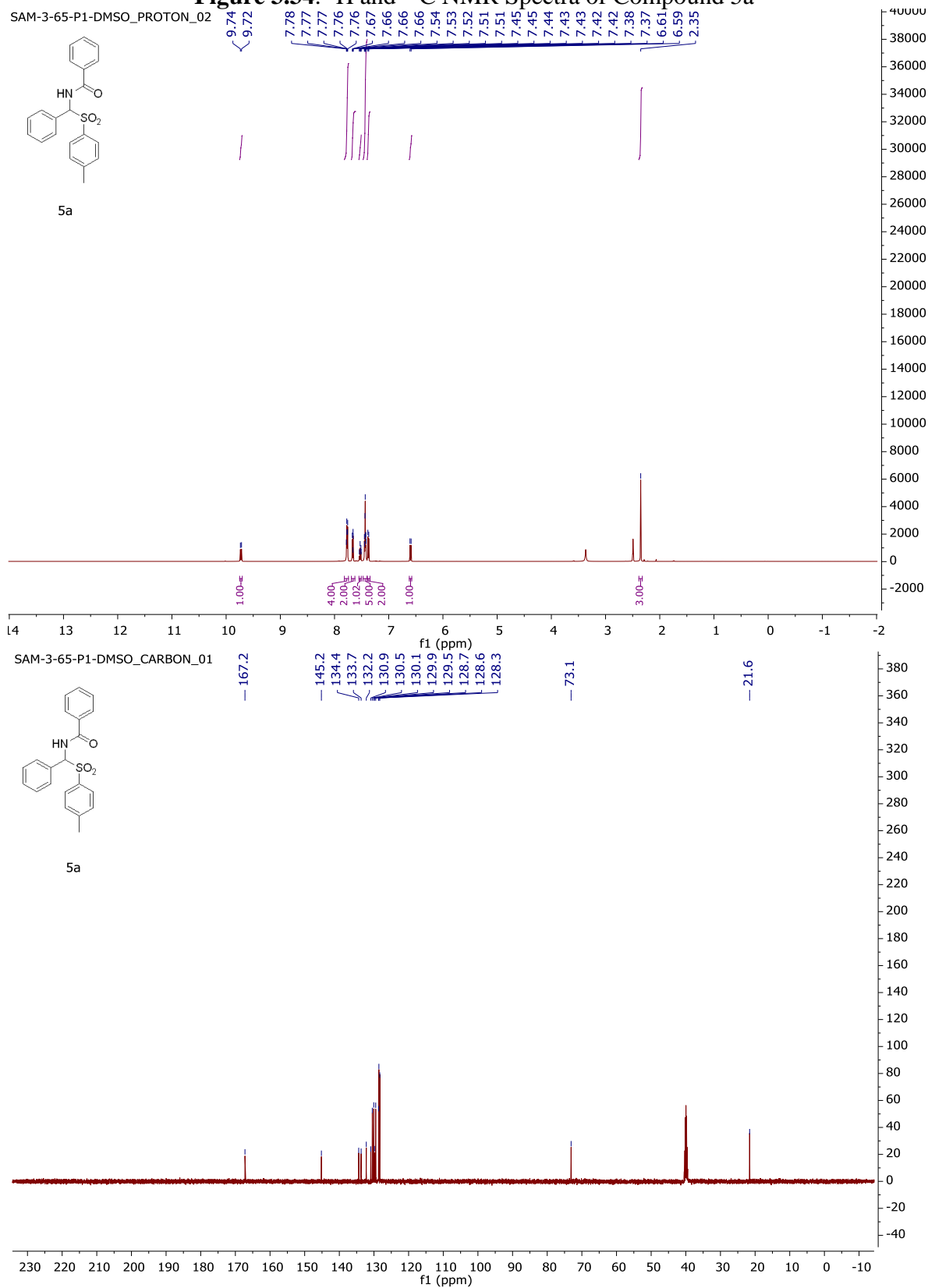


Figure 3.35. ^1H and ^{13}C NMR Spectra of Compound 5b

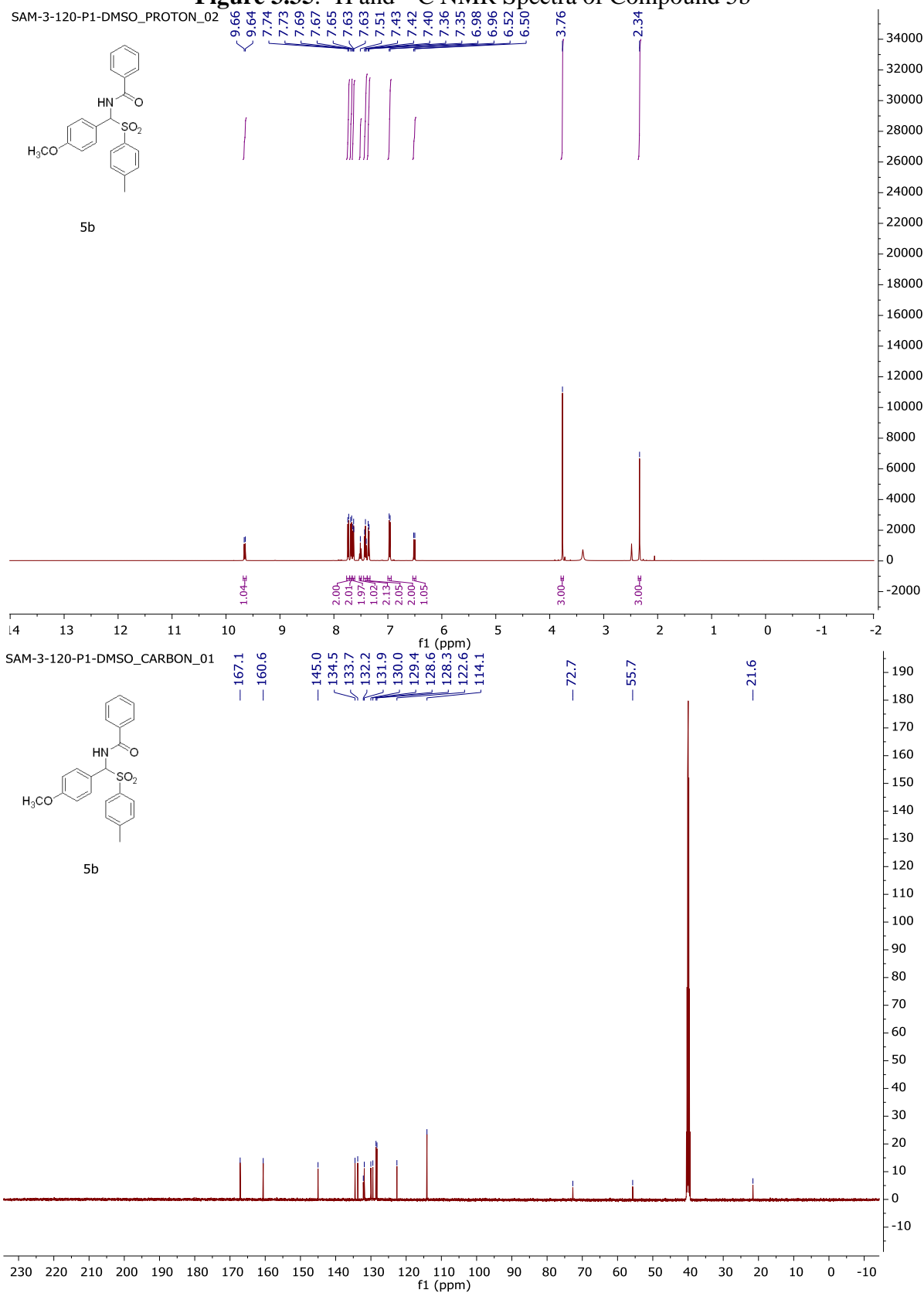


Figure 3.36. ^1H and ^{13}C NMR Spectra of Compound 5c

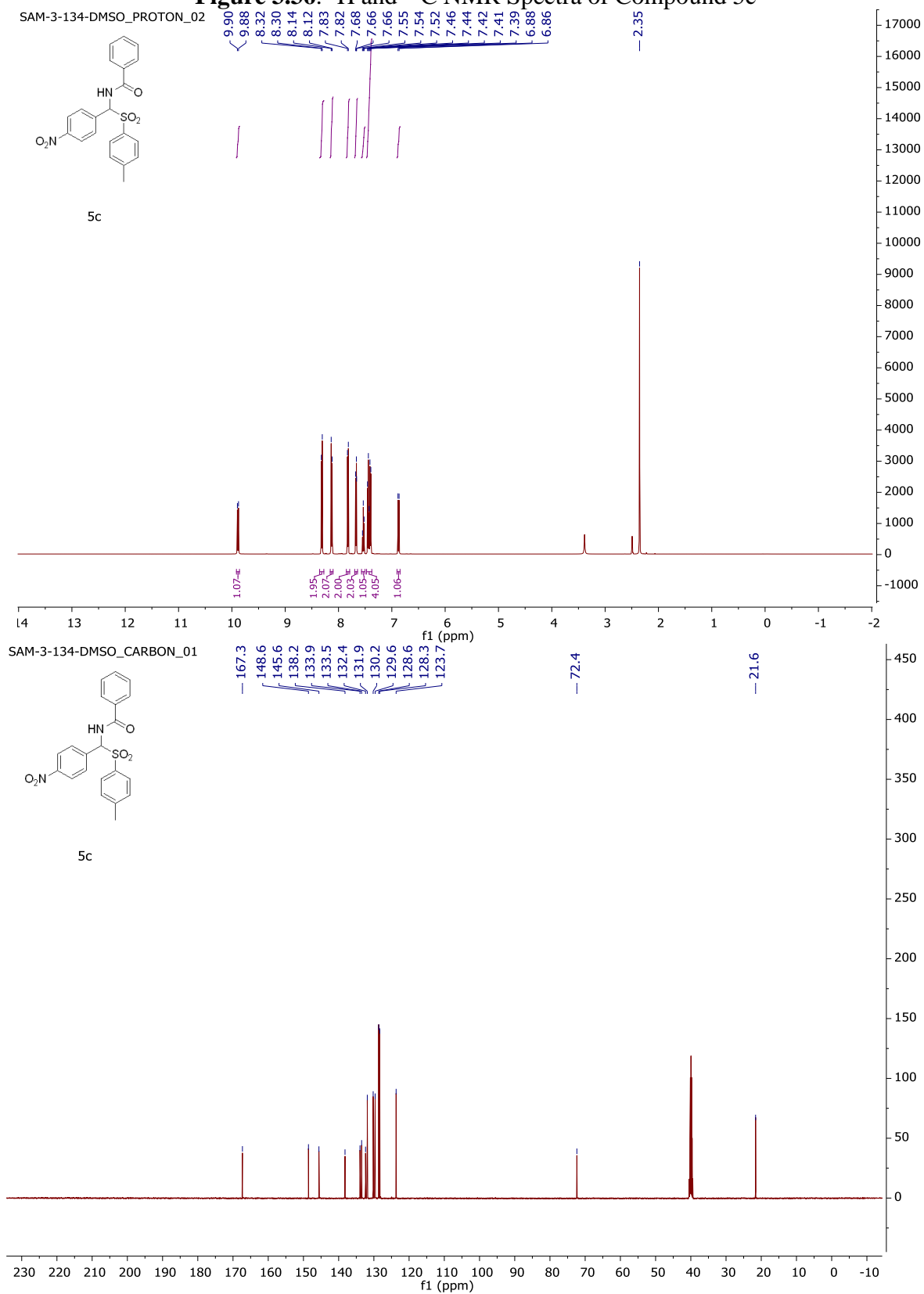


Figure 3.37. ^1H and ^{13}C NMR Spectra of Compound 5d

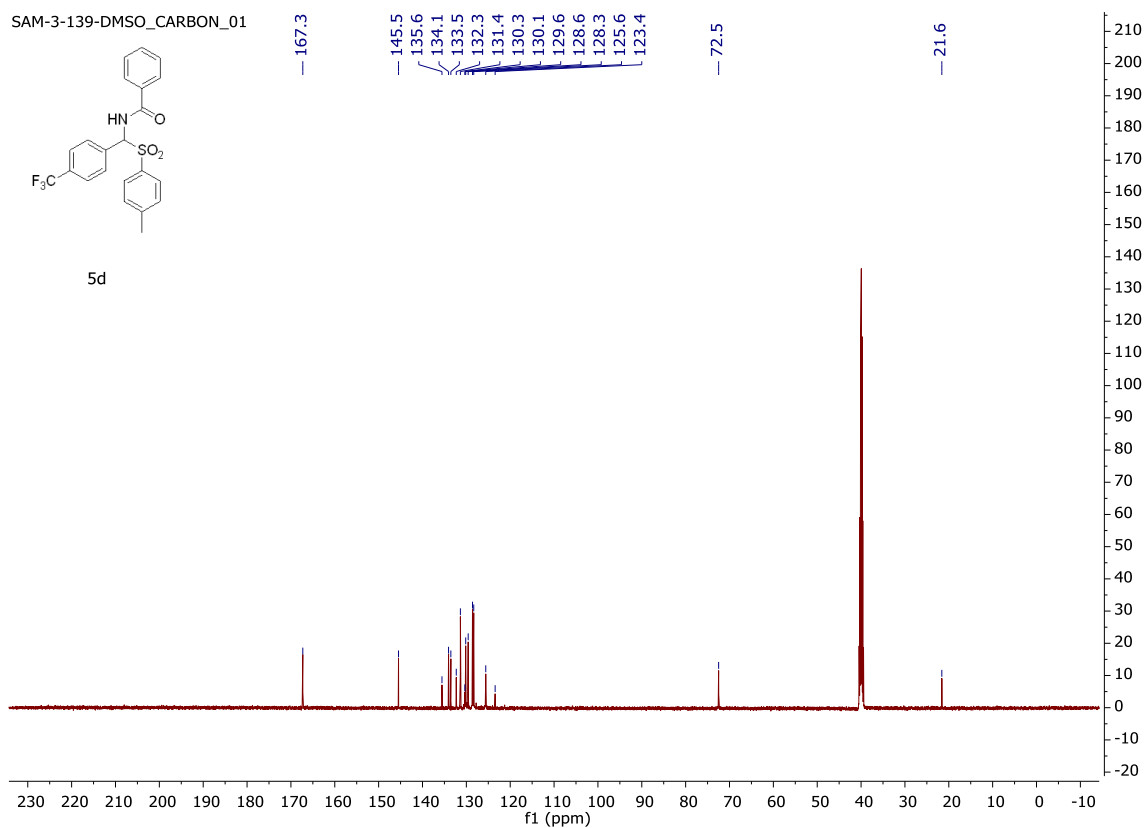
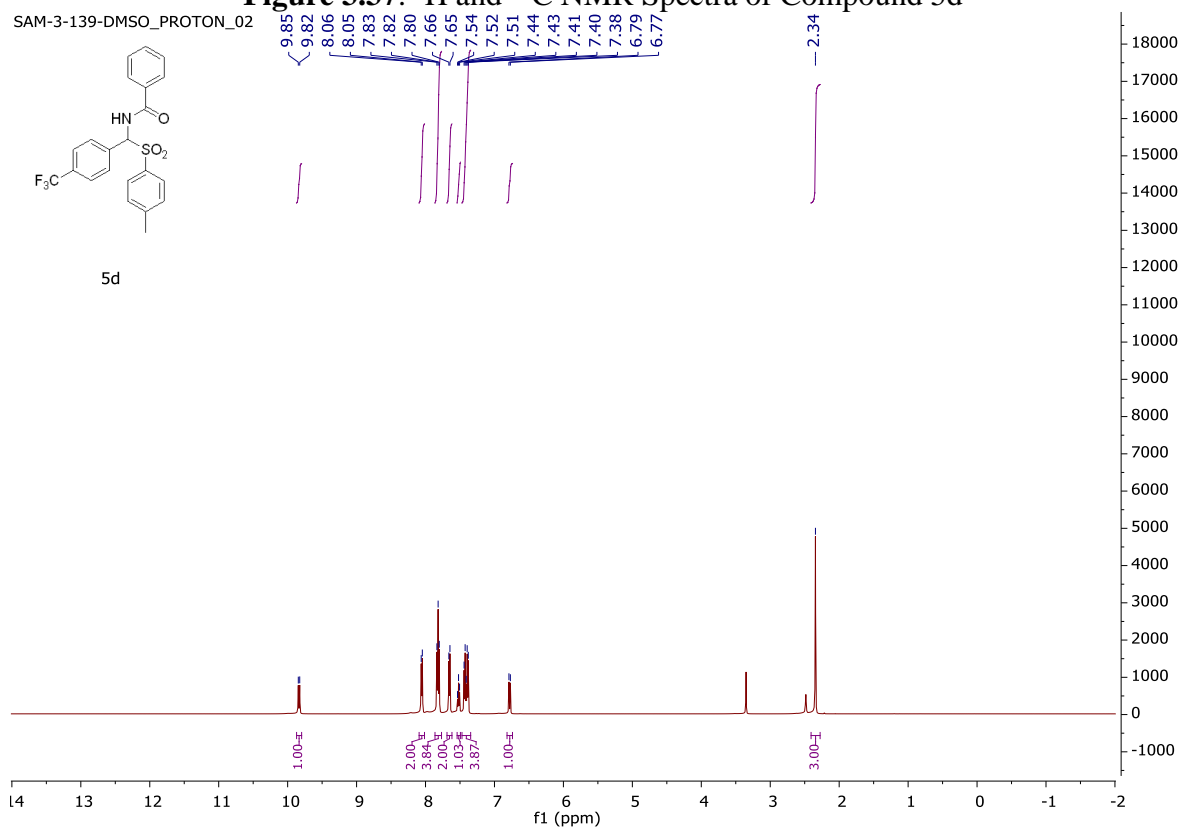


Figure 1 ¹H and ¹³C NMR spectra of compound 5e.

Top Panel: ¹H NMR Spectrum (DMSO-d₆)

Chemical structure of compound 5e is shown. The ¹H NMR spectrum displays peaks in the aromatic region (6.63–7.77 ppm) and a singlet at 2.35 ppm. Integration values are provided below the peaks.

Chemical Shift (ppm)	Integration
7.77	1.04
7.75	2.03
7.73	1.95
7.71	2.00
7.69	1.04
7.67	2.03
7.65	2.01
7.63	2.00
7.54	1.03
7.53	1.03
7.51	1.03
7.45	1.03
7.43	1.03
7.42	1.03
7.39	1.03
7.37	1.03
7.30	1.03
7.28	1.03
7.26	1.03
6.65	1.03
6.63	1.03
2.35	3.00

Bottom Panel: ¹³C NMR Spectrum (DMSO-d₆)

Chemical structure of compound 5e is shown. The ¹³C NMR spectrum displays peaks in the aromatic region (115.7–167.2 ppm) and a solvent peak at 72.3 ppm.

Chemical Shift (ppm)
167.2
162.3
145.2
134.2
133.6
132.8
132.3
130.1
129.5
128.6
128.3
127.3
115.7
72.3
21.6

Figure 3.39. ^1H and ^{13}C NMR Spectra of Compound 5f

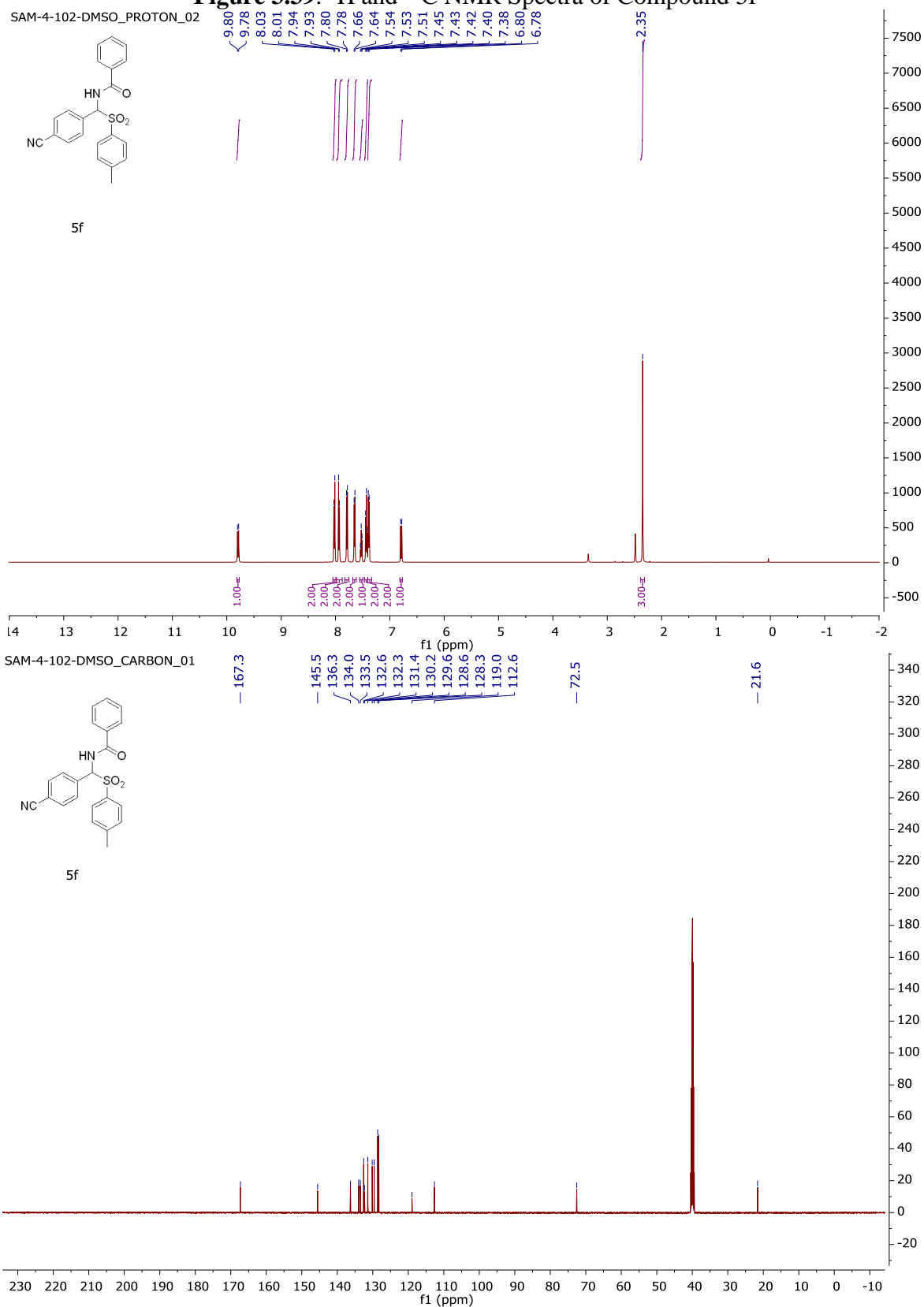


Figure 3.40. ^1H and ^{13}C NMR Spectra of Compound 5g

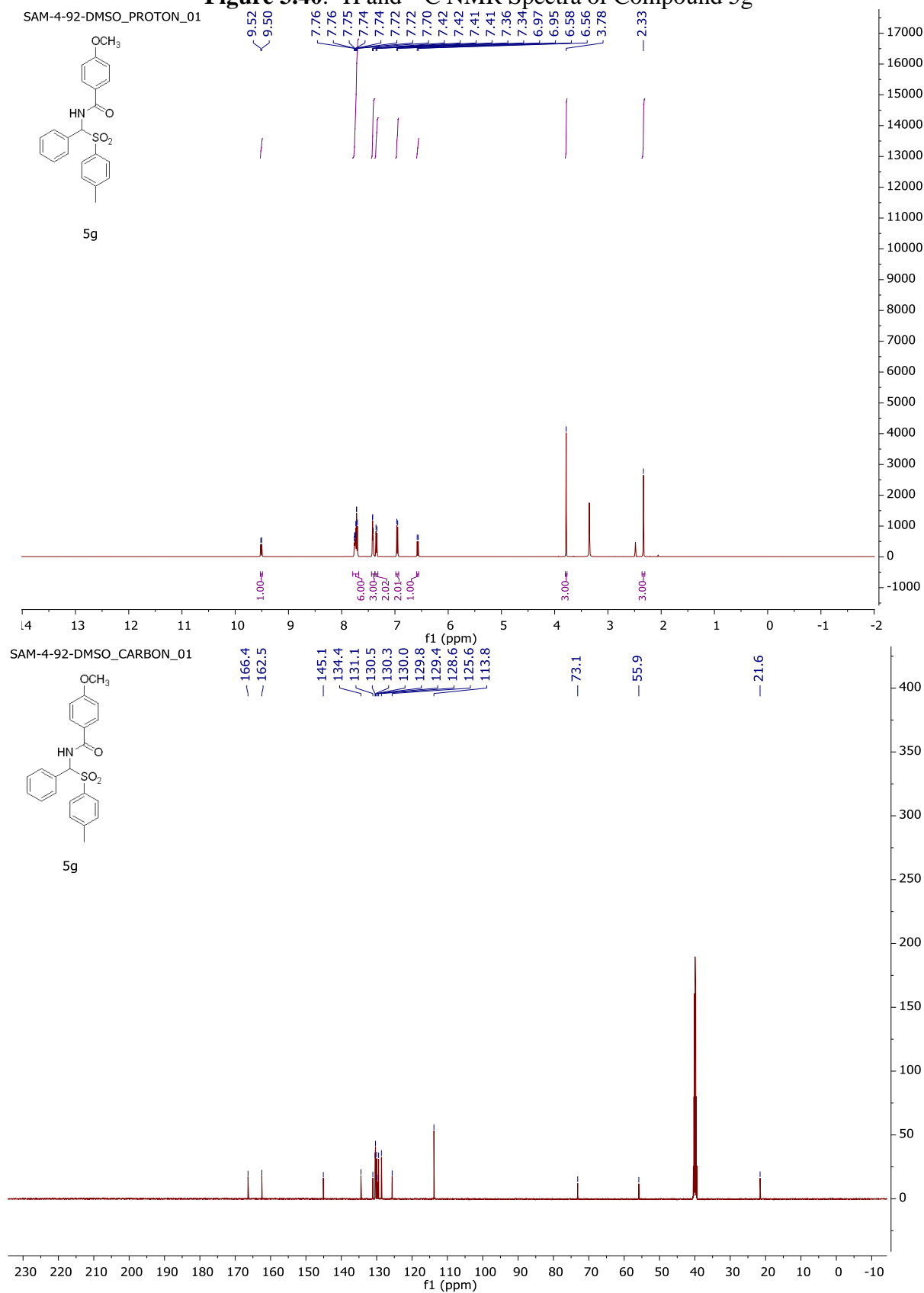


Figure 3.41. ^1H and ^{13}C NMR Spectra of Compound 5h

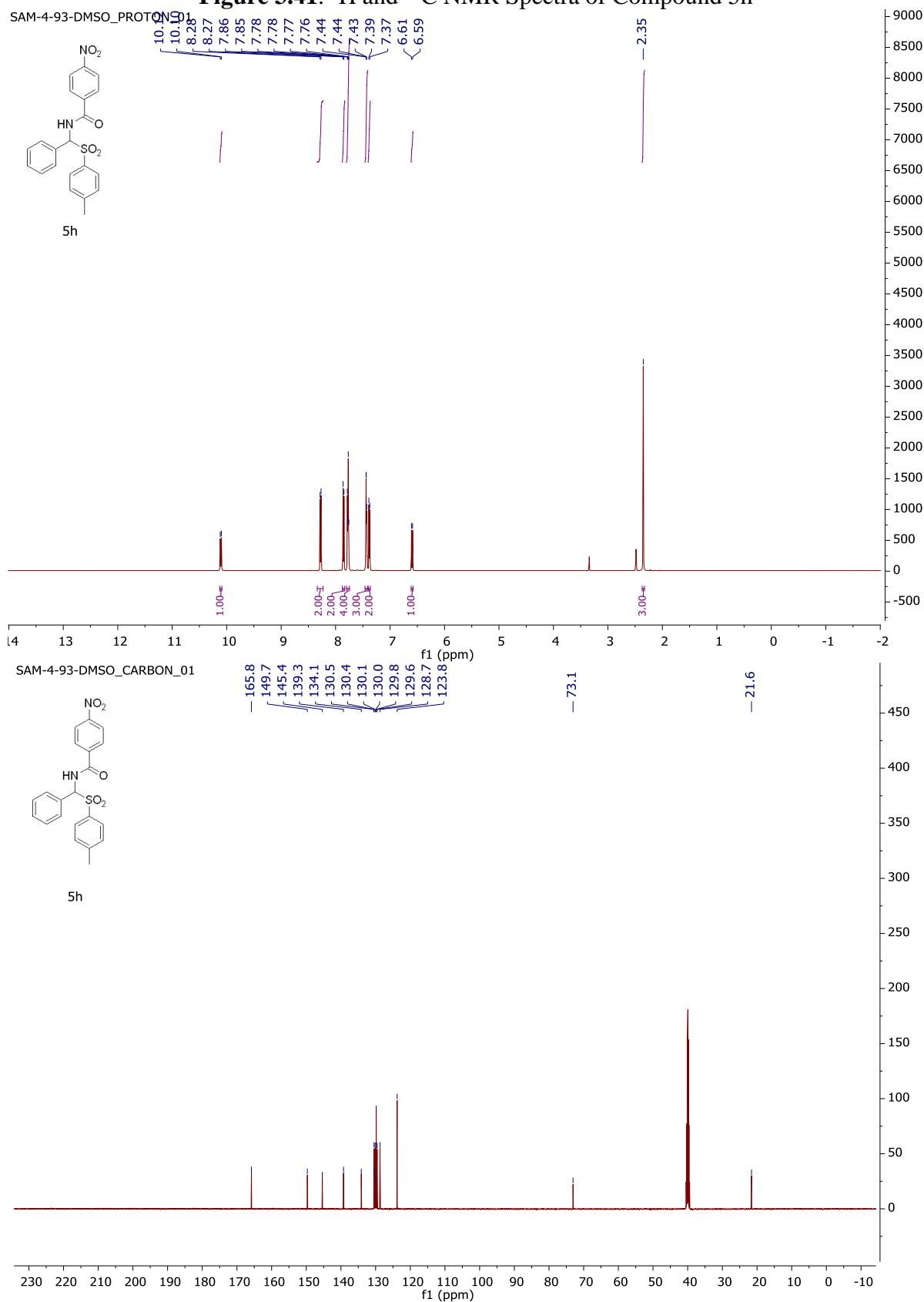


Figure 3.42. ^1H and ^{13}C NMR Spectra of Compound 6a

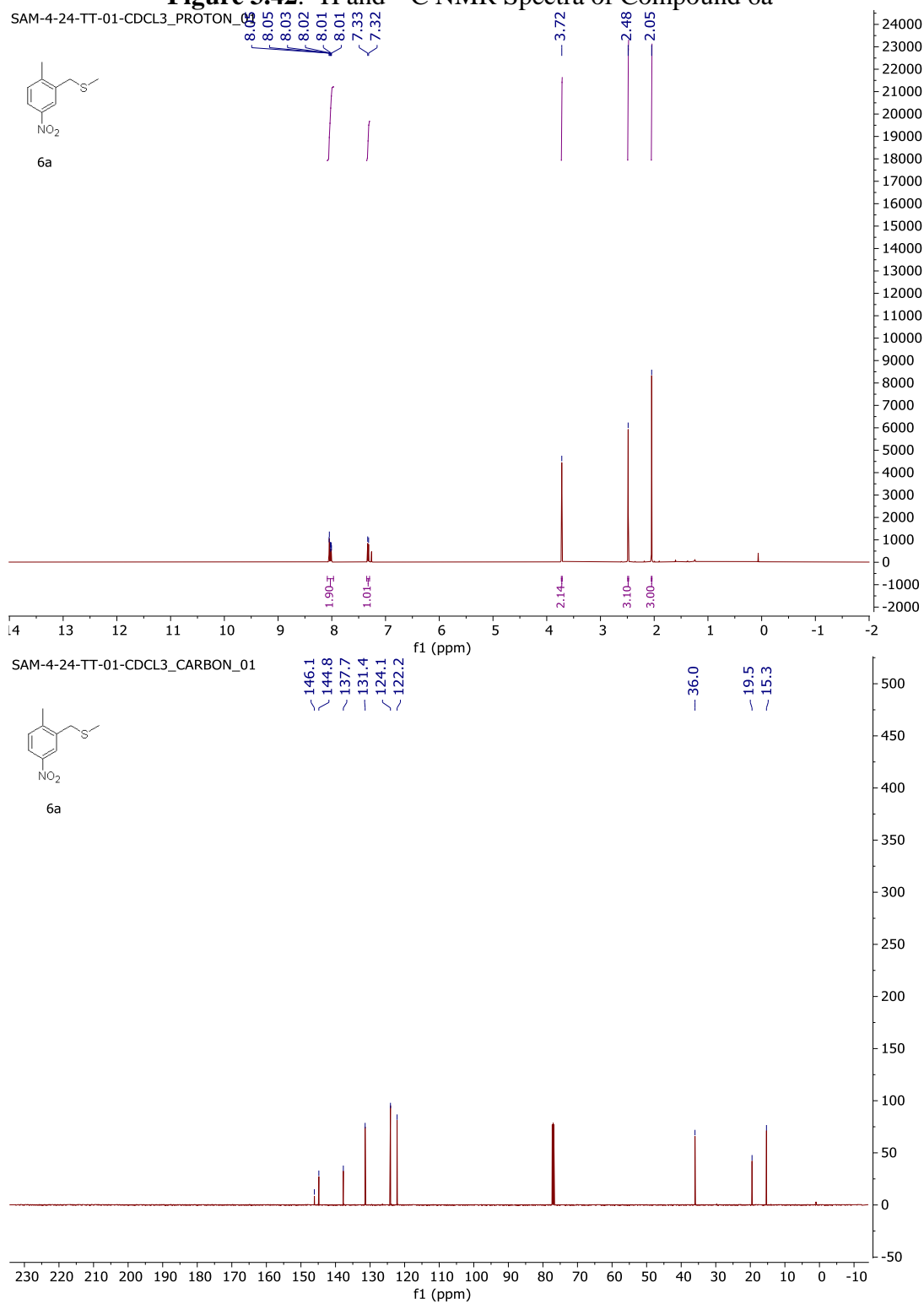
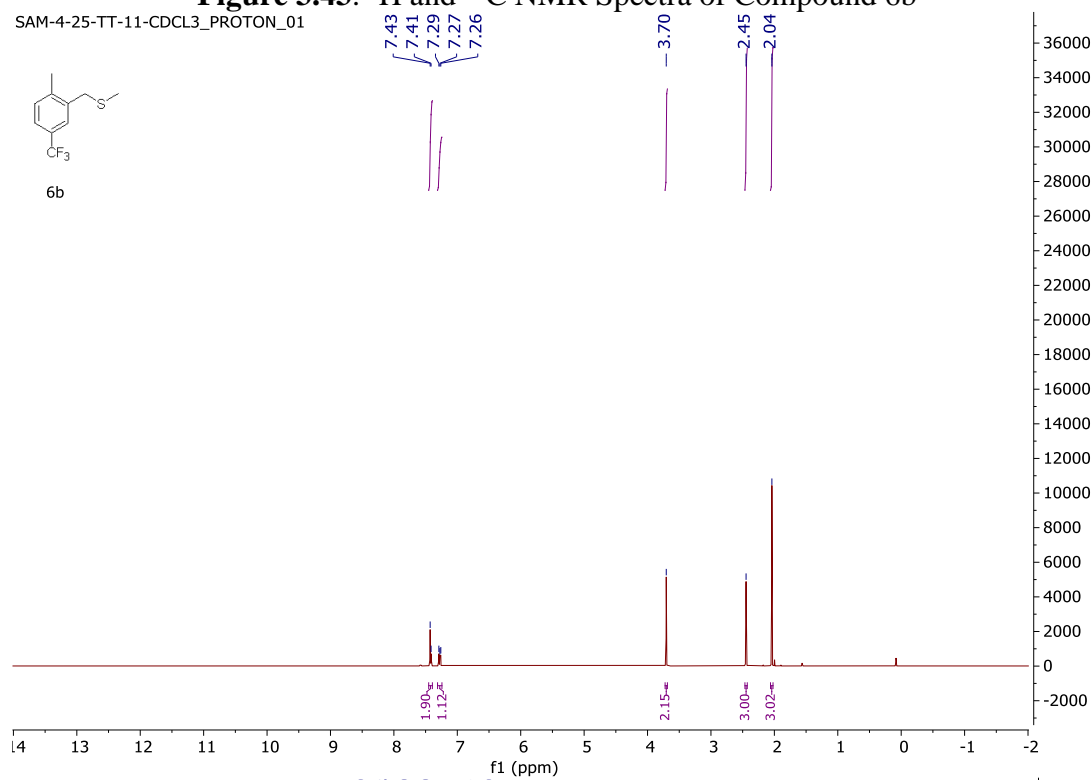


Figure 3.43. ^1H and ^{13}C NMR Spectra of Compound 6b

SAM-4-25-TT-11-CDCL3_PROTON_01



6b



SAM-4-25-TT-11-CDCL3_CARBON_01



6b

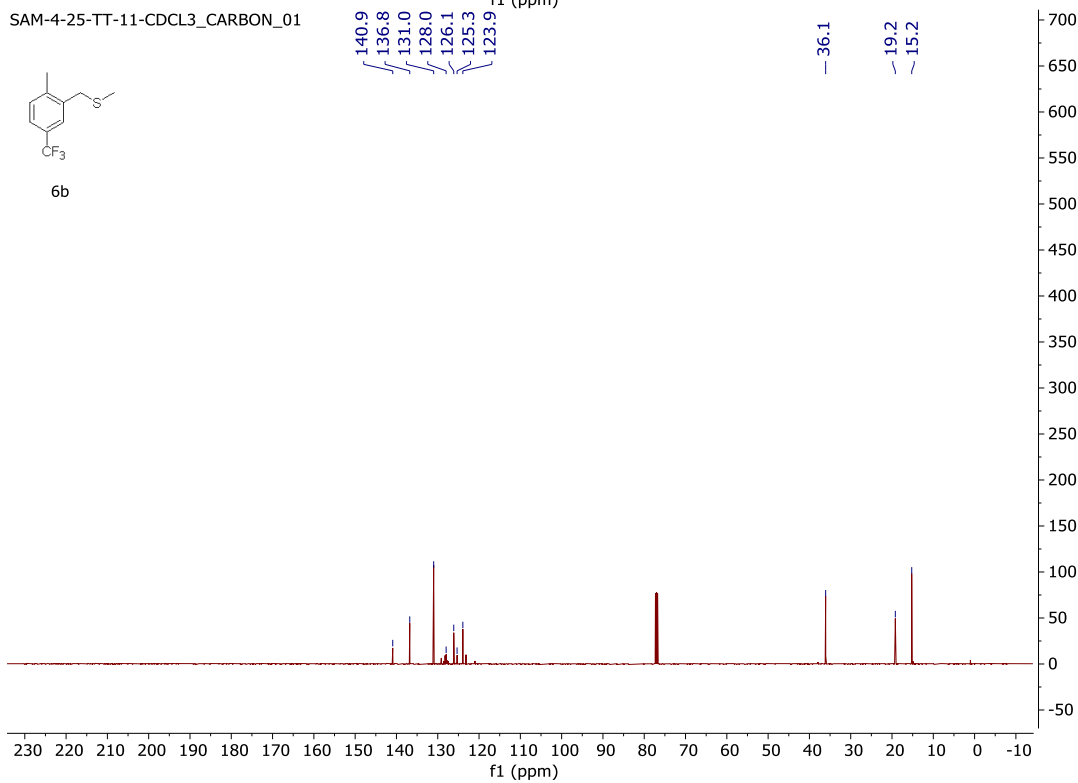


Figure 3.44. ^1H and ^{13}C NMR Spectra of Compound 6c

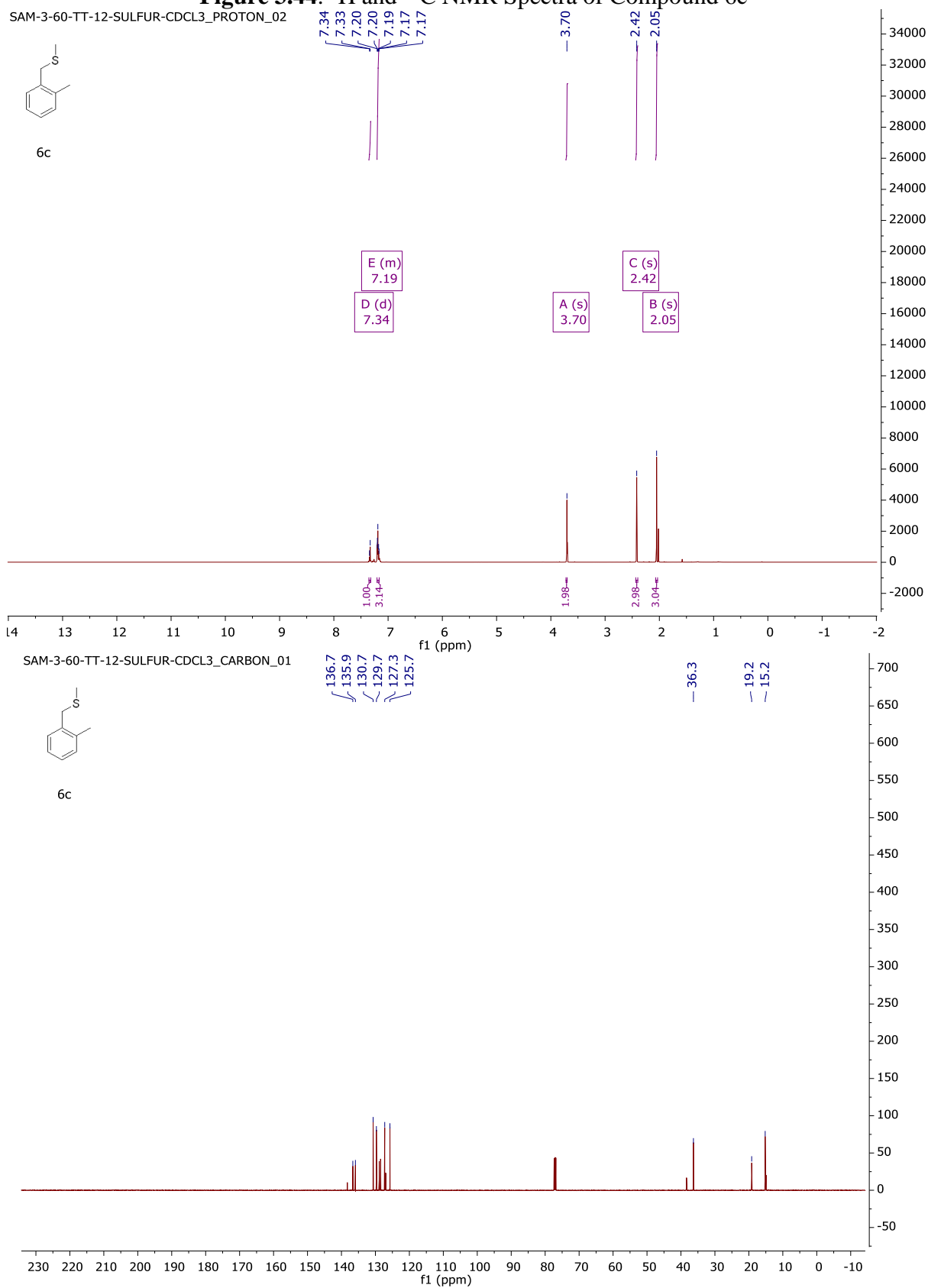
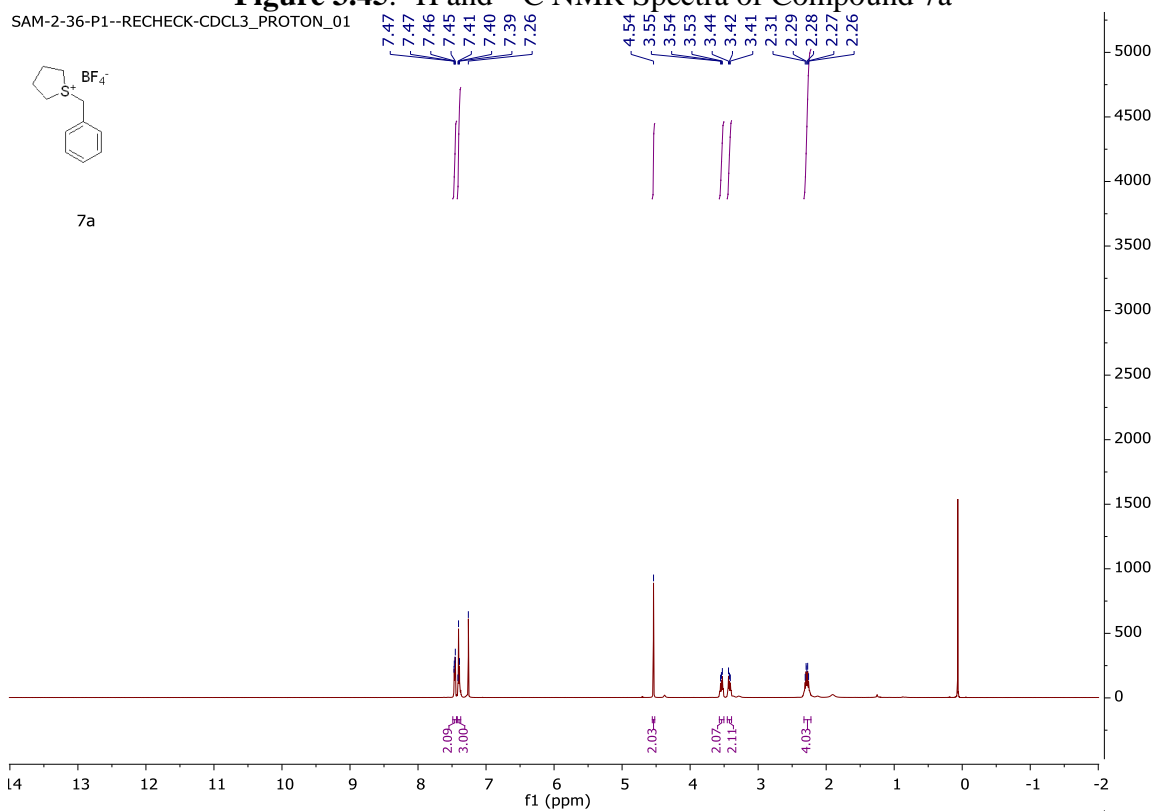
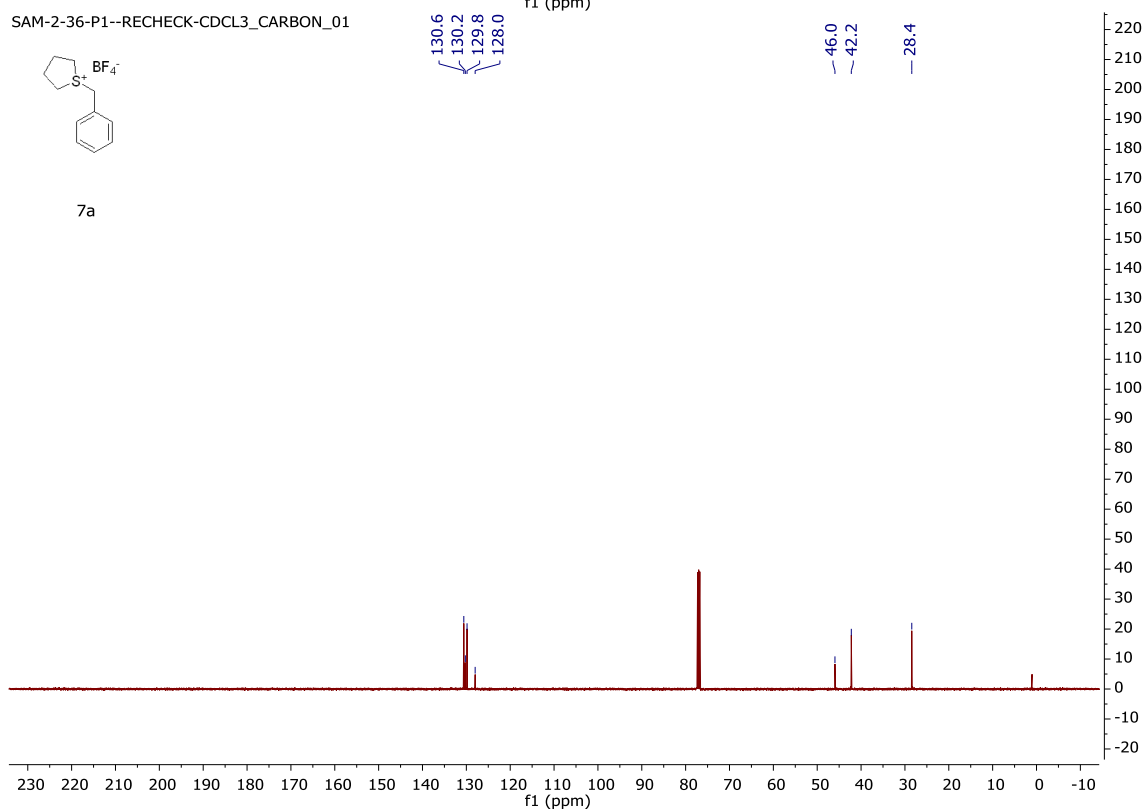


Figure 3.45. ^1H and ^{13}C NMR Spectra of Compound 7a

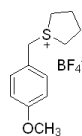
SAM-2-36-P1--RECHECK-CDCL3_PROTON_01



SAM-2-36-P1--RECHECK-CDCL3_CARBON_01



SAM-4-38-N-THF-DMSO_PROTON_01



7b

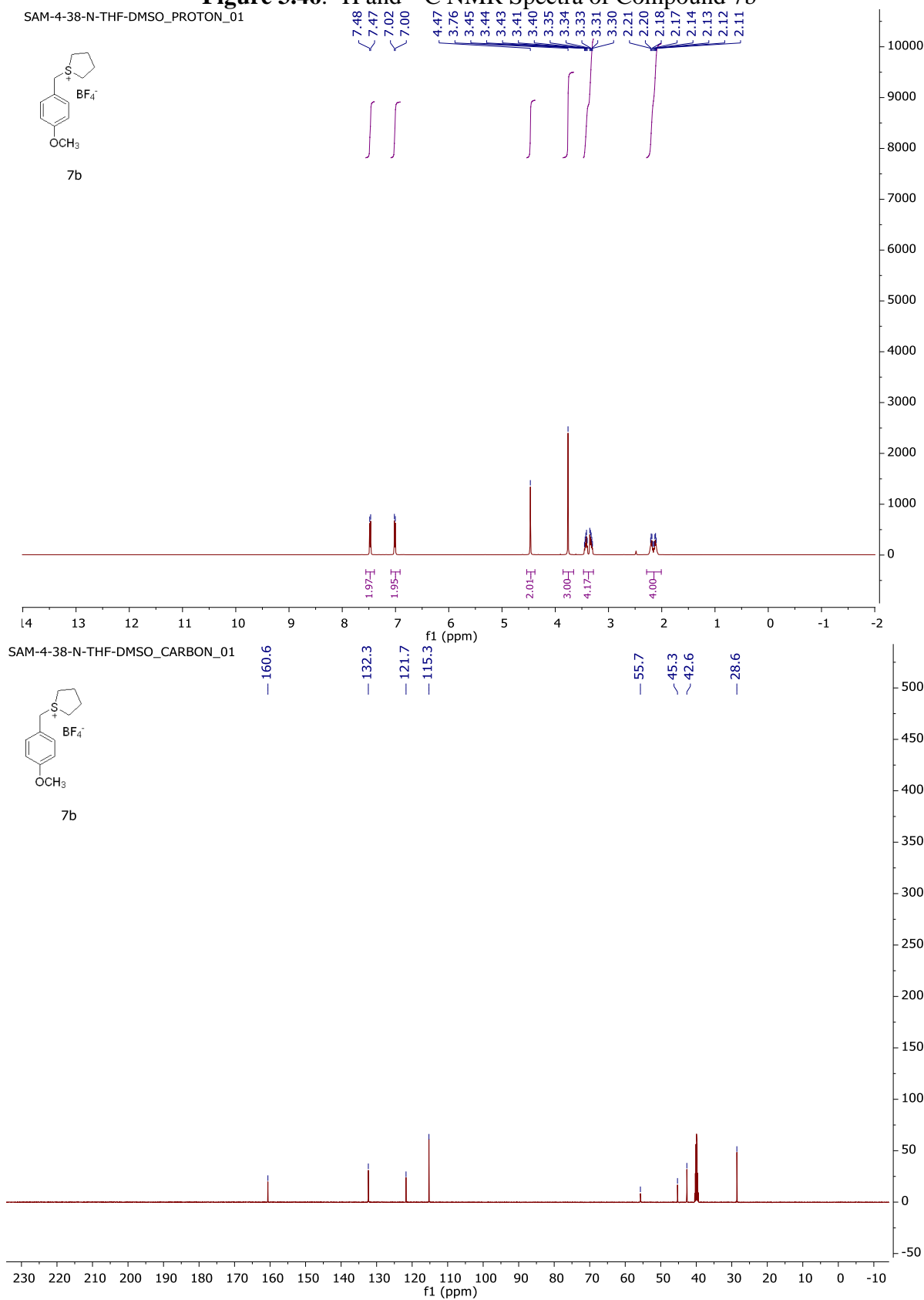
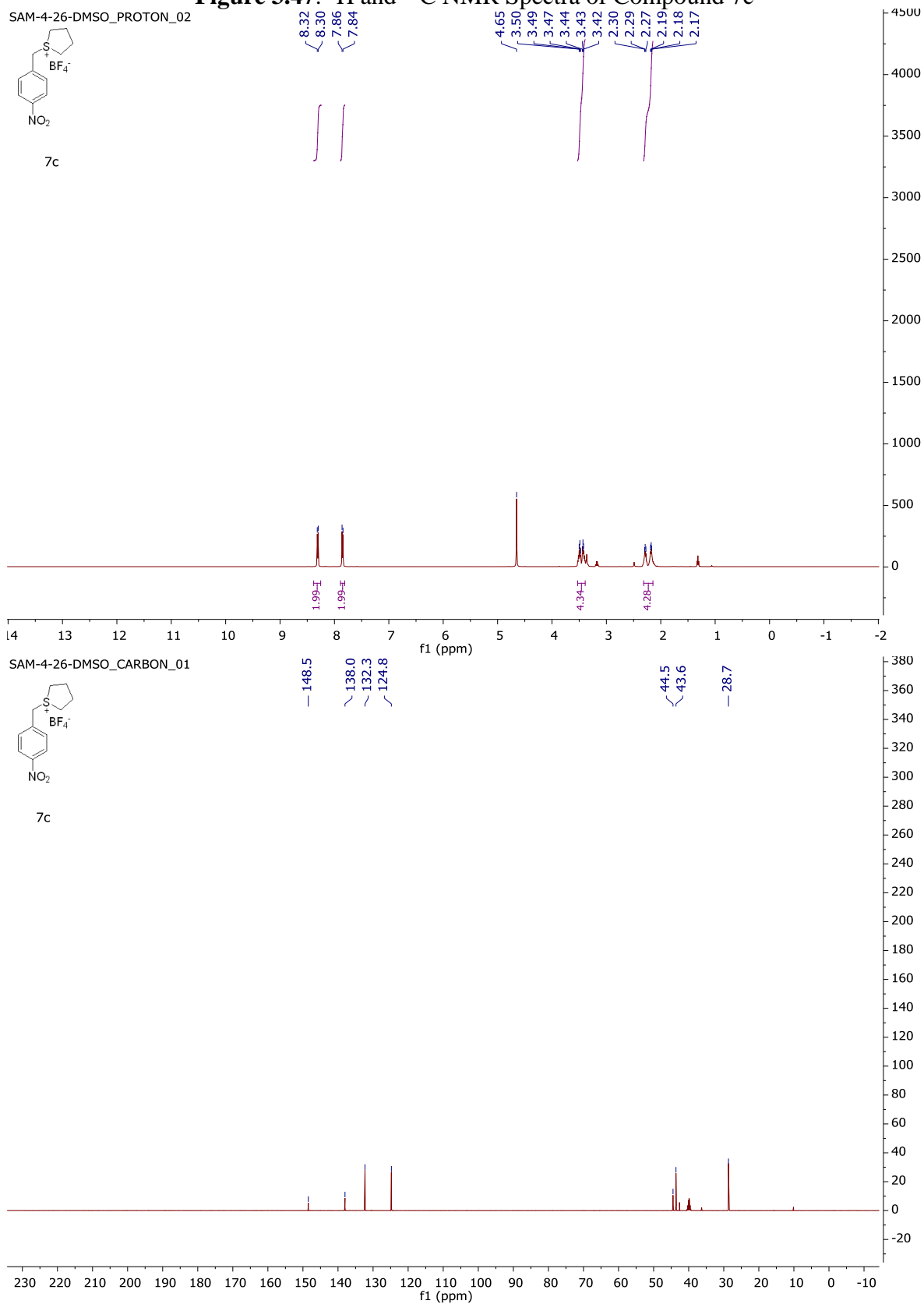


Figure 3.47. ^1H and ^{13}C NMR Spectra of Compound 7c



SAM-4-39-THF-DMSO_PROTON_01



Figure 3.49. ^1H and ^{13}C NMR Spectra of Compound 7h

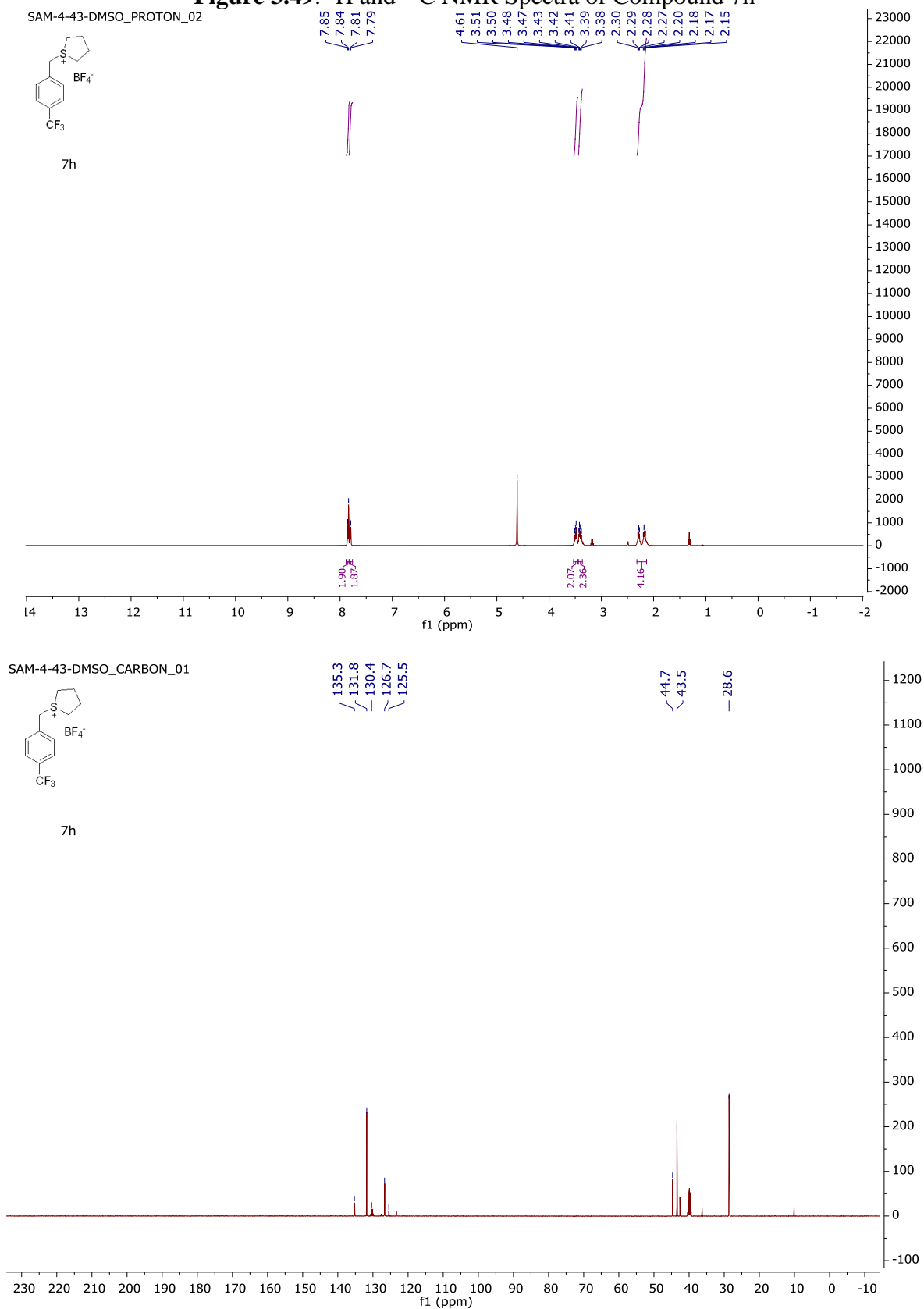
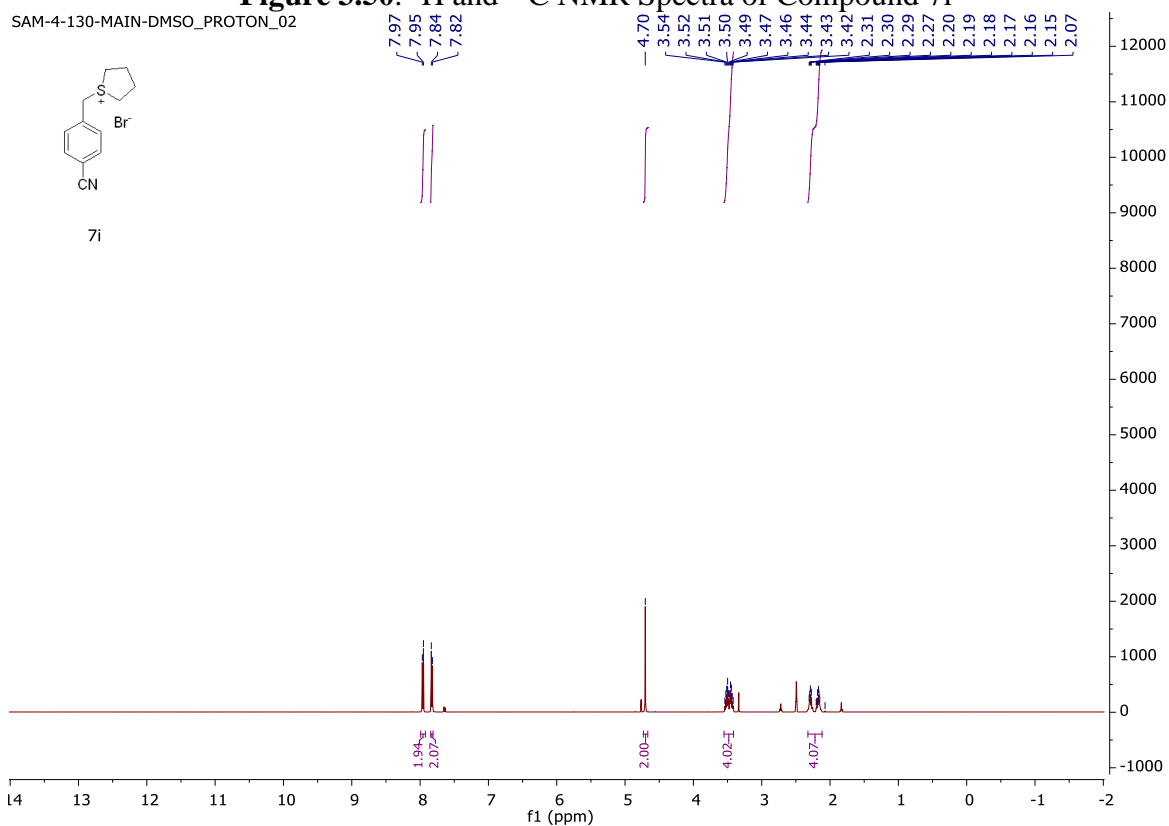
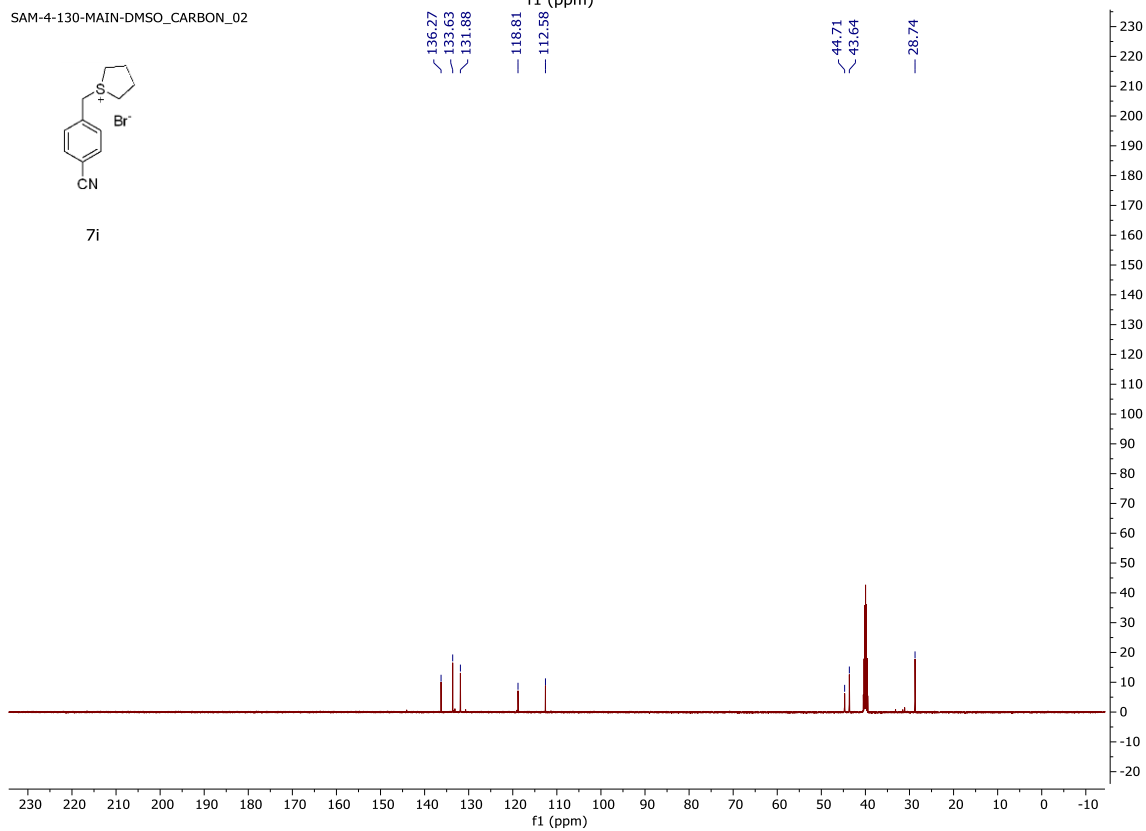


Figure 3.50. ^1H and ^{13}C NMR Spectra of Compound 7i

SAM-4-130-MAIN-DMSO_PROTON_02



SAM-4-130-MAIN-DMSO_CARBON_02



REFERENCES

REFERENCES

- [1] (a) Wipf, P., Pelletier, S. W., Ed. Pergamon: New York, 1998; pp 187; (b) Li, X.; Taechalertrpaisarn, J.; Xin, D.; Burgess, K. *Org. Lett.* **2015**, *17*, 632; (c) Plisson, F.; Prasad, P.; Xiao, X.; Piggott, A. M.; Huang, X. C.; Khalil, Z.; Capon, R. J. *Org. Biomol. Chem.* **2014**, *12*, 1579; (d) Moraski, G. C.; Chang, M.; Villegas-Estrada, A.; Franzblau, S. G.; Mollmann, U.; Miller, M. J. *Eur. J. Med. Chem.* **2010**, *45*, 1703;
- [2] (a) Cannon, J. S.; Overman, L. E. *Acc. Chem. Res.* **2016**, *49*, 2220; (b) Yang, G.; Zhang, W. *Chem. Soc. Rev.* **2018**, *47*, 1783; (c) Desimoni, G.; Faita, G.; Jorgensen, K. A. *Chem. Rev.* **2011**, *111*, PR284-437; (d) Johnson, J. S.; Evans, D. A. *Acc. Chem. Res.* **2000**, *33*, 325.
- [3] (a) Phillips, A. J.; Uto, Y.; Wipf, P.; Reno, M. J.; Williams, D. R. *Org. Lett.* **2000**, *2*, 1165; (b) Miley, G. P.; Rote, J. C.; Silverman, R. B.; Kelleher, N. L.; Thomson, R. J. *Org. Lett.* **2018**, *20*, 2369; (c) Cox, J. B.; Kimishima, A.; Wood, J. L. *J. Am. Chem. Soc.* **2019**, *141*, 25; (d) Brandstatter, M.; Roth, F.; Luedtke, N. W. *J. Org. Chem.* **2015**, *80*, 40.
- [4] (a) Wei, T.; Dixon, D. J. *Chem. Commun. (Camb)* **2018**, *54*, 12860; (b) Heath, R.; Muller-Bunz, H.; Albrecht, M. *Chem. Commun. (Camb)* **2015**, *51*, 8699.
- [5] (a) Wipf, P.; Wang, X. *J. Comb. Chem.* **2002**, *4*, 656; (b) Garg, P.; Chaudhary, S.; Milton, M. D. *J. Org. Chem.* **2014**, *79*, 8668.
- [6] Corey, E. J.; Chaykovsky, M. *J. Am. Chem. Soc.* **1962**, *84*, 867.
- [7] (a) Aggarwal, V. K.; Winn, C. L. *Acc. Chem. Res.* **2004**, *37*, 611; (b) Corey, E. J.; Chaykovsky, M. *J. Am. Chem. Soc.* **1965**, *87*, 1353; (c) Mondal, M.; Chen, S.; Kerrigan, N. J. *Molecules* **2018**, *23*, 738; (d) Xiang, Y.; Fan, X.; Cai, P.-J.; Yu, Z.-X. *Eur. J. Org. Chem.* **2019**, 582; (e) Hajra, S.; Roy, S.; Saleh, S. A. *Org. Lett.* **2018**, *20*, 4540; (f) Heravi, M. M.; Asadi, S.; Nazari, N.; Lashkariani, B. M. *Curr. Org. Syn.* **2016**, *13*, 308.
- [8] (a) Heine, H. W.; Kaplan, M. S. Aziridines. XVI. *J. Org. Chem.* **1967**, *32*, 3069; (b) Heine, H. W.; Kenyon, W. G.; Johnson, E. M. *J. Am. Chem. Soc.* **1961**, *83*, 2570; (c) Heine, H. W.; Bender, H. *J. Org. Chem.* **1960**, *25*, 461; (d) Kuszpit, M. R.; Wulff, W. D.; Tepe, J. J. *J. Org. Chem.* **2011**, *76*, 2913.
- [9] Aggarwal, V. K.; Vasse, J. L. *Org. Lett.* **2003**, *5*, 3987.
- [10] Katritzky, A. R.; Pernak, J.; Fan, W. Q.; Saczewski, F. *J. Org. Chem.* **1991**, *56*, 4439.
- [11] Mall, T.; Stamm, H. *Chem. Ber.* **1988**, *121*, 1353.
- [12] Katritzky, A. R.; Fan, W. Q.; Black, M.; Pernak, J. *J. Org. Chem.* **1992**, *57*, 547.

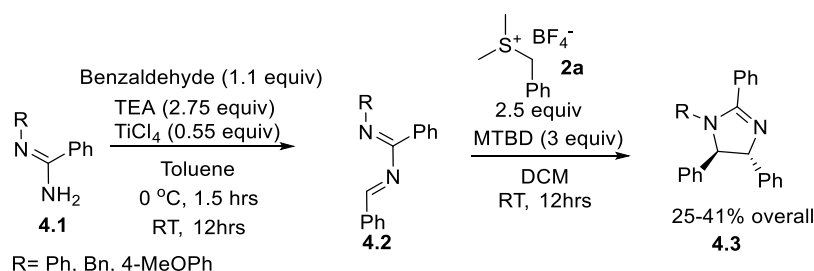
- [13] Murry, J. A.; Frantz, D. E.; Soheili, A.; Tillyer, R.; Grabowski, E. J.; Reider, P. J. *J. Am. Chem. Soc.* **2001**, *123*, 9696.
- [14] Burkhard, R. K.; Sellers, D. E.; DeCou, F.; Lambert, J. L. *J. Org. Chem.* **1959**, *24*, 767.
- [15] Cowen, B. J.; Saunders, L. B.; Miller, S. J. *J. Am. Chem. Soc.* **2009**, *131*, 6105.
- [16] Hauser, C. R.; Kantor, S. W.; Brasen, W. R. *J. Am. Chem. Soc.* **1953**, *75*, 2660.
- [17] Huisgen, R.; Raab, R. *Tetrahedron Lett.* **1966**, *6*, 649.
- [18] (a) Aggarwal, V. K.; Vasse, J.-L. *Org. Lett.* **2003**, *5*, 3987. (b) Katritzky, A. R.; Fan, W. Q.; Black, M.; Pernak, J. *J. Org. Chem.* **1992**, *57*, 547. (c) Katritzky, A. R.; Pernak, J.; Fan, W. Q.; Saczewski, F. *J. Org. Chem.* **1991**, *56*, 4439.
- [19] Forrester, J.; Jones, R. V. H.; Newton, L.; Preston, P. N. *Tetrahedron* **2001**, *57*, 2871.
- [20] Murry, J. A.; Frantz, D. E.; Soheili, A.; Tillyer, R.; Grabowski, E. J. J.; Reider, P. J. *J. Am. Chem. Soc.* **2001**, *123*, 9696.
- [21] Padwa, A.; Gasdaska, J. R. *Tetrahedron* **1988**, *44*, 4147.
- [22] Aggarwal, V. K.; Fang, G. Y.; Schmidt, A. T. *J. Am. Chem. Soc.* **2005**, *127*, 1642.
- [23] Fang, G. Y.; Aggarwal, V. K. *Angew. Chem. Int. Ed.* **2007**, *46*, 359.
- [24] Clergue, S.; Rousseau, O.; Delaunay, T.; Dequierez, G.; Tran, T.-V.; El Aakchioui, S.; Barozzino-Consiglio, G.; Robiette, R. *Chem. - Eur. J.* **2018**, *24*, 11417.
- [25] Okazaki, Y.; Ando, F.; Koketsu, J. *Bull. Chem. Soc. Jpn.* **2003**, *76*, 2155.
- [26] Clayden, J.; Clayton, J.; Harvey, R.; Karlubikova, O. *Synlett.* **2009**, 2836.
- [27] Clayden, J.; Parris, S.; Cabedo, N.; Payne, A. H. *Angew. Chem. Int. Ed. Engl.* **2008**, *47*, 5060.
- [28] Heine, H. W.; King, D. C.; Portland, L. A. *J. Org. Chem.* **1966**, *31*, 2662.

Chapter 4: Synthesis of imidazolines via reaction of 1,3-diaza-1,3-butadiene with sulfur ylides

4.1 Introduction

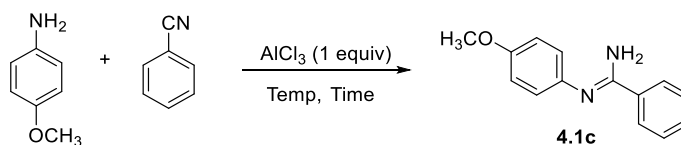
Imidazoline scaffolds have significant importance in the field of pharmaceutical, medicinal, and chemical sectors. The chapter one discussed the recent advancement in the synthesis of imidazoline scaffolds. To further extend the synthetic strategy of the imidazoline synthesis, 1,3-diaza-1,3-butadiene was used with sulfonium salts in the presence of a base (**Figure 4.1**).

Scheme 4.1. Synthesis of imidazoline



4.2 Results and discussion

The investigation was initiated by synthesizing amidine (**4.1c**) from the reaction of 4-methoxyaniline and a benzonitrile in the presence of 1 equivalent of AlCl_3 .¹ Unfortunately, the reaction provided only 21% of the amidine product, and a short optimization of the amidine synthesis was required before moving further to the next step. The optimizations were performed by treating the starting materials at different temperatures and times (**Table 4.1**). It was found that at $150\text{ }^\circ\text{C}$ for 50 minutes, the amidine product yield was increased to 65% from that initial 21%. After that, under these optimized conditions, various amidines (**4.1a-4.1f**) were synthesized in moderate to excellent yields (35-86%).

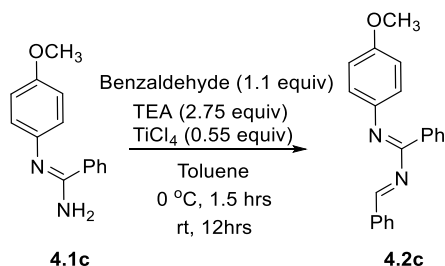
Table 4.1. Optimization of the amidine synthesis

Temp. °C	Time (min)	Yield% (4.1c)
140	30	21
160	40	45
200	10	18
150	30	31
150	50	65

Next, the 1,3-diaza-1,3-butadienes (**4.2**) were synthesized from the reaction of various amidine (**4.1a-4.1f**) with benzaldehyde.² But due to the instability of those compounds, purifications were tedious and not feasible. For optimizing this step, various temperatures (0 °C, room temperature, reflux), solvents (toluene, acetonitrile, dichloromethane), and different equivalents of starting materials were screened. From these investigations, we found that when we ran the reaction at room temperature and for a prolonged time, the reaction was forming 1,2-dihydro-1,3,5-triazine (**4.4**, see experimental section). This triazine was formed by a reaction of 1,3-diaza-1,3-butadiene (**4.2**) with an amidine starting material (**4.1**), or with another 1,3-diaza-1,3-butadiene (**4.2**), and further cyclized to that 1,2-dihydro-1,3,5-triazine (**4.4**).³ Later, to move further in the investigation, the most stable compound *N*-benzylidene-*N'*-(4-methoxyphenyl)benzimidamide (**4.2c**) was synthesized by reacting *N'*-(4-methoxyphenyl)benzimidamide (**4.1c**) with benzaldehyde in the presence of TEA and TiCl₄ (Scheme 4.2). The compound **4.2c** was then treated without further purification in the next step

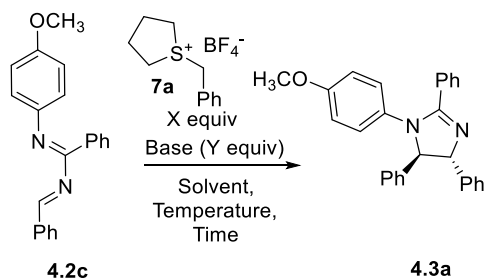
with sulfonium salt (**7a**, see chapter three) in the presence of a base to explore the optimization of the reaction.

Scheme 4.2. Synthesis of *N*-benzylidene-*N'*-(4-methoxyphenyl)benzimidamide



In this optimization step, different bases were screened with the sulfonium salt **7a**, at various temperatures and solvents (**Table 4.2**). The reaction of *n*BuLi, LiHMDS, and NaH, at -78 °C to room temperature in the solvent tetrahydrofuran or toluene did not provide any product formation. However, in the presence of 1,8-diazabicyclo[5.4.0]undec-7-ene (DBU), 5% of the imidazoline (**4.3a**) product was isolated. The isolated yield was calculated overall from the reaction of amidine (**4.1c**). To further explore the bases, the guanidine base 1,5,7-triazabicyclo[4.4.0]dec-5-ene (TBD) was tested, and the product formation increased to 13%.

Table 4.2. Optimization of new sulfur ylide reaction

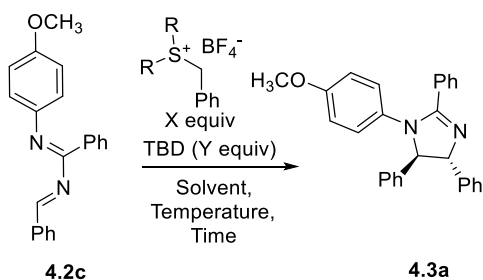


Base (Y equiv)	7a (X equiv)	Solvent	Temperature	Yield
<i>n</i> BuLi (1-2)	1-2 equiv	THF	-78 °C	N/A
LiHMDS (1)	1 equiv	THF	-78 °C to rt	N/A

Table 4.2. (cont'd)

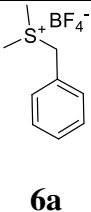
NaH (1)	1 equiv	Toluene	rt	N/A
DBU (2)	2 equiv	DCM	0 °C to rt	5%
TBD (2.5)	1.5 equiv	DCM	rt	13%

Further optimizations were performed by screening different equivalents of TBD base, sulfonium salts with the crude mixture of **4.2c**, in various solvents and temperatures (**Table 4.3**). The reaction provided the best yield at room temperature, whereas product formation dropped at low temperature, and no product formation was observed at the reflux condition in toluene. Changing the solvent from dichloromethane (DCM) to toluene also decreased product formation. Unfortunately, three equivalent of TBD base with the sulfonium salt **2a** (see chapter three) at room temperature in DCM offered the maximum overall yield of 14% from the reaction of amidine (**4.1c**).

Table 4.3. Optimization of imidazoline synthesis with TBD base

TBD equiv	Sulfur Ylide	Sulfur Ylide equiv	Solvent	Temperature	Yield
2.5		1.5	DCM	RT	13%
2.5		1.5	DCM	0 °C	8%
2.5		1.5	DCM	RT	11%
2.2		2	DCM	RT	8%

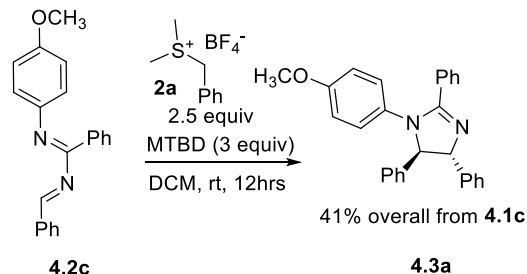
Table 4.3. (cont'd)

3	 6a	1.5	DCM	RT	14%
2.2		2	DCM	RT	8%
2.2		1	DCM	RT	5%
5		4	DCM	RT	4%
10		4	DCM	RT	4%
2.2		2	DCM	RT	N/A*
2.2		2	DCM	0 °C	N/A *
3		1.5	DCM	RT	N/A *
3		1.5	DCM	0 °C	N/A *
3		1.5	Toluene	RT	6%
5.5		5	Toluene	RT	5%
5.5		5	Toluene	reflux	N/A

* dropwise 1,3-diaza-1,3-butadiene

In the later stage of the optimization, the crude mixture of **4.2c** was treated with sulfonium salt (**2a**) in the presence of the MTBD base (found to be less hygroscopic, see chapter two) in DCM. The reaction afforded 41% overall yield (**Scheme 4.3**) of the imidazoline from the amidine **4.1c**. A similar reaction condition was employed with a crude mixture of *N*-benzylidene-*N'*-phenylbenzimidamide (**4.2b**), and the imidazoline **4.3b** was obtained in 25% overall yield from the amidine **4.1a**.

Scheme 4.3. Synthesis of imidazoline **4.3a** under the optimized condition



4.3 Conclusion

A new method to synthesize *trans*-imidazoline has been developed by reacting an *in situ* formed 1,3-diaza-1,3-butadiene with the sulfonium salt in the presence of base MTBD. The formed 1,3-diaza-1,3-butadiene was obtained by following the previous procedure from amidine. The overall yield of the imidazoline from amidine was low to moderate.

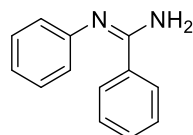
4.4 Experimental sections

The general method to synthesize amidines:

Under air, a pressure flask (75 mL in volume) equipped with a stirring bar was charged with *amine* (1.0 equiv, 20 mmol) followed by nitrile (1.0 equiv, 20 mmol). AlCl_3 (1.0 equiv, 20 mmol) was added in one portion while stirring the reaction. The flask was tightly sealed with a screw cap and placed into a preheated oil bath at 150 °C (Safety shield is recommended while running this reaction). The reaction mixture was stirred for 50 min and subsequently taken out of the oil bath. 20 mL of 1M ice-cold hydrochloric acid (HCl) solution was then added after 2 minutes to the mixture under vigorous stirring. Then, concentrated aqueous NaOH was added until a pH reached above 12. The aqueous layer was extracted with dichloromethane (3 X 50 mL). The combined organic layers were washed with water and then brine, and dried over Na_2SO_4 , filtered, and concentrated to 20 mL under reduced pressure. After that, 20 mL of hexane was added to the crude

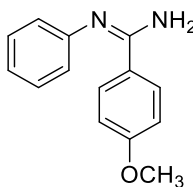
organic layer to precipitate out a solid product. The precipitate was washed with hexane, and the desired product was collected and confirmed by NMR.

N'-phenylbenzimidamide (**4.1a**):



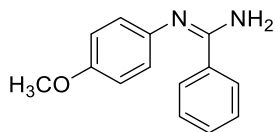
Whitish purple solid (43%), Melting Point: 116-118 °C. IR: 3465, 3058, 3013, 2968, 1632, 1597, 1335, 1230 cm^{-1} . ^1H NMR (500 MHz, $\text{DMSO-}d_6$) δ 7.96 (d, $J = 7.1$ Hz, 2H), 7.44 (dt, $J = 14.3$, 7.1 Hz, 3H), 7.31 (t, $J = 7.7$ Hz, 2H), 6.97 (t, $J = 7.7$ Hz, 1H), 6.86 (s, 2H), 6.25 (s, 2H). $^{13}\text{C}\{^1\text{H}\}$ NMR (126 MHz, $\text{DMSO-}d_6$) δ 154.1, 151.0, 136.3, 130.5, 129.6, 128.4, 127.5, 122.2, 122.0. HRMS (ESI-TOF) m/z : $[(\text{M}+\text{H})^+]$ calcd for ($\text{C}_{13}\text{H}_{13}\text{N}_2^+$) 197.1073; Found 197.1085.

4-methoxy-N'-phenylbenzimidamide (**4.1b**):



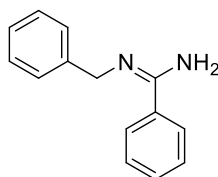
White colourless solid (35%), Melting Point: 139-141 °C. IR: 3460, 3295, 3035, 3010, 2954, 1621, 1608, 1495, 1235 cm^{-1} . ^1H NMR (500 MHz, $\text{DMSO-}d_6$) δ 7.93 (d, $J = 8.6$ Hz, 2H), 7.29 (t, $J = 7.8$ Hz, 2H), 6.96 (t, $J = 8.1$ Hz, 3H), 6.83 (d, $J = 7.8$ Hz, 2H), 6.12 (s, 2H), 3.79 (s, 3H). $^{13}\text{C}\{^1\text{H}\}$ NMR (126 MHz, $\text{DMSO-}d_6$) δ 161.2, 153.5, 151.3, 129.6, 129.0, 128.5, 122.2, 122.1, 113.6, 55.7. HRMS (ESI-TOF) m/z : $[(\text{M}+\text{H})^+]$ calcd for ($\text{C}_{14}\text{H}_{15}\text{N}_2\text{O}^+$) 227.1179; Found 227.1192.

N'-(4-methoxyphenyl)benzimidamide (**4.1c**):



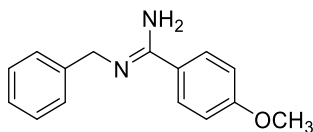
Whitish pink solid (2.94 gm, 65%), Melting point: 115-116 °C. IR: 3464, 3297, 3035, 3009, 2945, 2931, 1623, 1607, 1562, 1497, 1240, 1034 cm⁻¹. ¹H NMR (500 MHz, DMSO-*d*₆) δ 7.95 (d, *J* = 7.5 Hz, 2H), 7.48 – 7.36 (m, 3H), 6.89 (d, *J* = 8.7 Hz, 2H), 6.78 (d, *J* = 7.5 Hz, 2H), 6.19 (s, 2H), 3.72 (s, 3H). ¹³C{¹H} NMR (126 MHz, DMSO-*d*₆) δ 154.9, 154.4, 144.0, 136.5, 130.4, 128.4, 127.4, 122.8, 115.0, 55.5. HRMS (ESI-TOF) *m/z*: [(*M*+*H*)⁺] calcd for (C₁₄H₁₅N₂O⁺) 227.1179; Found 227.1180.

N'-benzylbenzimidamide (**4.1d**):



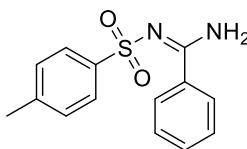
White solid (62%), Melting Point: 74-77 °C. IR: 3459, 3296, 3059, 2980, 1601, 1492, 1370, 1347 cm⁻¹. ¹H NMR (500 MHz, CHCl₃-*d*) δ 7.60 (d, *J* = 6.9 Hz, 2H), 7.50 – 7.34 (m, 7H), 7.33 – 7.27 (m, 1H), 5.55 (s, 2H), 4.56 (s, 2H). ¹³C NMR (126 MHz, CHCl₃-*d*) δ 138.9, 137.6, 130.2, 129.0, 128.7, 128.7, 127.8, 127.3, 126.1, 46.9. HRMS (ESI-TOF) *m/z*: [(*M*+*H*)⁺] calcd for (C₁₄H₁₅N₂⁺) 211.1230; Found 211.1235.

N'-benzyl-4-methoxybenzimidamide (**4.1e**):



White solid (47%), Melting Point: 89-91 °C. IR: 3196, 3161, 3060, 3018, 2954, 1604, 1503, 1350, 1250, 1174, 1031 cm^{-1} . ^1H NMR (500 MHz, $\text{DMSO}-d_6$) δ 9.33 (s, 2H), 7.79 (d, $J = 8.9$ Hz, 2H), 7.45 – 7.36 (m, 4H), 7.35 – 7.29 (m, 1H), 7.14 (d, $J = 8.9$ Hz, 2H), 4.67 (s, 2H), 3.84 (s, 3H). $^{13}\text{C}\{^1\text{H}\}$ NMR (126 MHz, $\text{DMSO}-d_6$) δ 163.8, 162.9, 136.1, 130.7, 129.1, 128.2, 128.0, 121.0, 114.8, 56.2, 45.9. HRMS (ESI-TOF) m/z : $[(\text{M}+\text{H})^+]$ calcd for $(\text{C}_{15}\text{H}_{17}\text{N}_2\text{O}^+)$ 241.1335; Found 241.1347.

N'-tosylbenzimidamide (**4.1f**):

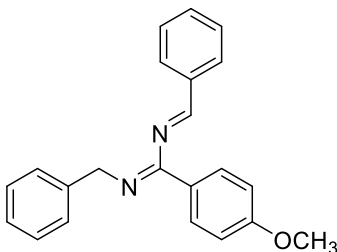


White solid (86%), Melting Point: 141-142 °C. IR: 3445, 3315, 3060, 2982, 1610, 1598, 1510, 1278, 1140, 1066 cm^{-1} . ^1H NMR (500 MHz, CHCl_3-d) δ 8.34 (s, 1H), 7.89 (d, $J = 8.0$ Hz, 2H), 7.78 (d, $J = 8.0$ Hz, 2H), 7.53 (t, $J = 7.6$ Hz, 1H), 7.42 (t, $J = 7.6$ Hz, 2H), 7.31 – 7.24 (d, $J = 8.0$ Hz, 2H), 6.34 (s, 1H), 2.41 (s, 3H). $^{13}\text{C}\{^1\text{H}\}$ NMR (126 MHz, CHCl_3-d) δ 162.6, 143.1, 139.2, 133.3, 132.8, 129.4, 128.8, 127.3, 126.5, 21.5. HRMS (ESI-TOF) m/z : $[(\text{M}+\text{H})^+]$ calcd for $(\text{C}_{14}\text{H}_{15}\text{N}_2\text{O}_2\text{S}^+)$ 275.0849; Found 275.0857.

The general method to synthesize 1,3-diaza-1,3-butadienes:

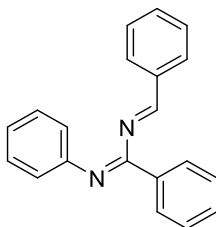
To a solution of dry toluene (30mL) in a 100 mL dry round bottom flask was added amidine (3.1) followed by benzaldehyde (1.1 equiv) and triethylamine (2.75 equiv). The solution was subsequently cooled to 0 °C under a nitrogen atmosphere. Then TiCl₄ (0.55 equiv) in dry toluene (1M solution in toluene) was slowly added dropwise for 90 min under a nitrogen atmosphere. After that, the mixture was stirred for additional 12 hours. The resulting white yellow suspension was rapidly filtered using an aspirator pressure through a Celite pad, and the clear liquid was stored in a sealed flask overnight at 4–6 °C. The cold, cloudy solution was re-filtered under reduced pressure over a well-pressed Celite pad and freed from solvent under reduced pressure without heating to give desired 1,3-diaza-1,3-butadiene (3.2) as a mixture compound, which is used in the next step without further purification.

N'-benzyl-N-benzylidene-4-methoxybenzimidamide (4.2a):



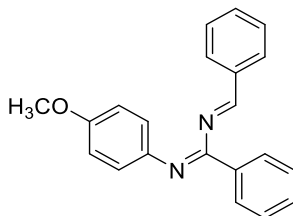
¹H NMR (500 MHz, DMSO-*d*₆) δ 8.43 (s, 1H), 7.96 (d, *J* = 7.3 Hz, 2H), 7.75 – 7.70 (m, 2H), 7.62 – 7.59 (m, 1H), 7.56 (t, *J* = 7.3 Hz, 2H), 7.36 (t, *J* = 5.0 Hz, 2H), 7.32 – 7.29 (m, 2H), 7.21 (t, *J* = 7.3 Hz, 1H), 6.99 – 6.95 (m, 2H), 4.46 (s, 2H), 3.77 (s, 3H). ¹³C{¹H} NMR (126 MHz, DMSO-*d*₆) δ 162.8, 162.2, 161.5, 141.6, 135.2, 134.7, 133.0, 129.5, 129.3, 129.2, 128.6, 128.0, 126.7, 114.2, 55.7, 52.5. HRMS (ESI-TOF) *m/z*: [(M+H+CH₃OH)⁺] calcd for (C₂₃H₂₅N₂O₂)⁺ 361.1911; Found 361.1911.

N-benzylidene-*N'*-phenylbenzimidamide (**4.2b**):



^1H NMR (500 MHz, $\text{DMSO}-d_6$) δ 8.43 (s, 1H), 7.88 (d, $J = 7.6$ Hz, 2H), 7.76 (d, $J = 7.6$ Hz, 2H), 7.51 (dt, 7H), 7.20 (t, $J = 8$ Hz, 2H), 6.89 (d, $J = 8.0$ Hz, 2H). $^{13}\text{C}\{^1\text{H}\}$ NMR (126 MHz, $\text{DMSO}-d_6$) δ 164.2, 162.3, 149.3, 135.1, 134.9, 133.0, 131.7, 130.0, 129.4, 129.2, 129.0, 128.2, 123.3, 122.3. HRMS (ESI-TOF) m/z : $[(\text{M}+\text{H})^+]$ calcd for $(\text{C}_{20}\text{H}_{17}\text{N}_2^+)$ 285.1386; Found 285.1388.

N-benzylidene-*N'*-(4-methoxyphenyl)benzimidamide (**4.2c**):

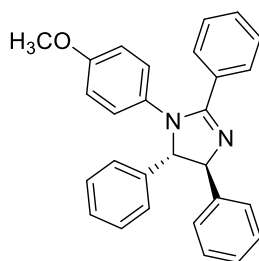


^1H NMR (500 MHz, CHCl_3-d) δ 8.19 (s, 1H), 7.97 – 7.94 (m, 2H), 7.79 – 7.76 (m, 2H), 7.26 – 7.24 (m, 2H), 7.19 – 7.17 (m, 4H), 7.03 – 6.99 (d, $J = 9$ Hz, 2H), 6.79 – 6.77 (d, $J = 9$ Hz, 2H), 3.74 (s, 3H). $^{13}\text{C}\{^1\text{H}\}$ NMR (126 MHz, CHCl_3-d) δ 162.7, 162.2, 158.4, 137.9, 132.3, 130.7, 129.0, 128.9, 128.7, 128.3, 128.1, 125.3, 124.2, 113.8, 55.3. HRMS (ESI-TOF) m/z : $[(\text{M}+\text{H})^+]$ calcd for $(\text{C}_{21}\text{H}_{19}\text{N}_2\text{O}^+)$ 315.1492; Found 315.1499.

Synthesis of Imidazolines:

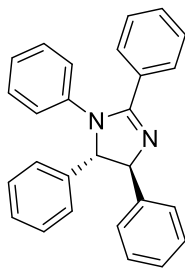
To a solution of dry dichloromethane (20 mL) in a 50 mL dry round bottom flask was added benzyldimethyl sulfonium tetrafluoroborate (2.5 equivalents) followed by MTBD (3 equivalents) and subsequently, crude 1,3-diaza-1,3-butadiene (**4.2b** or, **4.2c**) (1 equivalent). The reaction was stirred for 12 hours at room temperature. After that, the solvent was evaporated, and the crude product was purified using automated CombiFlash chromatography (silica gel 20-40 microns, using 25% ethyl acetate in hexane) to yield imidazoline (**4.3a-b**).

*1-(4-methoxyphenyl)-2,4,5-triphenyl-4,5-dihydro-1H-imidazole (**4.3a**):*



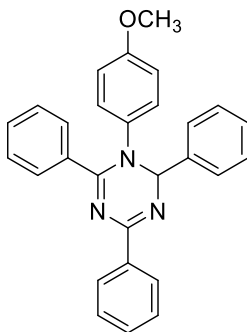
As an oil in 41% (42 mg) yield overall from amidine (**4.1c**). IR: 3053, 3027, 2922, 2837, 1611, 1570, 1504, 1149, 1424, 1374, 1330, 1285, 1245, 1173, 1125, 1074. ^1H NMR (500 MHz, CHCl_3 -*d*) δ 7.73 (d, $J = 7.4$ Hz, 2H), 7.45 – 7.26 (m, 13H), 6.70 (d, $J = 8.9$ Hz, 2H), 6.60 (d, $J = 8.9$ Hz, 2H), 5.12 (d, $J = 7.2$ Hz, 1H), 4.65 (d, $J = 7.2$ Hz, 1H), 3.67 (s, 3H). $^{13}\text{C}\{^1\text{H}\}$ NMR (126 MHz, CHCl_3 -*d*) δ 163.6, 156.9, 143.7, 143.4, 136.6, 131.0, 130.1, 129.2, 129.0, 128.7, 128.1, 127.8, 127.3, 126.9, 126.6, 126.1, 114.1, 79.3, 78.4, 55.3. HRMS (ESI-TOF) m/z : $[\text{M}+\text{H}]^+$ calcd for ($\text{C}_{28}\text{H}_{25}\text{N}_2\text{O}^+$) 405.1961; Found 405.1967.

1,2,4,5-tetraphenyl-4,5-dihydro-1H-imidazole (4.3b):



As an oil in 25% yield overall from amidine (3.1a). IR: 3030, 3006, 2961, 2836, 1611, 1601, 1570, 1508, 1449, 1382, 1262, 1245 cm^{-1} . ^1H NMR (500 MHz, CHCl_3 -*d*) δ 7.82 – 7.77 (m, 2H), 7.46 – 7.34 (m, 12H), 7.30 (tt, J = 6.1, 1.7 Hz, 1H), 7.11 – 7.05 (m, 2H), 7.01 – 6.96 (m, 1H), 6.76 (dt, J = 8.9, 1.7 Hz, 2H), 5.14 (d, J = 6.0 Hz, 1H), 4.80 (d, J = 6.0 Hz, 1H). $^{13}\text{C}\{^1\text{H}\}$ NMR (126 MHz, CHCl_3 -*d*) δ 163.0, 143.7, 143.5, 143.4, 131.0, 130.4, 129.2, 128.8, 128.3, 127.8, 127.5, 126.9, 126.6, 126.5, 125.5, 124.4, 123.7, 78.6, 78.2. HRMS (ESI-TOF) m/z : $[\text{M}+\text{H}]^+$ calcd for ($\text{C}_{27}\text{H}_{23}\text{N}_2^+$) 375.1856; Found 375.1858.

1-(4-methoxyphenyl)-2,4,6-triphenyl-1,2-dihydro-1,3,5-triazine (4.4):



Yellow oil. IR: 3056, 3027, 2960, 2925, 1611, 1575, 1504, 1445, 1365, 1341, 1288, 1236, 1170, 1097, 1026 cm^{-1} . ^1H NMR (500 MHz, CHCl_3 -*d*) δ 8.41 – 8.36 (m, 2H), 7.79 – 7.75 (m, 2H), 7.73 – 7.69 (m, 2H), 7.46 – 7.30 (m, 9H), 6.94 – 6.89 (d, J = 9.0 Hz, 2H), 6.71 – 6.67 (d, J = 9.0 Hz, 2H), 6.34 (s, 1H), 3.73 (s, 3H). $^{13}\text{C}\{^1\text{H}\}$ NMR (126 MHz, CHCl_3 -*d*) δ 160.8, 158.4, 157.7, 142.0,

137.2, 136.7, 135.0, 131.0, 130.4, 130.2, 129.0, 128.5, 128.3, 128.1, 128.1, 126.5, 126.2, 114.2, 79.1, 55.4. HRMS (ESI-TOF) m/z: $[M+H]^+$ calcd for $(C_{28}H_{24}N_3O^+)$ 418.1914; Found 418.1920.

APPENDIX

APPENDIX

Figure 4.1. ^1H and ^{13}C NMR Spectra of Compound 4.1a

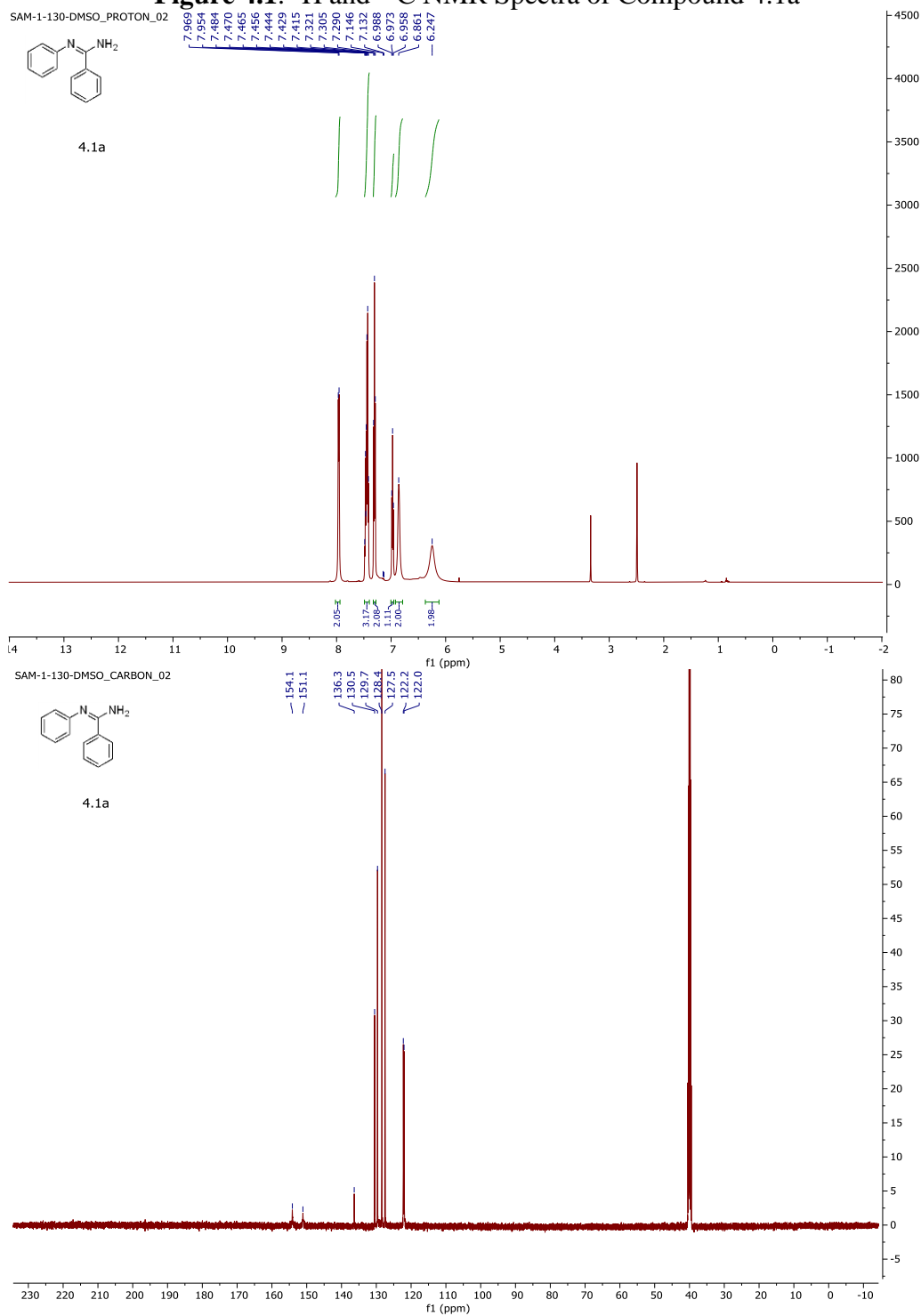


Figure 4.2. ^1H and ^{13}C NMR Spectra of Compound 4.1b

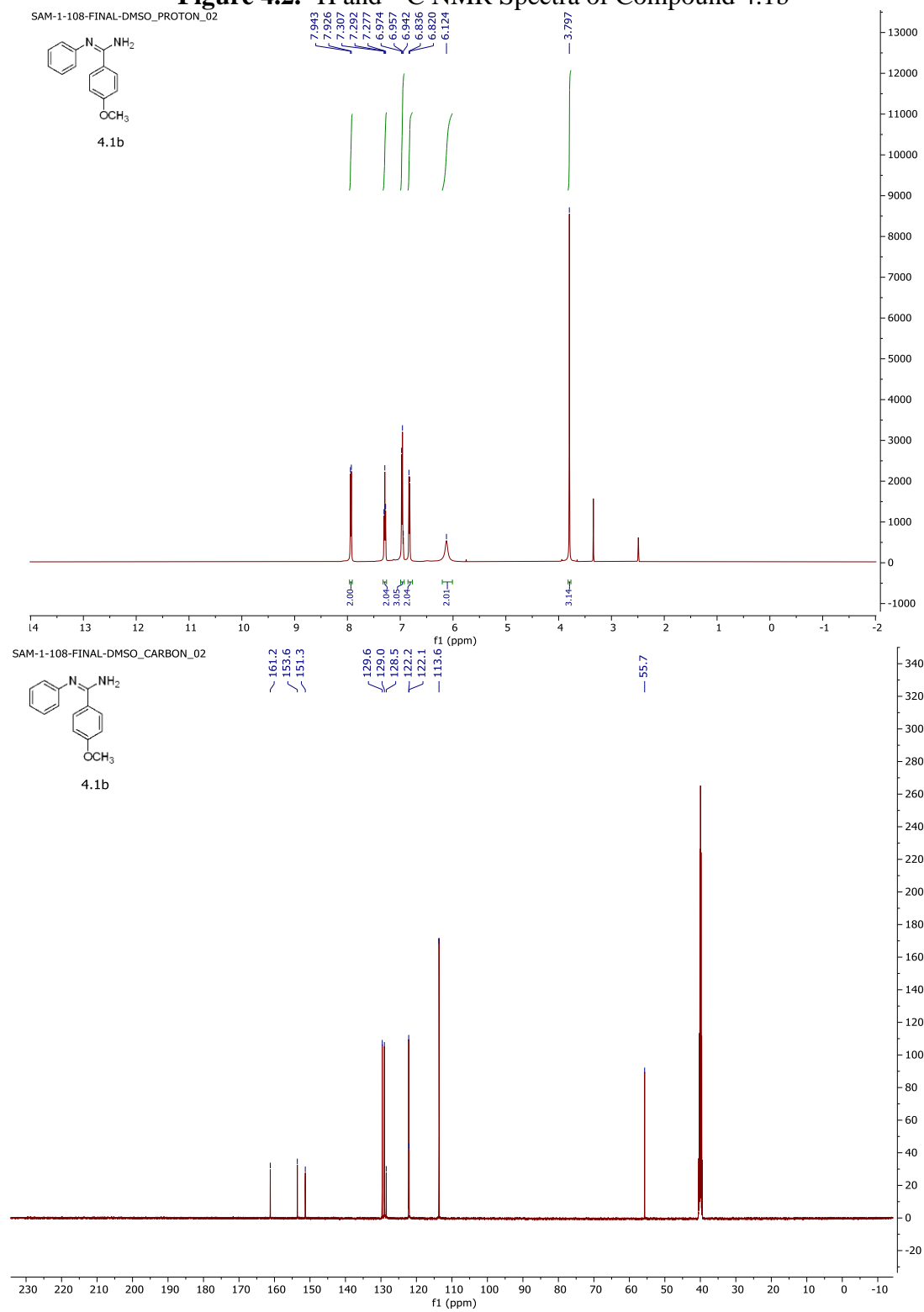


Figure 4.3. ^1H and ^{13}C NMR Spectra of Compound 4.1c

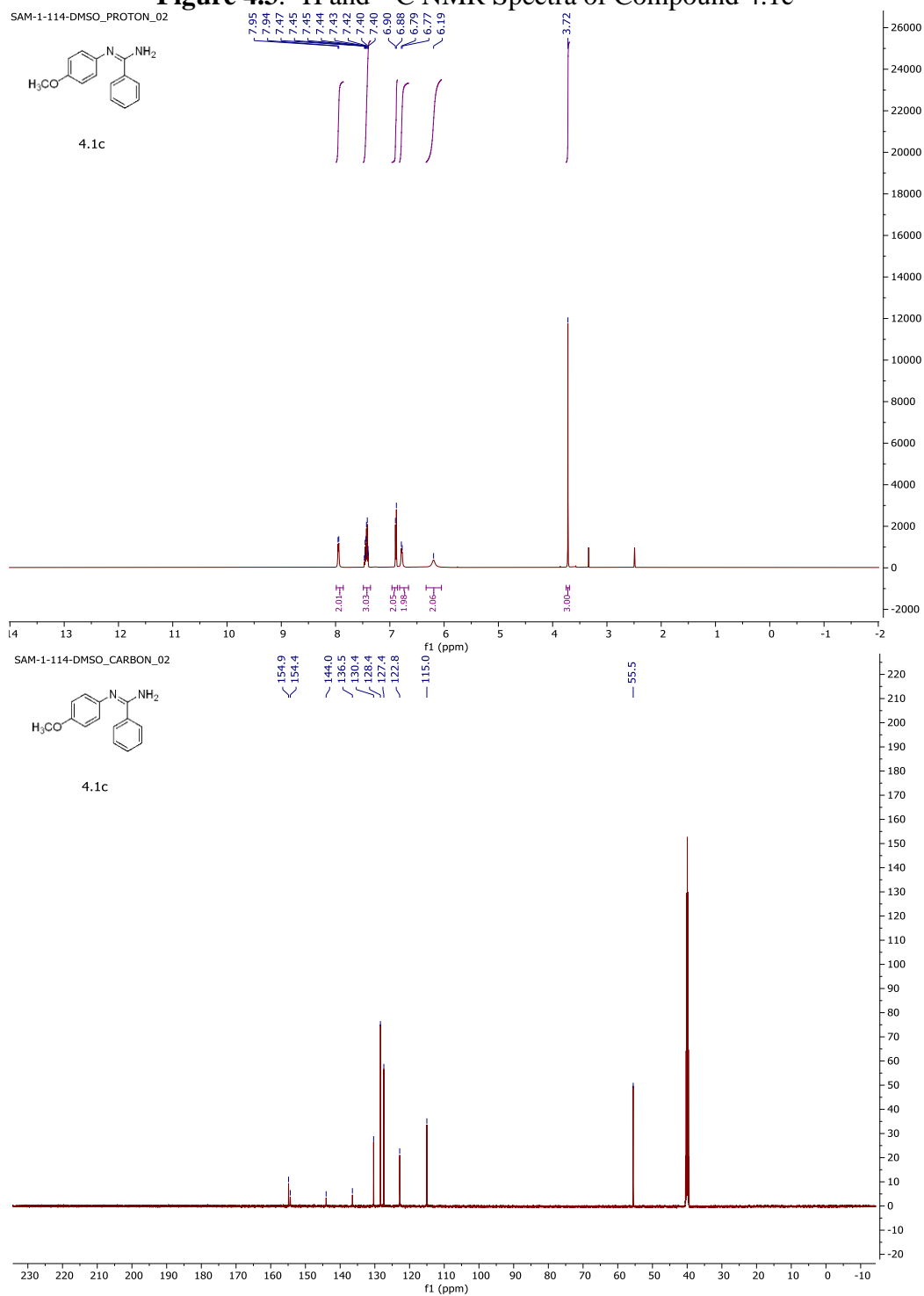


Figure 4.4. ^1H and ^{13}C NMR Spectra of Compound 4.1d

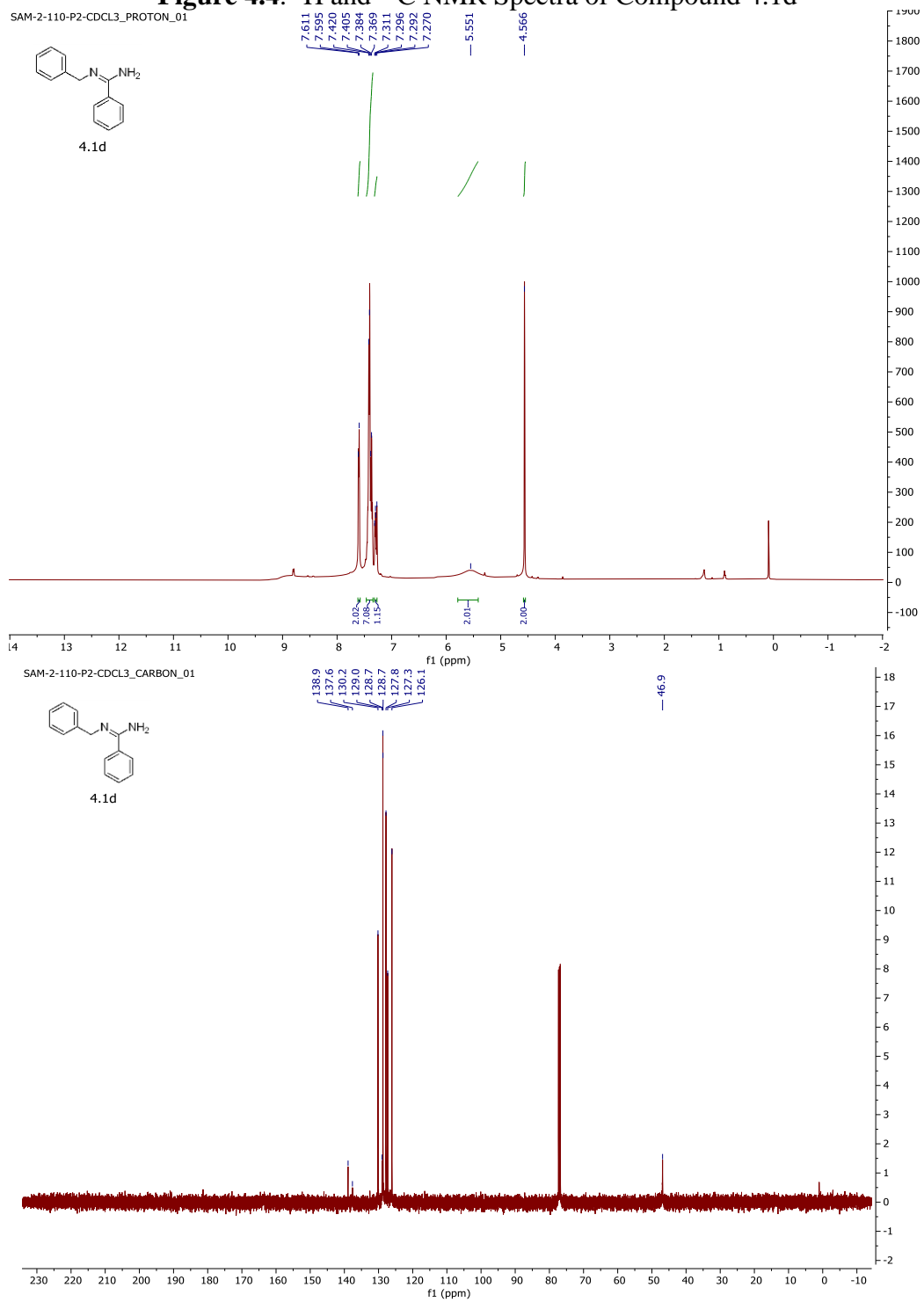


Figure 4.5. ^1H and ^{13}C NMR Spectra of Compound 4.1e

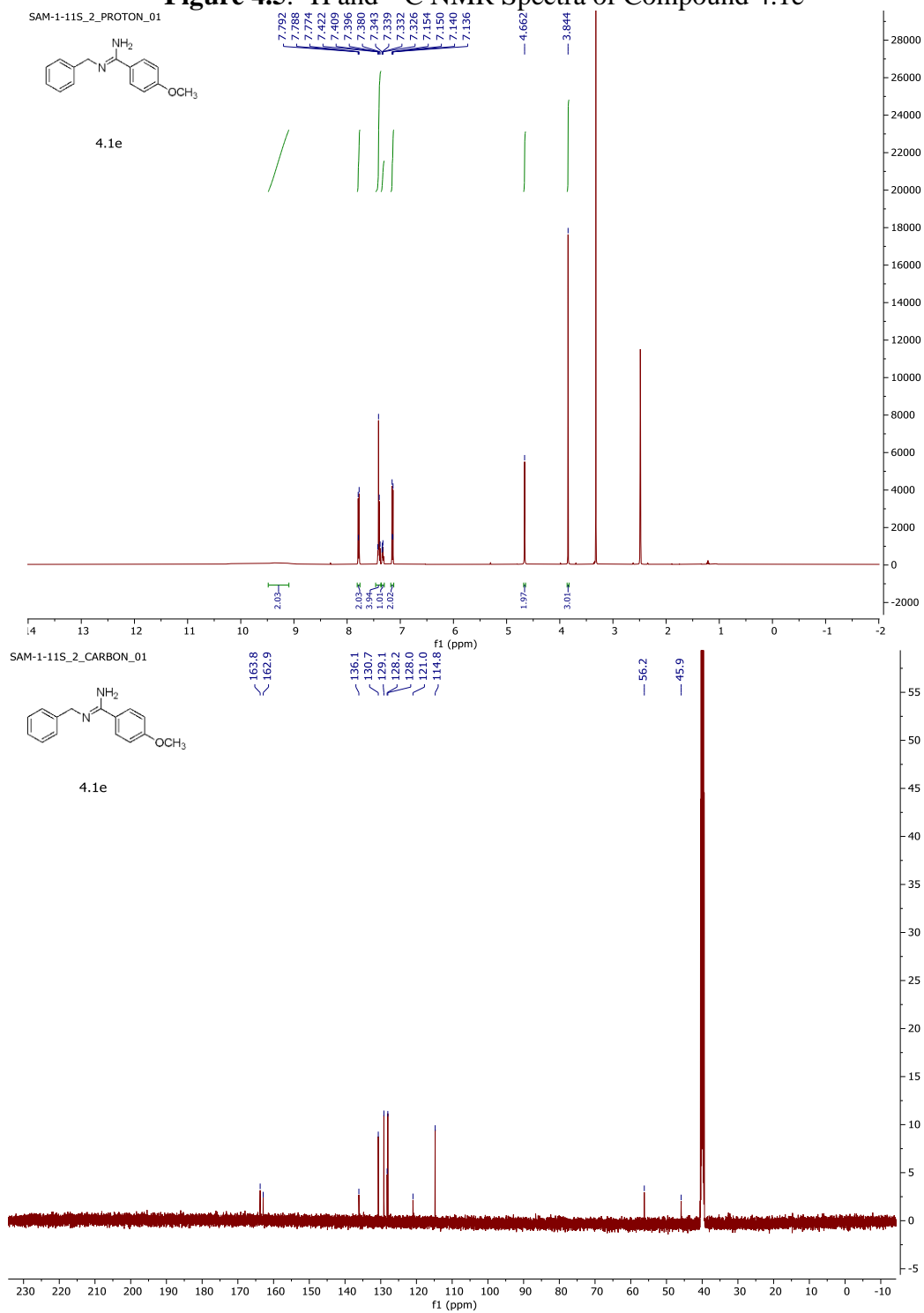


Figure 4.6. ^1H and ^{13}C NMR Spectra of Compound 4.1f

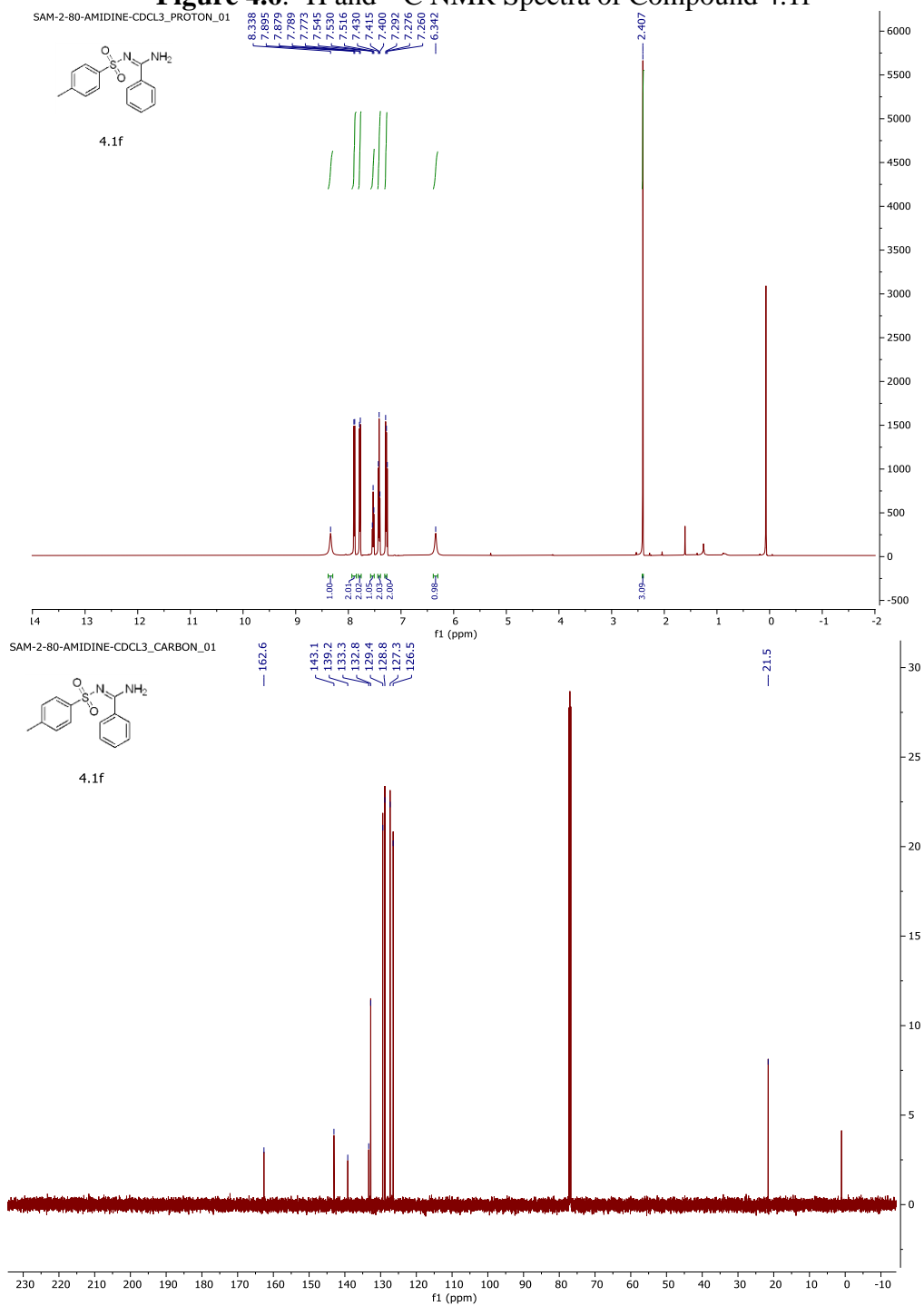


Figure 4.7. ^1H and ^{13}C NMR Spectra of Compound 4.2a

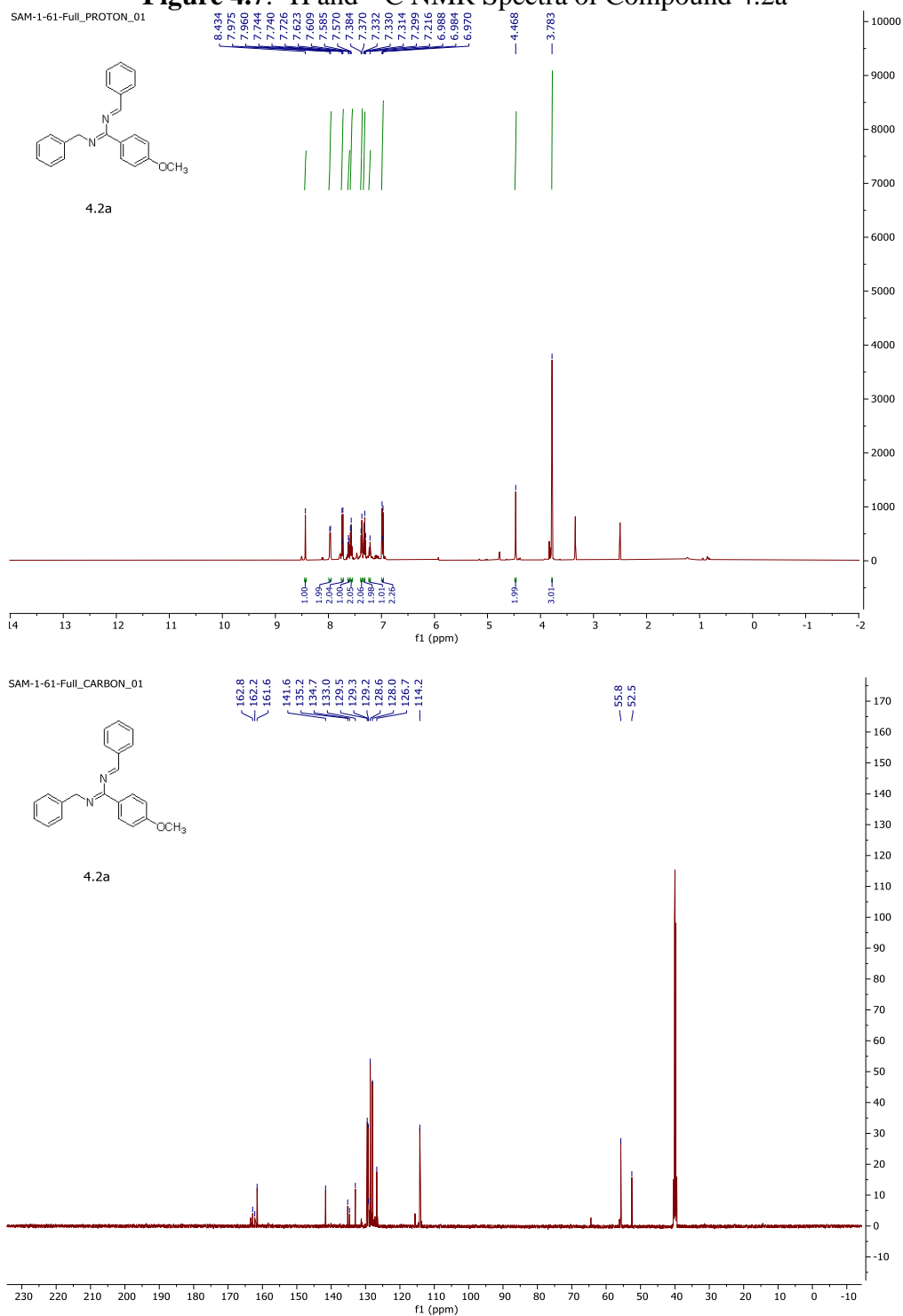


Figure 4.8. ^1H and ^{13}C NMR Spectra of Compound 4.2b

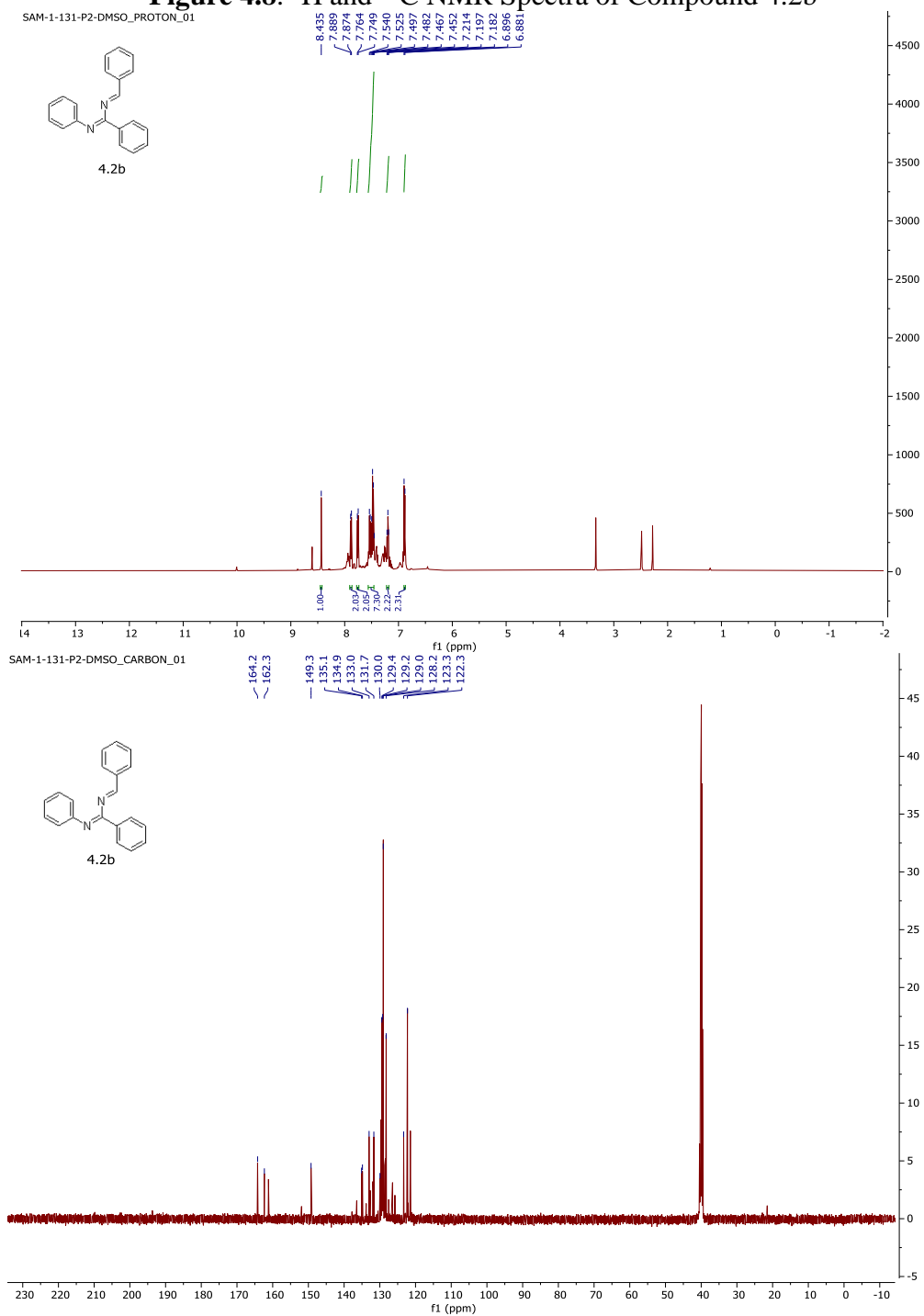


Figure 4.9. ^1H and ^{13}C NMR Spectra of Compound 4.2c

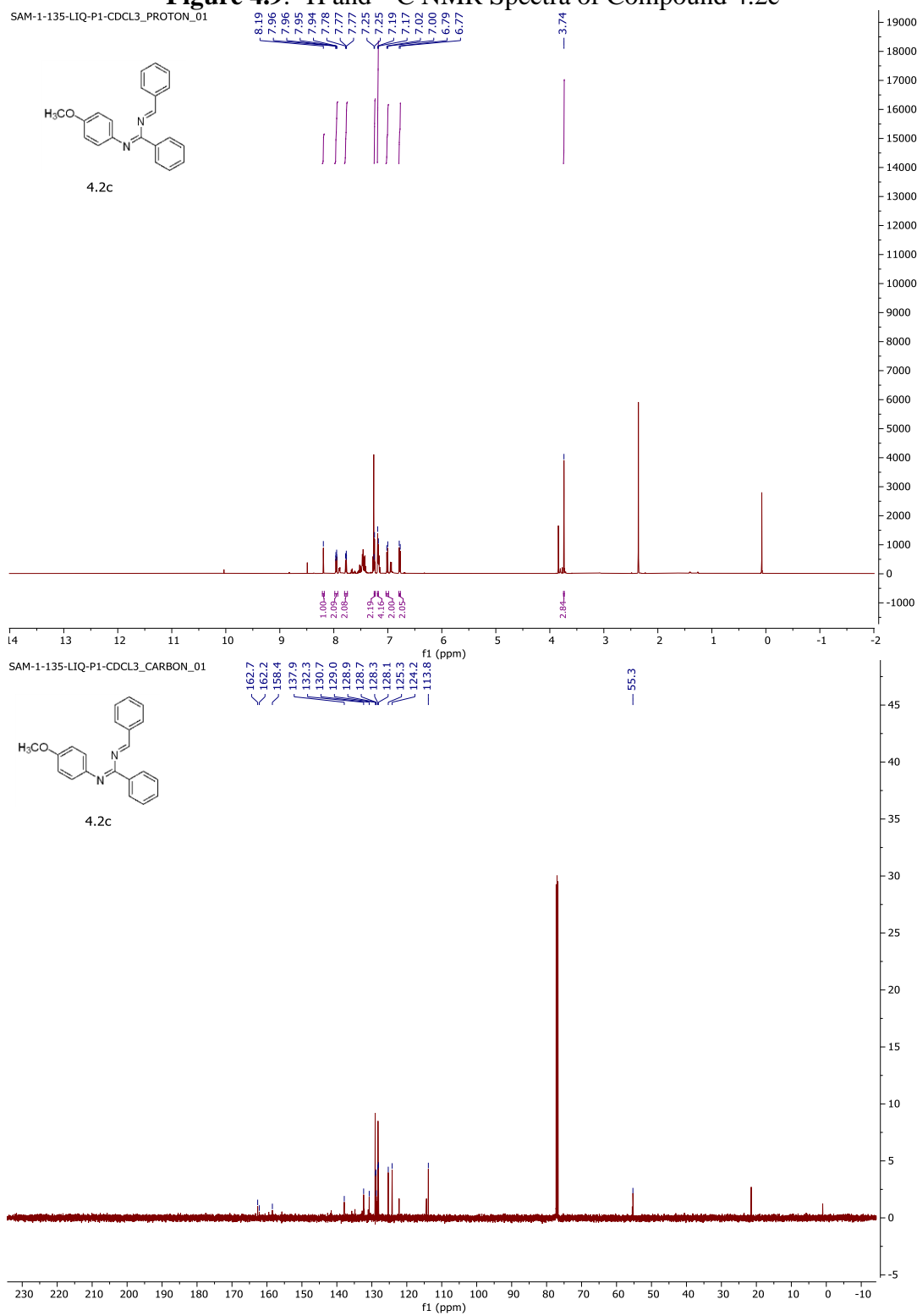


Figure 4.10. ^1H and ^{13}C NMR Spectra of Compound 4.3a

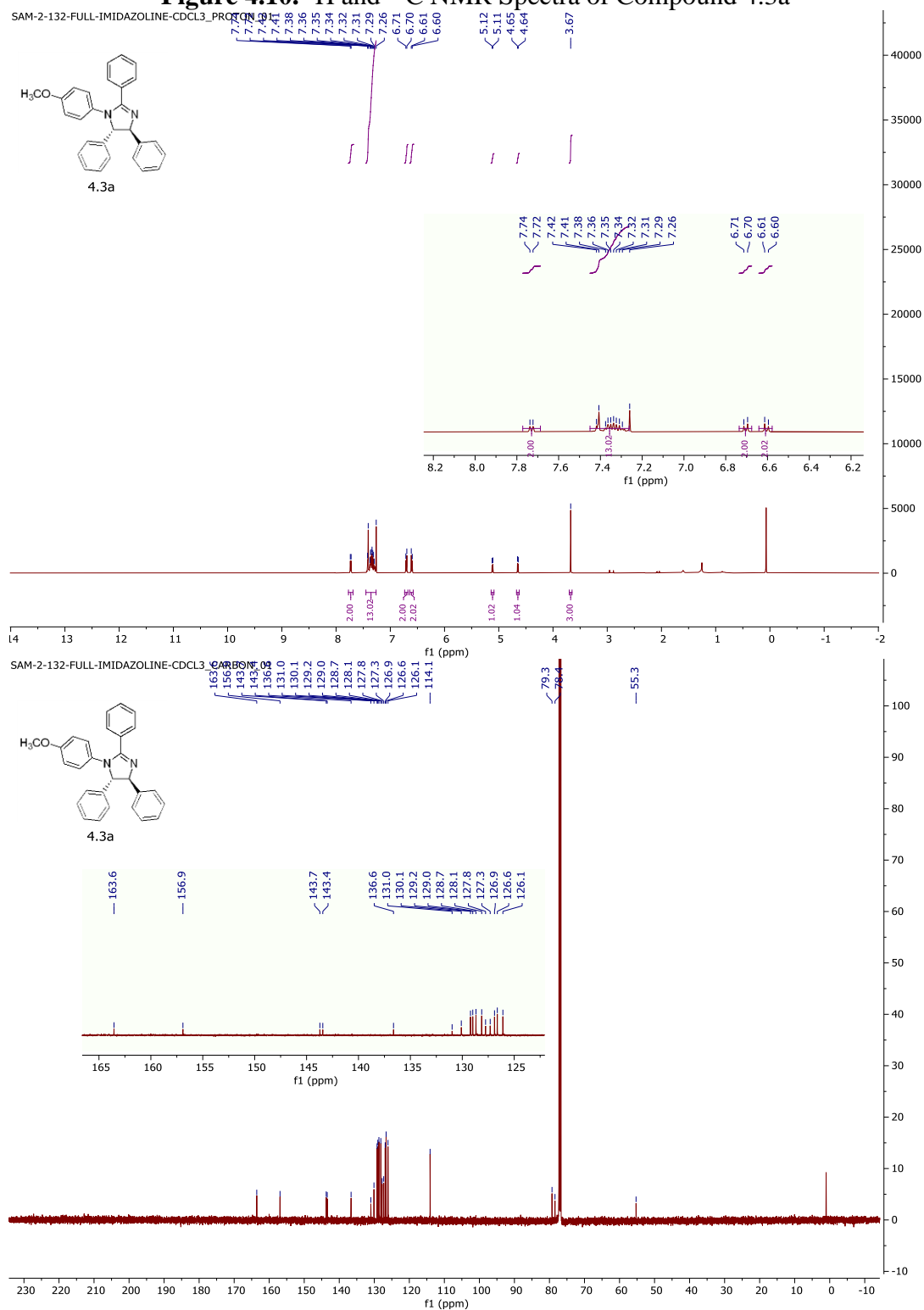


Figure 4.11. ^1H and ^{13}C NMR Spectra of Compound 4.3b

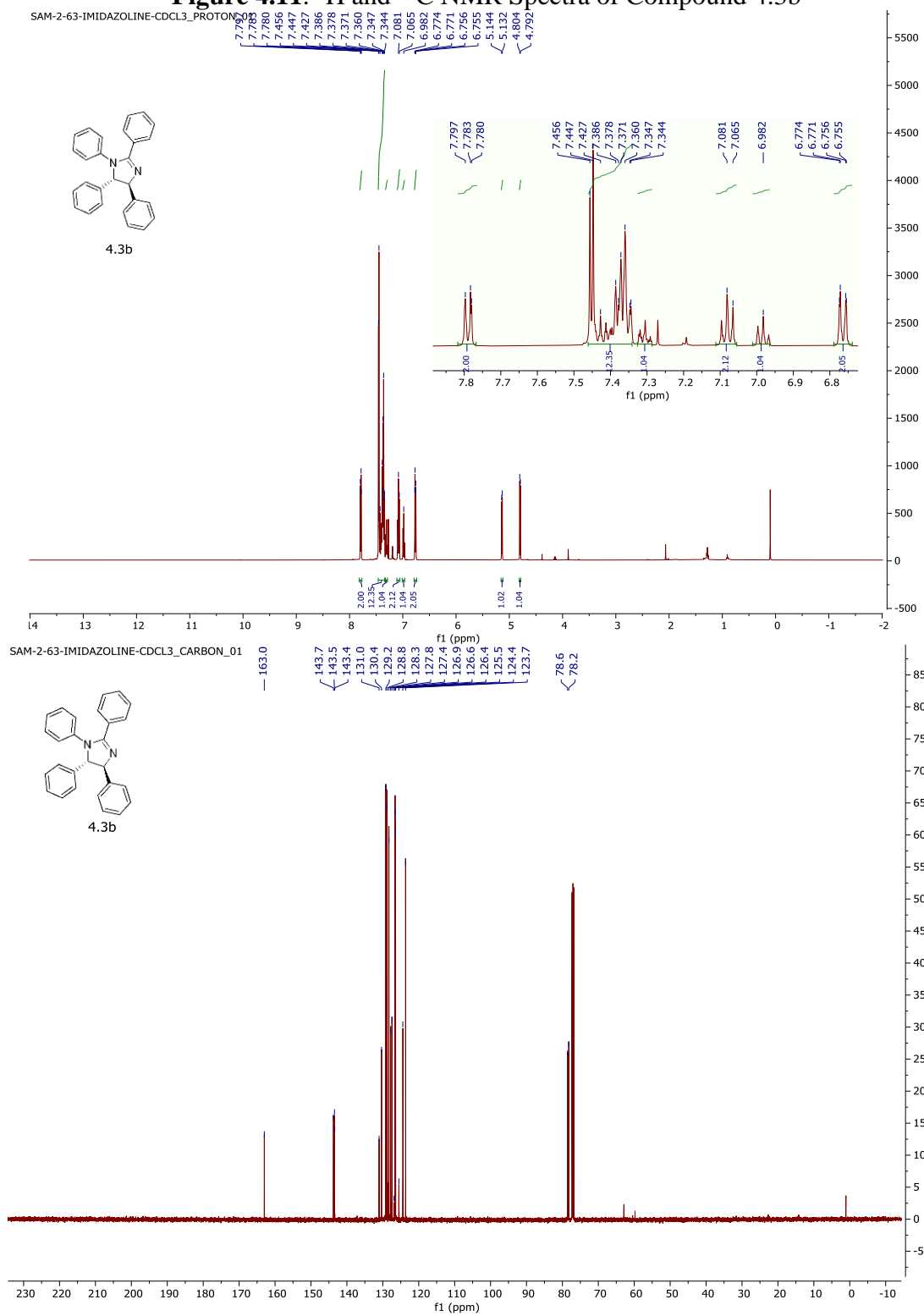
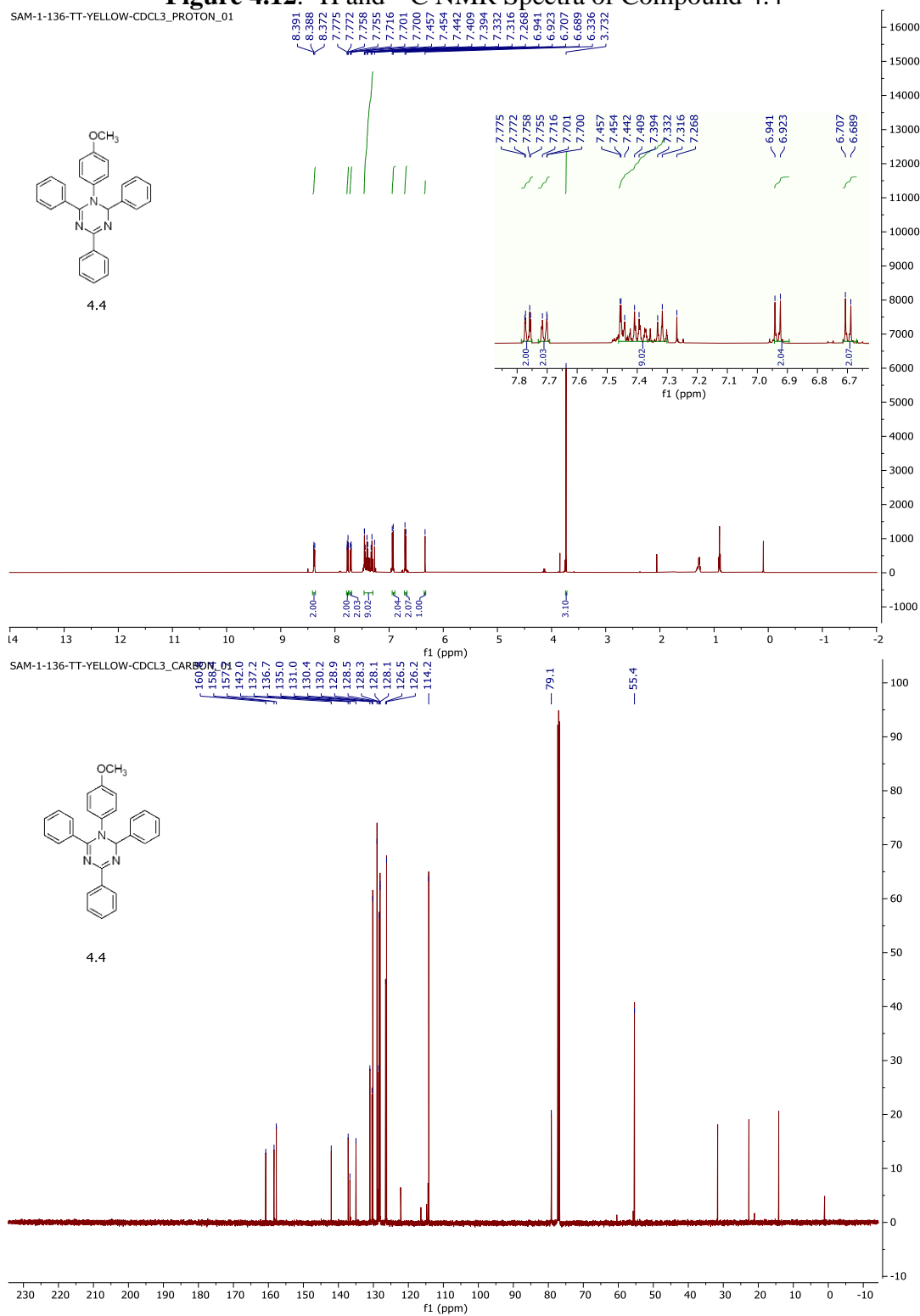


Figure 4.12. ^1H and ^{13}C NMR Spectra of Compound 4.4



REFERENCES

REFERENCES

- [1] Debnath, P.; Majumdar, K. C. *Tetrahedron Lett.* **2014**, *55*, 6976.
- [2] (a) Veer, S. D.; Katkar, K. V.; Akamanchi, K. G. *Tetrahedron Lett.* **2016**, *57*, 4039; (b) Abbiati, G.; Contini, A.; Nava, D.; Rossi, E. *Tetrahedron* **2009**, *65*, 4664.
- [3] (a) Meng, X.; Bi, X.; Wang, Y.; Chen, G.; Chen, B.; Jing, Z.; Zhao, P. *Catal. Commun.* **2017**, *89*, 34. (b) Rossi, E.; Abbiati, G.; Nava, D. *Heterocycles* **1999**, *51*, 1401.

Chapter 5: Synthesis of 2,3-disubstituted quinolines via reaction of anilines with epoxides in the presence of Lewis acids

5.1 Introduction

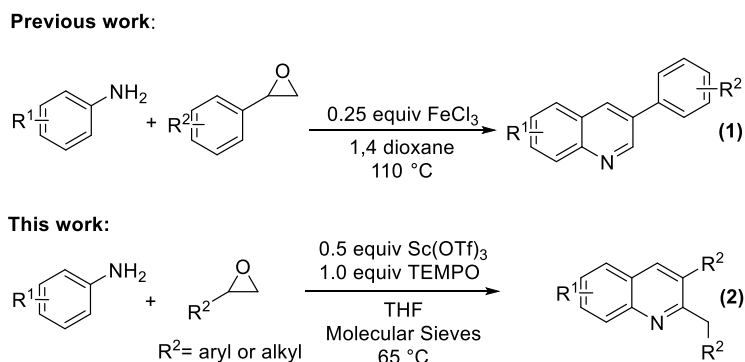
Quinoline is one of the most important scaffolds due to its widespread presence in biologically active synthetic and natural products.¹ Compounds possessing quinoline moieties play a substantial role in a wide range of therapeutic areas² including anti-malarial,³ anti-microbial,⁴ CNS,⁵ anti-inflammatory,⁶ anti-cancer agents⁷, and possibly in recent SARS-CoV-2 treatment.⁸ Various Substituted quinolines have also been employed as building blocks and catalysts.⁹ Moreover, they have been in various sectors, including agrochemicals,¹⁰ as anti-foaming agents in refineries,¹¹ and as ligands in sensors manufacturing industries.¹²

Different classical approaches to synthesize quinoline scaffolds, including the Friedlander reaction, Doebner-von Miller reaction, Skraup reaction, Conrad-Limpach-Knorr reaction, Pfitzinger reaction, Povarov reaction, and the Combes reaction, which have been well documented in the literature.¹³ However, these existing methods possess one or more limitations, including the need for high temperatures, limited availability of substrates, low yields, harsh reaction conditions, poor regioselectivity, and tedious multistep procedures that require isolation of the intermediates. In recent years, several modifications have been made to address some of these limitations.¹⁴ However, the synthesis of 2,3-disubstituted quinolines using readily available starting materials such as aldehydes, ketones, alkenes, alkynes, cyclobutanes or allyl alcohols is still limited to a few reports.¹⁵ This chapter discusses the utilization of readily available epoxides as a new approach to access 2,3-disubstituted quinolines.

In a preceding report, Zhang *et al.* investigated the synthesis of 3-substituted quinolines by the addition of epoxides and anilines in the presence of FeCl₃ (eq 1, **Scheme 5.1**).¹⁶ In their report,

the authors suggested a radical-mediated C-C bond cleavage, resulting in de-alkylation and isolation of solely the C-3 substituted quinolines. Motivated by their proposed reaction mechanism, here, a one-pot quinoline synthesis is described from the reaction epoxides and anilines, in the presence of $\text{Sc}(\text{OTf})_3$ and (2,2,6,6-tetramethylpiperidin-1-yl)oxyl (TEMPO), to synthesize the 2,3-disubstituted quinolines in up to 96% yields (eq 2, **Scheme 5.1**).

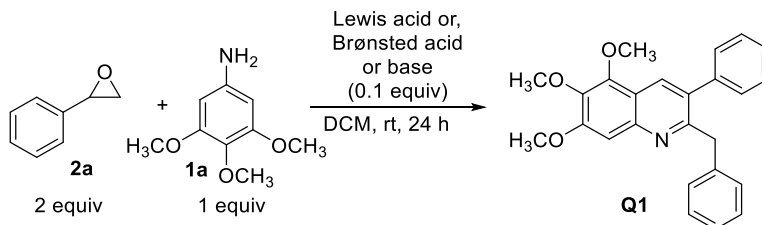
Scheme 5.1. Synthesis of quinolines from epoxides and aromatic amines



5.2 Results and discussion

We initiated our studies by treating one equivalent of 3,4,5-trimethoxyaniline (**1a**) with two equivalents of styrene oxide (**2a**), in the presence of 0.1 equivalent of various Lewis acids in DCM at room temperature (**Table 5.1**). Lewis acids included: AlCl_3 , AgOTf , AuCl , AuCl_3 , $\text{HAuCl}_4 \cdot 3\text{H}_2\text{O}$, $\text{BF}_3 \cdot \text{OEt}_2$, $\text{Sc}(\text{OTf})_3$, and others (**Table 5.1**). Among the Lewis acids screened, $\text{HAuCl}_4 \cdot 3\text{H}_2\text{O}$, AuCl_3 , and $\text{Sc}(\text{OTf})_3$ afforded better yields of our desired 2,3-substituted quinoline **Q1**. We screened a few Brønsted acids, including H_3PO_4 , trifluoroacetic acid (TFA), and triflic acid (TfOH), and the latter showed better conversion to the 2,3-disubstituted quinoline (**Table 5.1**). It needs to be noted that no product formation was observed in the absence of an acid, under basic (2,6-lutidine or Et_3N) nor neutral condition (**Table 5.1**). These studies exhibited that an acidic condition is required to proceed with the reaction. From this step, we chose our best acids (AuCl_3 , $\text{HAuCl}_4 \cdot 3\text{H}_2\text{O}$, $\text{Sc}(\text{OTf})_3$, and TfOH) to optimize the reaction conditions further.

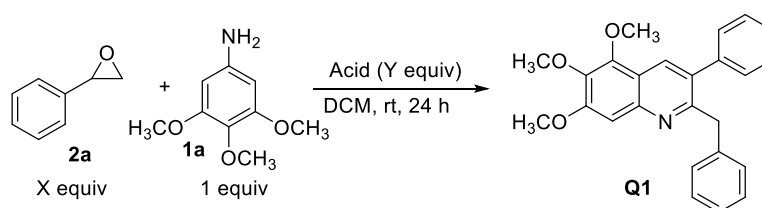
Table 5.1. Optimization of quinoline synthesis with different acids/bases



Lewis Acid	Yield of Q ₁ %	Lewis Acid	Yield of Q ₁ %
AlCl ₃	N/A	BF ₃ .OEt ₂	15
BI ₃	N/A	TMSCl	N/A
CuCl	N/A	Yb(OTf) ₃	N/A
CuCl ₂	N/A	Ho(OTf) ₃	13
Cu(OTf) ₂	15	Y(OTf) ₃	23
AgSbF ₆	10	HAuCl₄.3H₂O	39
AgOTf	N/A	Sn(OTf) ₂	10
AuCl₃	30	Eu(OTf) ₃	10
FeCl ₃	10	Sm(OTf) ₃	14
Zn(OTf) ₂	N/A	Er(OTf) ₃	12
TMSOTf	14	Dy(OTf) ₃	26
Sc(OTf)₃	37	AuBr ₃	10
Brønsted Acid	Yield of Q ₁ %	Base	Yield of Q ₁ %
H ₃ PO ₄	8	TEA	N/A
TFA	23	2,6-lutidine	N/A
TfOH	36	No acid/base	N/A

The reaction was further optimized by altering the equivalents of epoxide, amine, and acids (**Table 5.2**), indicating an increase of epoxide (to 3 equivalents) and higher catalyst loading offer higher product formation. A further rise in the epoxide resulted in lower product formation, most likely due to epoxides' unwanted interactions. Here on, two sets of conditions were selected for the optimization studies: (a) three equivalents of epoxide with 0.5 equivalents of Sc(OTf)₃, and (b) four equivalents of epoxide with one equivalent of TfOH.

Table 5.2. Optimization of quinoline synthesis (acid)



X equiv of epoxide	Acid	Y equiv of acid	Yield of Q1 %
3	AuCl ₃	0.1	19
3	HAuCl ₄ .3H ₂ O	0.1	24
3	Sc(OTf) ₃	0.1	36
3	Sc(OTf)₃	0.5	43
3	TfOH	1	26
4	AuCl ₃	0.5	20
4	HAuCl ₄ .3H ₂ O	0.5	23
4	Sc(OTf) ₃	0.5	40
4	TfOH	0.5	21
4	HAuCl ₄ .3H ₂ O	1	16
4	Sc(OTf) ₃	1	40

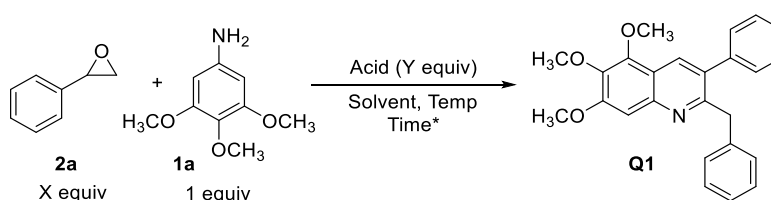
Table 5.2. (cont'd)

4	TfOH	1	42
4	TfOH	1.5	35
4	Sc(OTf) ₃	0.3	27
5	Sc(OTf) ₃	0.5	30
5	TfOH	1	29
8	AuCl ₃	0.5	16
8	HAuCl ₄ .3H ₂ O	0.5	25
8	Sc(OTf) ₃	0.5	32
8	TfOH	1.5	37
8	TfOH	2	38
8	AuCl ₃	1	8
8	HAuCl ₄ .3H ₂ O	1	19
8	Sc(OTf) ₃	1	26
8	TfOH	3	37

After optimizing the Lewis acids, various solvents and temperature effects were studied to observe product formation. Of the solvents screened (acetonitrile, tetrahydrofuran (THF), chloroform, toluene, acetone, and water), THF offered the best yield, possibly via a scandium-THF complex (**Table 5.3**). In THF, two extra equivalents of epoxide were added, and the quinoline yield was increased to 81%. In the investigation of temperature effects, there was a direct correlation observed between temperature and product yield. The high temperature provided more product, whereas at -78 °C, no product formation was observed (**Table 5.1**). Some additional

solvents, including dichloroethane (DCE), 1,4-dioxane, dimethylsulfoxide (DMSO), and 2-methyl THF, were screened to further explore higher temperatures. Interestingly, at 80 °C in 2-methyl THF, a lower amount of product was isolated. Additionally, further temperature increases induced de-alkylation of C-2, forming the 3-substituted quinolines. The reaction pathway (**Scheme 5.3**) likely involved an intermediate imine, which led to adding molecular sieves (4Å); thus, the product yield increased to 85%.

Table 5.3. Optimization of quinoline synthesis (solvent and temperature)



X Equiv epoxide	Solvent	Acid	Y Equiv Acid	Temp °C	Yield of Q1 %
3	DCM	Sc(OTf) ₃	0.5	rt	43
3	MeCN	Sc(OTf) ₃	0.5	rt	36
3	THF	Sc(OTf) ₃	0.5	rt	44
3	CHCl ₃	Sc(OTf) ₃	0.5	rt	41
3	Toluene	Sc(OTf) ₃	0.5	rt	36
3	Acetone	Sc(OTf) ₃	0.5	rt	25
3	Water	Sc(OTf) ₃	0.5	rt	N/A
3	THF	Sc(OTf) ₃	0.5	65	48
3	THF	Sc(OTf) ₃	0.5	0	26
3	THF	Sc(OTf) ₃	0.5	-40	10

Table 5.3. (cont'd)

3	THF	Sc(OTf) ₃	0.5	-78	N/A
2 ^c	THF	Sc(OTf) ₃	0.5	65	42
2+0.5 ^{a,c}	THF	Sc(OTf) ₃	0.5	65	56
3+2 ^a	THF	Sc(OTf) ₃	0.5	65	81
3+2 ^{a,b}	THF	Sc(OTf) ₃	0.5	65	59
3 ^c	THF	Sc(OTf) ₃	0.5	65	51
3+2 ^{a,c}	THF	Sc(OTf) ₃	0.5	65	85
3+2^{a,c,d}	THF	Sc(OTf)₃	0.5	65	91
3+2 ^{a,c,e}	THF	Sc(OTf) ₃	0.5	65	56
3+1 ^{a,c}	THF	Sc(OTf) ₃	0.5	65	75
4	THF	Sc(OTf) ₃	0.5	65	77
5	THF	Sc(OTf) ₃	0.5	65	69
3+2 ^a	2-methyl THF	Sc(OTf) ₃	0.5	80	65
3	DCE	Sc(OTf) ₃	0.5	reflux	24
3+2 ^a	DCE	Sc(OTf) ₃	0.5	reflux	39
3	1,4-dioxane	Sc(OTf) ₃	0.5	reflux	35
3+2 ^a	1,4-dioxane	Sc(OTf) ₃	0.5	reflux	51
3	DMSO	Sc(OTf) ₃	0.5	140	33

Table 5.3. (cont'd)

3+2 ^a	DMSO	Sc(OTf) ₃	0.5	140	45
4	DCM	TfOH	1	rt	42
4	MeCN	TfOH	1	rt	26
4	THF	TfOH	0.5	rt	40
4	THF	TfOH	1	rt	42
4	THF	TfOH	2	rt	36
4	THF	TfOH	1	65	42
4	THF	TfOH	0.5	65	69
4+2 ^a	THF	TfOH	1	65	64
4+2 ^a	THF	TfOH	0.5	65	68

rt=room temperature. *all reactions above rt ran for 18 h, otherwise 24 h. ^aadditional equiv of epoxide was after 6 h. ^b0.1ml H₂O was added at the beginning. ^c4Å molecular sieve was added. ^d1 equiv TEMPO was added. ^e5 equiv TEMPO was added.

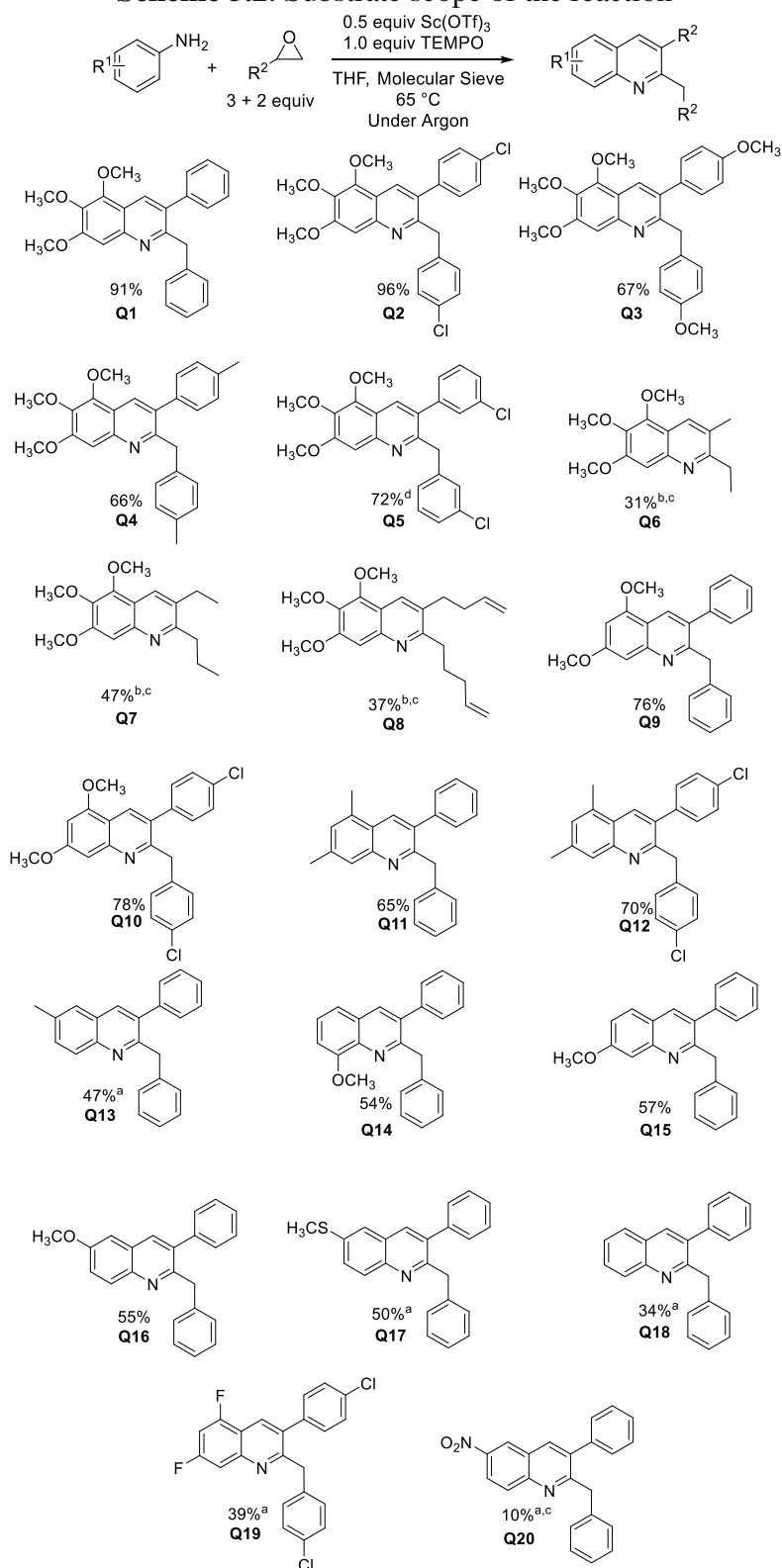
Previous reports indicate that Fe or Cu initiate a radical-mediated dealkylation of the C-2 position.^{14(a),16} Although Sc(OTf)₃ is not anticipated to evoke radical formation, to prevent unwanted C-2 de-alkylation, the radical scavenger TEMPO was added to our previously optimized conditions, which further increased yield to 91% (**Scheme 5.2, Q1**). This result suggested that one equivalent of the radical scavenger's addition prevents unwanted oxidation by trapping any radical formed in the reaction vessel. Additional equivalents of TEMPO did not improve product formation. The optimized conditions (3+2 equivalents of epoxide, 0.5 equivalents of Sc(OTf)₃, and

1.0 equivalent of TEMPO in THF at 65 °C) were used to explore the substrate scope of this reaction using different epoxides and anilines.

Initially, 3,4,5-trimethoxy aniline (**1a**) was added with various substituted styrene oxides (**2**). As shown in **Scheme 5.2**, both electron-donating and electron-withdrawing groups were well tolerated, and the corresponding quinolines were obtained in 66-96% yields (**Q2-Q5**). Epoxides with an electron-withdrawing group (4-chlorostyrene oxide) afforded the best yield of 96% (**Q2**), likely due to the reduction of oxidative C-2 de-alkylation.¹⁷ A few aliphatic epoxides named as Propylene oxide, butylene oxide, and 1,2-epoxy-5-hexene moderately reacted with **1a** to provide the highly substituted quinolines (**Q6-Q8**) in 31-47% yield.

Next, several aromatic amines (**1**) bearing different substituents, including electron-withdrawing and electron-donating groups, were treated with styrene oxide (**2a**) or 4-chlorostyrene oxide. It was discovered that the reduction of the electron density in the aromatic amine directly impacted product yields. Removal of one methoxide from 3,4,5-trimethoxy aniline (**1a**) to 3,5-dimethoxyaniline dropped the yield to 76% and 78% of quinoline **Q9** and **Q10**, respectively. A similar trend was observed with alkyl-substituted aromatic amines, which provided quinolines **Q11-Q13** in 47-70% yields. Anilines with one methoxy group on their ortho-, meta-, or para-position provided quinolines **Q14-Q16**, in a similar yield of 54-57%. It should be noted that only one regioisomer (**Q15**) was isolated when *m*-methoxy aniline was used as starting aniline. As anticipated from the previous results, treating aniline with **2a** gave 34% of the quinoline product (**Q18**). Only 10% product (**Q20**) was isolated when we used the most electron deficient group (-NO₂) at the para position of the aromatic amine. Moreover, a gram scale reaction was conducted with styrene oxide (**2a**) and 3,4,5-trimethoxy aniline (**1a**), and the quinoline product **Q1** was obtained with a 78% yield.

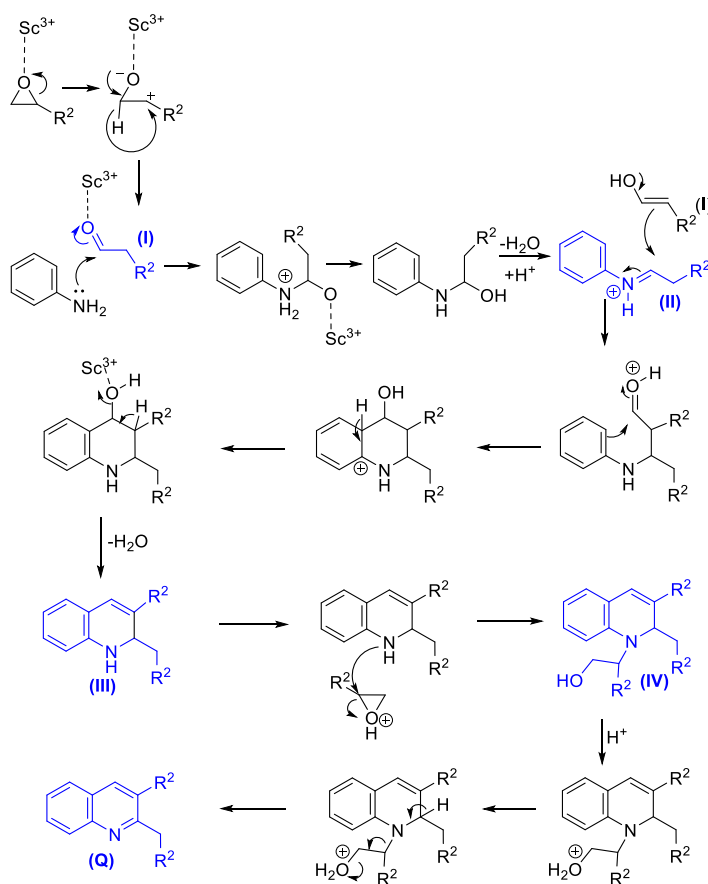
Scheme 5.2. Substrate scope of the reaction



^aAdditional 1 equivalent of epoxide was added at 12 h, and the reaction ran for 24 h. ^bReaction ran with a total of 3 equivalents of epoxide. ^cReaction ran without TEMPO. ^dTemperature at 60 °C.

Based on the observed results and mechanistic experiments (**5.3**), a plausible mechanism is proposed in **Scheme 5.3**. The reaction initiates by the rapid *in situ* generations of aldehyde **I** (observed by NMR within 5 minutes, see *Mechanistic Experiment-3*) by Sc^{3+} to generate the iminium **II** (observed in MS, **Figure 5.1**). A second equivalent of the enol tautomer of aldehyde **I** reacts with the iminium **II**, which then undergoes cyclization with aryl group to form the 1,2-dehydroquinoline **III** (observed in MS, **Figure 5.1**). Oxidation of the dihydroquinoline can be envisioned, following the addition of another epoxide to **III**, to form the intermediate **IV** (observed in MS, **Figure 5.2** and **Figure 5.3**), to yield the desired quinoline **Q**.

Scheme 5.3. Proposed mechanism of the reaction



5.3 Mechanistic experiments

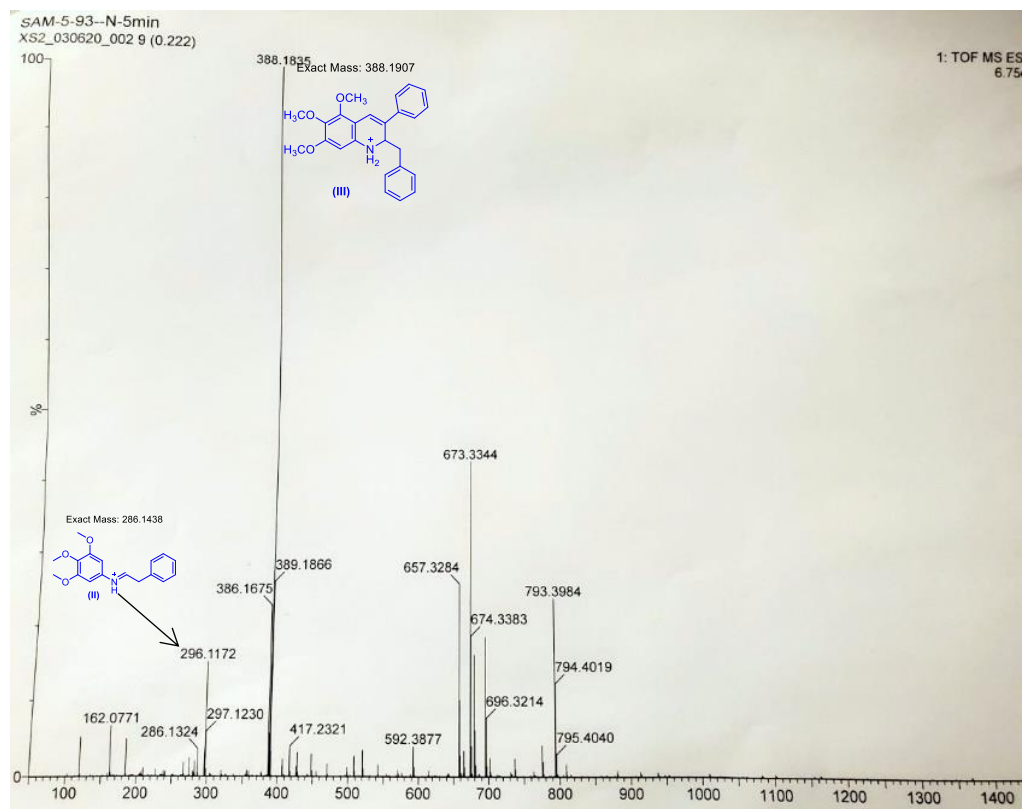
Experiment-1:

To a solution of dry tetrahydrofuran (THF) (10 mL) in a 50 mL dry round bottom flask, phenyl acetaldehyde (3 equiv, 0.75 mmol) were added, followed by $\text{Sc}(\text{OTf})_3$ (0.5 equiv, 0.125 mmol) at room temperature. Then 3,4,5-trimethoxy aniline (1 equiv, 0.25 mmol) was added at room temperature. The reaction was placed under argon gas and was stirred for 6 hours at 65 °C in an oil bath. Then, another 2 equiv of the same aldehyde was added dropwise, and the reaction was allowed to stir for additional 12 hours. After that, the reaction mixture was cooled to room temperature, and the solvent was evaporated under reduced pressure. Then 10mL of dichloromethane and 10ml saturated NaHCO_3 solution were added, and the solution was extracted with 3×10mL of dichloromethane. The combined organic layers were collected and evaporated under reduced pressure, and the crude products were purified using automated CombiFlash chromatography (silica gel, 20-40 microns, gradient 7.5% ethyl acetate in hexane). Yield: 43mg (45%).

Experiment-2:

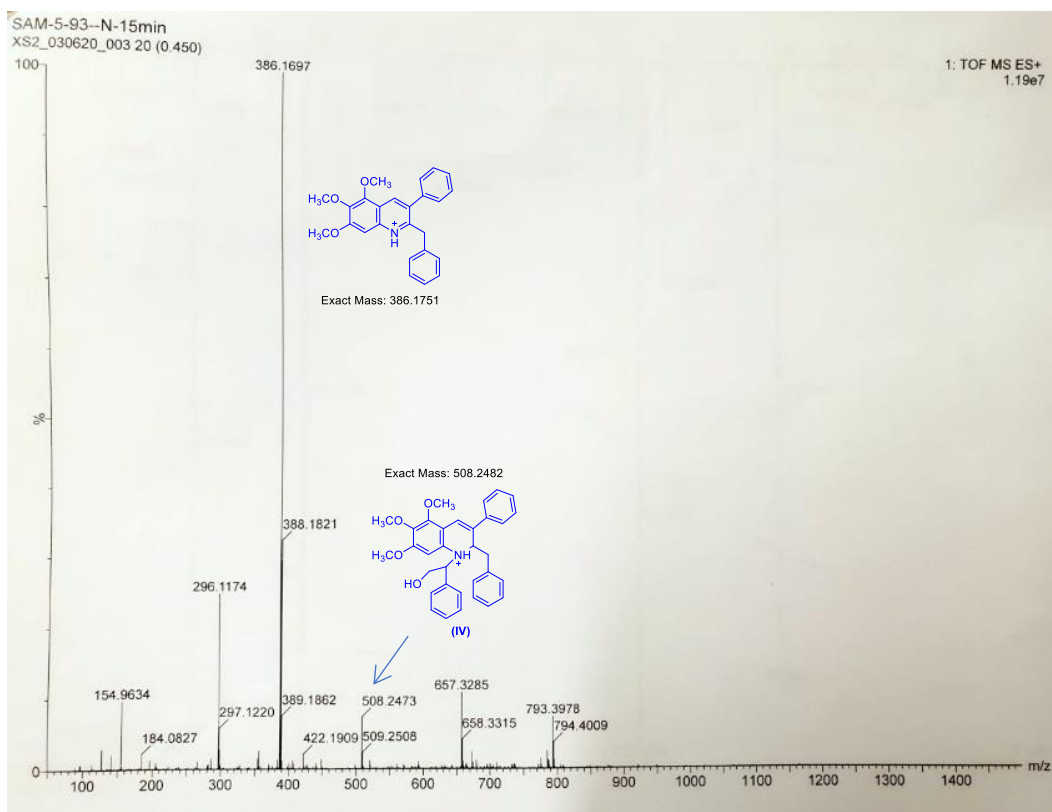
To a solution of dry tetrahydrofuran (2.5 mL) in a 20 mL vial, styrene oxide (5 equiv, 0.5 mmol) was added, followed by $\text{Sc}(\text{OTf})_3$ (0.5 equiv, 0.05 mmol) at room temperature. Then 3,4,5-trimethoxy aniline (1 equiv, 0.1 mmol) was added at room temperature. The reaction was stirred at room temperature, and the crude mass was checked after 5 minutes, 15 minutes, and 30 minutes time intervals using a mass spectrometer by ESI (+) method with a Quadrupole detector. After 5 minutes (**Figure 5.1**), mass spec indicated major peaks corresponding to the masses of the protonated structures II, III (see also **Scheme 5.3**).

Figure 5.1. Crude mass spectrum five minutes into the reaction



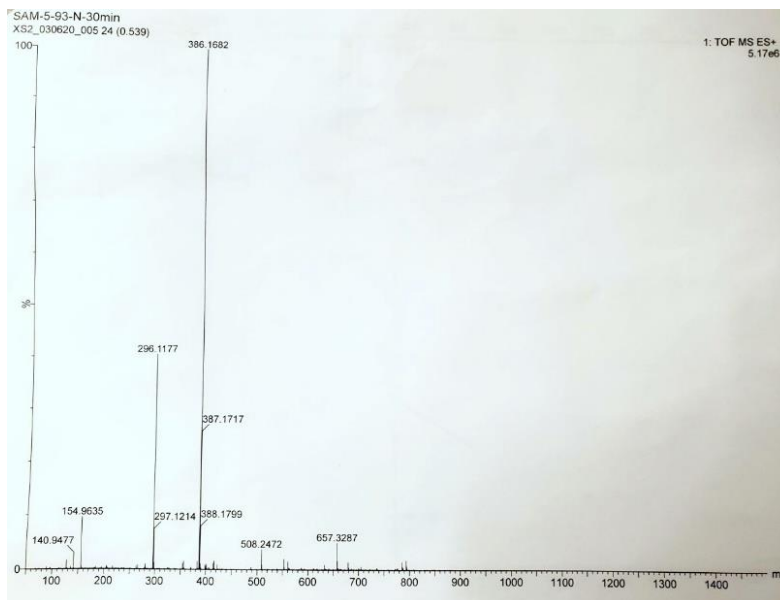
After 15 minutes (**Figure 5.2**), mass spec indicated major peaks corresponding to the masses of the protonated quinoline **Q1** and **IV** (see also **Scheme 5.3**).

Figure 5.2. Crude mass spectrum fifteen minutes into the reaction



In 30 minutes (**Figure 5.3**), the relative ratio between protonated quinoline **Q** and intermediate **IV** increased, indicating possible conversion of intermediate **IV** to quinoline.

Figure 5.3. Crude mass spectrum thirty minutes into the reaction



Experiment-3:

To a solution of dry tetrahydrofuran (2.5 mL) in a 10 mL dry round bottom flask, styrene oxide (6 equiv, 0.6 mmol) was added, followed by $\text{Sc}(\text{OTf})_3$ (1 equiv, 0.1 mmol) at room temperature and stirred for 60 minutes at 65 °C in an oil bath. Within 5 minutes, the formation of phenylacetaldehyde was observed, and within 1 hour, the phenylacetaldehyde peak was detected as a major peak in the crude NMR (see below ^{13}C NMR spectrum in CD_2Cl_2).

Figure 5.4. ^{13}C Spectrum: Reaction of styrene oxide with $\text{Sc}(\text{OTf})_3$ at 1 hour

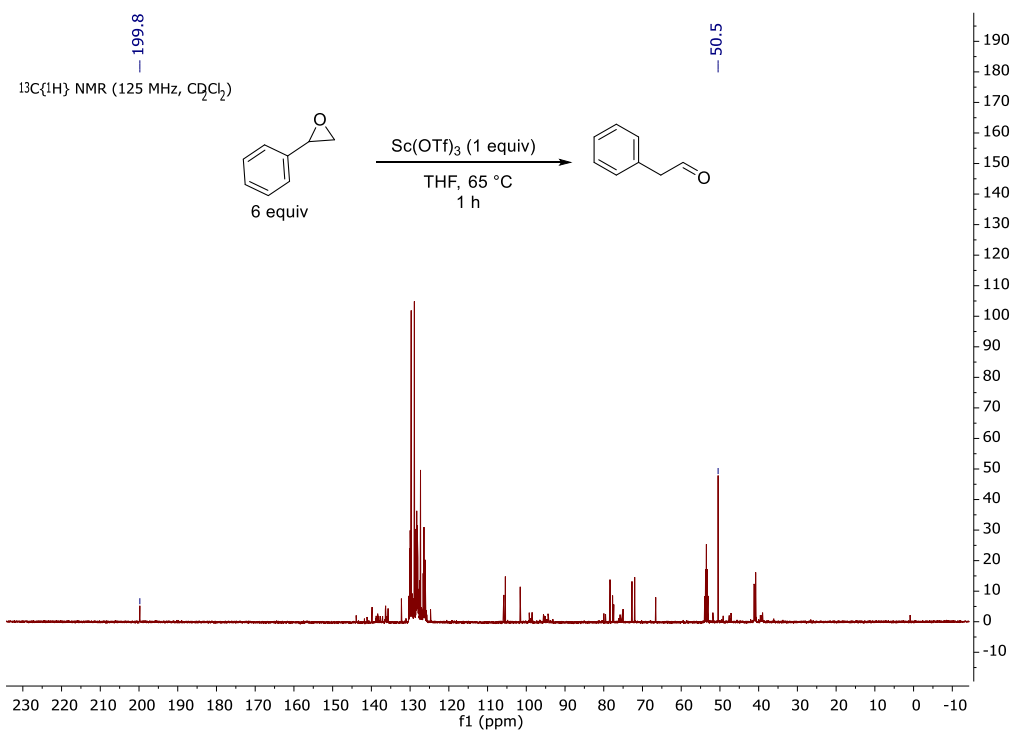
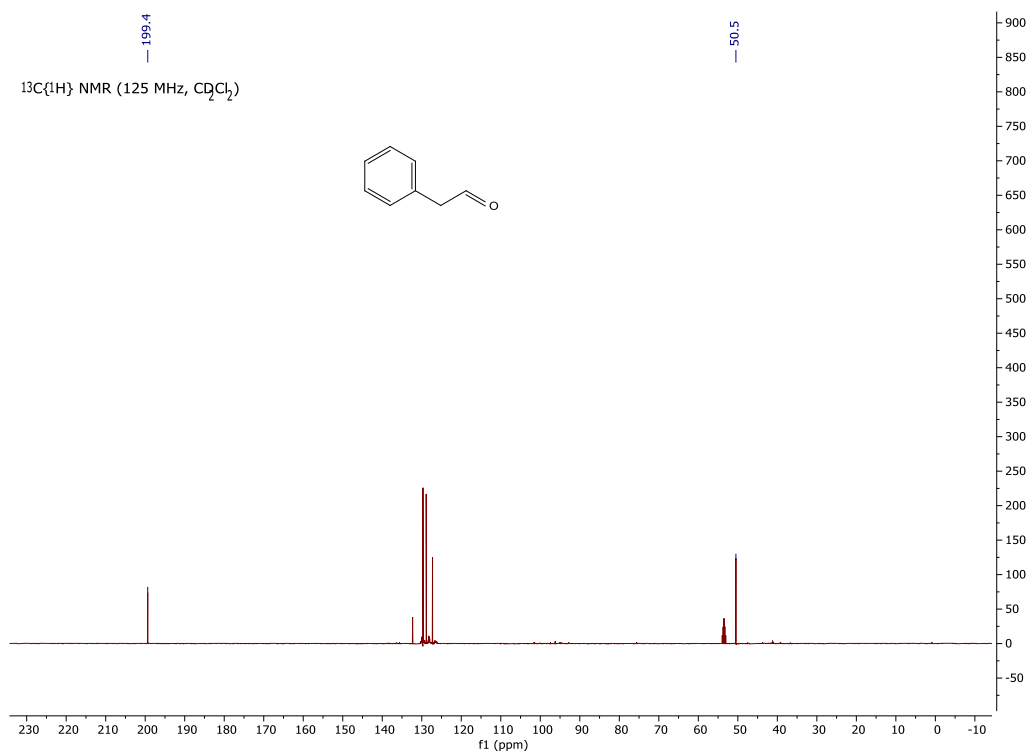


Figure 5.5. ^{13}C NMR of phenylacetaldehyde



5.4 Conclusion

In conclusion, a new method for the synthesis of 2,3-disubstituted quinolines from epoxides and aromatic amines is described in this chapter. This reaction tolerates various electron-donating aromatic amines with both aliphatic and aromatic epoxides to provide the quinoline analogs in moderate to excellent yields.

5.5 Experimental sections

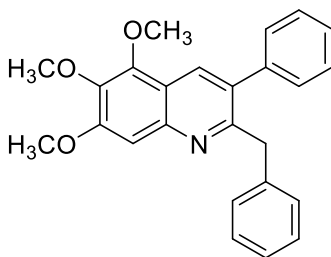
General information. Commercially available reagents were used without additional purification. All reactions were performed under an argon atmosphere with commercial-grade reagents. THF was dried under 3 Å molecular sieve and checked for any water content before using it in the reaction. The molecular sieve (3 Å and 4 Å) was freshly activated before use. All flasks were oven-dried overnight and cooled under argon. All NMR spectra were recorded on a 500 MHz spectrometer. The mass spectrometer ionization method was ESI with a Quadrupole detector, and infrared spectra were recorded on a Jasco Series 6600 FTIR spectrometer.

The general method to synthesize of 2,3-substituted quinoline (Q)

To a solution of dry tetrahydrofuran (THF) (10 mL) in a 50 mL dry round bottom flask, different substituted epoxides (3 equiv, 0.75 mmol) were added, followed by Sc(OTf)₃ (0.5 equiv, 0.125 mmol) at room temperature. Then different substituted aromatic amines (1 equiv, 0.25 mmol), followed by TEMPO (1 equiv, 0.25 mmol) was added at room temperature. The reaction was placed under argon gas and was stirred for 6 hours at 65 °C in a sand bath (Compound Q1, Q5, Q7, and Q19 in an oil bath). Then, another 2 equiv of the same epoxide was added dropwise, and the reaction was allowed to stir for additional 12 hours. After that, the reaction mixture was cooled to room temperature, and the solvent was evaporated under reduced pressure. Then 10mL of

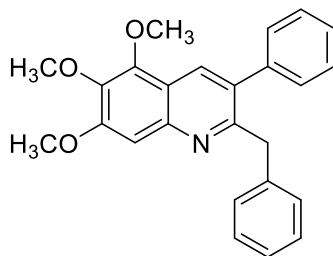
dichloromethane and 10ml saturated NaHCO_3 solution were added, and the solution was extracted with $3 \times 10 \text{ mL}$ of dichloromethane. The combined organic layers were collected and evaporated under reduced pressure, and the crude products were purified using automated CombiFlash chromatography (silica gel, 20-40 microns, gradient 1.5-20% ethyl acetate in hexane).

Method to synthesize gram scale 2-benzyl-5,6,7-trimethoxy-3-phenylquinoline (Q1):



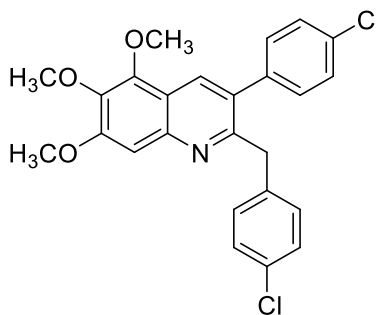
To a solution of dry tetrahydrofuran (THF) (40 mL) in a 100 mL dry round bottom flask, styrene oxide (3 equiv, 15 mmol) was added, followed by $\text{Sc}(\text{OTf})_3$ (0.5 equiv, 2.5 mmol) at room temperature. Then 3,4,5-trimethoxy aniline (1 equiv, 5 mmol) was added at room temperature. The reaction was placed under argon gas and was stirred for 6 hours at 65°C in an oil bath. Then, another 2 equiv (10 mmol) of styrene oxide was added dropwise, and the reaction was continued to stir for additional 12 hours. After that, the reaction mixture was cooled to room temperature, and the solvent was evaporated under reduced pressure. Then 40 mL of dichloromethane and 40ml saturated NaHCO_3 solution were added, and the solution was extracted with $3 \times 40 \text{ mL}$ of dichloromethane. The combined organic layers were collected and evaporated under reduced pressure, and the product was purified using automated CombiFlash chromatography (silica gel, 20-40 microns, gradient 7.5% ethyl acetate in hexane). Yield: 1.497 gm (78%).

2-benzyl-5,6,7-trimethoxy-3-phenylquinoline (Q1).



Colorless oil (88 mg, 91%). Isolated with 7.5% ethyl acetate in hexane. IR: 3058, 3027, 2936, 1616, 1591, 1563, 1480, 1370, 1101 cm^{-1} . ^1H NMR (500 MHz, CD_2Cl_2) δ 8.19 (s, 1H), 7.42 (m, 3H), 7.32 – 7.30 (m, 2H), 7.26 (s, 1H), 7.23 – 7.08 (m, 3H), 7.00 (d, $J = 7.0$ Hz, 2H), 4.28 (s, 2H), 4.05 (s, 3H), 4.03 (s, 3H), 3.96 (s, 3H). $^{13}\text{C}\{^1\text{H}\}$ NMR (125 MHz, CD_2Cl_2) δ 158.1, 156.1, 146.9, 145.1, 140.7, 140.2, 140.1, 133.6, 131.1, 129.6, 128.8, 128.2, 128.0, 127.3, 125.8, 117.6, 103.7, 61.5, 61.0, 56.0, 42.1. HRMS (ESI-TOF) m/z : $[(\text{M}+\text{H})^+]$ calcd for $(\text{C}_{25}\text{H}_{24}\text{NO}_3^+)$ 386.1751; Found 386.1756.

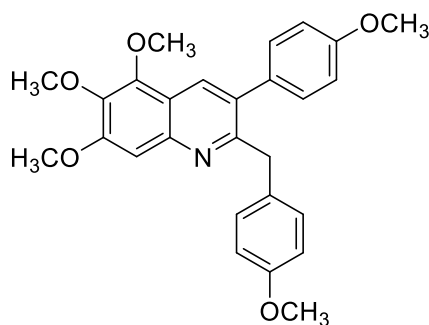
2-(4-chlorobenzyl)-3-(4-chlorophenyl)-5,6,7-trimethoxyquinoline (Q2).



Colorless oil (108 mg, 96%). Isolated with 10% ethyl acetate in hexane. IR: 3060, 3026, 2917, 1600, 1585, 1493, 1073, 760, 695 cm^{-1} . ^1H NMR (500 MHz, CD_2Cl_2) δ 8.14 (s, 1H), 7.40 (d, $J = 8.4$ Hz, 2H), 7.24 (s, 1H), 7.20 (d, $J = 8.4$ Hz, 2H), 7.15 (d, $J = 8.4$ Hz, 2H), 6.93 (d, $J = 8.4$ Hz, 2H), 4.20 (s, 2H), 4.03 (s, 3H), 4.02 (s, 3H), 3.95 (s, 3H). $^{13}\text{C}\{^1\text{H}\}$ NMR (125 MHz, CD_2Cl_2) δ 157.3, 156.4, 146.9, 145.1, 140.8, 138.6, 138.3, 133.4, 132.2, 131.6, 131.3, 130.9, 130.2, 128.3,

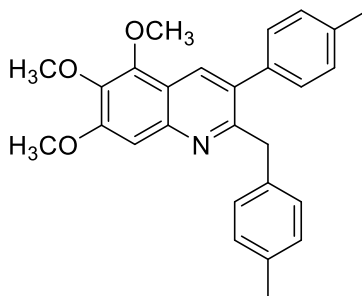
128.1, 117.6, 103.6, 61.5, 61.0, 56.1, 41.6. HRMS (ESI-TOF) m/z : $[(M+H)^+]$ calcd for $(C_{25}H_{22}Cl_2NO_3^+)$ 454.0971; Found 454.0986.

5,6,7-trimethoxy-2-(4-methoxybenzyl)-3-(4-methoxyphenyl)quinoline (Q3).



Colorless oil (30 mg, 67%; ran with 0.1mmol of aromatic amine as 1 equiv). Isolated with 10% ethyl acetate in hexane. IR: 3062, 3031, 2933, 1611, 1510, 1371, 1210, 1101, 1033 cm^{-1} . 1H NMR (500 MHz, CD_2Cl_2) δ 8.16 – 8.11 (m, 1H), 7.24 (s, 1H), 7.23 – 7.20 (m, 2H), 6.99 – 6.89 (m, 4H), 6.75 – 6.69 (m, 2H), 4.20 (s, 2H), 4.03 (s, 3H), 4.02 (s, 3H), 3.95 (s, 3H), 3.87 (s, 3H), 3.74 (s, 3H). $^{13}C\{^1H\}$ NMR (125 MHz, CD_2Cl_2) δ 159.1, 158.7, 157.8, 156.0, 146.9, 144.9, 140.6, 133.2, 132.5, 132.1, 131.1, 130.7, 129.7, 117.6, 113.5, 113.4, 103.6, 61.5, 61.0, 56.0, 55.3, 55.1, 41.2. HRMS (ESI-TOF) m/z : $[(M+H)^+]$ calcd for $(C_{27}H_{28}NO_5^+)$ 446.1962; Found 446.1973.

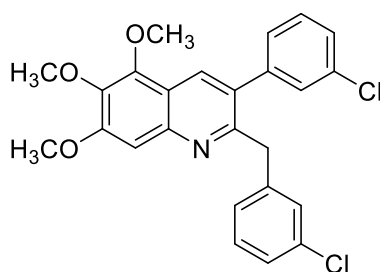
5,6,7-trimethoxy-2-(4-methylbenzyl)-3-(p-tolyl)quinoline (Q4).



Colorless oil (27 mg, 66%; ran with 0.1mmol of aromatic amine as 1 equiv). Isolated with 7.5% ethyl acetate in hexane. IR: 3051, 3019, 2935, 1616, 1480, 1370, 1101 cm^{-1} . 1H NMR (500 MHz,

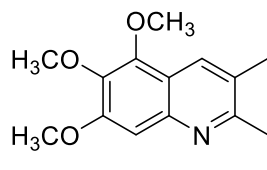
CD₂Cl₂) δ 8.17 (s, 1H), 7.27 – 7.21 (m, 5H), 7.01 (d, J = 8.0 Hz, 2H), 6.91 (d, J = 8.0 Hz, 2H), 4.23 (s, 2H), 4.04 (s, 3H), 4.03 (s, 3H), 3.96 (s, 3H), 2.44 (s, 3H), 2.28 (s, 3H). ¹³C{¹H} NMR (125 MHz, CD₂Cl₂) δ 158.4, 156.0, 146.9, 145.0, 140.7, 137.3, 137.2, 137.1, 135.3, 133.5, 131.1, 129.5, 128.8, 128.7, 128.6, 117.6, 103.6, 61.5, 61.0, 56.0, 41.5, 20.9, 20.7. HRMS (ESI-TOF) m/z : [(M+H)⁺] calcd for (C₂₇H₂₈NO₃⁺) 414.2064; Found 414.2074.

2-(3-chlorobenzyl)-3-(3-chlorophenyl)-5,6,7-trimethoxyquinoline (Q5).



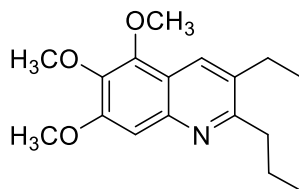
Colorless oil (82 mg, 72%). Isolated with 12.5% ethyl acetate in hexane. IR: 3059, 2936, 1615, 1475, 1369, 1104, 1037, 783, 683 cm⁻¹. ¹H NMR (500 MHz, CD₂Cl₂) δ 8.17 (s, 1H), 7.42 – 7.35 (m, 2H), 7.26 (s, 1H), 7.23 (t, J = 1.8 Hz, 1H), 7.18 – 7.11 (m, 3H), 6.98 (s, 1H), 6.90 – 6.86 (m, 1H), 4.22 (s, 2H), 4.05 (s, 3H), 4.04 (s, 3H), 3.96 (s, 3H). ¹³C{¹H} NMR (125 MHz, CD₂Cl₂) δ 156.9, 156.5, 146.9, 145.2, 141.8, 140.9, 133.9, 133.7, 132.0, 131.3, 129.6, 129.5, 129.4, 128.8, 127.8, 127.5, 127.3, 127.1, 126.1, 117.6, 103.6, 61.5, 61.0, 56.1, 42.1. HRMS (ESI-TOF) m/z : [(M+H)⁺] calcd for (C₂₅H₂₂Cl₂NO₃⁺) 454.0971; Found 454.0980.

2-ethyl-5,6,7-trimethoxy-3-methylquinoline (Q6).



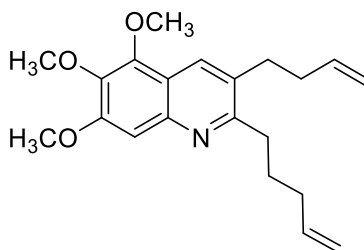
Colorless solid (20 mg, 31%). Isolated with 15% ethyl acetate in hexane. MP: 95-97 °C. IR: 3017, 2964, 2925, 1604, 1484, 1389, 1238, 1093, 1002 cm^{-1} . ^1H NMR (500 MHz, CD_2Cl_2) δ 8.04 (s, 1H), 7.17 (s, 1H), 4.03 (s, 3H), 3.98 (s, 3H), 3.93 (s, 3H), 2.93 (q, $J = 7.5$ Hz, 2H), 2.46 (s, 3H), 1.33 (t, $J = 7.5$ Hz, 3H). $^{13}\text{C}\{^1\text{H}\}$ NMR (125 MHz, CD_2Cl_2) δ 162.2, 155.1, 146.5, 144.1, 140.2, 130.0, 127.0, 117.8, 103.4, 61.4, 60.9, 55.9, 28.9, 18.7, 12.3. HRMS (ESI-TOF) m/z : $[(\text{M}+\text{H})^+]$ calcd for ($\text{C}_{15}\text{H}_{20}\text{NO}_3^+$) 262.1438; Found 262.1449.

3-ethyl-5,6,7-trimethoxy-2-propylquinoline (Q7).



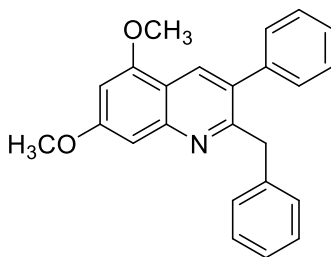
Colorless oil (34 mg, 47%). Isolated with 20% ethyl acetate in hexane. IR: 3010, 2961, 2937, 1601, 1479, 1373, 1236, 1094, 1001 cm^{-1} . ^1H NMR (500 MHz, CD_2Cl_2) δ 8.05 (s, 1H), 7.14 (s, 1H), 4.04 (s, 3H), 3.98 (s, 3H), 3.92 (s, 3H), 2.91 – 2.87 (m, 2H), 2.82 (q, $J = 7.5$ Hz, 2H), 1.81 (dd, $J = 15.5$, 7.5 Hz, 2H), 1.32 (t, $J = 7.5$ Hz, 3H), 1.05 (t, $J = 7.5$ Hz, 3H). $^{13}\text{C}\{^1\text{H}\}$ NMR (125 MHz, CD_2Cl_2) δ 161.0, 155.1, 146.6, 144.1, 140.1, 133.1, 128.1, 117.8, 103.5, 61.4, 60.9, 55.9, 37.4, 25.2, 22.6, 14.6, 14.1. HRMS (ESI-TOF) m/z : $[(\text{M}+\text{H})^+]$ calcd for ($\text{C}_{17}\text{H}_{24}\text{NO}_3^+$) 290.1751; Found 290.1758.

3-(but-3-en-1-yl)-5,6,7-trimethoxy-2-(pent-4-en-1-yl)quinoline (Q8).



Colorless oil (32 mg, 37%). Isolated with 12% ethyl acetate in hexane. IR: 3074, 3001, 2934, 1616, 1566, 1481, 1243, 1093 cm^{-1} . ^1H NMR (500 MHz, CD_2Cl_2) δ 8.05 (s, 1H), 7.15 (s, 1H), 6.04 – 5.85 (m, 2H), 5.18 – 4.98 (m, 4H), 4.04 (s, 3H), 3.99 (s, 3H), 3.94 (s, 3H), 2.95 – 2.86 (m, 4H), 2.48 – 2.43 (m, 2H), 2.23 (q, $J = 7.3$ Hz, 2H), 1.90 (dt, $J = 15.4, 7.6$ Hz, 2H). $^{13}\text{C}\{^1\text{H}\}$ NMR (125 MHz, CD_2Cl_2) δ 160.8, 155.2, 146.5, 144.3, 140.2, 138.7, 137.9, 130.7, 129.2, 117.6, 115.0, 114.5, 103.5, 61.4, 61.0, 55.9, 34.7, 34.6, 33.8, 31.7, 28.5. HRMS (ESI-TOF) m/z : $[(\text{M}+\text{H})^+]$ calcd for $(\text{C}_{21}\text{H}_{28}\text{NO}_3^+)$ 342.2064; Found 342.2066.

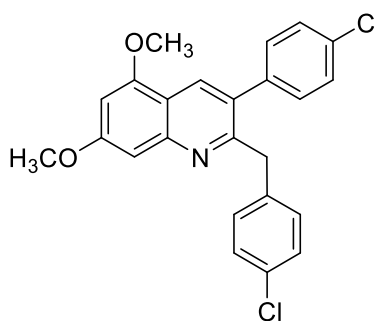
2-benzyl-5,7-dimethoxy-3-phenylquinoline (Q9).



Yellow solid (68 mg, 76%). Isolated with 6.5% ethyl acetate in hexane. MP: 80-82 $^{\circ}\text{C}$. IR: 3059, 3019, 2920, 1628, 1575, 1493, 1382, 1204, 1117, 1044 cm^{-1} . ^1H NMR (500 MHz, CD_2Cl_2) δ 8.27 (s, 1H), 7.44 – 7.37 (m, 3H), 7.32 – 7.29 (m, 2H), 7.21 – 7.15 (m, 2H), 7.13 (dd, $J = 8.4, 6.0$ Hz, 1H), 7.08 – 6.95 (m, 3H), 6.54 (d, $J = 2.1$ Hz, 1H), 4.28 (s, 2H), 3.97 (s, 3H), 3.96 (s, 3H). $^{13}\text{C}\{^1\text{H}\}$ NMR (125 MHz, CD_2Cl_2) δ 161.4, 159.3, 156.1, 149.4, 140.2, 140.0, 132.9, 131.5, 129.6, 128.8,

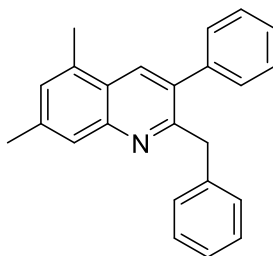
128.1, 128.0, 127.2, 125.8, 115.0, 99.2, 97.8, 55.8, 55.6, 42.2. HRMS (ESI-TOF) m/z : $[(M+H)^+]$ calcd for $(C_{24}H_{22}NO_2^+)$ 356.1645; Found 356.1653.

2-(4-chlorobenzyl)-3-(4-chlorophenyl)-5,7-dimethoxyquinoline (Q10).



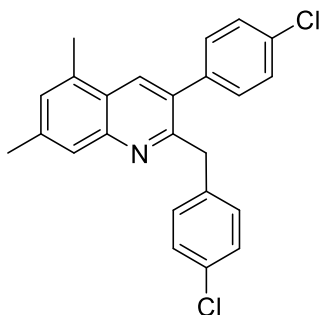
Light yellow oil (83 mg, 78%). Isolated with 8% ethyl acetate in hexane. IR: 3063, 3007, 2931, 1621, 1575, 1490, 1379, 1204, 1014, 809, 732, 673 cm^{-1} . 1H NMR (500 MHz, CD_2Cl_2) δ 8.23 (s, 1H), 7.39 (d, $J = 8.4$ Hz, 2H), 7.17 (dd, $J = 17.2, 8.4$ Hz, 4H), 7.01 (d, $J = 1.8$ Hz, 1H), 6.94 (d, $J = 8.4$ Hz, 2H), 6.55 (d, $J = 1.8$ Hz, 1H), 4.20 (s, 2H), 3.96 (s, 3H), 3.95 (s, 3H). $^{13}C\{^1H\}$ NMR (125 MHz, CD_2Cl_2) δ 161.6, 158.5, 156.1, 149.5, 138.6, 138.3, 133.3, 131.7, 131.6, 131.4, 130.9, 130.2, 128.3, 128.1, 115.0, 99.2, 98.0, 55.8, 55.7, 41.7. HRMS (ESI-TOF) m/z : $[(M+H)^+]$ calcd for $(C_{24}H_{20}Cl_2NO_2^+)$ 424.0866; Found 424.0846.

2-benzyl-5,7-dimethyl-3-phenylquinoline (Q11).



Colorless oil (53 mg, 65%). Isolated with 4% ethyl acetate in hexane. IR: 3026, 2960, 2919, 1622, 1595, 1494, 1257, 1073, 1007 cm^{-1} . ^1H NMR (500 MHz, CD_2Cl_2) δ 8.09 (s, 1H), 7.72 (s, 1H), 7.42 – 7.39 (m, 3H), 7.32 – 7.29 (m, 2H), 7.24 (s, 1H), 7.13 (dd, $J = 13.3, 7.0$ Hz, 3H), 6.98 (d, $J = 7.0$ Hz, 2H), 4.31 (s, 2H), 2.64 (s, 3H), 2.54 (s, 3H). $^{13}\text{C}\{^1\text{H}\}$ NMR (125 MHz, CD_2Cl_2) δ 158.3, 147.8, 140.3, 139.9, 139.3, 134.6, 134.2, 133.2, 129.6, 129.0, 128.8, 128.2, 128.0, 127.4, 126.0, 125.8, 124.2, 42.3, 21.5, 18.3. HRMS (ESI-TOF) m/z : $[(\text{M}+\text{H})^+]$ calcd for $(\text{C}_{24}\text{H}_{22}\text{N}^+)$ 324.1747; Found 324.1756.

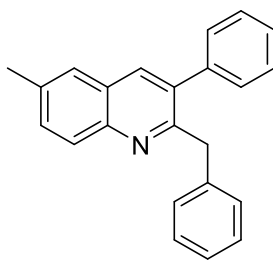
2-(4-chlorobenzyl)-3-(4-chlorophenyl)-5,7-dimethylquinoline (Q12).



Colorless oil (69 mg, 70%). Isolated with 4% ethyl acetate in hexane. IR: 3045, 2972, 2916, 1621, 1591, 1489, 1369, 1263, 1015, 807, 712, 667 cm^{-1} . ^1H NMR (500 MHz, CD_2Cl_2) δ 8.08 (s, 1H), 7.74 (s, 1H), 7.43 (d, $J = 8.4$ Hz, 2H), 7.26 (s, 1H), 7.23 (d, $J = 8.4$ Hz, 2H), 7.16 (d, $J = 8.4$ Hz, 2H), 6.95 (d, $J = 8.4$ Hz, 2H), 4.26 (s, 2H), 2.64 (s, 3H), 2.55 (s, 3H). $^{13}\text{C}\{^1\text{H}\}$ NMR (125 MHz, CD_2Cl_2) δ 157.5, 147.9, 139.7, 138.6, 138.2, 134.3, 133.5, 133.4, 133.2, 131.6, 130.9, 130.2, 129.3,

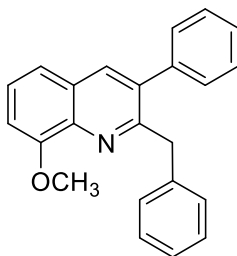
128.4, 128.1, 126.0, 124.1, 41.8, 21.6, 18.2. HRMS (ESI-TOF) m/z : $[(M+H)^+]$ calcd for $(C_{24}H_{20}Cl_2N^+)$ 392.0967; Found 392.0944.

2-benzyl-6-methyl-3-phenylquinoline (Q13).



Light yellow oil (36 mg, 47%). Isolated with 3% ethyl acetate in hexane. IR: 3025, 2915, 1601, 1489, 1368, 1073, 1030 cm^{-1} . 1H NMR (500 MHz, CD_2Cl_2) δ 7.98 (d, J = 8.5 Hz, 1H), 7.92 (s, 1H), 7.61 (s, 1H), 7.58 (d, J = 8.6 Hz, 1H), 7.46 – 7.39 (m, 3H), 7.30 (d, J = 7.4 Hz, 2H), 7.20 – 7.08 (m, 3H), 6.98 (d, J = 7.4 Hz, 2H), 4.31 (s, 2H), 2.56 (s, 3H). $^{13}C\{^1H\}$ NMR (125 MHz, CD_2Cl_2) δ 158.0, 145.8, 139.9, 139.8, 136.2, 136.0, 135.9, 131.5, 129.4, 128.8, 128.4, 128.2, 128.0, 127.4, 126.9, 126.2, 125.8, 42.4, 21.3. HRMS (ESI-TOF) m/z : $[(M+H)^+]$ calcd for $(C_{23}H_{20}N^+)$ 310.1590; Found 310.1599.

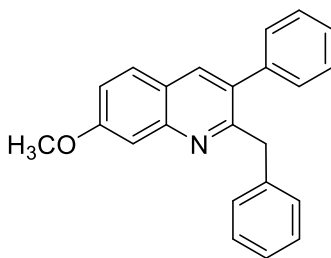
2-benzyl-8-methoxy-3-phenylquinoline (Q14).



Light yellow oil (44 mg, 54%). Isolated with 5% ethyl acetate in hexane. IR: 3058, 3025, 2926, 1614, 1594, 1564, 1494, 1272, 1113, 1030 cm^{-1} . 1H NMR (500 MHz, CD_2Cl_2) δ 7.97 (s, 1H), 7.50

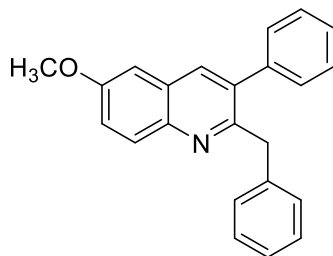
– 7.47 (m, 1H), 7.43 – 7.39 (m, 4H), 7.28 – 7.25 (m, 2H), 7.16 – 7.09 (m, 4H), 6.96 – 6.91 (m, 2H), 4.36 (s, 2H), 4.10 (s, 3H). $^{13}\text{C}\{^1\text{H}\}$ NMR (125 MHz, CD_2Cl_2) δ 157.6, 155.3, 139.9, 139.7, 139.1, 136.7, 136.4, 129.3, 128.7, 128.2, 128.1, 128.0, 127.5, 126.5, 125.7, 119.2, 107.8, 56.0, 42.5. HRMS (ESI-TOF) m/z : $[(\text{M}+\text{H})^+]$ calcd for $(\text{C}_{23}\text{H}_{20}\text{NO}^+)$ 326.1539; Found 326.1542.

2-benzyl-7-methoxy-3-phenylquinoline (Q15).



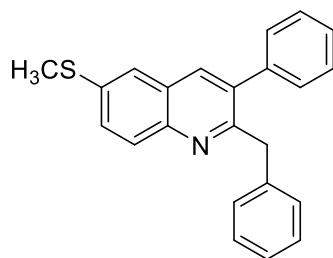
Light yellow oil (46 mg, 57%). Isolated with 5% ethyl acetate in hexane. IR: 3058, 3026, 2927, 1619, 1601, 1492, 1375, 1209, 1026 cm^{-1} . ^1H NMR (500 MHz, CD_3OD) δ 8.00 (s, 1H), 7.78 (d, J = 8.9 Hz, 1H), 7.44 (d, J = 2.4 Hz, 1H), 7.37 – 7.34 (m, 3H), 7.23 – 7.18 (m, 3H), 7.10 – 7.05 (m, 3H), 6.85 – 6.81 (m, 2H), 4.28 (s, 2H), 3.97 (s, 3H). $^{13}\text{C}\{^1\text{H}\}$ NMR (125 MHz, CD_3OD) δ 161.4, 158.9, 148.2, 139.3, 139.1, 137.4, 134.1, 129.2, 128.7, 128.2, 128.0, 127.8, 127.3, 125.7, 122.3, 119.5, 105.1, 54.7, 41.5. HRMS (ESI-TOF) m/z : $[(\text{M}+\text{H})^+]$ calcd for $(\text{C}_{23}\text{H}_{20}\text{NO}^+)$ 326.1539; Found 326.1545.

2-benzyl-6-methoxy-3-phenylquinoline (Q16).



Light yellow oil (45 mg, 55%). Isolated with 5% ethyl acetate in hexane. IR: 3058, 3030, 2921, 1622, 1492, 1224, 1028 cm^{-1} . ^1H NMR (500 MHz, CD_2Cl_2) δ 7.98 (d, $J = 9.2$ Hz, 1H), 7.91 (s, 1H), 7.45 – 7.40 (m, 3H), 7.37 (dd, $J = 9.2, 2.8$ Hz, 1H), 7.31 – 7.28 (m, 2H), 7.19 – 7.08 (m, 4H), 7.02 – 6.95 (m, 2H), 4.28 (s, 2H), 3.94 (s, 3H). $^{13}\text{C}\{^1\text{H}\}$ NMR (125 MHz, CD_2Cl_2) δ 157.7, 156.4, 143.3, 140.0, 139.9, 136.2, 135.6, 130.2, 129.4, 128.8, 128.2, 128.0, 127.8, 127.4, 125.8, 121.9, 104.8, 55.5, 42.2. HRMS (ESI-TOF) m/z : $[(M+H)^+]$ calcd for $(\text{C}_{23}\text{H}_{20}\text{NO}^+)$ 326.1539; Found 326.1544.

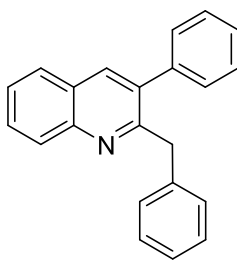
2-benzyl-6-(methylthio)-3-phenylquinoline (Q17).



Light yellow oil (43 mg, 50%). Isolated with 3% ethyl acetate in hexane. IR: 3025, 2917, 1600, 1585, 1493, 1261, 1073, 823, 728 cm^{-1} . ^1H NMR (500 MHz, CD_2Cl_2) δ 7.97 (d, $J = 8.9$ Hz, 1H), 7.89 (s, 1H), 7.60 (dd, $J = 8.9, 2.2$ Hz, 1H), 7.56 (d, $J = 2.2$ Hz, 1H), 7.44 – 7.41 (m, 3H), 7.30 – 7.27 (m, 2H), 7.17 – 7.11 (m, 3H), 7.00 – 6.95 (m, 2H), 4.29 (s, 2H), 2.60 (s, 3H). $^{13}\text{C}\{^1\text{H}\}$ NMR (125 MHz, CD_2Cl_2) δ 158.2, 145.4, 139.7, 139.7, 137.1, 136.5, 135.4, 129.4, 129.0, 128.8, 128.7,

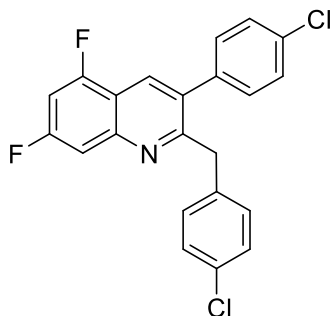
128.2, 128.0, 127.5, 127.4, 125.8, 122.0, 42.3, 15.5. HRMS (ESI-TOF) m/z : $[(M+H)^+]$ calcd for $(C_{23}H_{20}NS^+)$ 342.1311; Found 342.1318.

2-benzyl-3-phenylquinoline (Q18).



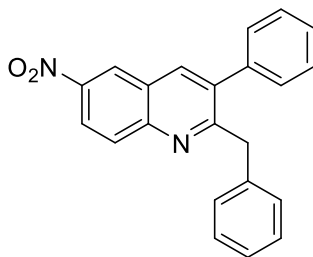
Light yellow oil (25 mg, 34%). Isolated with 1.5% ethyl acetate in hexane. IR: 3025, 2922, 1601, 1592, 1486, 1410, 1073 cm^{-1} . 1H NMR (500 MHz, CD_2Cl_2) δ 8.10 (d, $J = 8.5$ Hz, 1H), 8.01 (s, 1H), 7.86 (d, $J = 8.1$ Hz, 1H), 7.74 (d, $J = 7.0$ Hz, 1H), 7.58-7.56 (dd, $J = 7.0$ Hz, $J = 8.1$ Hz, 1H), 7.46 – 7.40 (m, 3H), 7.32 – 7.29 (m, 2H), 7.19 – 7.11 (m, 3H), 6.99 (d, $J = 7.4$ Hz, 2H), 4.34 (s, 2H). $^{13}C\{^1H\}$ NMR (125 MHz, CD_2Cl_2) δ 159.1, 147.2, 139.7, 139.7, 136.7, 136.0, 129.4, 129.3, 128.8, 128.8, 128.2, 128.0, 127.5, 127.5, 126.9, 126.3, 125.8, 42.5. HRMS (ESI-TOF) m/z : $[(M+H)^+]$ calcd for $(C_{22}H_{18}N^+)$ 296.1434; Found 296.1444.

2-(4-chlorobenzyl)-3-(4-chlorophenyl)-5,7-difluoroquinoline (**Q19**).



White solid (39 mg, 39%). Isolated with 1.5% ethyl acetate in hexane. MP: 62-63 °C. IR: 3059, 3026, 2917, 1639, 1573, 1443, 1373, 1233, 1133, 1052, 1004, 854, 755, 696 cm^{-1} . ^1H NMR (500 MHz, CD_2Cl_2) δ 8.18 (s, 1H), 7.61 – 7.55 (m, 1H), 7.44 (d, J = 8.4 Hz, 2H), 7.22 – 7.15 (m, 4H), 7.10 (m, 1H), 6.94 (d, J = 8.4 Hz, 2H), 4.26 (s, 2H). $^{13}\text{C}\{^1\text{H}\}$ NMR (125 MHz, CD_2Cl_2) δ 161.5 (dd, J = 248, 14 Hz), 160.9 (dd, J = 256, 15 Hz), 157.4, 148.0 (dd, J = 14, 4.5 Hz), 137.4, 137.3, 134.3 (dd, J = 6, 3 Hz), 134.0, 131.9, 130.8, 130.3, 130.2 (dd, J = 3.5, 2 Hz), 128.6, 128.2, 114.6 (dd, J = 15, 2 Hz), 108.7 (dd, J = 21, 4.5 Hz), 102.0 (dd, J = 21, 6 Hz), 42.0. m/z : $[(\text{M}+\text{H})^+]$ calcd for $(\text{C}_{22}\text{H}_{14}\text{Cl}_2\text{F}_2\text{N}^+)$ 400.0466; Found 400.0445.

2-benzyl-6-nitro-3-phenylquinoline (**Q20**).



Light yellow oil (9 mg, 10%). Isolated with 3% ethyl acetate in hexane. IR: 3025, 2921, 1601, 1575, 1520, 1494, 1403, 1021 cm^{-1} . ^1H NMR (500 MHz, CD_2Cl_2) δ 8.81 (s, 1H), 8.48 (d, J = 9.2 Hz, 1H), 8.23 (d, J = 9.2 Hz, 1H), 8.18 (s, 1H), 7.48 (s, 3H), 7.31 – 7.30 (m, 2H), 7.18 – 7.16 (m,

3H), 7.00 – 6.98 (m, 2H), 4.37 (s, 2H). $^{13}\text{C}\{^1\text{H}\}$ NMR (125 MHz, CD_2Cl_2) δ 163.5, 152.2, 144.1, 138.7, 138.5, 138.1, 137.9, 130.6, 129.3, 128.9, 128.5, 128.1, 128.1, 126.2, 125.7, 124.4, 122.6, 42.8. HRMS (ESI-TOF) m/z : $[(\text{M}+\text{H})^+]$ calcd for $(\text{C}_{22}\text{H}_{17}\text{N}_2\text{O}_2^+)$ 341.1285; Found 341.1292.

APPENDIX

APPENDIX

Figure 5.6. ^1H and ^{13}C NMR Spectra of Compound Q1

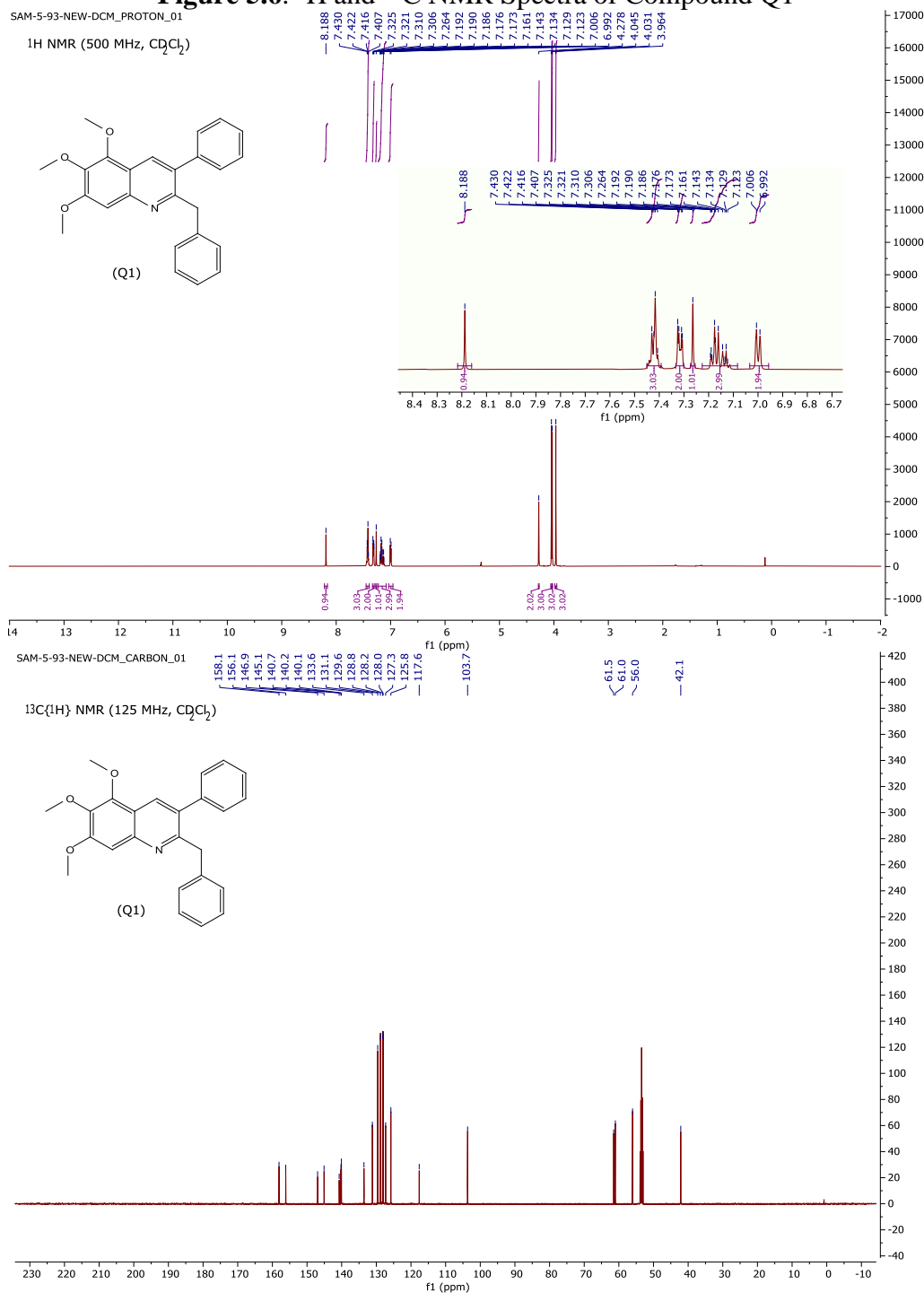


Figure 5.7. ^1H and ^{13}C NMR Spectra of Compound Q2

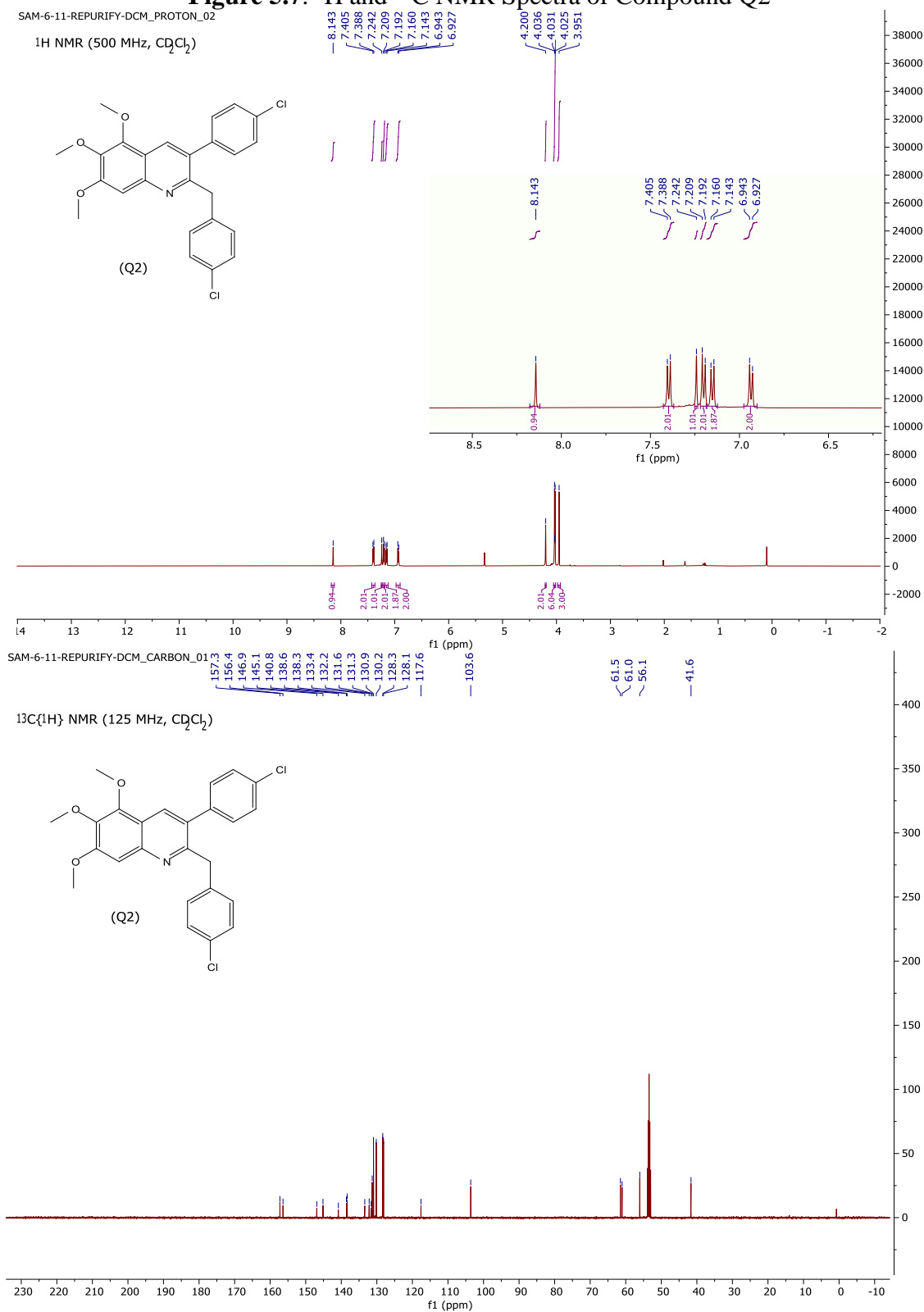
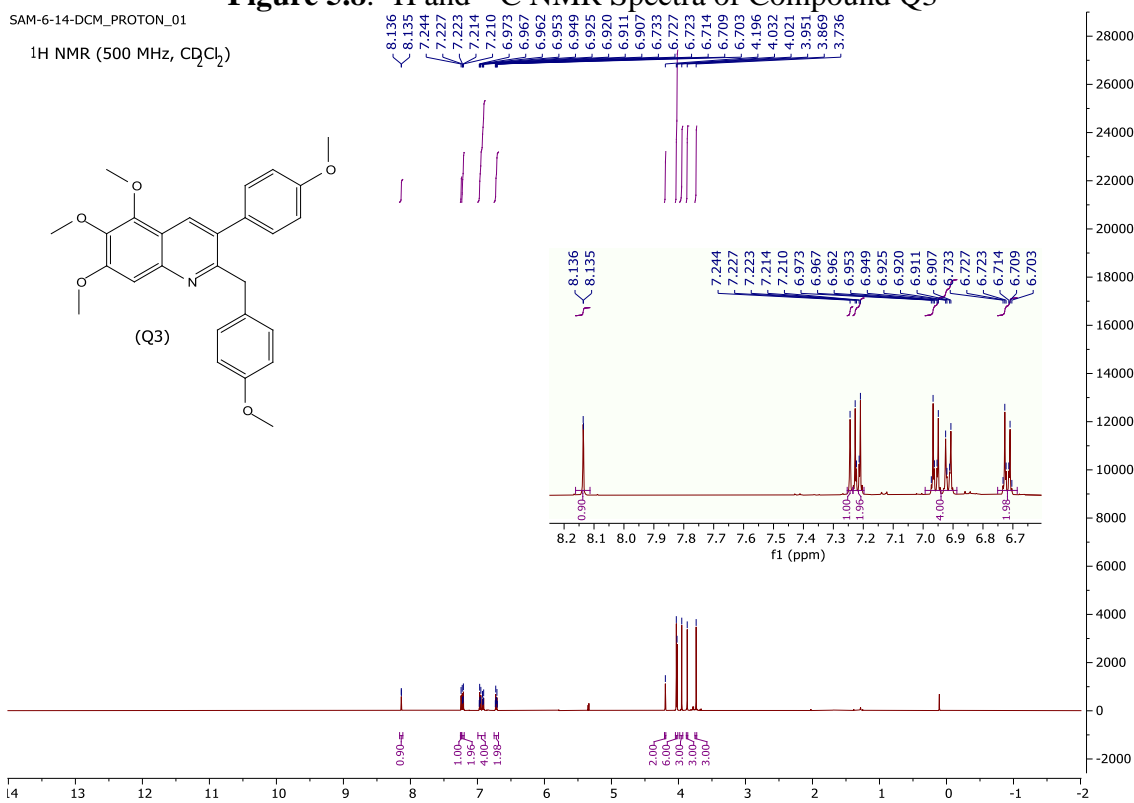


Figure 5.8. ^1H and ^{13}C NMR Spectra of Compound Q3

SAM-6-14-DCM_PROTON_01

^1H NMR (500 MHz, CDCl_3)



SAM-6-14-DCM_CARBON_01

$^{13}\text{C}\{^1\text{H}\}$ NMR (125 MHz, CDCl_3)

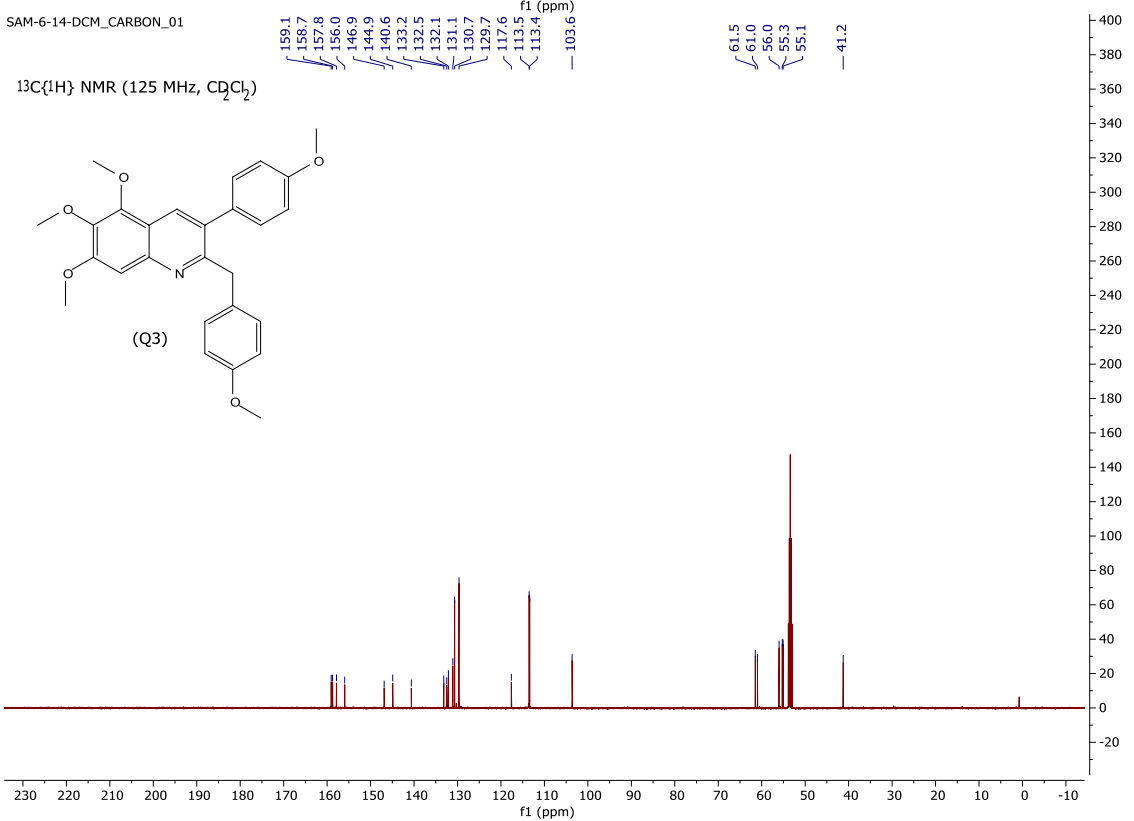


Figure 5.9. ^1H and ^{13}C NMR Spectra of Compound Q4

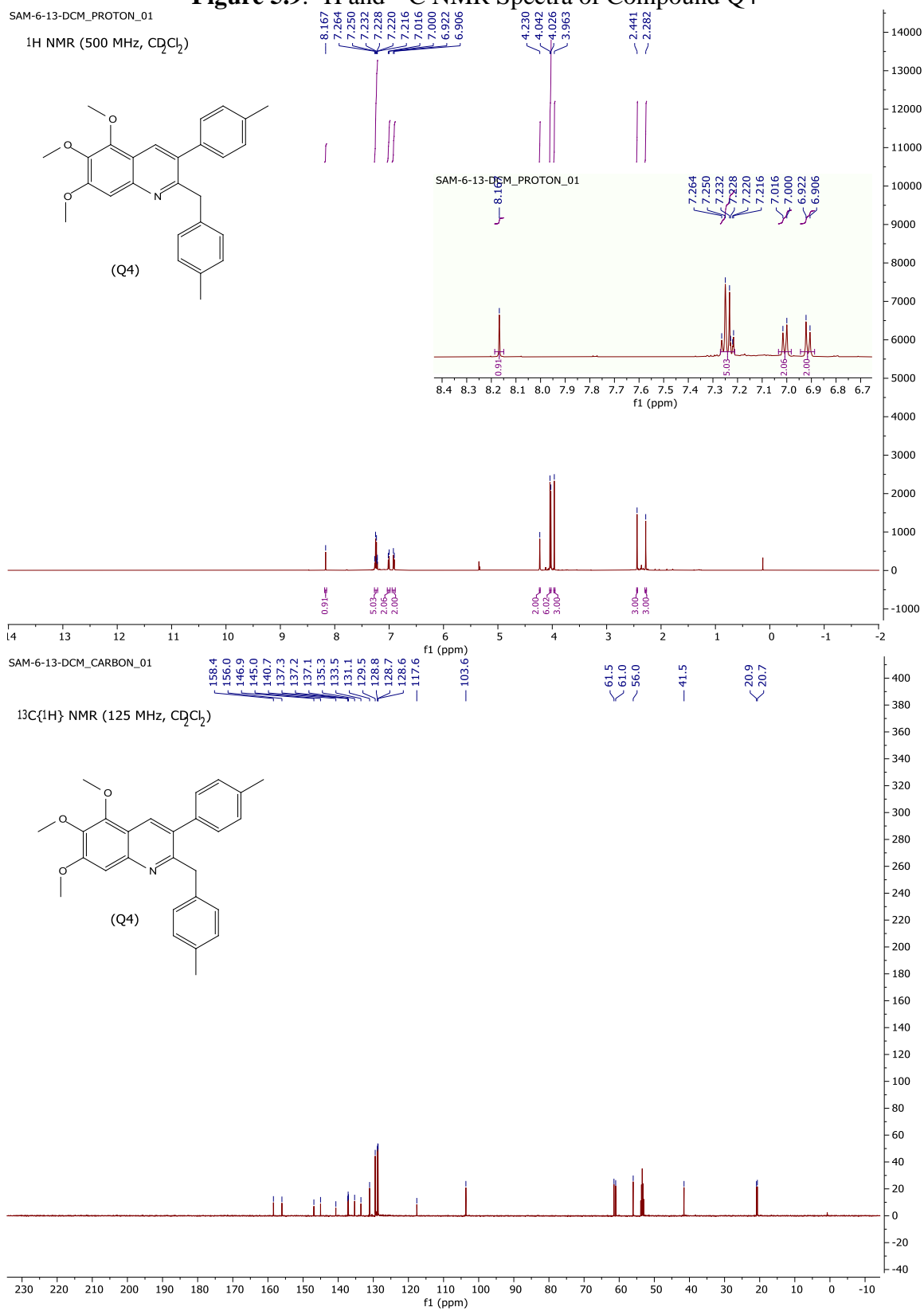
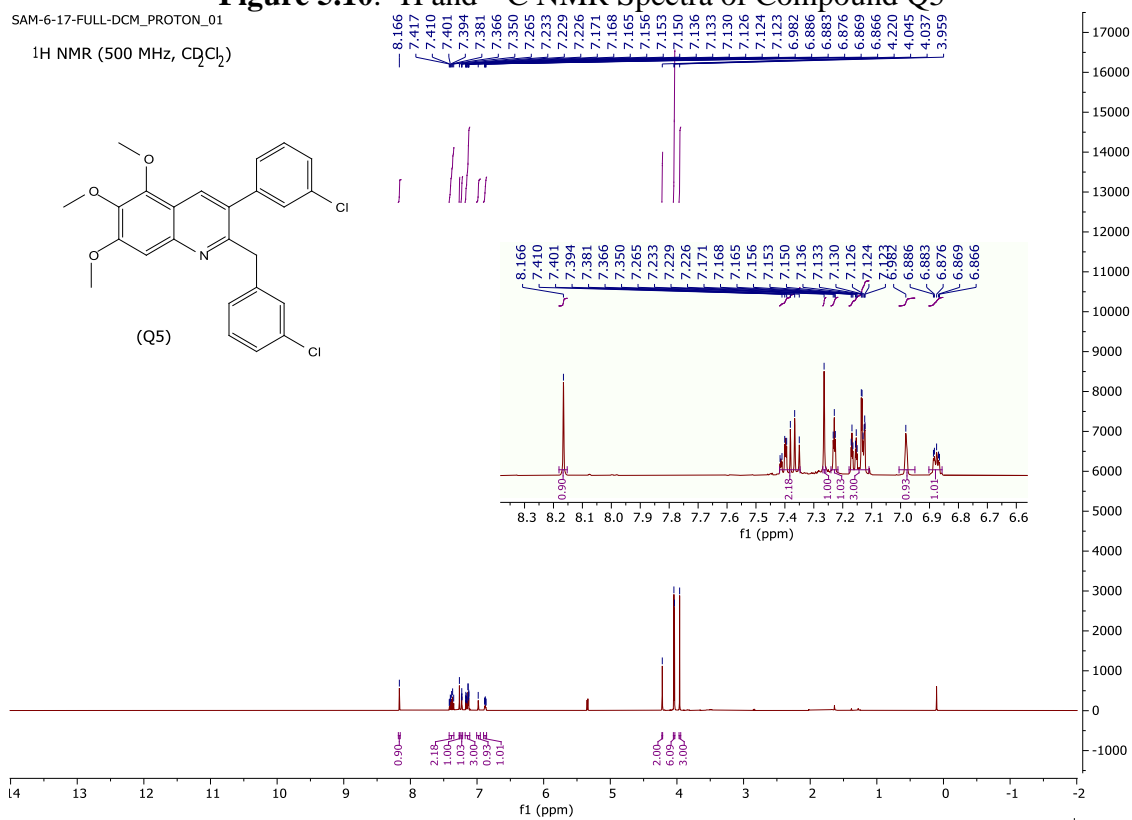
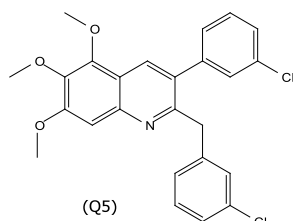


Figure 5.10. ^1H and ^{13}C NMR Spectra of Compound Q5

SAM-6-17-FULL-DCM_PROTON_01

^1H NMR (500 MHz, CD_2Cl_2)



SAM-6-17-FULL-DCM_CARBON_01

$^{13}\text{C}\{^1\text{H}\}$ NMR (125 MHz, CD_2Cl_2)

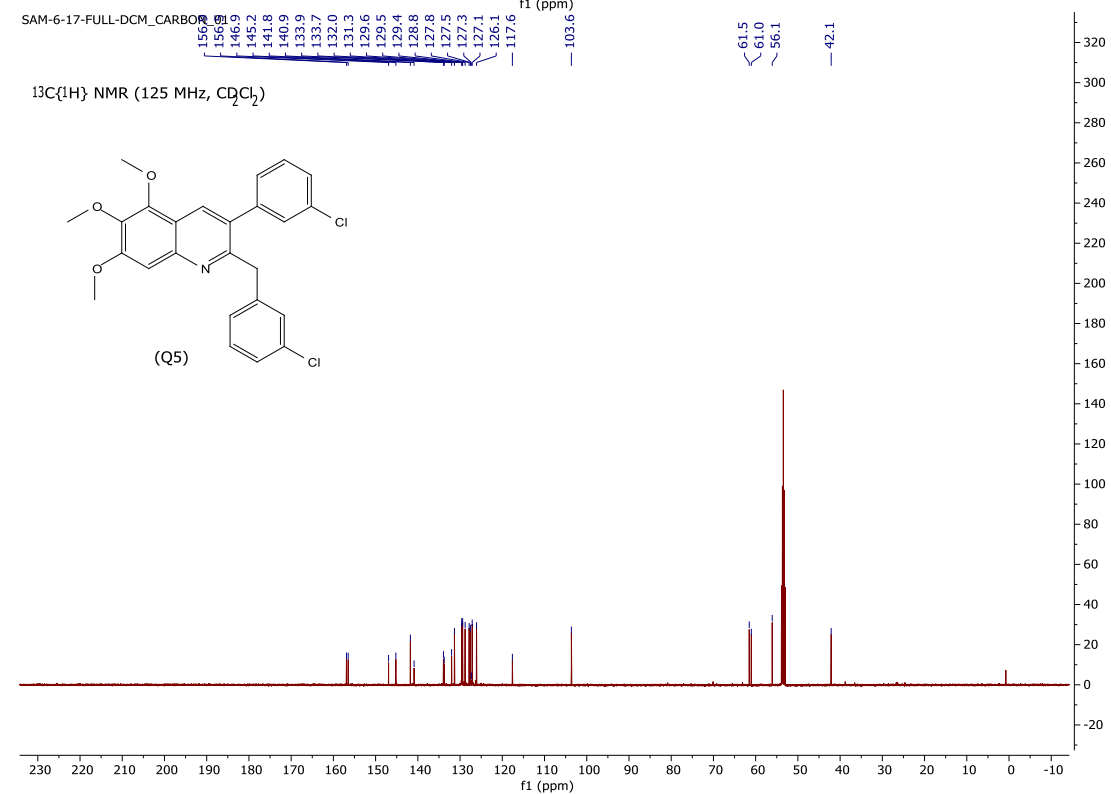
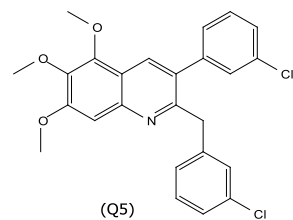
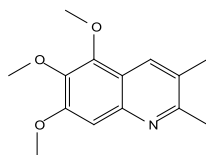


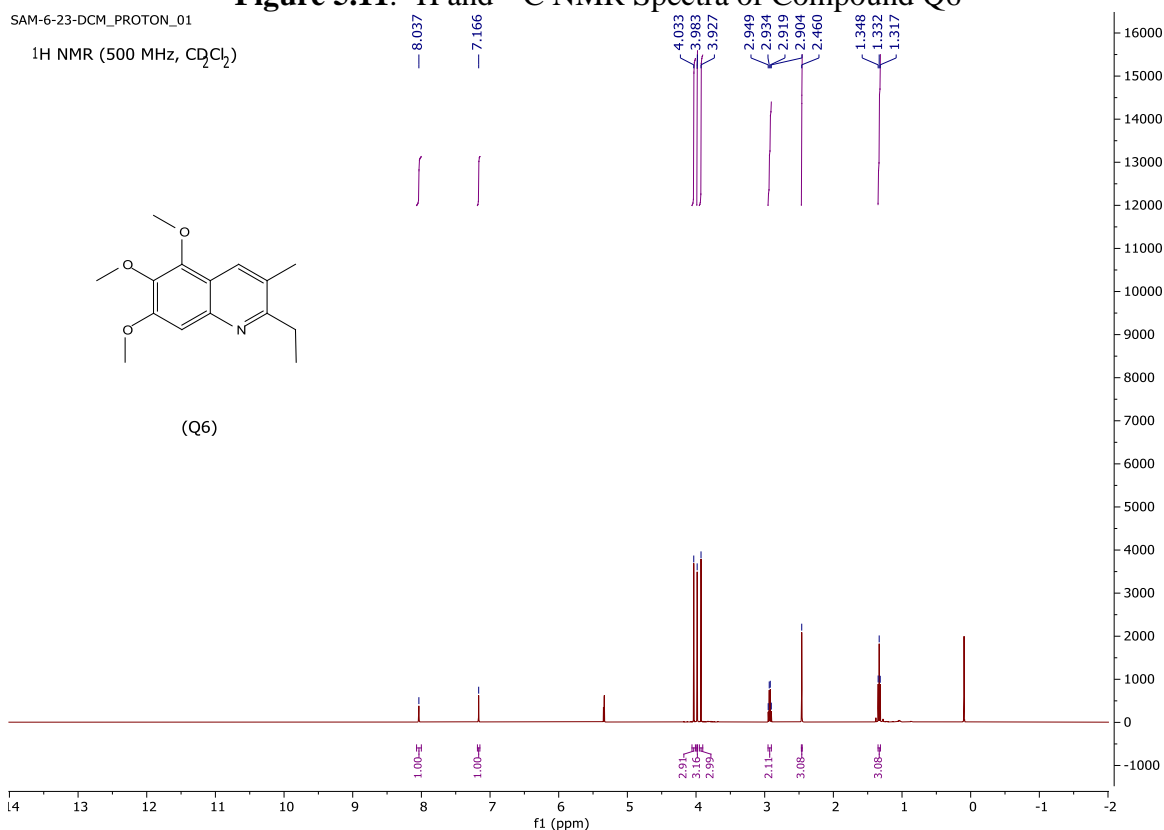
Figure 5.11. ^1H and ^{13}C NMR Spectra of Compound Q6

SAM-6-23-DCM_PROTON_01

^1H NMR (500 MHz, CD_2Cl_2)

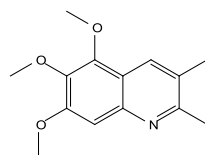


(Q6)



SAM-6-23-DCM_CARBON_02

$^{13}\text{C}\{^1\text{H}\}$ NMR (125 MHz, CD_2Cl_2)



(Q6)

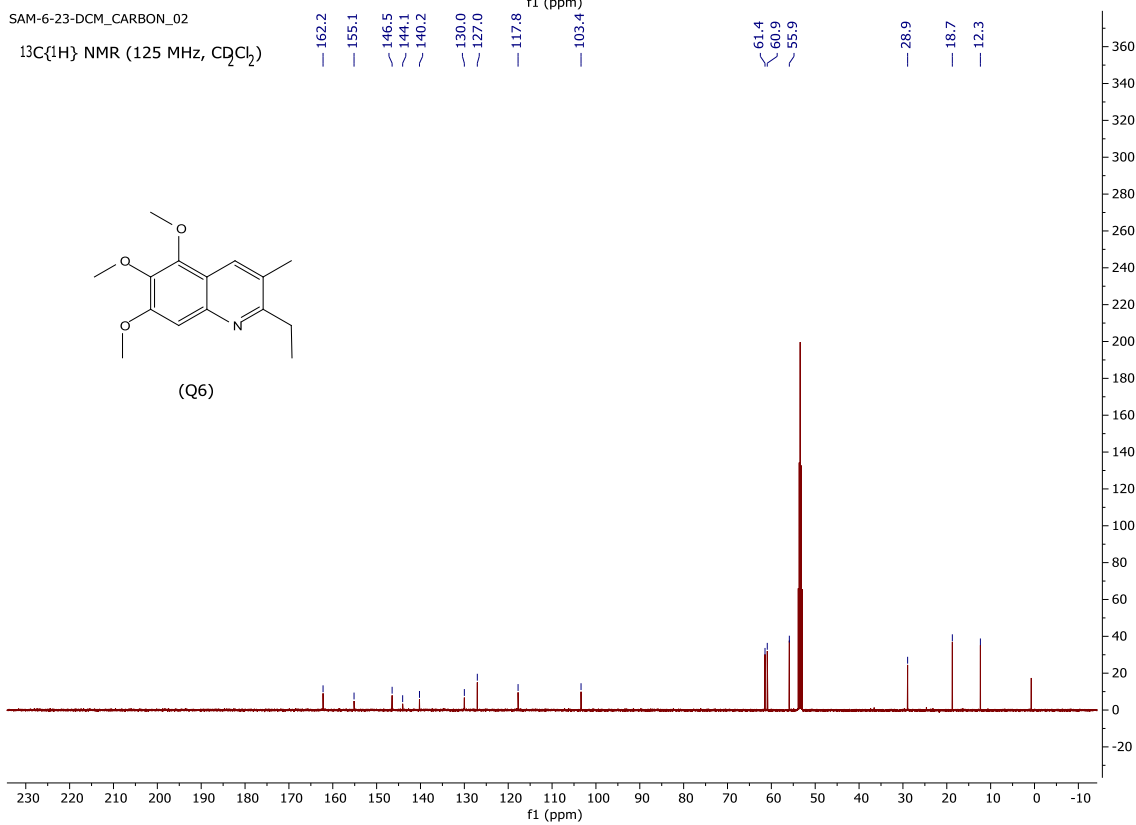


Figure 5.12. ^1H and ^{13}C NMR Spectra of Compound Q7

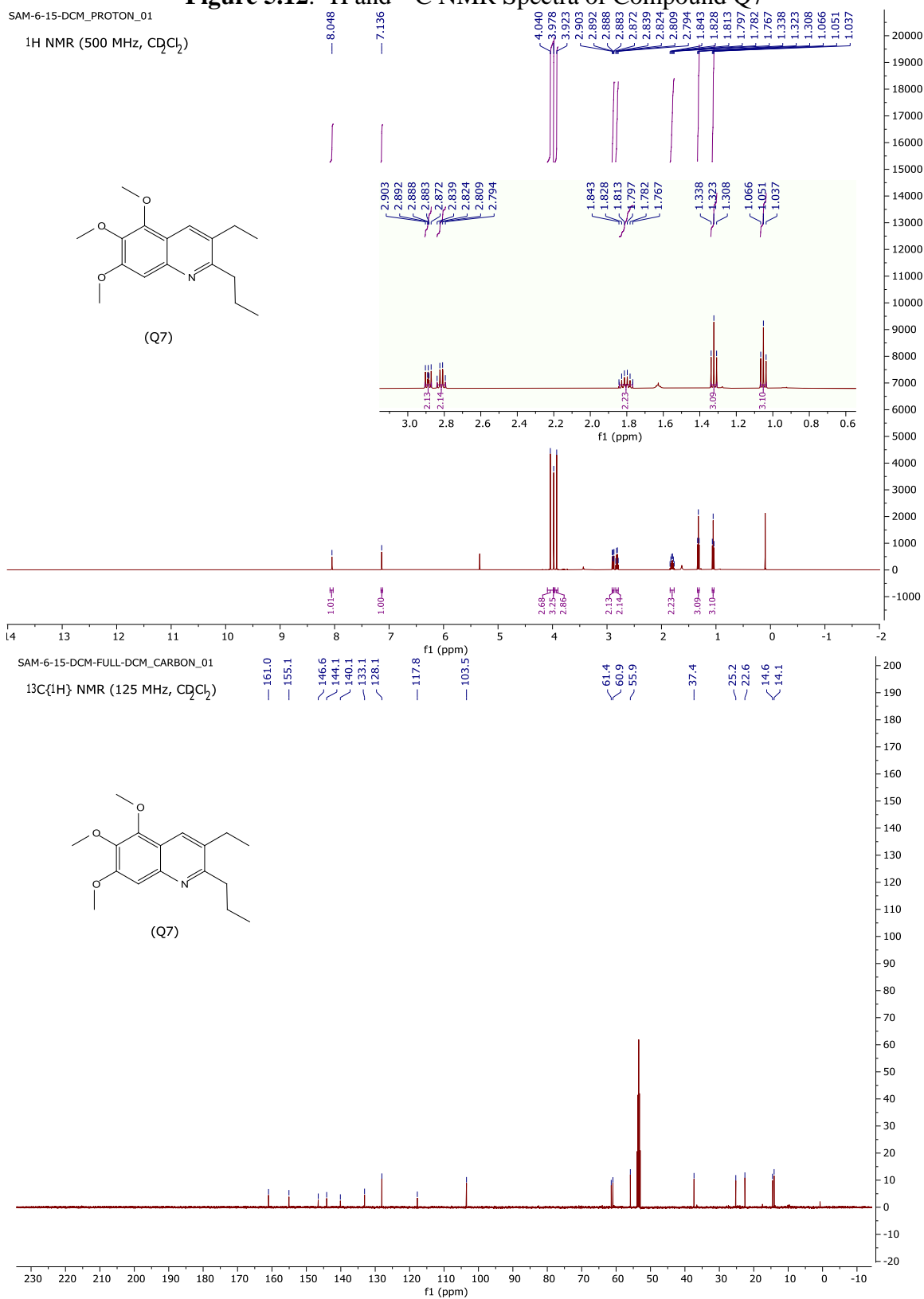


Figure 5.13. ^1H and ^{13}C NMR Spectra of Compound Q8

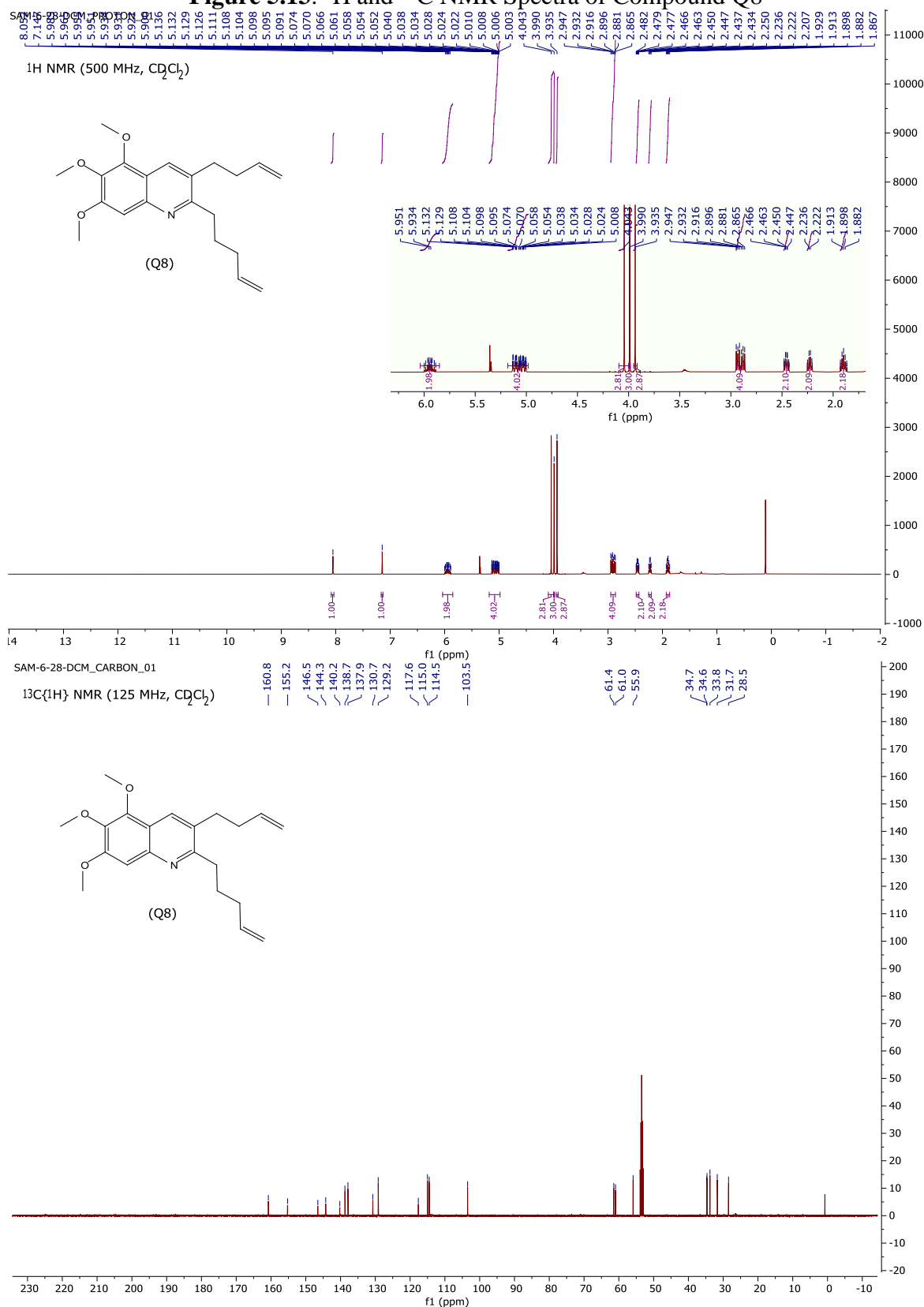


Figure 5.14. ^1H and ^{13}C NMR Spectra of Compound Q9

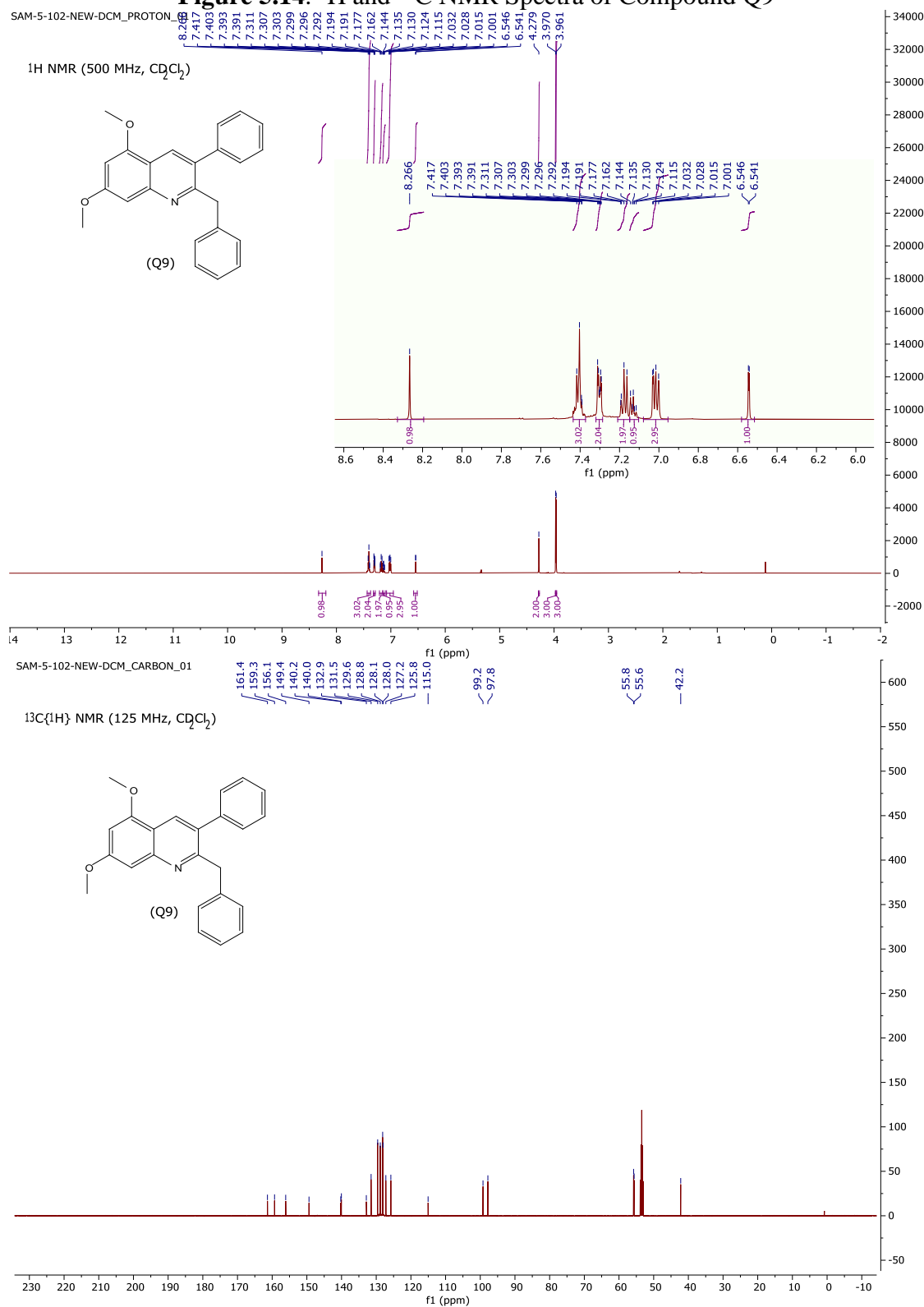
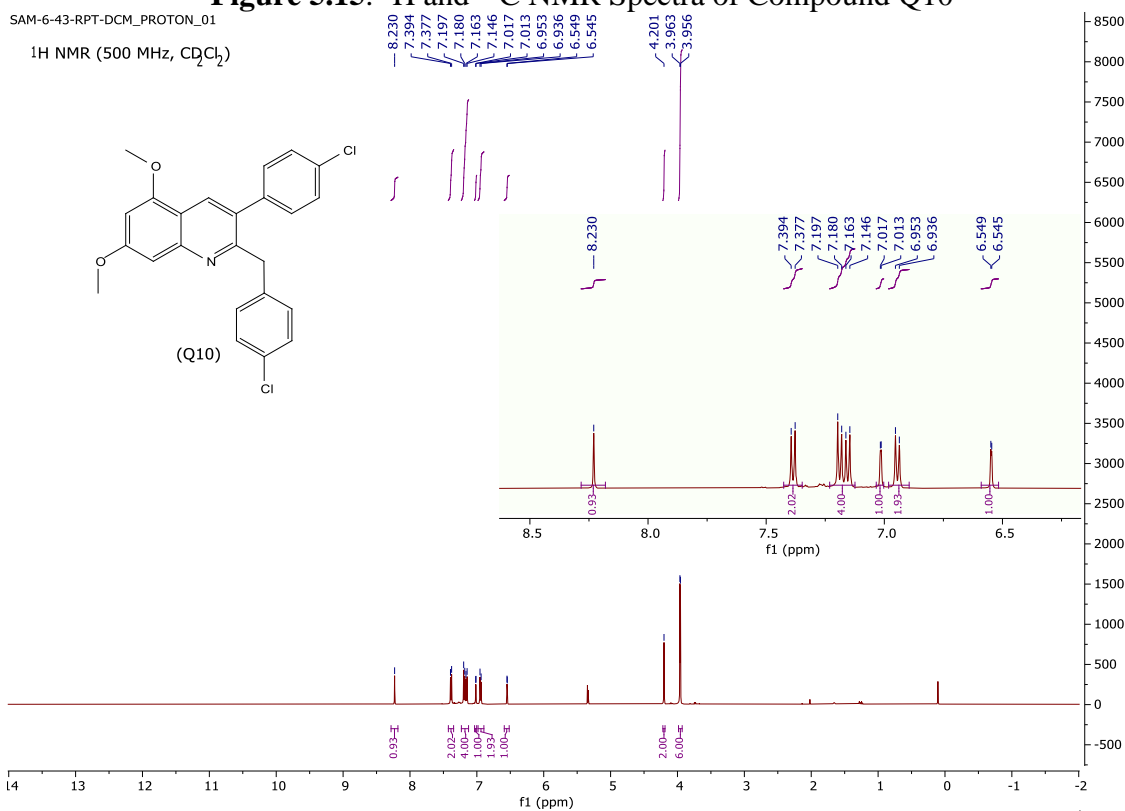


Figure 5.15. ^1H and ^{13}C NMR Spectra of Compound Q10

SAM-6-43-RPT-DCM_PROTON_01

^1H NMR (500 MHz, CD_2Cl_2)



SAM-6-43-RPT-DCM_CARBON_01

$^{13}\text{C}\{^1\text{H}\}$ NMR (125 MHz, CD_2Cl_2)

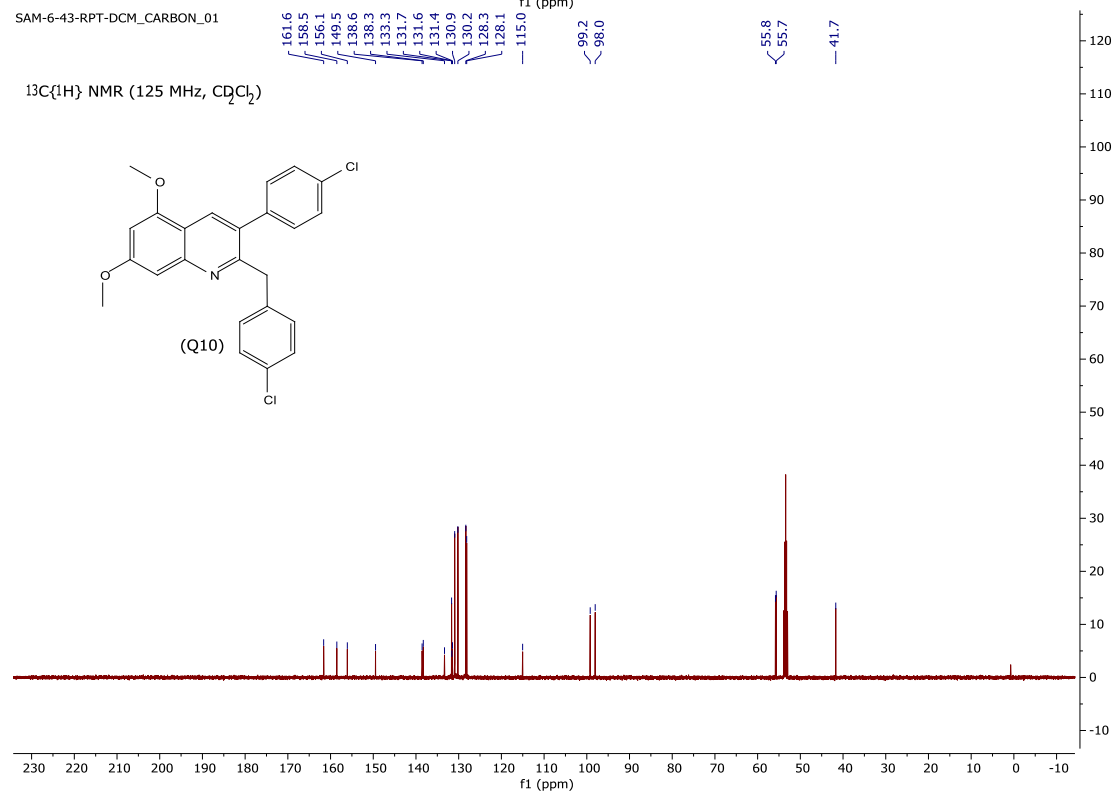


Figure 5.16. ^1H and ^{13}C NMR Spectra of Compound Q11

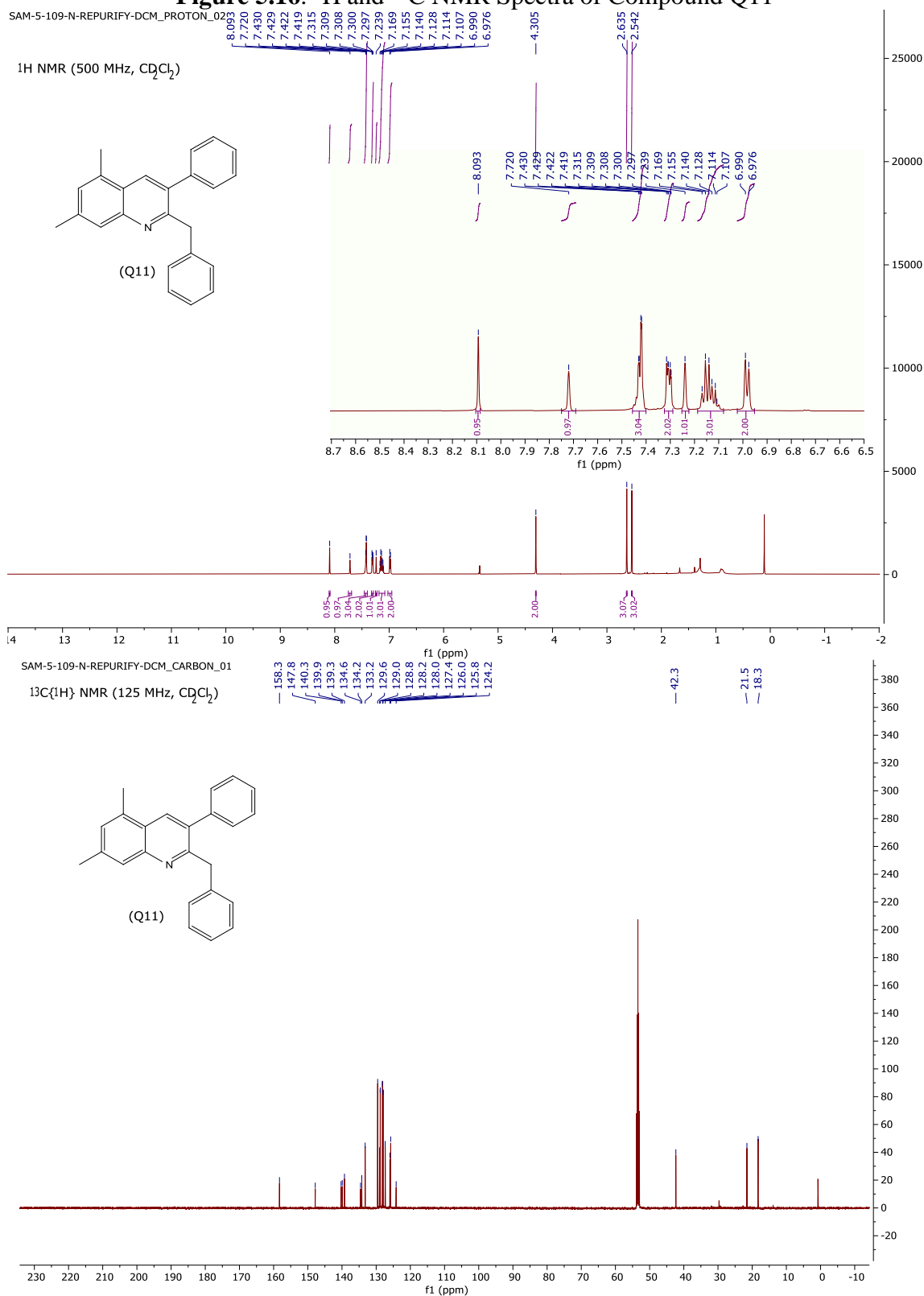


Figure 5.17. ^1H and ^{13}C NMR Spectra of Compound Q12

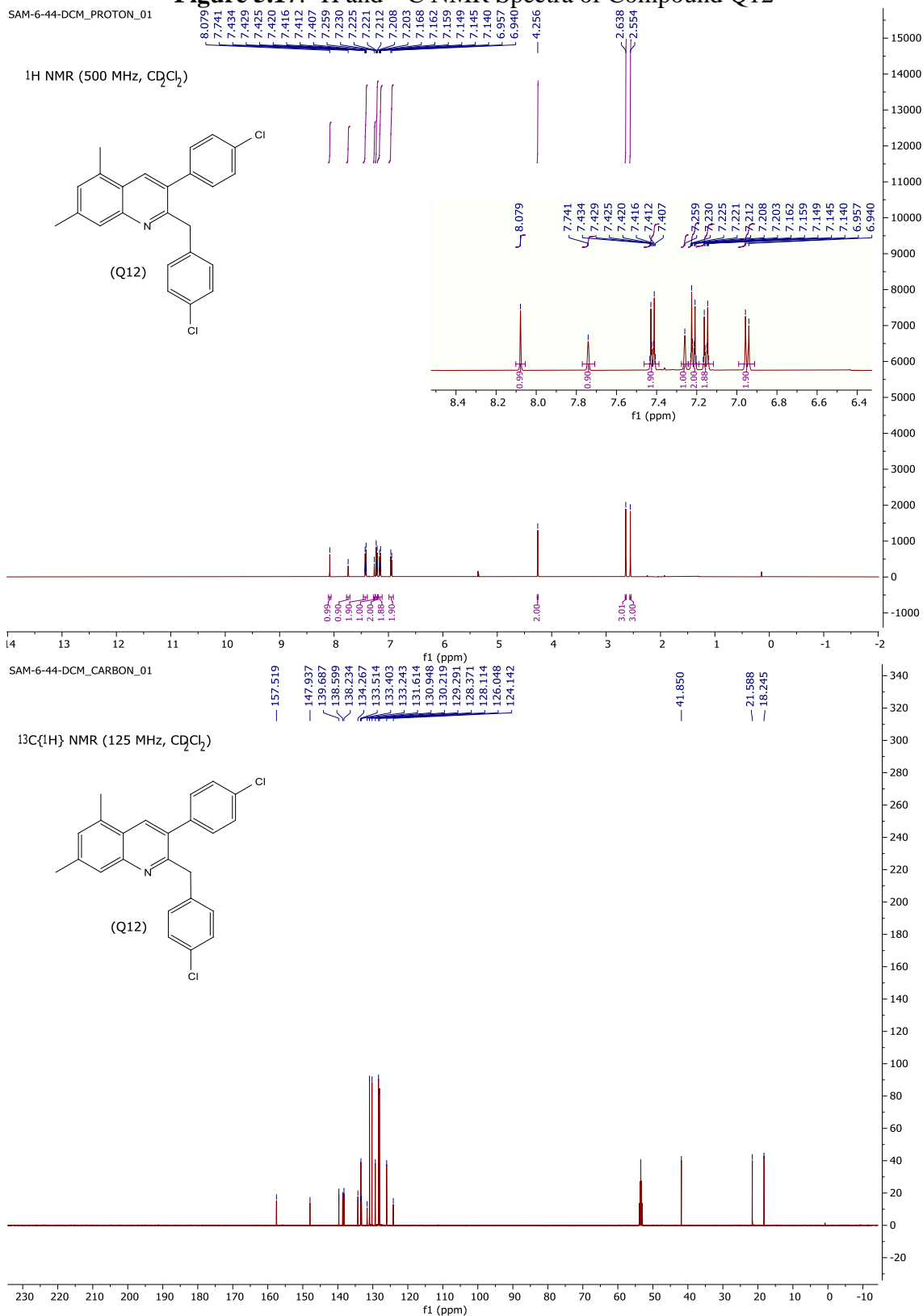


Figure 5.18. ^1H and ^{13}C NMR Spectra of Compound Q13

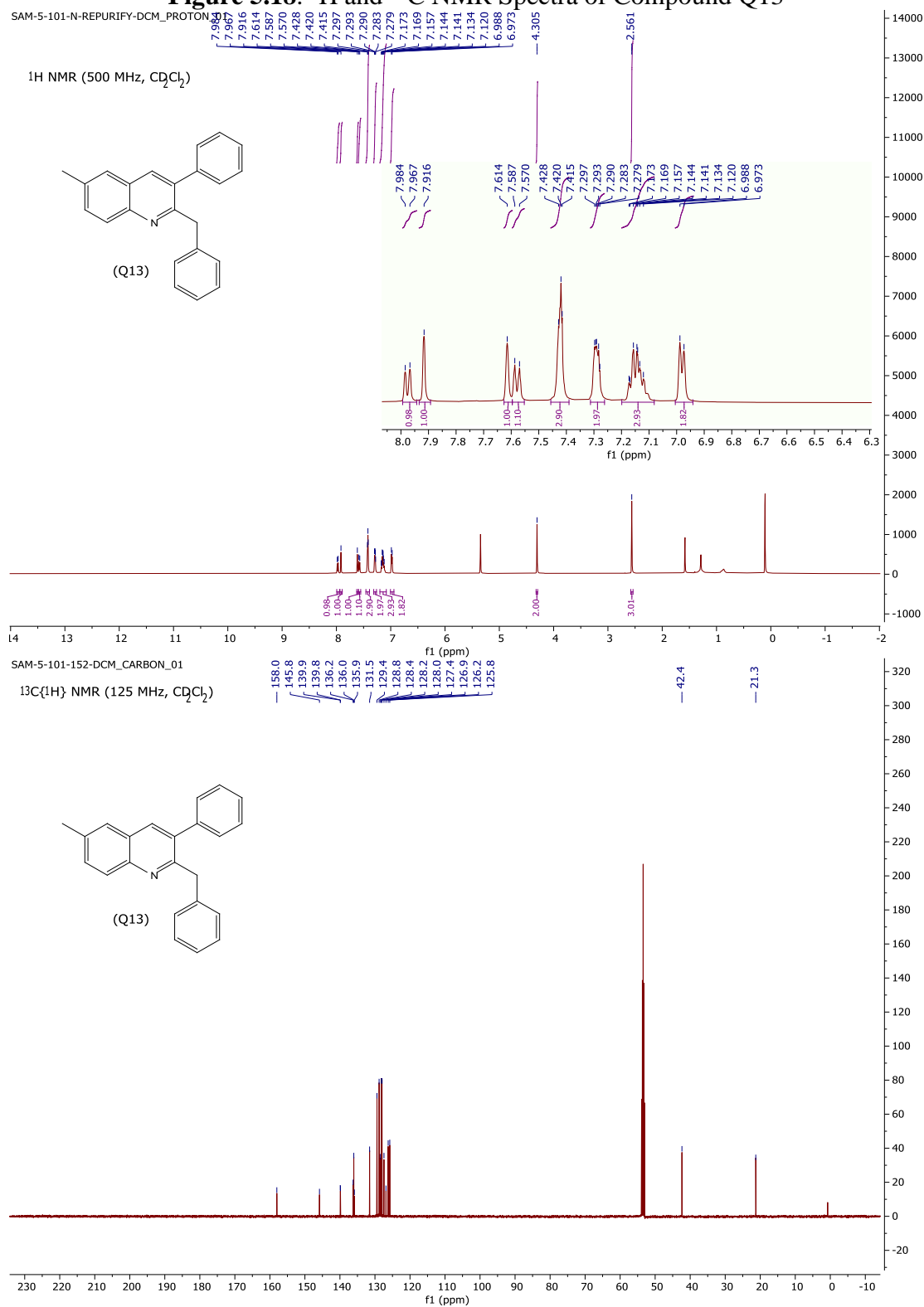


Figure 5.19. ^1H and ^{13}C NMR Spectra of Compound Q14

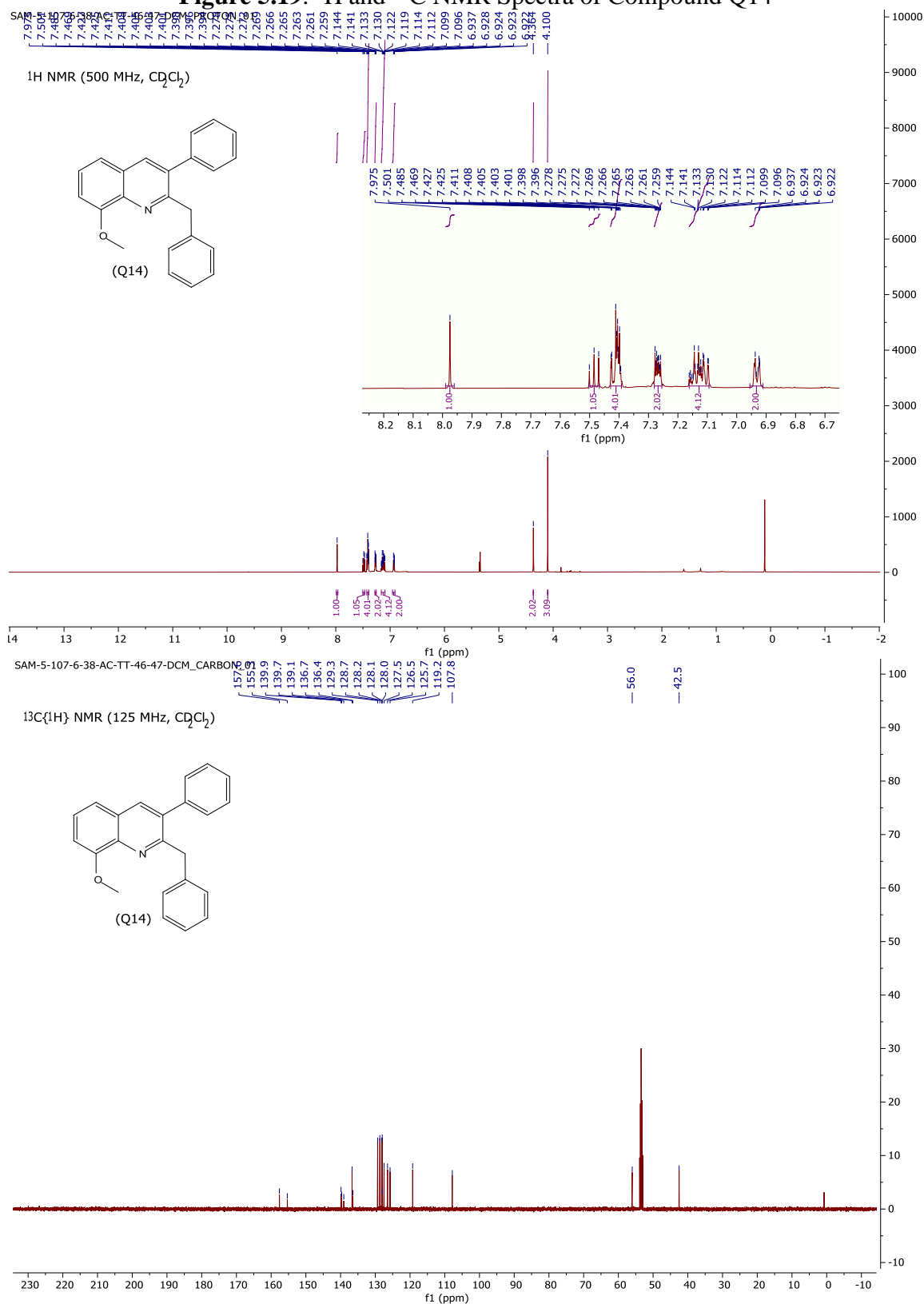


Figure 5.20. ^1H and ^{13}C NMR Spectra of Compound Q15

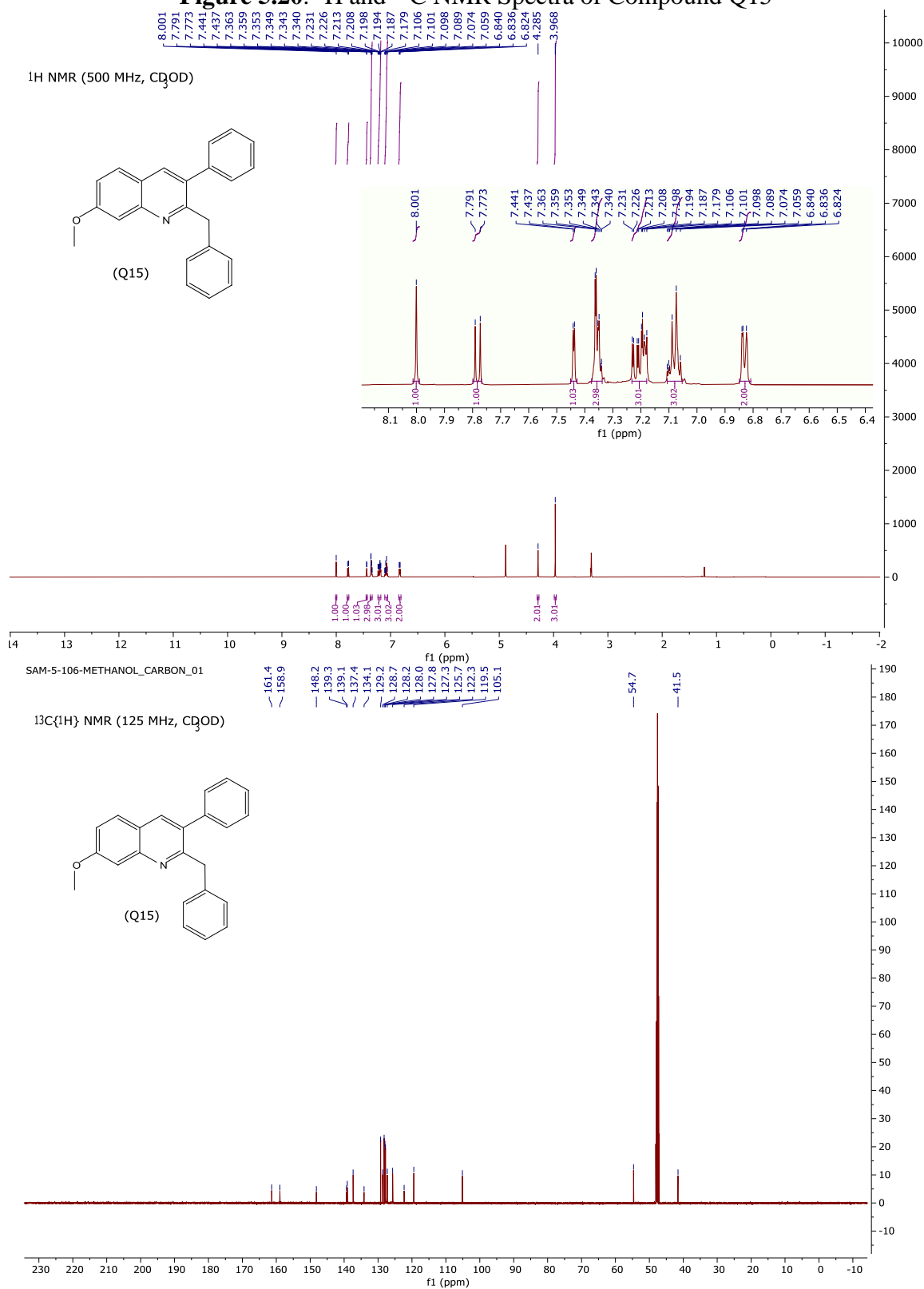


Figure 5.21. ^1H and ^{13}C NMR Spectra of Compound Q16

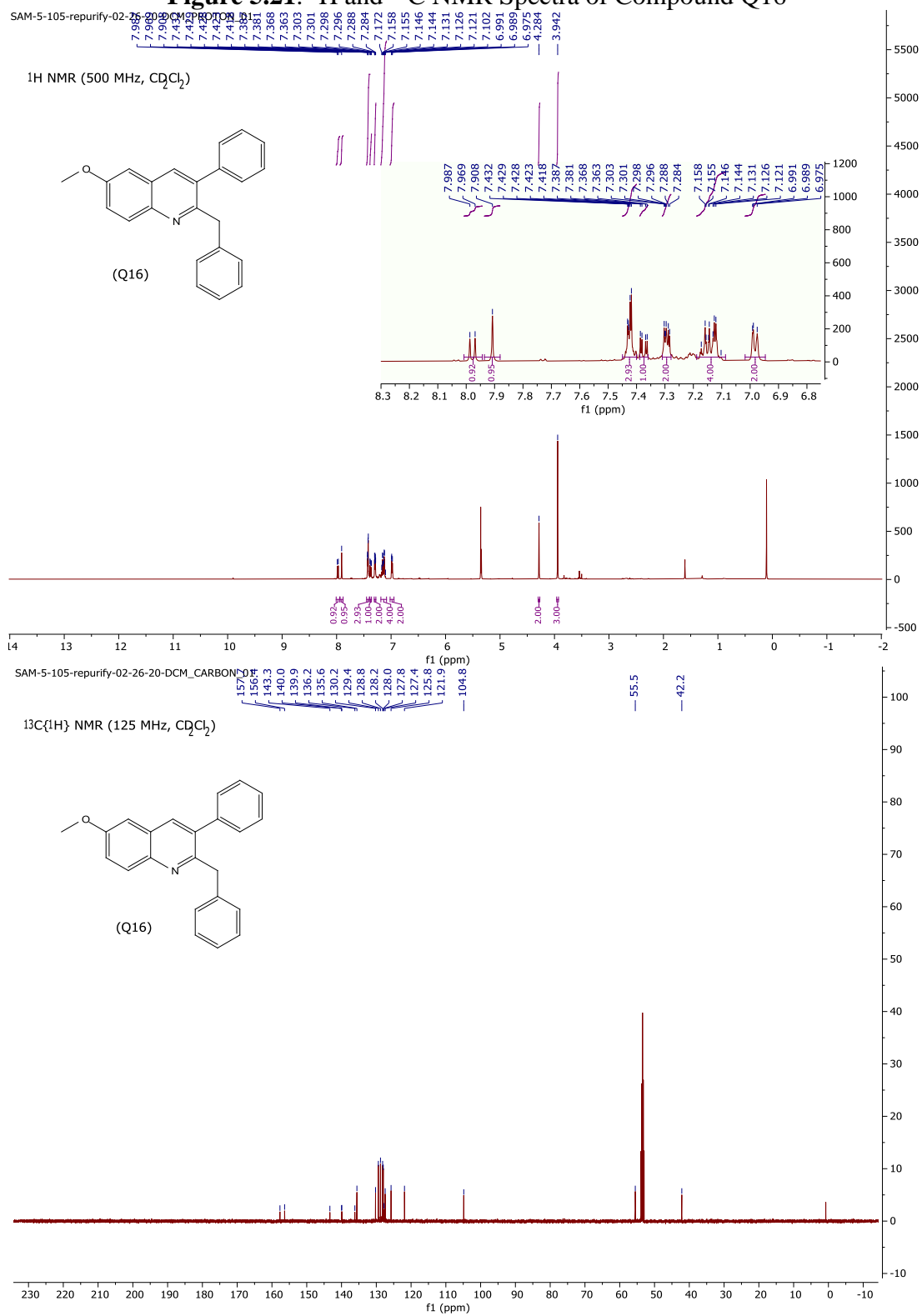


Figure 5.22. ^1H and ^{13}C NMR Spectra of Compound Q17

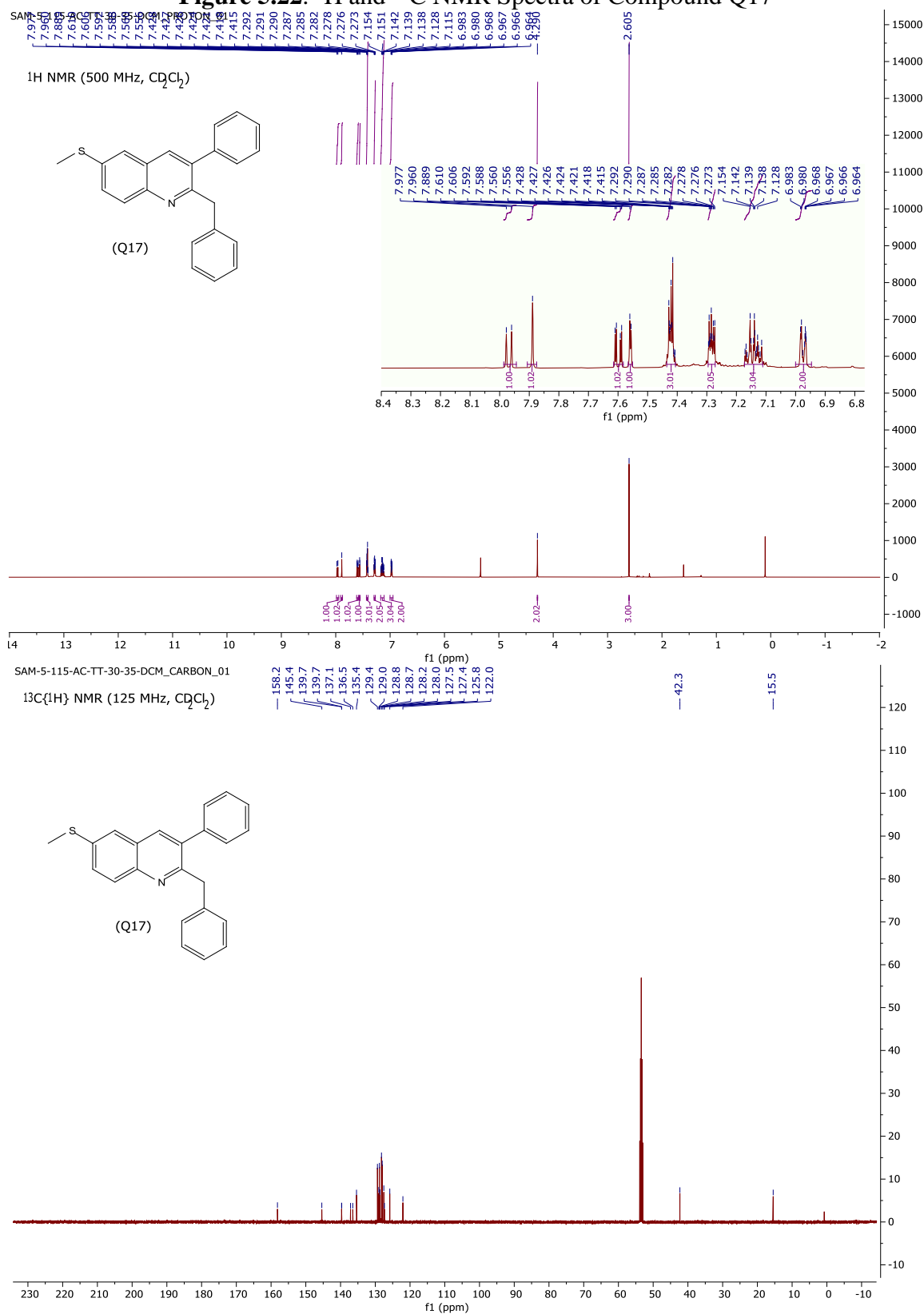


Figure 5.23. ^1H and ^{13}C NMR Spectra of Compound Q18

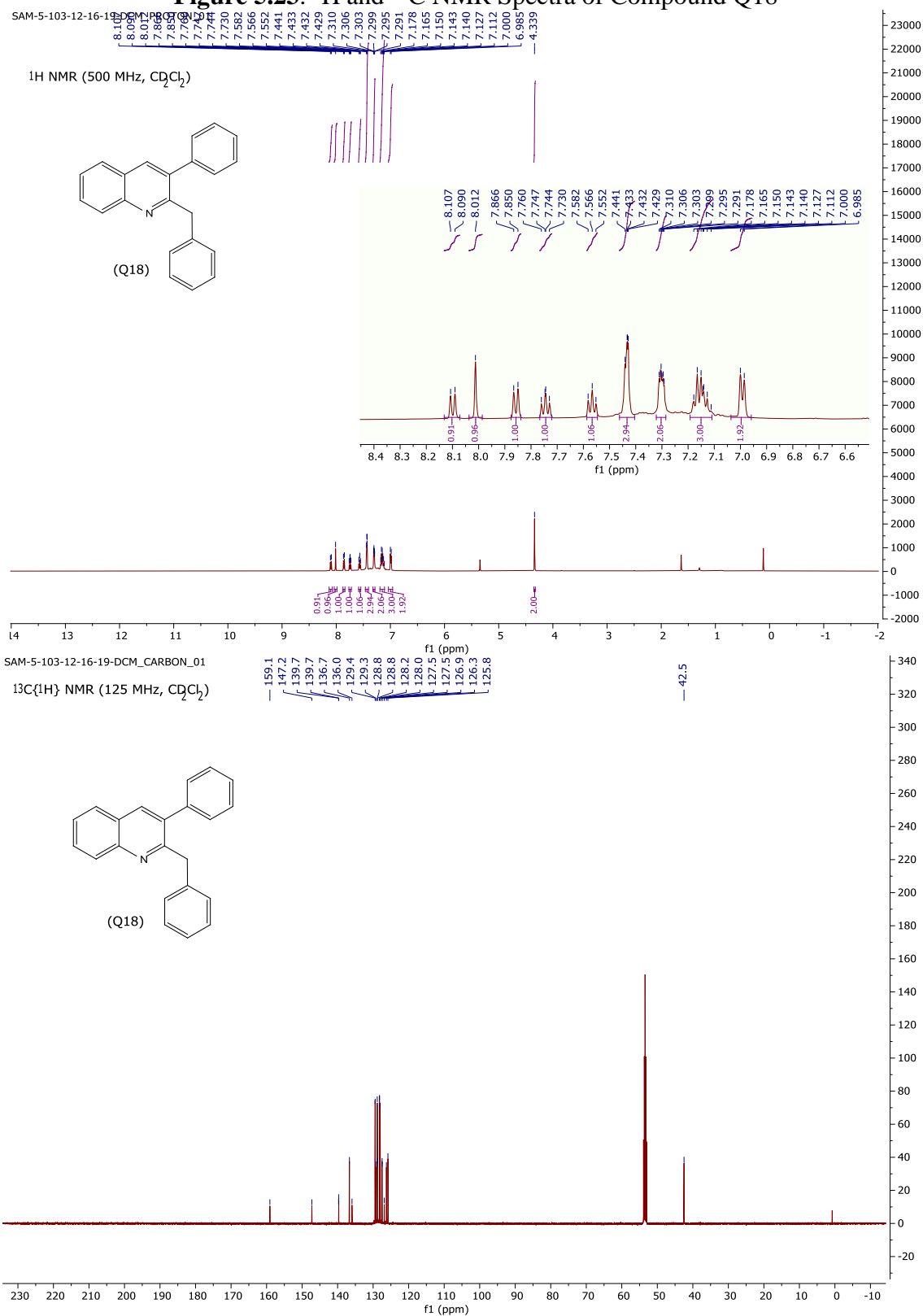


Figure 5.24. ^1H and ^{13}C NMR Spectra of Compound Q19

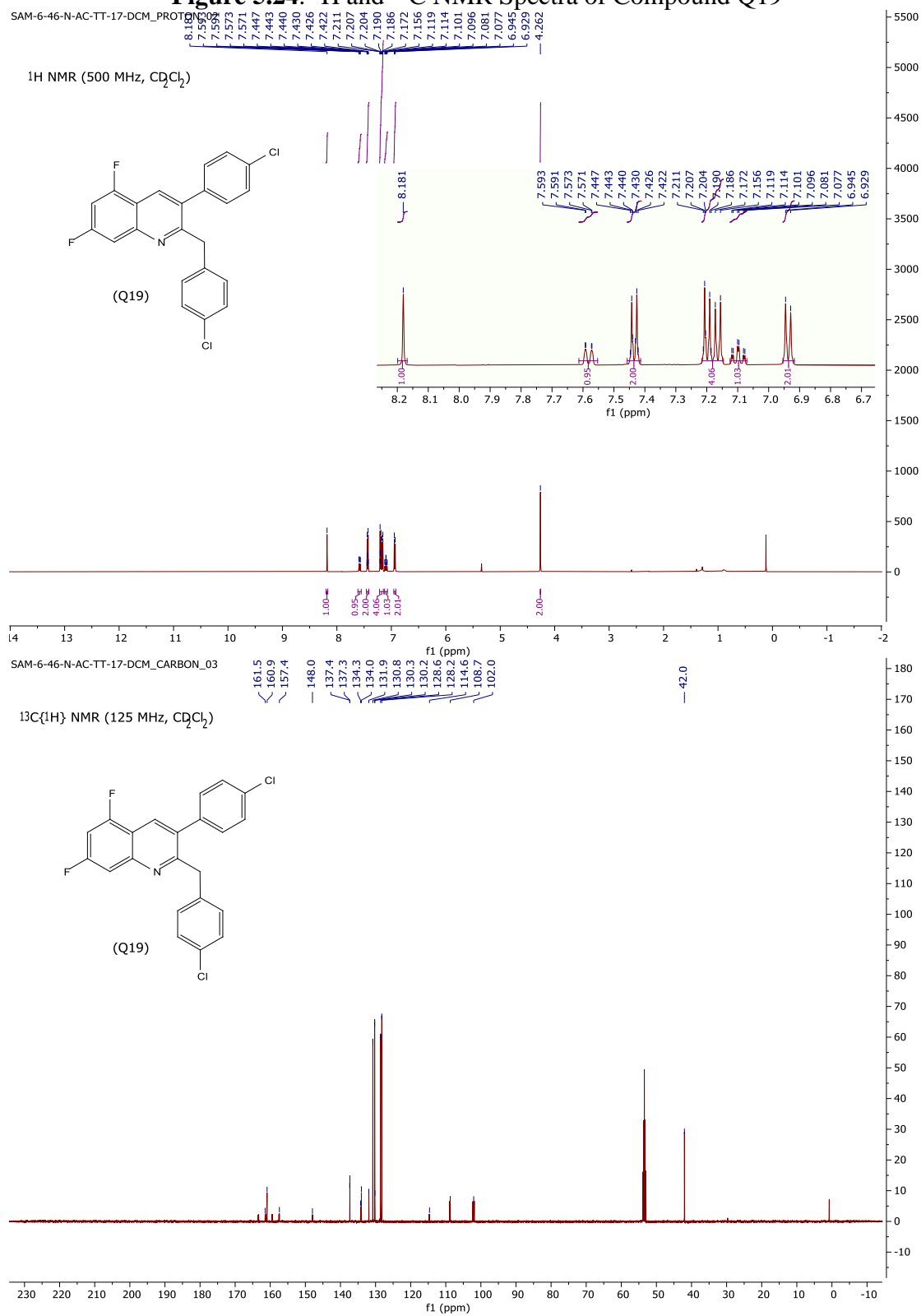
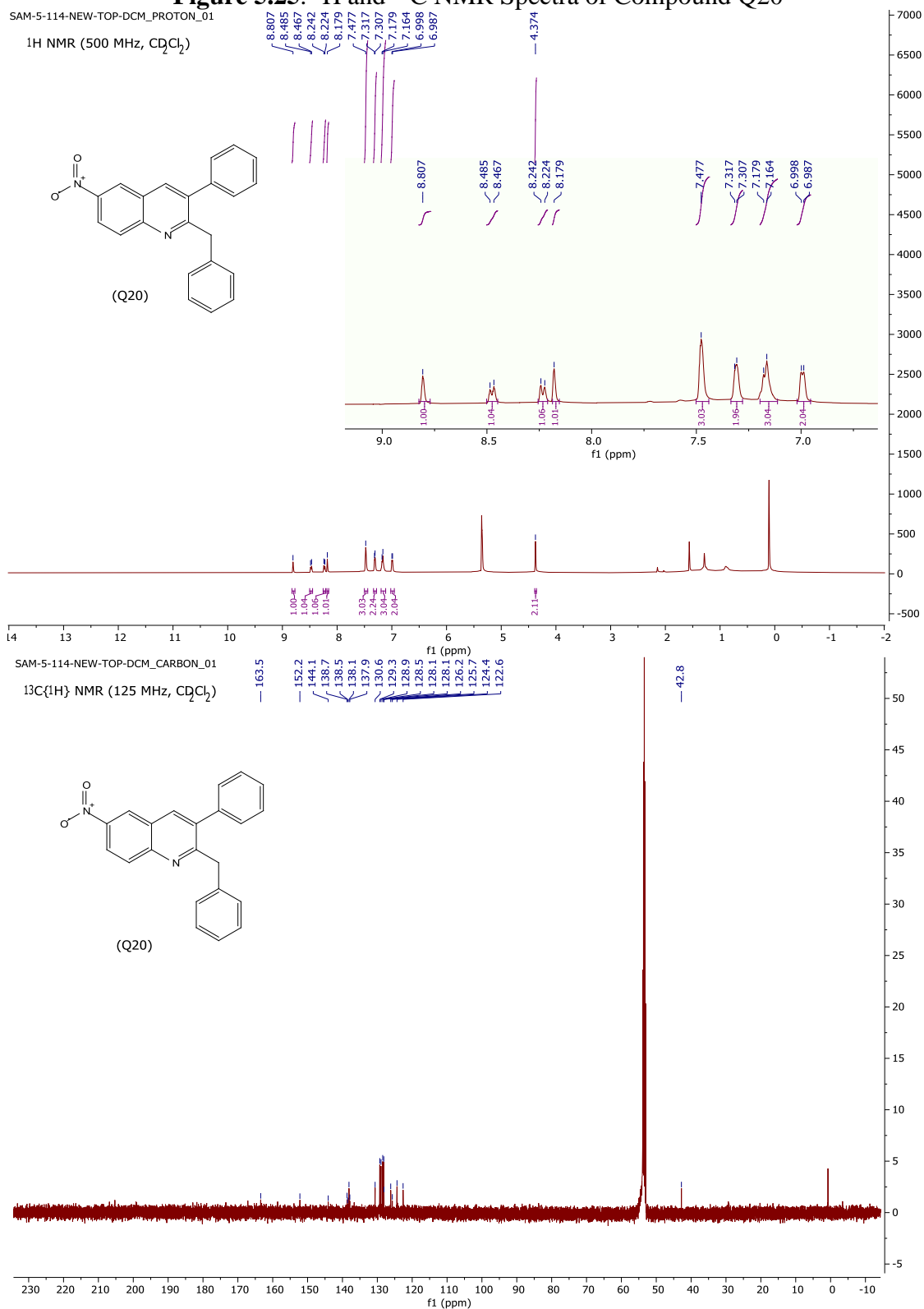


Figure 5.25. ^1H and ^{13}C NMR Spectra of Compound Q20



REFERENCES

REFERENCES

- [1] (a) Michael, J. P. *Nat. Prod. Rep.* **2008**, 25, 166. (b) Shang, X.-F.; Morris-Natschke, S. L.; Liu, Y.-Q.; Guo, X.; Xu, X.-S.; Goto, M.; Li, J.-C.; Yang, G.-Z.; Lee, K.-H. *Med. Res. Rev.* **2018**, 38, 775.
- [2] (a) Chung, P.; Bian, Z.; Pun, H.; Chan, D.; Chan, A. S.; Chui, C.; Tang, J. C.; Lam, K. *Future Med. Chem.* **2015**, 7, 947. (b) Hussaini, S. M. A. *Expert Opin. Ther. Pat.* **2016**, 26, 1201. (c) Kumari, L.; Salahuddin; Mazumder, A.; Pandey, D.; Yar, M. S.; Kumar, R.; Mazumder, R.; Sarafroz, M.; Ahsan, M. J.; Kumar, V.; Gupta, S. *Mini-Rev. Org. Chem.* **2019**, 16, 653.
- [3] Collet, J. W.; Ackermans, K.; Lambregts, J.; Maes, B. U. W.; Orru, R. V. A.; Ruijter, E. *J. Org. Chem.* **2018**, 83, 854.
- [4] Zhang, G.-F.; Zhang, S.; Pan, B.; Liu, X.; Feng, L.-S. *Eur. J. Med. Chem.* **2018**, 143, 710.
- [5] Smith, P. W.; Wyman, P. A.; Lovell, P.; Goodacre, C.; Serafinowska, H. T.; Vong, A.; Harrington, F.; Flynn, S.; Bradley, D. M.; Porter, R.; Coggon, S.; Murkitt, G.; Searle, K.; Thomas, D. R.; Watson, J. M.; Martin, W.; Wu, Z.; Dawson, L. A. *Bioorg. Med. Chem. Lett.* **2009**, 19, 837.
- [6] Tseng, C.-H.; Tung, C.-W.; Peng, S.-I.; Chen, Y.-L.; Tzeng, C.-C.; Cheng, C.-M. *Molecules* **2018**, 23, 1036.
- [7] McDaniel, T. J.; Lansdell, T. A.; Dissanayake, A. A.; Azevedo, L. M.; Claes, J.; Odom, A. L.; Tepe, J. J. *Bioorg. Med. Chem.* **2016**, 24, 2441.
- [8] (a) Liu, J.; Cao, R.; Xu, M.; Wang, X.; Zhang, H.; Hu, H.; Li, Y.; Hu, Z.; Zhong, W.; Wang, M. *Cell Discov.* **2020**, 6, 1. (b) Gao, J.; Tian, Z.; Yang, X. *Biosci. Trends* **2020**, 14, 72. (c) Cortegiani, A.; Ingoglia, G.; Ippolito, M.; Giarratano, A.; Einav, S. *J. Crit. Care* **2020**, 57, 279.
- [9] (a) Dobish, M. C.; Johnston, J. N. *J. Am. Chem. Soc.* **2012**, 134, 6068. (b) Knowe, M. T.; Danneman, M. W.; Sun, S.; Pink, M.; Johnston, J. N. *J. Am. Chem. Soc.* **2018**, 140, 1998. (c) Kim, A. N.; Ngamnithiporn, A.; Welin, E. R.; Daiger, M. T.; Grünanger, C. U.; Bartberger, M. D.; Virgil, S. C.; Stoltz, B. M. *ACS Catal.* **2020**, 10, 3241. (d) Xu-Xu, Q.-F.; Zhang, X.; You, S.-L. *Org. Lett.* **2020**, 22, 1530. (e) Lu, G.; Xie, F.; Xie, R.; Jiang, H.; Zhang, M. *Org. Lett.* **2020**, 22, 2308.
- [10] Aribi, F.; Panossian, A.; Vors, J.-P.; Pazenok, S.; Leroux, F. R. *Eur. J. Org. Chem.* **2018**, 2018, 3792.
- [11] Caeiro, G.; Lopes, J.; Magnoux, P.; Ayrault, P.; Ramoaribeiro, F. *J. Catal.* **2007**, 249, 234.

- [12] (a) Jiang, B.; Ning, X.; Gong, S.; Jiang, N.; Zhong, C.; Lu, Z.-H.; Yang, C. *J. Mater. Chem. C* **2017**, *5*, 10220. (b) Mandapati, P.; Braun, J. D.; Killeen, C.; Davis, R. L.; Williams, J. A. G.; Herbert, D. E. *Inorg. Chem.* **2019**, *58*, 14808.
- [13] (a) Bharate, J. B.; Vishwakarma, R. A.; Bharate, S. B. *RSC Adv.* **2015**, *5*, 42020. (b) Ramann, G.; Cowen, B. *Molecules* **2016**, *21*, 986. (c) Sharma, R.; Kour, P.; Kumar, A. *J. Chem. Sci.* **2018**, *130*, 73.
- [14] (a) Yan, R.; Liu, X.; Pan, C.; Zhou, X.; Li, X.; Kang, X.; Huang, G. *Org. Lett.* **2013**, *15*, 4876. (b) Kong, L.; Zhou, Y.; Huang, H.; Yang, Y.; Liu, Y.; Li, Y. *J. Org. Chem.* **2015**, *80*, 1275. (c) Fedoseev, P.; Van der Eycken, E. *Chem. Commun.* **2017**, *53*, 7732. (d) Jadhav, S. D.; Singh, A. *Org. Lett.* **2017**, *19*, 5673. (e) Kumar, G. S.; Kumar, P.; Kapur, M. *Org. Lett.* **2017**, *19*, 2494. (f) Pang, X.; Wu, M.; Ni, J.; Zhang, F.; Lan, J.; Chen, B.; Yan, R. *J. Org. Chem.* **2017**, *82*, 10110. (g) Sharghi, H.; Aberi, M.; Khataminejad, M.; Shiri, P. *Beilstein J. Org. Chem.* **2017**, *13*, 1977. (h) Wakade, S. B.; Tiwari, D. K.; Ganesh, P. S. K. P.; Phanindrudu, M.; Likhar, P. R.; Tiwari, D. K. *Org. Lett.* **2017**, *19*, 4948. (i) Ahmed, W.; Zhang, S.; Yu, X.; Yamamoto, Y.; Bao, M. *Green Chem.* **2018**, *20*, 261. (j) Lee, S. Y.; Jeon, J.; Cheon, C.-H. *J. Org. Chem.* **2018**, *83*, 5177. (k) Phanindrudu, M.; Wakade, S. B.; Tiwari, D. K.; Likhar, P. R.; Tiwari, D. K. *J. Org. Chem.* **2018**, *83*, 9137. (l) Rubio-Presa, R.; Suárez-Pantiga, S.; Pedrosa, M. R.; Sanz, R. *Adv. Synth. Catal.* **2018**, *360*, 2216. (m) Das, S.; Sinha, S.; Samanta, D.; Mondal, R.; Chakraborty, G.; Brandañ, P.; Paul, N. D. *J. Org. Chem.* **2019**, *84*, 10160. (n) Dhiman, A. K.; Chandra, D.; Kumar, R.; Sharma, U. *J. Org. Chem.* **2019**, *84*, 6962. (o) Zhao, P.; Wu, X.; Zhou, Y.; Geng, X.; Wang, C.; Wu, Y.; Wu, A.-X. *Org. Lett.* **2019**, *21*, 2708. (p) Zou, L.-H.; Zhu, H.; Zhu, S.; Shi, K.; Yan, C.; Li, P.-G. *J. Org. Chem.* **2019**, *84*, 12301.
- [15] (a) Sugimoto, M.; Fukuda, T.; Ito, Y. *Org. Lett.* **1999**, *1*, 1977. (b) Beller, M.; Thiel, O. R.; Trauthwein, H.; Hartung, C. G. *Chem. - Eur. J.* **2000**, *6*, 2513. (c) McNaughton, B. R.; Miller, B. L. *Org. Lett.* **2003**, *5*, 4257. (d) Shan, G.; Sun, X.; Xia, Q.; Rao, Y. *Org. Lett.* **2011**, *13*, 5770. (e) Ji, X.; Huang, H.; Li, Y.; Chen, H.; Jiang, H. *Angew. Chem. Int. Ed.* **2012**, *51*, 7292. (f) Jin, H.; Tian, B.; Song, X.; Xie, J.; Rudolph, M.; Rominger, F.; Hashmi, A. S. K. *Angew. Chem. Int. Ed.* **2016**, *55*, 12688. (g) Li, Y.; Cao, X.; Liu, Y.; Wan, J.-P. *Org. Biomol. Chem.* **2017**, *15*, 9585. (h) Tiwari, D. K.; Phanindrudu, M.; Wakade, S. B.; Nanubolu, J. B.; Tiwari, D. K. *Chem. Commun.* **2017**, *53*, 5302. (i) Xu, J.; Sun, J.; Zhao, J.; Huang, B.; Li, X.; Sun, Y. *RSC Adv.* **2017**, *7*, 36242. (j) Zhang, J.; Wang, L.; Xiang, J.; Cui, J.; Hu, B.; Yang, L.; Tang, Y. *ChemistrySelect* **2019**, *4*, 9392.
- [16] Zhang, Y.; Wang, M.; Li, P.; Wang, L. *Org. Lett.* **2012**, *14*, 2206.
- [17] (a) Batista, V. S.; Crabtree, R. H.; Konezny, S. J.; Luca, O. R.; Praetorius, J. M. *New J. Chem.* **2012**, *36*, 1141. (b) Tanwar, L.; Börgel, J.; Ritter, T. *J. Am. Chem. Soc.* **2019**, *141*, 17983.

Chapter 6: Conclusion and future works

My research work in Prof. Tepe's lab was focused on the development of new methods to synthesize novel heterocyclic analogs. The modified Corey-Chaykovsky sulfur ylide reaction was described in this report to synthesize oxazolines. The reactions provided exclusively diastereoselective *trans*-oxazoline products in moderate to high yields. A similar method was also utilized to synthesize *trans*-imidazolines in moderate yields. However, the enantioselective synthesis of those scaffolds yet remains unexplored. In the future, these may be achievable by using enantiopure sulfonium salts or bases in similar reaction conditions. In addition, the synthesis of oxazoline and imidazoline scaffolds are still limited to the aromatic sulfonium salts. Moreover, the development of stable precursors in the imidazoline synthesis may further improve the yields of the imidazoline analogs.

In this work, the synthesis of 2,3-disubstituted quinolines were also reported from the reaction of anilines and aromatic or aliphatic epoxides in the presence of the Lewis acid $\text{Sc}(\text{OTf})_3$ and the radical scavenger TEMPO. The reaction provided excellent yields with aromatic epoxides and the electron-donating group containing anilines, whereas aliphatic epoxides provided moderate yields of the quinolines. The reaction worked poorly with the electron-donating aromatic amines, which may need further development in the future. In addition, these optimized reaction conditions to form the *in situ* aldehydes from the epoxides can be used to synthesize other heterocyclic scaffolds such as pyridines, pyrazole, etc.